ON ITERATIVE LEARNING CONTROL FOR SOLVING NEW CONTROL PROBLEMS

XUEFANG LI

NATIONAL UNIVERSITY OF SINGAPORE

2016

ON ITERATIVE LEARNING CONTROL FOR SOLVING NEW CONTROL PROBLEMS

XUEFANG LI

(M.Sc., Sichuan University, China)

A THESIS SUBMITTED

FOR THE DEGREE OF DOCTOR OF PHILOSOPHY

DEPARTMENT OF ELECTRICAL AND COMPUTER ENGINEERING

NATIONAL UNIVERSITY OF SINGAPORE

2016

Declaration

I hereby declare that the thesis is my original work

and it has been written by me in its entirely. I have

duly acknowledged all the sources of information

which have been used in the thesis.

This thesis has also not been submitted for any

degree in any university previously.

XUEFANG LI

31 July, 2016

Acknowledgments

I would like to express my sincere appreciation to my supervisor Professor Jian-Xin Xu for his inspiration, excellent guidance, support and encouragement. Through our countless discussions, I have benefited a lot from his erudite knowledge, originality of thought, and rich experience in research. I owe an immense debt of gratitude to him for having given me the curiosity about the learning and research in the domain of control. Besides, Professor Xu's rigorous attitude and endless enthusiasm towards research have influenced me greatly. Without his help, this thesis and many others would have been impossible.

I would also like to thank A/Professor Abdullah Al Mamun, A/Professor Cheng Xiang at National University of Singapore, Professor Weinian Zhang at Sichuan University and Professor Deqing Huang at Southwest Jiaotong University, who provided me kind encouragement and constructive suggestions for my research.

Special thanks go to Electrical and Computer Engineering Department in National University of Singapore for the financial support during my pursuit of PhD degree and the research facilities provided throughout my research work.

I am grateful to all my colleagues at the Control & Simulation Lab, for their kind assistance, friendship, and support during my stay at National University of Singapore. Special mention has to be given to Dr. Qinyuan Ren, Dr. Zhaoqin Guo, Dr. Xin Deng, Dr. Shiping Yang, Verma Saurab, Dr. Yue Yang, for their encouragement and support in my research. I would also like to thank my good friend Qian Wang for being there through the good times and the bad.

Last but not least, I would like to thank my husband, Dr. Zihong Yuan, for his encouragement, patience and love. I would also express my deepest gratitude to my parents for their constant support, understanding and love during all these years. This thesis is dedicated to them.

Contents

Summary

Iterative learning control (ILC) is an approach for improving the transient performance of uncertain systems that operate repetitively over a fixed time interval. Over the past three decades, although ILC has been well established in terms of the underlying theory, there are several limitations in traditional ILC that hinder its applicability. Motivated by this observation, the main contributions of this thesis are to apply ILC approach to solve new control problems, such as uncertain systems with non-repeatable factors, systems with unstructured uncertainties, applicability of ILC in systems of partial differential equations (PDEs), and motion control of robotic fish via ILC.

The first main objective of this research is to deal with temporal and/or spatial factors in the control system that are not strictly repeatable (non-uniform) along the iteration axis. Three different ILC schemes are developed to deal with learning control systems with iteration-varying trial lengths. Firstly, a modified ILC scheme is proposed for discrete-time linear systems with randomly varying trial lengths. By considering the stochastic property of trial lengths, a stochastic variable satisfying the Bernoulli distribution and an iteration-average operator are introduced into the classic ILC algorithm to handle the variation of trial lengths. Based on the contraction mapping method and λ-norm, the convergence of tracking error is guaranteed in the sense of mathematical expectation. Next, a novel ILC scheme with an embedded iteratively-moving-average operator is developed for continuous-time nonlinear dynamic systems with randomly varying trial lengths. It is shown that for nonlinear affine and non-affine systems, the proposed learning algorithm works effectively to nullify the tracking error. Furthermore, in practice a control system may implement different but highly correlated motion tasks. Whether

a control system can learn consecutively from different but highly correlated tracking tasks is of great interest and challenge. In this thesis, a new adaptive ILC (AILC) scheme with a time-scaling factor is proposed for control tasks with different magnitude and time scales. The major advantage of the proposed AILC algorithm is the ability to utilize all the learned knowledge despite the iteratively varying tracking tasks

The second main objective is to deal with the norm-bounded uncertainties. A new robust ILC (RILC) scheme is developed for state tracking control of nonlinear MIMO systems. By introducing a composite energy function (CEF), the asymptotical convergence of tracking error is proved. The idea behind the proposed controller is to parameterize the bounding functions, and then learn those parametric uncertainties pointwisely in the iteration domain. In such sense, ILC of systems with non-parametric uncertainties is fulfilled by a parametric adaptation method. The results are first derived for systems without input disturbance, and then generalized to systems with uncertain input distribution matrix and state-dependent input disturbance.

Despite the great progress of ILC for lumped parameter systems (LPSs) modeled by ordinary differential equations (ODEs), studies of ILC for distributed parameter systems (DPSs) governed by partial differential equations (PDEs) are limited. Thus, the third main objective of this research is to explore the applicability of learning rules to PDE systems. Firstly, a design and analysis framework of ILC for linear inhomogeneous distributed parameter systems (LIDPSs) is constructed. Owing to the system model characteristics, LIDPSs are first reformulated into a matrix form in the frequency domain. Then, through the determination of a fundamental matrix, the transfer function of LIDPS is precisely evaluated in a closed form. The derived transfer function provides

the direct input-output relationship of the LIDPS, and thus facilitates the consequent ILC design and convergence analysis in the frequency domain. Subsequently, a D-type anticipatory ILC scheme is applied to the boundary control of a class of nonlinear inhomogeneous heat equations. By transforming the inhomogeneous heat equation into its integral form and exploiting the properties of the embedded Jacobi Theta functions, the learning convergence of ILC is obtained through CM method. The adopted ILC scheme is capable of dealing with state-independent or state-dependent uncertainties.

To the end, as a real-time application, an ILC approach is presented for precise speed tracking of a two-link Carangiform robotic fish. By virtue of the Lagrangian mechanics method, a mathematical model for the robotic fish is first established, which is highly nonlinear and non-affine-in-input. In this thesis, a P-type ILC algorithm is adopted, which can significantly improve the tracking performance despite the high nonlinearity in fish model. It is shown, from both theoretical analysis and real-time experiments, that ILC is an appropriate and powerful motion control method for robotic fish because of its partial model-free property and the simplicity of the control algorithm.

List of Figures

List of Tables

Chapter 1

Introduction

1.1 Iterative Learning Control

Iterative learning control (ILC), as an effective control strategy, is designed to improve the current performance of uncertain systems by fully utilizing the past control experience. Specifically, ILC is usually designed for systems that are able to complete some tasks over a fixed time interval and perform them repeatedly. By synthesizing the control input from the previous control input and tracking error, the controller learns from the past experience and improves the current tracking performance. ILC was initially developed by S. Arimoto [1], and has been widely explored by the control community since then [2–9].

Fig. 1 shows the schematic diagram of ILC, where the subscript i denotes the iteration index and y_d denotes the reference trajectory. Based on the input signal u_i at the ith iteration, as well as the tracking error $e_i \triangleq y_d - y_i$, the input u_{i+1} for the next iteration, namely, the $(i+1)$th iteration, is constructed. Meanwhile, the input signal u_{i+1} is also stored into the memory for the $(i+2)$th iteration.

It is important to note that in Fig. 1.1, a closed loop feedback is formed in the

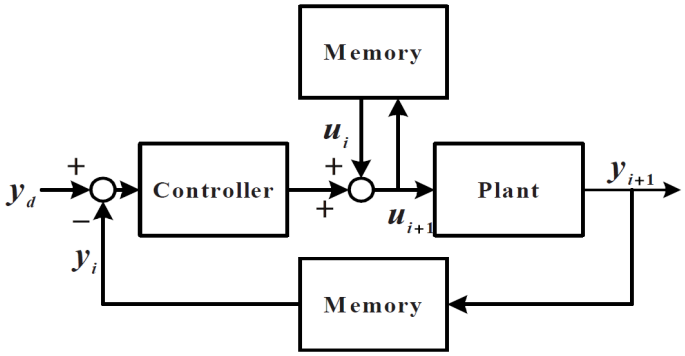

Figure 1.1: Framework of ILC

iteration domain rather than the time domain. Comparing to other control methods such as proportional-integral-derivative (PID) control and sliding mode control, there is a number of distinct features about ILC. First, ILC is designed to handle repetitive control tasks, while other control techniques are difficult to take advantage of the task repetition. Under a repeatable control environment, repeating the same feedback would yield the same control performance. While by incorporating learning, ILC is able to improve the control performance iteratively. Second, the control objective is different. ILC aims at achieving perfect tracking during the whole operation interval. Whereas, most control methods target at achieving asymptotic convergence property along the time axis. Third, ILC is a feedforward control method if viewing in the time domain, and the plant shown in Fig. 1.1 is a generalized plant, that is, the generalized plant can actually include a feedback loop. ILC is used to further improve the performance of the generalized plant. As such, the generalized plant could be made stable in the time domain, which is helpful in guaranteeing transient response while learning proceeds. Last but not least, ILC is a partial model-free control method. As long as an appropriate learning gain is chosen, perfect tracking can be achieved without using the perfect plant model.

Generally speaking there are two main frameworks for ILC, namely contraction-

mapping (CM)-based and composite energy function (CEF)-based approaches. CM-based iterative learning controller has a very simple structure and it is extremely easy to implement. A correction term in the controller is constructed by the output tracking error. To ensure convergence, an appropriate learning gain can be selected based on the system gradient information instead of accurate dynamic model. As it is a partial model-free control method, CM-based ILC is applicable to non-affine-in-input systems. These features are highly desirable in practice as there are plenty of data available in the industry processes but are lack of accurate system models. CM-based ILC has been adopted in many applications, for example X-Y table, chemical batch reactors, laser cutting system, motor control, water heating system, freeway traffic control, wafer manufacturing, and etc [9]. A limitation of CM-based ILC is that it is only applicable to global Lipschitz continuous (GLC) systems. GLC is required by ILC in order to form a contractive mapping, and rule out the finite escape time phenomenon. In comparison, CEF-based ILC, a complementary part of CM-based ILC, applies Lyapunov-like method to design learning rules. CEF is an effective method to handle local Lipschitz continuous (LLC) systems, because the system dynamics is used in the design of learning and feedback mechanisms. It is however worthwhile pointing out that in CM-based ILC, the learning mechanism only requires output signals, while in CEF-based ILC, the full state information is usually required. CEF-based ILC has been applied in satellite trajectory keeping [10] and robotic manipulators control [11–13].

1.2 Motivations and Contributions

ILC is an intelligent control methodology based on strict system environment, where the strict system environment includes that every trial (pass, cycle, and iteration) must

end in a fixed time of duration, that the initial state must be reset to the same point in each iteration, and that the invariance of systems must be ensured throughout the repetition, etc. Due to its structural simplicity as well as almost model-free nature in the process of controller design, ILC has been widely used in industries for control of repetitive motions, such as robotic manipulator, hard disk drives, chemical plants, and so forth [13–15]. In the past few decades, ILC has been well established in terms of both the underlying theory and experimental applications ([6, 14, 16–23]). However, there are still several open problems to be solved in traditional ILC, such as ILC for systems with non-uniform trial lengths, ILC for systems with norm-bounded uncertainties, ILC for infinite dimensional (PDE) systems, and ILC for motion control of robotic fish, etc. This thesis follows the line of ILC for ODE systems, ILC for PDE systems and real-time application of ILC.

In traditional ILC, it is required that the control tasks repeat in a fixed time interval. In many applications of ILC, nevertheless, fixed time of duration may not hold. A pass might be terminated early or late, either by events that depend on the states of the system or on the controller performance or by randomly occurring events. For instance, as introduced in [24], when stroke patients walk on a treadmill, depending on their strength and abilities, the steps will be usually cut short by suddenly putting the foot down. Assuming that up to this point the movement of hip and knee was hardly different from the movement in a full-length step, the data gathered in these aborted steps should be used for learning under the framework of ILC. Similarly, as demonstrated in [25], the gait problems of humanoid robots are divided into phases defined by foot strike times, where the durations of the phases are usually not the same from cycle to cycle during the learning process. Thus, when ILC is applied, the non-uniform trial length problem

occurs. One more example is the timing belt drive system that might be used in a copy machine [25]. When the velocity of output shaft varies, the period of rotation changes accordingly because of the inaccuracies of gearing, thus also hinders the application of classic ILC schemes. Besides those cases, the presence of limiting constraints might also pose pass length questions in the applications of ILC. One example is the functional electrical stimulation for upper limb movement [24]. For reasons of safety, a trial needs to be terminated whenever the output and reference begin to differ too much, and the data gathered outside the neighborhood of reference trajectory cannot be used for learning. If ILC is used for such systems, the trial length might be different from iteration to iteration. Another example is the trajectory tracking with output constraints on a lab-scale gantry crane [26]. When the output constraints are violated, the load is wound up and the trial is terminated, which results in variable pass lengths for ILC. Additionally, there exists another type of non-uniform trial length problem. For example, a robotic manipulator draws a circle in Cartesian space with the same radius but different periods. For such kind of non-repeatable learning control problem, in spite of the variation of the trial lengths, it should be noted that the underlying dynamic properties of the controlled system remain the same. Therefore, how to deal with systems with iteration-varying trial lengths under the framework of ILC is an open and challenging topic.

In the research field of ILC, two categories of uncertainties are considered, namely, parametric ones and non-parametric/unstructured ones. For the former class, the system model is assumed to be linear in parameters, and adaptive ILC scheme is developed to learn the unknown system parameters pointwisely in the iteration domain [27–30]. For the latter class, there are mainly three types of unstructured uncertainties [31]: (1) the uncertainty itself is norm-bounded by a known function $\rho(\mathbf{x},t)$: $\|\eta(\mathbf{x},t)\|_2 \leq \rho(\mathbf{x},t)$, (2)

the variation of uncertainty is norm-bounded by a known function $\rho(\mathbf{x}_1,\mathbf{x}_2,t)$: $\|\eta(\mathbf{x}_1,t)-\eta(\mathbf{x}_2,t)\|_2 \leq \rho(\mathbf{x}_1,\mathbf{x}_2,t)\|\mathbf{x}_1-\mathbf{x}_2\|_2$, and (3) the uncertainty itself is norm-bounded but with unknown coefficient θ: $\|\eta(\mathbf{x},t)\|_2 \leq \theta\rho(\mathbf{x},t)$. Much effort has been made to address ILC design for the second type of non-parametric uncertainties, which may be globally Lipschitz continuous (GLC) [5] or locally Lipschitz continuous (LLC) [32, 33]. When the system is GLC, the popular methodology for convergence analysis is based on contraction mapping. However, for LLC systems, the contraction mapping methodology is not globally applicable any more, and as an alternative, CEF-based ILC design has been well exploited, e.g., [5, 28, 30, 31]. Relatively, there are few works that focus on learning controller design for systems with the other two types of non-parametric uncertainties. The second part of this thesis aims to deal with systems with uncertainties of type (1) and (3) under the framework of ILC.

Despite the significant progress of ILC for finite dimensional systems, studies on ILC for distributed parameter processes or infinite-dimensional processes are limited due to the interweave of 3D dynamics in the time, space, and iteration domains. In practice, many important industrial processes are described by distributed parameter systems (DPSs) governed by partial differential equations (PDEs), such as heat exchanger, industrial chemical reactor, biochemical reactors, fluid flow, etc. Currently, there has been some works reported on ILC of PDE systems. In [34], an iterative learning approach is applied for the constrained digital regulation of a class of linear hyperbolic PDE systems, where the plant model is first reduced to ordinary differential equation (ODE) systems and then approximated by the discrete-time equivalence. In [35], ILC scheme is presented for more general spatio-temporal dynamics using nD discrete linear system models. Without any discretization of system, [36] considers the

design of P-type and D-Type ILC laws for a class of infinite-dimensional linear systems using semigroup theory. Furthermore, to address the application of ILC for some specific DPSs, [37] considers ILC of flow rate in a center pivot irrigator used in dry-land farming, which can be modeled as a spatial-temporal diffusion process in three spatial dimensions coupled with flow in one dimension. Besides, based on Lyapunov theory, differential-difference type ILC is augmented with proportional controller to attenuate the unknown periodic speed variation for a stretched string system on a transporter in [38]. In [39], the similar ILC scheme is combined with proportional-derivative controller to compensate for the unknown periodic motion on the right end for a class of axially moving material systems. In [38] and [39], ILC is mainly designed for the stability maintenance of mechanical processes. Recently, under the framework of ILC, velocity boundary control of a quasi-linear PDE process is considered in [40], where the convergence of output regulation is guaranteed in the steady-state stage. Additionally, there are some works investigating trajectory tracking problems for both linear and nonlinear DPSs ([41–46]) under the framework of ILC. While the ILC design in [41–46] lies in "in domain" control, i.e., actuation penetrates inside the domain of PDE systems. Boundary control, by contrast, is physically more realistic because actuation and sensing are non-intrusive. Hence, as a third extension of ILC strategy, ILC design of boundary tracking control for both linear and nonlinear PDE systems will be addressed. The main difficulty is how to develop the direct input-output relationship of the PDE systems.

As a real-time application of ILC, we are now at the position of considering the precise speed tracking control of a robotic fish via ILC approach. With the increasing underwater activities, many kinds of autonomous underwater vehicles (AUVs) have

been applied for ocean exploration, scientific research, and commercial missions, etc. Among different kinds of AUVs, robotic fish is regarded as one of the most remarkable one because of its high efficiency, high maneuverability and low noise. In previous robotic fish studies, the majority of works investigate how to model various fish behaviors and generate fish-like locomotion [47–55], as well as how to replicate the bodily motion of swimming fish in a robot, etc. Nevertheless, the control issue of robotic fish is still challenging due to nonlinearity, time variance, unpredictable external disturbances, the difficulty in accurately modeling the hydrodynamic effect, etc. Up to now, efforts in studying motion control and motion planning of robotic fish have been made, such as speed and orientation control [56], efficient swimming control [57], target-tracking [58–60], etc. However, as an essential part of motion control and motion planning, the research on precise speed tracking control of robotic fish is limited. This motivates us to apply ILC approach to robotic fish. Owning to its partial model-free property, ILC is proven to work well despite the high nonlinearity and uncertainties in hydrodynamics, and the speed tracking control performance can be improved significantly via ILC.

The objective of the thesis is to extend ILC approach to solve new control problems. The main contributions lie in the following aspects: ILC design for systems with non-uniform trial lengths, systems with unstructured uncertainties, infinite dimensional (PDE) systems, and real-time application of ILC. The contributions of the thesis are summarized in Table 1.1.

In details, the contributions of this thesis are list as follows.

1. In Chapter 2, an ILC design problem for discrete-time linear systems with randomly varying trial lengths is investigated. The novelty is that a stochastic variable satisfying the Bernoulli distribution is introduced due to the stochastic prop-

Table 1.1: The Contribution of The Thesis.

System (Plant)			Trial lengths	Uncertainty	Method	Performance
Discrete time	Linear		Non-uniform	Linear	CM-ILC	$\|\cdot\|_E$
Continuous time	ODE	Nonlinear	Non-uniform	GLC	CM-ILC	Asym. conv.
			Non-uniform	Parametric	CEF-ILC	$\|\cdot\|_{L^2}$
			Uniform	Norm-bounded	CEF-ILC	$\|\cdot\|_{L^2}$
	PDE	Linear	Uniform	Linear	CM-ILC	Asym. conv.
		Nonlinear	Uniform	GLC	CM-ILC	$\|\cdot\|_\lambda$
	Robotic fish	Nonlinear	Uniform	LLC	CEF-ILC	Unif. conv.

[1] ODE: ordinary differential equation, PDE: partial differential equation, ILC: iterative learning control, GLC: global Lipschitz continuous, LLC: local global Lipschitz continuous, CM: contraction mapping, CEF: composite energy function, CM-ILC: CM-based ILC, CEF-ILC: CEF-based ILC, Conv.: convergence.

[2] $\|\cdot\|_E$: convergence in the sense of mathematical expectation, $\|\cdot\|_{L^2}$: convergence in the sense of L^2-norm $\|\cdot\|_\lambda$: convergence in the sense of λ-norm, Asym. conv.: asymptotic convergence in iteration domain, Unif. conv.: uniform convergence.

erty of trial lengths. Furthermore, a unified expression of ILC scheme for systems with different trial lengths is presented by introducing an iteration-average operator. It turns out that the proposed ILC algorithm is able to handle tracking tasks with non-uniform trial lengths, which thus mitigates the requirement on classic ILC that all trial lengths must be identical. Considering the stochastic property of trial lengths, the learning convergence condition of ILC is derived in the sense of mathematical expectation through CM methodology.

2. In Chapter 3, ILC with non-uniform varying trial lengths is extended to continuous-time nonlinear dynamical systems. By considering the fact that the latest trials could provide more accurate control information than those 'older' trials, an ILC scheme based on an iteratively-moving-average operator is introduced, where the iteratively-moving-average operator incorporates control information of the few

most recent trials. It is shown that for nonlinear affine and non-affine systems, the proposed learning algorithm works effectively to handle the randomness of trial lengths and nullify the tracking error.

3. In practice, a control system may implement different but highly correlated motion tasks. Whether a control system can learn consecutively from different but highly correlated tracking tasks is of great interest and challenge. In Chapter 4, a new adaptive ILC (AILC) scheme with a time-scaling function is proposed for control tasks with different magnitude and time scales. The rigorous convergence analysis for nonlinear systems with time-invariant and time-varying parametric uncertainties are derived by applying CEF approach. As such, the learning control system is capable of fully utilizing all the learned knowledge to solve different but somehow correlated control problems.

4. In Chapter 5, a new robust ILC (RILC) scheme is presented for state tracking control of nonlinear MIMO systems. The main characteristic of the proposed controller lies in its ability to deal with unstructured uncertainties that are norm-bounded but not globally or locally Lipschitz continuous as usual. The classical resetting condition of ILC is removed and replaced with more practical alignment condition. Furthermore, the proposed ILC law is extended to more general systems with input distribution uncertainties.

5. Chapter 6 aims to construct a design and analysis framework for ILC of linear inhomogeneous distributed parameter systems (LIDPSs), which may be hyperbolic, parabolic, or elliptic, and include many important physical processes such as diffusion, vibration, heat conduction and wave propagation as special cases. Owing to the system model characteristics, LIDPSs are first reformulated into a matrix

form in the Laplace transform domain. Then, through the determination of a fundamental matrix, the transfer function of LIDPS is precisely evaluated in a closed form. The derived transfer function provides the direct input-output relationship of the LIDPS, and thus facilitates the consequent ILC design and convergence analysis in the frequency domain. The proposed control design scheme is able to deal with parametric and non-parametric uncertainties and make full use of the process repetition, while avoid any simplification or discretization for the 3D dynamics of LIDPS in the time, space, and iteration domains.

6. In Chapter 7, a D-type anticipatory ILC scheme is applied to the boundary control of a class of nonlinear inhomogeneous heat equations, where the heat flux at one side is the control input while the temperature measurement at the other side is the control output. By transforming the inhomogeneous heat equation into its integral form and exploiting the properties of the embedded Jacobi Theta function, the learning convergence of ILC is guaranteed through rigorous analysis. One of the major advantages of the adopted ILC scheme is the ability to deal with state-independent or state-dependent uncertainties. Meanwhile, due to the feedforward characteristic of ILC, the proposed scheme not only makes anticipatory compensation possible to overcome the heat conduction delay in boundary output tracking, but also eliminates the gain margin limitation encountered in feedback control.

7. In Chapter 8, an ILC approach is applied to a two-link Carangiform robotic fish in real time and achieves precise speed tracking performance. Firstly, a mathematical model for the robotic fish is established by virtue of Newton's second law, which is highly nonlinear and non-affine in control input. Then a P-type ILC

algorithm is adopted for speed tracking tasks of the robotic fish, and the convergence of tracking error is derived based on CEF method. By employing ILC, the speed tracking control performance can be improved significantly without using the perfect model. ILC is thus shown to be an appropriate and powerful motion control method for robotic fish from both theoretical analysis and real-time experiments.

Chapter 2

ILC for Discrete-time Linear Systems with Randomly Varying Trial Lengths

2.1 Introduction

ILC is usually designed for control tasks that repeat in a fixed time interval. In many applications of ILC, nevertheless, it would not be the case that every trial ends in a fixed time of duration. A pass might be terminated early or late, either by events that depend on the states of the system or on the controller performance or by randomly occurring events. Therefore, how to design ILC algorithms for systems with different trial lengths is an interesting and challenging problem.

In existing literature, there are some works investigating the ILC problems with non-uniform trial lengths. In [61] a non-standard ILC approach is developed for the systems operating continuously in time. The ILC approach was applied by defining a

"trial" in terms of completion of a single "period" of the output trajectory, where the actual trial lengths will likely be different from the desired trial length. In [25], the authors investigate the utilization of ILC and repetitive control to implement periodic gaits. In [24], the monotonic convergence of linear ILC systems with varying pass lengths is considered by using the lifting method, where a concept maximum pass length error is introduced. As an application, the ILC algorithm with variable pass lengths in [24] is applied to trajectory tracking on a lab-scale gantry crane with output constraints in [26]. However, to the best of our knowledge, there are no works applying the iteration-average operator to the ILC problems with non-uniform trial lengths. In our case, the trial lengths will randomly vary in the iteration domain. If the previous trial ends before we want it to end, it implies that some of the tracking information are missing, which thus cannot be used to improve the current performance. When introducing the iteration-average operator, all tracking information of the past trials will be applied for learning simultaneously. Thus, the absent tracking information in the last trial will be made up by that of other previous trials if there are any. Then the current performance will be improved by fully utilizing the past control experience. Furthermore, it is practically hard or even impossible to set the initial state of the system at the same value perfectly, the study on the initial resetting conditions has become a hotspot research in recent years, such as [62–64], etc. In [24–26, 61], the identical initialization condition is one of the fundamental requirements for their controller design. While by introducing the iteration-average operator, this requirement would be removed.

In this chapter, considering the stochastic property of trial lengths, a modified ILC scheme is developed by adopting an iteration-average operator. The learning condition of ILC that guarantees the convergence of tracking error in mathematical expectation is

derived through rigorous analysis. The proposed ILC scheme mitigates the requirement on classic ILC that all trial lengths must be identical. In addition, the identical initialization condition can be removed. Moreover, the extension from time-invariant systems to time-varying systems is also addressed parallelly.

This chapter is organized as follows. Section 2.2 formulates the ILC problems with randomly varying trial lengths. In Section 2.3, controller design and convergence analysis are presented. Further, the proposed ILC law is extended to time-varying systems in Section 2.4. Section 2.5 gives two illustrative examples.

2.2 Problem Formulation

First of all, some notations are presented. Throughout this chapter, denote $\|\cdot\|$ the Euclidean norm or any consistent norm, and $\|\mathbf{f}(t)\|_\lambda = \sup_{t\in\{0,1,\ldots,T\}} \alpha^{-\lambda t}\|\mathbf{f}(t)\|$ the λ-norm of a vector function $\mathbf{f}(t)$ with $\lambda > 0$ and $\alpha > 1$. Denote $\mathscr{N}$ the set of natural numbers, and I the identity matrix. Moreover, define $\mathscr{I}_d \triangleq \{0,1,\ldots,T_d\}$, where T_d is the desired trial length, and $\mathscr{I}_i \triangleq \{0,1,\ldots,T_i\}$, where T_i is the trial length of the ith iteration. When $T_i < T_d$, it follows that $\mathscr{I}_i \subset \mathscr{I}_d$. Define $\mathscr{I}_d/\mathscr{I}_i \triangleq \{t \in \mathscr{I}_d : t \notin \mathscr{I}_i\}$ as the complementary set of $\mathscr{I}_i$ in $\mathscr{I}_d$. Given two integers N_1 and N_2 satisfying $0 \le N_1 < T_d$ and $N_2 \ge 0$, respectively. Set $\mathscr{I}_N \triangleq \{0,1,\ldots,\ldots,T_d+N_2\}$ and it may be divided into two subsets, $\mathscr{I}_a \triangleq \{0,1,\ldots,T_d-N_1-1\}$ and $\mathscr{I}_b \triangleq \{T_d-N_1,\ldots,T_d+N_2\}$. On the set $\mathscr{I}_a$, the control system is deterministic, whereas on the set $\mathscr{I}_b$ the system trial length is randomly varying. Denote $\tau_m \triangleq T_d - N_1 + m$, $m \in \{0,1,\ldots,N_1+N_2\}$, which implies $\tau_m \in \mathscr{I}_b$.

Consider a class of linear time-invariant systems

$$\begin{cases} \mathbf{x}_i(t+1) = A\mathbf{x}_i(t) + B\mathbf{u}_i(t), \\ \mathbf{y}_i(t) = C\mathbf{x}_i(t), \end{cases} \tag{2.1}$$

where $i \in \mathscr{N}$ and $t \in \mathscr{I}_i$ denote the iteration index and discrete time, respectively. Meanwhile, $\mathbf{x}_i(t) \in \mathbf{R}^n$, $\mathbf{u}_i(t) \in \mathbf{R}^p$, and $\mathbf{y}_i(t) \in \mathbf{R}^r$ denote state, input, and output of the system (2.1), respectively. Further, A, B and C are constant matrices with appropriate dimensions, and CB is full-rank. Let $\mathbf{y}_d(t)$, $t \in \mathscr{I}_d$ be the desired output trajectory. Assume that, for any realizable output trajectory $\mathbf{y}_d(t)$, there exists a unique control input $\mathbf{u}_d(t) \in \mathbf{R}^p$ such that

$$\begin{cases} \mathbf{x}_d(t+1) = A\mathbf{x}_d(t) + B\mathbf{u}_d(t), \\ \mathbf{y}_d(t) = C\mathbf{x}_d(t), \end{cases} \tag{2.2}$$

where $\mathbf{u}_d(t)$ is uniformly bounded for all $t \in \mathscr{I}_d$.

The main difficulty in designing ILC scheme for the system (2.1) is that the actual trial length T_i is iteration-varying and different from the desired trial length T_d. Here a simple example is illustrated in Fig. 2.1 to show the variation of the trial lengths in the iteration domain. Assume that the desired trial length is 10, namely, $T_d = 10$, and $N_1 = 3$, $N_2 = 2$. Clearly, there have $\mathscr{I}_d = \{0,1,\ldots,10\}$, $\mathscr{I}_N = \{0,1,\ldots,12\}$, $\mathscr{I}_a = \{0,1,\ldots,6\}$ and $\mathscr{I}_b = \{7,8,\ldots,12\}$. The span of curve i, $i \in \{1,2,\ldots,5\}$ in Fig. 2.1 represents the trial length of the control process at the ith iteration, and the dashed line stands for the possible values, $\{T_d - N_1,\ldots,T_d + N_2\}$, of the stochastic variable T_i. As can be seen from Fig. 2.1, $T_1 = 7$, $T_2 = 11$, $T_3 = 9$, $T_4 = 10$ and $T_5 = 12$. For $i = 1,3$, there has $T_i < T_d$, namely, $\mathscr{I}_i \subset \mathscr{I}_d$. It is easy to verify that $\mathscr{I}_d/\mathscr{I}_1 = \{8,9,10\}$ and $\mathscr{I}_d/\mathscr{I}_3 = \{10\}$. Fig. 2.1 shows that the trial lengths randomly vary between 7 and 12 and they are likely different from the desired trial length.

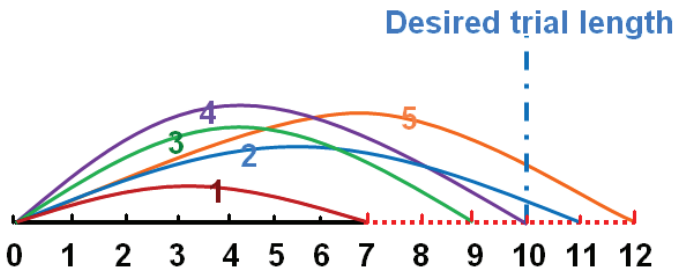

Figure 2.1: Randomly varying trial lengths.

Before addressing the ILC design problem with non-uniform trial lengths, let us give some notations and assumptions that would be useful in the derivation of our main result.

Definition 2.1 $\mathbf{E}\{f\}$ *stands for the expectation of the stochastic variable* f. $\mathbf{P}[f]$ *means the occurrence probability of the event* f.

Assumption 2.1 *Assume that* $T_i \in \mathscr{I}_b$ *is a stochastic variable with* $\mathbf{P}[T_i = \tau_m] = p_m$, $m \in \{0,1,\ldots,N_1+N_2\}$, *where* $\tau_m = T_d - N_1 + m$, *and* $0 \leq p_m < 1$ *is a known constant.*

Assumption 2.2 $\mathbf{E}\{\mathbf{x}_i(0)\} = \mathbf{x}_d(0)$.

Remark 2.1 *The contraction mapping based ILC usually requires the identical initial condition in each iteration. In Assumption 2.2, the condition is extended clearly. The initial states of system could change randomly with* $\mathbf{E}\{\mathbf{x}_i(0)\} = \mathbf{x}_d(0)$ *and there are no limitations to the variance of* $\mathbf{x}_i(0)$.

If the control process (2.1) repeats with the same trial length T_d, namely, $T_i = T_d$, and under the identical initial condition, a simple and effective ILC [65] for the linear system (2.1) is

$$\mathbf{u}_{i+1}(t) = \mathbf{u}_i(t) + L\mathbf{e}_i(t+1), \tag{2.3}$$

where $\mathbf{e}_i(t+1) \triangleq \mathbf{y}_d(t+1) - \mathbf{y}_i(t+1)$, and $L \in \mathbf{R}^{p\times r}$ is an appropriate learning gain matrix. The convergence analysis of (2.3) is given in *Appendix A.1*. However, when the trial length T_i is iteration-varying, which corresponds to a non-standard ILC process, the learning control scheme (2.3) has to be re-designed.

2.3 ILC Design and Convergence Analysis

In this section, based on the assumptions and notations that are given in Section 2.2, ILC design and convergence analysis are addressed, respectively.

In practice, for one scenario that the ith trial ends before the desired trial length, namely, $T_i < T_d$, both the output $\mathbf{y}_i(t)$ and the tracking error $\mathbf{e}_i(t)$ on the time interval $\mathscr{I}_d/\mathscr{I}_i$ are missing, which thus cannot be used for learning. For the other scenario that the ith trial is still running after the time instant we want it to stop, i.e., $T_i > T_d$, the signals $\mathbf{y}_i(t)$ and $\mathbf{e}_i(t)$ after the time instant T_d are redundant and useless for learning. In order to cope with those missing signals or redundant signals in different scenarios, a sequence of stochastic variables satisfying Bernoulli distribution is defined. By using those stochastic variables, a newly defined tracking error $\mathbf{e}_i^*(t)$ is introduced to facilitate the modified ILC design.

The main procedure for deriving a modified ILC scheme can be described as follows:

(1) Define a stochastic variable $\gamma_i(t)$ in the ith iteration.

Let $\gamma_i(t), t \in \mathscr{I}_N$ be a stochastic variable satisfying Bernoulli distribution and taking binary values 0 and 1. On the one hand, the relationship $\gamma_i(t) = 1$ represents the event that the control process (2.1) can continue to the time instant t in the ith iteration, which occurs with a probability of $p(t)$, where $0 < p(t) \leq 1$ is a prespecified function of

time t. On the other hand, the relationship $\gamma_i(t) = 0$ denotes the event that the control process (2.1) cannot continue to the time instant t in the ith iteration, which occurs with a probability of $1 - p(t)$.

(2) Compute the probability $\mathbf{P}[\gamma_i(t) = 1]$.

Since the control process (2.1) will not stop within the time interval $\mathscr{I}_a$, the event that $\gamma_i(t) = 1$ surely occurs when $t \in \mathscr{I}_a$, which implies that $p(t) = 1$, $\forall t \in \mathscr{I}_a$. While for the scenario of $t \in \mathscr{I}_b$, denote A_m the event that the control process (2.1) stops at τ_m, where $\tau_m = T_d - N_1 + m$, $m \in \{0, 1, \ldots, N_1 + N_2\}$. Then it follows from Assumption 2.1 that $\mathbf{P}[A_m] = p_m$ and the events A_m, $m \in \{0, 1, \ldots, N_1 + N_2\}$, are mutually exclusive clearly. For $t \in \mathscr{I}_b$, the event $\gamma_i(t) = 1$ corresponds to the statement that the control process (2.1) stops at or after the time instant t. Thus,

$$\begin{aligned} \mathbf{P}[\gamma_i(t) = 1] &= \mathbf{P}[\bigcup_{m=t-T_d+N_1}^{N_1+N_2} A_m] \\ &= \sum_{m=t-T_d+N_1}^{N_1+N_2} \mathbf{P}[A_m] \\ &= \sum_{m=t-T_d+N_1}^{N_1+N_2} p_m. \end{aligned} \tag{2.4}$$

Thus, it follows that

$$p(t) = \begin{cases} 1, & t \in \mathscr{I}_a, \\ \sum_{m=t-T_d+N_1}^{N_1+N_2} p_m, & t \in \mathscr{I}_b. \end{cases} \tag{2.5}$$

Further, there has that $0 < p(t) \leq 1$. In order to demonstrate the calculation of the probability $\mathbf{P}[\gamma_i(t) = 1]$ more clearly, a simple example is illustrated in Fig. 2.2. In addition, since $\gamma_i(t)$ satisfies Bernoulli distribution, the expectation $\mathbf{E}\{\gamma_i(t)\} = 1 \cdot p(t) + 0 \cdot (1 - p(t)) = p(t)$.

(3) Define a modified tracking error.

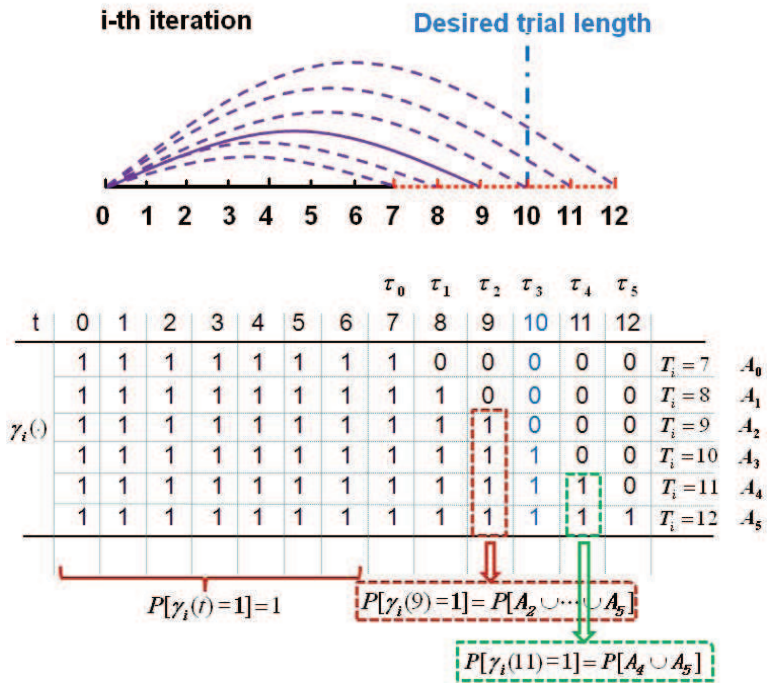

Figure 2.2: Similarly as Fig. 2.1, set $T_d = 10$, $N_1 = 3$ and $N_2 = 2$, the stochastic variable T_i has six possible values $\tau_m = 7+m$, $m \in \{0,1,\ldots,5\}$. All of the possible outcomes are shown in the table and the probability of the event $\gamma_i(t) = 1$ is related to the number of the character 1 in the corresponding column. It is easy to verify the formulation (2.4). For instance, when $t = 9$, there are four 1s in its corresponding column. Then, $\mathbf{P}[\gamma_i(9) = 1] = \mathbf{P}[A_2 \bigcup \cdots \bigcup A_5] = \sum_{m=2}^{5} \mathbf{P}[A_m] = \sum_{m=2}^{5} p_m$. Similarly, when $t = 11$, there are only two 1s in its corresponding column. Thus, it follows that $\mathbf{P}[\gamma_i(11) = 1] = \mathbf{P}[A_4 \bigcup A_5] = \sum_{m=4}^{5} \mathbf{P}[A_m] = \sum_{m=4}^{5} p_m$.

Denote

$$\mathbf{e}_i^*(t) \triangleq \gamma_i(t)\mathbf{e}_i(t), \quad t \in \mathscr{I}_d \tag{2.6}$$

as a modified tracking error, which renders to

$$\mathbf{e}_i^*(t) = \begin{cases} \mathbf{e}_i(t), & t \in \mathscr{I}_i, \\ 0, & t \in \mathscr{I}_d / \mathscr{I}_i, \end{cases} \tag{2.7}$$

when $T_i < T_d$, and

$$\mathbf{e}_i^*(t) = \mathbf{e}_i(t), \quad t \in \mathscr{I}_d, \tag{2.8}$$

when $T_i \geq T_d$.

Remark 2.2 *Since the absent signals are unavailable, and the redundant signals are useless for learning, it is reasonable to define a modified tracking error* $\mathbf{e}_i^*(t)$ *as in*

(2.6), or equivalently (2.7) and (2.8). In the modified tracking error $\mathbf{e}_i^*(t)$*, the redundant signals in* $\mathbf{e}_i(t)$ *are cut off when* $T_i > T_d$*, and the unavailable signals in* $\mathbf{e}_i(t)$ *are set as zero when* $T_i < T_d$*.*

(4) The modified ILC scheme.

Introduce an iteration-average operator [22],

$$\mathbf{A}\{f_i(\cdot)\} \triangleq \frac{1}{i+1}\sum_{j=0}^{i} f_j(\cdot), \tag{2.9}$$

for a sequence $f_0(\cdot), f_1(\cdot), \ldots, f_i(\cdot)$, which plays a pivotal role in the proposed controller. The modified ILC scheme is given as follows,

$$\mathbf{u}_{i+1}(t) = \mathbf{A}\{\mathbf{u}_i(t)\} + \frac{i+2}{i+1} L \sum_{j=0}^{i} \mathbf{e}_j^*(t+1),\ t \in \mathscr{I}_d, \tag{2.10}$$

for all $i \in \mathscr{N}$, where the learning gain matrix L will be determined in the following.

Remark 2.3 *As a matter of fact, the second term on the right hand side of (2.10) can be rewritten as* $(i+2)L\mathbf{A}\{\mathbf{e}_i^*(t+1)\}$*. In* $\mathbf{A}\{\mathbf{e}_i^*(t+1)\}$*, the error profiles* $\mathbf{e}_j^*(t+1)$*,* $j = 0, 1, 2, \ldots, i$*, have been reduced by* $(i+1)$ *times. Nevertheless, by multiplying the factor* $(i+2)$ *in the feedback loop, their magnitudes can be retained even when* $i \to \infty$*.*

The following theorem presents the first main result of this chapter.

Theorem 2.1 *For the discrete-time linear system (2.1) and the ILC scheme (2.10), choose the learning gain matrix L such that, for any constant* $0 \le \rho < 1$*,*

$$\sup_{t \in \mathscr{I}_d} \|I - p(t)LCB\| \le \rho, \tag{2.11}$$

then the expectation of the error, $\mathbf{E}\{\mathbf{e}_i(t)\}$*,* $t \in \mathscr{I}_d$*, will converge to zero asymptotically as* $i \to \infty$*.*

Remark 2.4 *In practice, the probability distribution of the trial length T_i could be estimated in advance based on previous multiple experiments or by experience. In consequence, the probability p_m in Assumption 2.1 is known. Finally, $p(t)$ can be calculated by (2.5), thus is available for controller design.*

Remark 2.5 *From the convergence condition* (2.11) *and Remark 2.4, it can be found that the only system knowledge needed for ILC is the system gradient information CB. In the next chapter, it will be discussed that the accurate mathematical expression of $p(t)$ is not actually required, and we only need its upper and lower bounds when design ILC law.*

Proof. The proof consists of two parts. Part I proves the convergence of the input error in iteration-average and expectation by using the λ-norm. Part II proves the convergence of the tracking error in expectation.

Part I. Let $\triangle \mathbf{u}_i(t) \triangleq \mathbf{u}_d(t) - \mathbf{u}_i(t)$ and $\triangle \mathbf{x}_i(t) \triangleq \mathbf{x}_d(t) - \mathbf{x}_i(t)$ be the input and state errors, respectively, then there have

$$\begin{cases} \triangle \mathbf{x}_i(t+1) = A\triangle \mathbf{x}_i(t) + B\triangle \mathbf{u}_i(t), \\ \mathbf{e}_i(t) = C\triangle \mathbf{x}_i(t). \end{cases} \tag{2.12}$$

By the definition of iteration-average operator (2.9), $\mathbf{A}\{\triangle \mathbf{u}_{i+1}(t)\}$ can be rewritten as

$$\mathbf{A}\{\triangle \mathbf{u}_{i+1}(t)\} = \frac{1}{i+2}[\triangle \mathbf{u}_{i+1}(t) + (i+1)\mathbf{A}\{\triangle \mathbf{u}_i(t)\}]. \tag{2.13}$$

In addition, subtracting $u_d(t)$ from both sides of the ILC law (2.10) implies

$$\triangle \mathbf{u}_{i+1}(t) = \mathbf{A}\{\triangle \mathbf{u}_i(t)\} - \frac{i+2}{i+1} L \sum_{j=0}^{i} \mathbf{e}_i^*(t+1). \tag{2.14}$$

Then substituting (2.14) into the right hand side of (2.13) and applying the operator

$\mathbf{E}\{\cdot\}$ on both sides of (2.13) yield

$$\mathbf{E}\{\mathbf{A}\{\triangle\mathbf{u}_{i+1}(t)\}\} = \mathbf{E}\{\mathbf{A}\{\triangle\mathbf{u}_i(t)\}\} - L\mathbf{E}\{\mathbf{A}\{\mathbf{e}_i^*(t+1)\}\}. \tag{2.15}$$

Since both $\mathbf{E}\{\cdot\}$ and $\mathbf{A}\{\cdot\}$ are linear operators, the operation orders of $\mathbf{E}\{\cdot\}$ and $\mathbf{A}\{\cdot\}$ can be exchanged, yielding

$$\mathbf{E}\{\mathbf{A}\{\mathbf{e}_i^*(t+1)\}\} = p(t+1)\mathbf{E}\{\mathbf{A}\{\mathbf{e}_i(t+1)\}\}, \tag{2.16}$$

where $\mathbf{E}\{\gamma_j(t+1)\mathbf{e}_j(t+1)\} = p(t+1)\mathbf{E}\{\mathbf{e}_j(t+1)\}$ is applied as $\gamma_j(t+1)$ and $\mathbf{e}_j(t+1)$ are independent with each other. Meanwhile, from (2.12), it follows that

$$\mathbf{e}_i(t+1) = CA\triangle\mathbf{x}_i(t) + CB\triangle\mathbf{u}_i(t). \tag{2.17}$$

Then, combining (2.16) and (2.17) gives

$$\begin{aligned}\mathbf{E}\{\mathbf{A}\{\mathbf{e}_i^*(t+1)\}\} &= p(t+1)CA\mathbf{E}\{\mathbf{A}\{\triangle\mathbf{x}_i(t)\}\} \\ &\quad + p(t+1)CB\mathbf{E}\{\mathbf{A}\{\triangle\mathbf{u}_i(t)\}\}.\end{aligned} \tag{2.18}$$

In consequence, substituting (2.18) into (2.15) yields

$$\begin{aligned}\mathbf{E}\{\mathbf{A}\{\triangle\mathbf{u}_{i+1}(t)\}\} &= [I - p(t+1)LCB]\mathbf{E}\{\mathbf{A}\{\triangle\mathbf{u}_i(t)\}\} \\ &\quad - p(t+1)LCA\mathbf{E}\{\mathbf{A}\{\triangle\mathbf{x}_i(t)\}\}.\end{aligned} \tag{2.19}$$

Further, since the solution of the reference system (2.2) is

$$\mathbf{x}_d(t) = A^t\mathbf{x}_d(0) + \sum_{k=0}^{t-1} A^{t-k-1}B\mathbf{u}_d(k), \tag{2.20}$$

it can be obtained similarly from (2.12) that

$$\triangle\mathbf{x}_i(t) = A^t(\mathbf{x}_d(0) - \mathbf{x}_i(0)) + \sum_{k=0}^{t-1} A^{t-1-k}B\triangle\mathbf{u}_i(k). \tag{2.21}$$

Applying both operators $\mathbf{E}\{\cdot\}$ and $\mathbf{A}\{\cdot\}$ on both sides of (2.21) and noticing Assumption 2.2, it concludes that

$$\mathbf{E}\{\mathbf{A}\{\triangle\mathbf{x}_i(t)\}\} = \sum_{k=0}^{t-1} A^{t-1-k}B\mathbf{E}\{\mathbf{A}\{\triangle\mathbf{u}_i(k)\}\}. \tag{2.22}$$

Then substituting (2.22) into (2.19) and taking the norm $\|\cdot\|$ on both sides lead to

$$\begin{aligned}\|\mathbf{E}\{\mathbf{A}\{\triangle\mathbf{u}_{i+1}(t)\}\}\| &\leq \|I-p(t+1)LCB\|\|\mathbf{E}\{\mathbf{A}\{\triangle\mathbf{u}_i(t)\}\}\| \\ &\quad +\beta\sum_{k=0}^{t-1}\alpha^{t-k}\|\mathbf{E}\{\mathbf{A}\{\triangle\mathbf{u}_i(k)\}\}\|, \end{aligned} \tag{2.23}$$

where the parameter α satisfies $\alpha \geq \|A\|$ and $\beta \triangleq \sup_{t\in\mathscr{I}_d}\|p(t+1)LC\|\|B\|$. Multiplying both sides of (2.23) by $\alpha^{-\lambda t}$, and taking the supremum over $\mathscr{I}_d$, there have

$$\begin{aligned}\sup_{t\in\mathscr{I}_d}\alpha^{-\lambda t}\|\mathbf{E}\{\mathbf{A}\{\triangle\mathbf{u}_{i+1}(t)\}\}\| &\leq \rho\sup_{t\in\mathscr{I}_d}\alpha^{-\lambda t}\|\mathbf{E}\{\mathbf{A}\{\triangle\mathbf{u}_i(t)\}\}\| \\ &\quad +\beta\sup_{t\in\mathscr{I}_d}\alpha^{-\lambda t}\sum_{k=0}^{t-1}\alpha^{t-k}\|\mathbf{E}\{\mathbf{A}\{\triangle\mathbf{u}_i(k)\}\}\|, \end{aligned} \tag{2.24}$$

where the constant ρ is chosen such that (2.11) holds. From the definition of λ-norm, it follows that

$$\begin{aligned}&\sup_{t\in\mathscr{I}_d}\alpha^{-\lambda t}\sum_{k=0}^{t-1}\alpha^{t-k}\|\mathbf{E}\{\mathbf{A}\{\triangle\mathbf{u}_i(k)\}\}\| \\ &= \sup_{t\in\mathscr{I}_d}\alpha^{-(\lambda-1)t}\sum_{k=0}^{t-1}\alpha^{-\lambda k}\|\mathbf{E}\{\mathbf{A}\{\triangle\mathbf{u}_i(k)\}\}\|\alpha^{(\lambda-1)k} \\ &\leq \|\mathbf{E}\{\mathbf{A}\{\triangle\mathbf{u}_i(t)\}\}\|_\lambda\sup_{t\in\mathscr{I}_d}\alpha^{-(\lambda-1)t}\sum_{k=0}^{t-1}\alpha^{(\lambda-1)k} \\ &\leq \frac{1-\alpha^{-(\lambda-1)T_d}}{\alpha^{\lambda-1}-1}\|\mathbf{E}\{\mathbf{A}\{\triangle\mathbf{u}_i(t)\}\}\|_\lambda. \end{aligned} \tag{2.25}$$

Then, combining (2.24) and (2.25), there finally have

$$\|\mathbf{E}\{\mathbf{A}\{\triangle\mathbf{u}_{i+1}(t)\}\}\|_\lambda \leq \rho_0\|\mathbf{E}\{\mathbf{A}\{\triangle\mathbf{u}_i(t)\}\}\|_\lambda, \tag{2.26}$$

where $\rho_0 \triangleq \rho+\beta\frac{1-\alpha^{-(\lambda-1)T_d}}{\alpha^{\lambda-1}-1}$. Since $0\leq\rho<1$ by the condition (2.11), it is possible to choose a sufficiently large λ such that $\rho_0<1$. Therefore, (2.26) implies that

$$\lim_{i\to\infty}\|\mathbf{E}\{\mathbf{A}\{\triangle\mathbf{u}_i(t)\}\}\|_\lambda = 0. \tag{2.27}$$

Part II: Now prove the convergence of $\mathbf{e}_i(t)$ in expectation. Multiplying both sides of (2.26) by $(i+2)$, it follows that

$$\|\mathbf{E}\{\sum_{j=0}^{i+1}\triangle\mathbf{u}_j(t)\}\|_\lambda \leq \rho_0\|\mathbf{E}\{\sum_{j=0}^{i}\triangle\mathbf{u}_j(t)\}\|_\lambda + \rho_0\|\mathbf{E}\{\mathbf{A}\{\triangle\mathbf{u}_i(t)\}\}\|_\lambda. \tag{2.28}$$

According to the boundedness of $\|\mathbf{E}\{\mathbf{A}\{\triangle\mathbf{u}_i(t)\}\}\|_\lambda$ from (2.26), (2.27) and Lemma 1 in [22], $\lim_{i\to\infty}\|\mathbf{E}\{\sum_{j=0}^{i}\triangle\mathbf{u}_j(t)\}\|_\lambda = 0$ is further derived, thus

$$\lim_{i\to\infty}\mathbf{E}\{\triangle\mathbf{u}_i(t)\} = \lim_{i\to\infty}[\mathbf{E}\{\sum_{j=0}^{i}\triangle\mathbf{u}_j(t)\} - \mathbf{E}\{\sum_{j=0}^{i-1}\triangle\mathbf{u}_j(t)\}] = 0. \tag{2.29}$$

Pre multiplying the matrix C on both sides of (2.21) and taking the operator $\mathbf{E}\{\cdot\}$ on both sides of yield

$$\mathbf{E}\{\mathbf{e}_i(t)\} = \sum_{k=0}^{t-1} CA^{t-1-k}B\mathbf{E}\{\triangle\mathbf{u}_i(k)\}, \tag{2.30}$$

where Assumption 2.2 is applied. Finally, since (2.29) holds for any $t \in \mathscr{I}_d$, it is proved that $\lim_{i\to\infty}\mathbf{E}\{\mathbf{e}_i(t)\} = 0$, $t \in \mathscr{I}_d$. ■

2.4 Extension to Time-varying Systems

In this section, the proposed ILC scheme is extended to time-varying systems

$$\begin{cases} \mathbf{x}_i(t+1) = A(t)\mathbf{x}_i(t) + B(t)\mathbf{u}_i(t), \\ \mathbf{y}_i(t) = C(t)\mathbf{x}_i(t), \end{cases} \tag{2.31}$$

where $A(t)$, $B(t)$ and $C(t)$ are time-varying matrices with appropriate dimensions and $C(t)B(t)$ is full-rank. The result is summarized in the following theorem.

Theorem 2.2 *For the discrete-time linear time-varying system (2.31) and the ILC algorithm (2.10), choose the learning gain matrix L such that, for any constant* $0 \le \rho < 1$,

$$\sup_{t\in\mathscr{I}_d}\|I - p(t)L(t)C(t)B(t)\| \le \rho, \tag{2.32}$$

the expectation of the error, $\mathbf{E}\{\mathbf{e}_i(t)\}$, $t \in \mathscr{I}_d$, *will converge to zero asymptotically as* $i \to \infty$.

Proof. The proof can be performed similarly as in the proof of Theorem 1.

Considering the desired dynamics that corresponds to (2.31), namely, (2.2) with the matrices A,B,C replaced by $A(t),B(t)$, and $C(t)$, respectively, there has

$$\begin{aligned}\mathbf{x}_d(t) &= \left(\prod_{k=0}^{t-1}A(k)\right)\mathbf{x}_d(0) \\ &\quad+\sum_{k=0}^{t-1}\left(\prod_{l=0}^{t-k-2}A(t-1-l)\right)B(k)\mathbf{u}_d(k).\end{aligned} \tag{2.33}$$

Since a similar relationship also holds at the ith iteration, it follows that

$$\begin{aligned}\triangle\mathbf{x}_i(t) &= \left(\prod_{k=0}^{t-1}A(k)\right)(\mathbf{x}_d(0)-\mathbf{x}_i(0)) \\ &\quad+\sum_{k=0}^{t-1}\left(\prod_{l=0}^{t-k-2}A(t-1-l)\right)B(k)\triangle\mathbf{u}_i(k).\end{aligned} \tag{2.34}$$

Now, replacing (2.20) and (2.21) in the proof of Theorem 2.1 with (2.33) and (2.34), respectively, we can obtain that the inequality (2.26) holds, where the parameter α satisfies $\alpha \geq \sup_{t\in\mathscr{I}_d}\|A(t)\|$ and $\beta \triangleq \sup_{t\in\mathscr{I}_d}\|p(t+1)L(t)C(t)\|\cdot\sup_{t\in\mathscr{I}_d}\|B(t)\|$. By choosing a sufficient large λ and noticing the condition (2.32), it follows that $\rho_0<1$. Hence $\lim_{i\to\infty}\|\mathbf{E}\{\mathbf{A}\{\triangle\mathbf{u}_i(t)\}\}\|_\lambda = 0$ can be obtained similarly. Following the second part of the proof of Theorem 2.1, it gives that $\lim_{i\to\infty}\mathbf{E}\{\mathbf{e}_i(t)\}=0,\ \ t\in\mathscr{I}_d$. ■

Remark 2.6 *In Theorems 2.1 and 2.2, the identical initialization condition is replaced by* $\mathbf{E}\{\mathbf{x}_i(0)\}=\mathbf{x}_d(0)$. *According to (2.21), it has*

$$\mathbf{e}_i(t)=CA^t(\mathbf{x}_d(0)-\mathbf{x}_i(0))+\sum_{k=0}^{t-1}CA^{t-1-k}B\triangle\mathbf{u}_i(k).$$

So, other than deriving the convergence of tracking error, its expectation converges asymptotically is proved by using the expectation operator and the proposed iteration-average based ILC scheme.

Remark 2.7 *The proposed ILC law (2.10) can be extended to the following m-th (*$m\geq 2$*) order ILC scheme,*

$$\mathbf{u}_{i+1}(t)=\sum_{j=1}^{m}\alpha_j\mathbf{u}_{i-j+1}(t)+\sum_{j=1}^{m}\beta_j\mathbf{e}^*_{i-j+1}(t+1),\ t\in\mathscr{I}_d, \tag{2.35}$$

where α_j and β_j are design parameters. Similarly as the proofs of Theorems 1 and 2, the convergence of the expectation of tracking error, $\mathbf{E}\{\mathbf{e}_i(t)\}$, can be derived by the contraction mapping method, and the learning convergence conditions are $\sum_{j=1}^{m}\alpha_j = 1$ and $\sum_{j=1}^{m}\gamma_j < 1$, where $\gamma_j \triangleq \sup_{t\in\mathscr{I}_d}\|\alpha_j \cdot I - \beta_j p(t)CB\|$. In (2.35), only the tracking information of the last m trials are adopted.

2.5 Illustrative Example

In order to show the effectiveness of the proposed ILC scheme, two examples are considered.

Example 1: Time-invariant system.

Consider the following discrete-time linear time-invariant system

$$\begin{aligned}\mathbf{x}_i(t+1) &= \begin{pmatrix} 0.50 & 0 & 1.00 \\ 0.15 & 0.30 & 0 \\ -0.75 & 0.25 & -0.25 \end{pmatrix}\mathbf{x}_i(t) + \begin{pmatrix} 0 \\ 0 \\ 1.00 \end{pmatrix}\mathbf{u}_i(t), \qquad (2.36)\\ y_i(t) &= \begin{pmatrix} 0 & 0 & 1.00 \end{pmatrix}\mathbf{x}_i(t),\end{aligned}$$

where $\mathbf{x}_i(0) = [0,0,0]^T, i \in \mathscr{N}$. Let the desired trajectory be $y_d(t) = \sin(2\pi t/50) + \sin(2\pi t/5) + \sin(50\pi t)$, $t \in \mathscr{I}_d \triangleq \{0,1,\ldots,50\}$, as shown in Fig. 2.3, and thus, $T_d = 50$. Without loss of generality, set $u_0(t) = 0$, $t \in \mathscr{I}_d$ in the first iteration. Moreover, assume that $N_1 = N_2 = 5$ and that T_i is a stochastic variable satisfying discrete uniform distribution. Then, $T_i \in \{45,46,\ldots,55\}$ and $P[T_i = \tau_m] = 1/11$, where $\tau_m = 45 + m$, $m \in \{0,1,\ldots,10\}$. Further, the learning gain is set as $L = 0.5$, which renders to $\sup_{t\in\mathscr{I}_d}\|I - p(t)LCB\| \approx 0.7273 < 1$. The performance of the maximal tracking error, $\|e_i\|_s \triangleq \sup_{t\in\mathscr{I}_d}\|e_i\|$, is presented in Fig. 2.4. It shows that the maximal tracking error $\|e_i\|_s$ decreases from 1.801 to 0.0098 within 42 iterations.

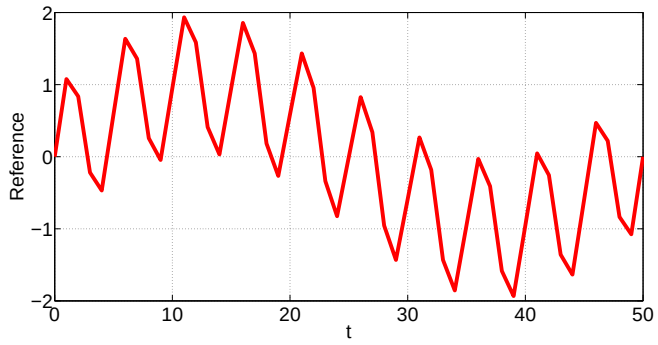

Figure 2.3: The reference y_d with desired trial length $T_d = 50$.

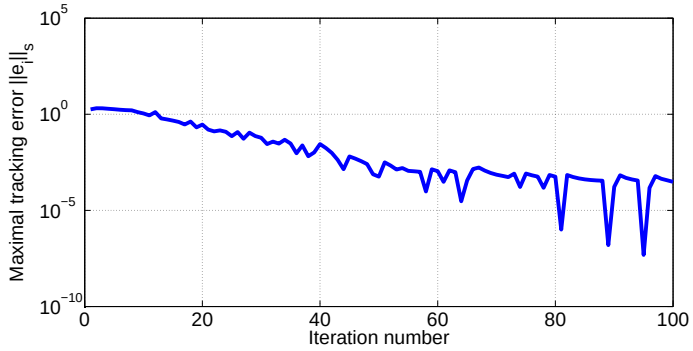

Figure 2.4: Maximal tracking error profile of ILC with non-uniform trial length: $N_1 = N_2 = 5$.

Moreover, Fig. 2.5 gives the tracking error profiles for 10th, 20th, 40th, 80th iterations, respectively. The ends of these trials are marked with the dots A, B, C and D, respectively.

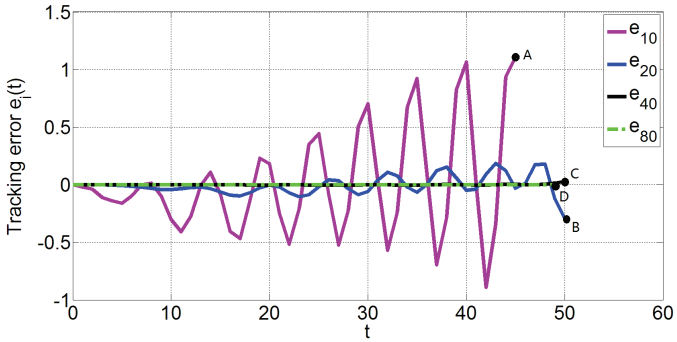

Figure 2.5: Tracking error profiles of ILC with non-uniform trial length: $N_1 = N_2 = 5$.

To demonstrate the effects of N_1 and N_2 on the convergence speed of the tracking error, the learning gain is fixed as $L = 0.5$, and it is assumed $N_1 = N_2 = 30$. Here $T_i \in \{20, 21, \ldots, 80\}$ and $P[T_i = \tau_m] = 1/61$, where $\tau_m = 20 + m$, $m \in \{0, 1, \ldots, 60\}$,

then it follows that $\sup_{t\in\mathscr{I}_d}\|I-p(t)LCB\|\approx 0.7417<1$. It can be seen from Fig. 2.6 that more than 60 iterations are needed to decrease the $\|e_i\|_s$ from 1.801 to 0.0097. The convergence speed is obviously slower than the case $N_1=N_2=5$.

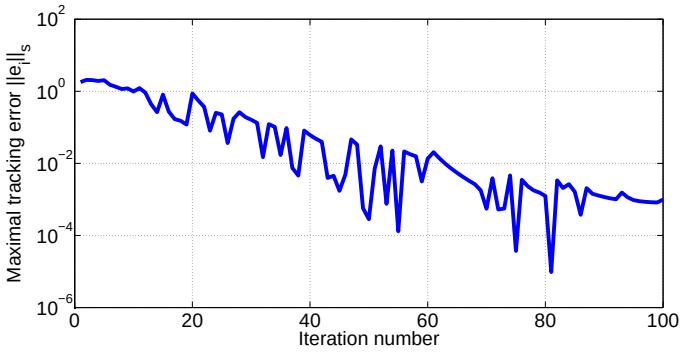

Figure 2.6: Maximal tracking error profile of ILC with non-uniform trial length: $N_1=N_2=30$.

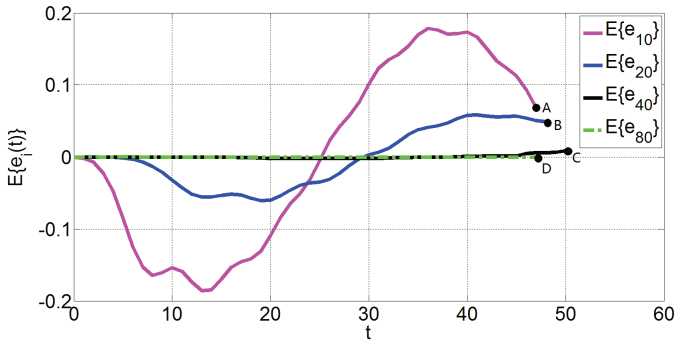

Figure 2.7: The expectation of tracking errors when the proposed ILC scheme is applied in (2.36).

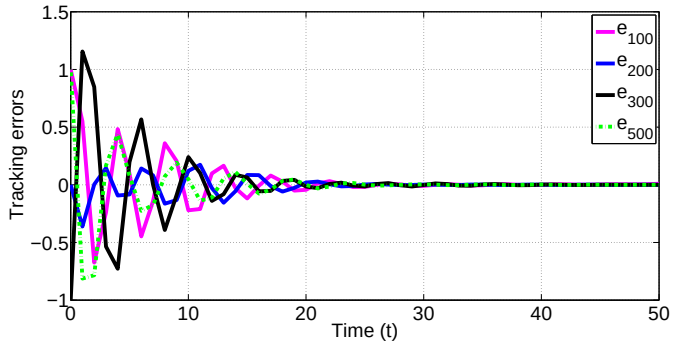

Figure 2.8: Tracking error profiles when the proposed ILC scheme is applied in (2.36).

To show the effectiveness of the proposed ILC scheme with randomly varying initial states, it is assumed that the learning gain $L=0.5$ and $N_1=N_2=5$. Assume $\mathbf{x}_i(0)$ is

a stochastic variable with probability $P[\mathbf{x}_i(0) = \mathbf{v}_1] = 1/3$, $P[\mathbf{x}_i(0) = \mathbf{v}_2] = 1/3$ and $P[\mathbf{x}_i(0) = \mathbf{v}_3] = 1/3$, where $\mathbf{v}_1 = [0,0,-1]^T$, $\mathbf{v}_2 = [0,0,0]^T$, $\mathbf{v}_3 = [0,0,1]^T$. Fig. 2.7 shows that the expectation of the tracking error $\mathbf{E}\{\mathbf{e}_i(t)\}$ will converge to zero within 80 iterations. The tracking error profiles of the proposed ILC scheme and the ILC scheme in [24] are illustrated in Fig. 2.8 and Fig. 2.9, respectively. It is obvious that the performance of the proposed ILC scheme is superior to that of the ILC scheme in [24] under the situation of randomly varying initial states. Similarly, in [25] and [61], the identical initialization condition is also indispensable.

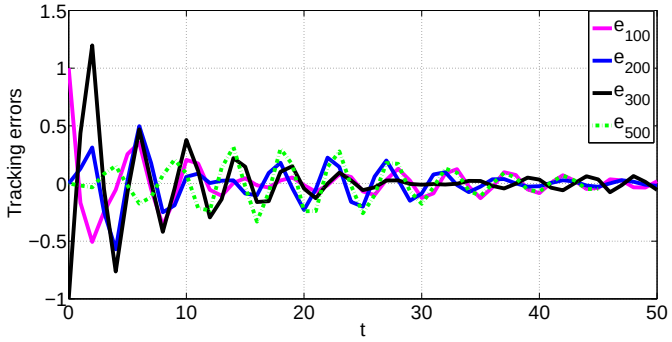

Figure 2.9: Tracking error profiles when the ILC scheme in [24] is applied in (2.36).

Example 2: Time-varying system.

In order to show effectiveness of our proposed ILC algorithm for time-varying systems, the following discrete-time linear time-varying system is considered

$$\begin{aligned} \mathbf{x}_i(t+1) &= \begin{pmatrix} 0.2e^{-t/100} & -0.6 & 0 \\ 0 & 0.5 & \sin(t) \\ 0 & 0 & 0.7 \end{pmatrix} \mathbf{x}_i(t) + \begin{pmatrix} 1.3 \\ 0.5 \\ 0.6 \end{pmatrix} \mathbf{u}_i(t), \quad (2.37) \\ y_i(t) &= \begin{pmatrix} -0.5 & 1.5 & 0 \end{pmatrix} \mathbf{x}_i(t), \end{aligned}$$

where $\mathbf{x}_i(0) = [0,0,0]^T, i \in \mathscr{N}$. Similarly as example 1, let the desired trajectory be $y_d(t) = \sin(2\pi t/50) + \sin(2\pi t/5) + \sin(50\pi t)$, $t \in \mathscr{I}_d = \{0,1,\ldots,50\}$. Set $u_0(t) = 0$, $t \in \mathscr{I}_d$ in the first iteration. Assume that $N_1 = N_2 = 5$ and T_i satisfies the binomial

distribution with $\mathbf{P}[T_i = \tau_m] = C_{11}^m p^m (1-p)^{11-m}$ and $p = 0.5$, where $\tau_m = 45 + m$, $m \in \{0, 1, \ldots, 10\}$. Set the learning gain as $L = 2$, then it follows that $\sup_{t \in \mathscr{I}_d} \|I - p(t)LCB\| = \|1 - 0.5 \cdot 0.2\| = 0.9 < 1$. The performance of the maximal tracking error $\|e_i\|_s$ is presented in Fig. 2.10, where $\|e_i\|_s$ decreases from 1.553 to 0.0058 within 80 iterations.

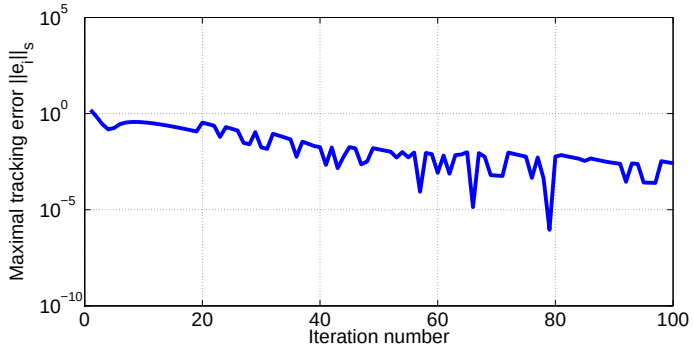

Figure 2.10: Maximal tracking error profile of ILC with non-uniform trial length: $N_1 = N_2 = 5$.

Remark 2.8 *When $\mathbf{x}_i(0)$ is a stochastic variable, the tracking error $\mathbf{e}_i(t)$ is also a stochastic variable, and satisfies the same probability distribution with $\mathbf{x}_i(0)$. If $\mathbf{x}_i(0)$ is fixed, $\mathbf{E}\{\mathbf{e}_i(t)\} = \mathbf{e}_i(t)$, and plotting $||\mathbf{e}_i||_s$ would be a rational and clear way to demonstrate the efficacy of the proposed ILC scheme.*

2.6 Conclusion

This chapter presents the ILC design and analysis results for discrete-time linear time-invariant or time-varying systems with non-uniform trial lengths. Due to the variation of the trial lengths, a modified ILC scheme is developed by applying an iteration-average operator. The learning condition of ILC that guarantees the convergence of tracking error in expectation is derived through rigorous analysis. The proposed ILC scheme mitigates the requirement on classic ILC that each trial must end in a fixed time of duration. In addition, the identical initialization condition might be removed.

Therefore, the proposed ILC scheme is applicable to more repetitive control processes. The formulation of ILC with non-uniform trial lengths is novel and could be extended to other control problems that are perturbed by random factors, for instance, control systems with random factors in communication channels. In the next chapter, how to extend the proposed ILC scheme to nonlinear control systems will be addressed.

Chapter 3

ILC for Continuous-time Nonlinear Systems with Randomly Varying Trial Lengths

3.1 Introduction

In Chapter 2, an ILC design problem for discrete-time linear systems with randomly varying trial lengths is addressed, where an ILC scheme based on the iteration-average operator is proposed. The novelty is that a stochastic variable satisfying the Bernouli distribution is introduced due to the stochastic property of trial lengths. Furthermore, a unified expression of ILC scheme for systems with different trial lengths is presented. Motivated by the ideas in Chapter 2, the ILC design problem for continuous-time nonlinear dynamical systems with randomly varying trial lengths will be addressed in this chapter.

The main contributions of this chapter can be summarized as: (i) A new formulation

is presented for continuous-time nonlinear dynamic systems with randomly varying trial lengths, where the trial lengths satisfy a continuous probability distribution; (ii) Different from Chapter 2 that considers linear systems, ILC for nonlinear affine and non-affine dynamic systems with non-uniform trial lengths is investigated; (iii) Instead of using the iteration-average operator that includes all the past tracking information as in Chapter 2, an iteratively-moving-average operator that incorporates the most recent few trials is introduced. With the ILC convergence, it is clear that, the latest trials could provide more accurate control information than those "older" trials.

This chapter is organized as follows. Section 3.2 formulates the ILC problems with randomly varying trial lengths. In Section 3.3, controller design and convergence analysis are presented. Further, the proposed ILC law is extended to nonlinear non-affine systems in Section 3.4. Section 3.5 gives two illustrative examples. Throughout this chapter, denote $\mathscr{N}$ the set of natural numbers, and I the identity matrix. Moreover, denote T_d the desired trial length, and $T_i,\ i \in \mathscr{N}$ the trial length of the ith iteration.

3.2 Problem Formulation

Consider a nonlinear dynamical system

$$\begin{cases} \dot{\mathbf{x}}_i(t) = \mathbf{f}(\mathbf{x}_i(t),t) + \mathbf{b}u_i(t), \\ y_i(t) = \mathbf{c}^T\mathbf{x}_i(t), \end{cases} \tag{3.1}$$

where $i \in \mathscr{N}$ and $t \in [0,T_i]$ denote the iteration index and time, respectively. Meanwhile, $\mathbf{x}_i(t) \in \mathbf{R}^n$, $u_i(t) \in \mathbf{R}$, and $y_i(t) \in \mathbf{R}$ denote state, input, and output of the system (3.1), respectively. $\mathbf{f}(\mathbf{x},t)$ is Lipschitz continuous with respect to $\mathbf{x}$, i.e., $\|\mathbf{f}(\mathbf{x}_1,t) - \mathbf{f}(\mathbf{x}_2,t)\| \leq f_0\|\mathbf{x}_1 - \mathbf{x}_2\|$. Further, $\mathbf{b} \in \mathbf{R}^n$ and $\mathbf{c} \in \mathbf{R}^n$ are constant vectors, and $\mathbf{c}^T\mathbf{b} \neq 0$. Let $y_d(t) \in \mathbf{R},\ t \in [0,T_d]$ be the desired output trajectory. Assume that, for any realizable output

trajectory $y_d(t)$, there exists a unique control input $u_d(t) \in \mathbf{R}$ such that

$$\begin{cases} \dot{\mathbf{x}}_d(t) = \mathbf{f}(\mathbf{x}_d(t), t) + \mathbf{b}u_d(t), \\ y_d(t) = \mathbf{c}^T \mathbf{x}_d(t), \end{cases} \tag{3.2}$$

where $u_d(t)$ is uniformly bounded for all $t \in [0, T_d]$. The main difficulty in designing ILC scheme for the system (3.1) is that the actual trial length T_i is iteration-varying and may be different from the desired trial length T_d.

Before addressing the ILC design problem with non-uniform trial lengths, let us give some notations and assumptions that would be useful in the derivation of our main result.

Definition 3.1 $\mathbf{E}\{\eta\}$ *stands for the expectation of the stochastic variable* η. $\mathbf{P}[\eta \leq t]$ *means the occurrence probability of the event* $\eta \leq t$ *with a given* t.

Assumption 3.1 *Assume that* T_i *is a stochastic variable and its probability distribution function is*

$$F_{T_i}(t) \triangleq \mathbf{P}[T_i \leq t] = \begin{cases} 0, & t \in [0, T_d - N_1), \\ p(t), & t \in [T_d - N_1, T_d + N_2], \\ 1, & t > T_d + N_2, \end{cases} \tag{3.3}$$

where $0 \leq p(t) \leq 1$ *is a known function, and* $0 \leq N_1 < T_d$ *and* $N_2 \geq 0$ *are two given constants.*

Assumption 3.2 $\mathbf{x}_i(0) = \mathbf{x}_d(0)$.

If the control process (3.1) repeats with the same trial length T_d, namely, $T_i = T_d$, and under the identical initial condition, a simple and effective ILC for system (3.1) is

$$u_{i+1}(t) = u_i(t) + L\dot{e}_i(t), \tag{3.4}$$

where $e_i(t) \triangleq y_d(t) - y_i(t)$ is the tracking error on the interval $[0, T_d]$, $\dot{e}_i(t)$ is the derivative of $e_i(t)$ on $[0, T_d]$, and $L \in \mathbf{R}$ is the learning gain. However, when the trial length T_i is iteration-varying, which corresponds to a non-standard ILC process, the learning control scheme (3.4) has to be re-designed.

3.3 ILC Design and Convergence Analysis

In this section, based on the assumptions and notations that are given in Section 3.2, ILC design and convergence analysis are addressed, respectively.

In practice, for one scenario that the ith trial ends before the desired trial length, namely, $T_i < T_d$, both the output $y_i(t)$ and the derivative of tracking error $\dot{e}_i(t)$ on the time interval $(T_i, T_d]$ are missing, which thus cannot be used for learning. For the other scenario that the ith trial is still running after the time instant we want it to stop, i.e., $T_i > T_d$, the signals $y_i(t)$ and $\dot{e}_i(t)$ after the time instant T_d are redundant and useless for learning. In order to cope with those missing signals or redundant signals in different scenarios, a sequence of stochastic variables satisfying Bernoulli distribution is defined. By using those stochastic variables, a newly defined tracking error $\dot{e}_i^*(t)$ is introduced to facilitate the modified ILC design.

The main procedure for deriving a modified ILC scheme can be described as follows:

(1) Define a stochastic variable $\gamma_i(t)$ at the ith iteration.

Let $\gamma_i(t)$, $t \in [0, T_d + N_2]$ be a stochastic variable satisfying Bernoulli distribution and taking binary values 0 and 1. The relationship $\gamma_i(t) = 1$ represents the event that the control process (3.1) can continue to the time instant t in the ith iteration, which occurs with a probability of $q(t)$, where $0 < q(t) \leq 1$ is a prespecified function of time t. The

relationship $\gamma_i(t) = 0$ denotes the event that the control process (3.1) cannot continue to the time instant t in the ith iteration, which occurs with a probability of $1 - q(t)$.

(2) Compute the probability $\mathbf{P}[\gamma_i(t) = 1]$.

Since the control process (3.1) will not stop within the time interval $[0, T_d - N_1)$, the event that $\gamma_i(t) = 1$ surely occurs when $t \in [0, T_d - N_1)$, which implies that $q(t) = 1$, $\forall t \in [0, T_d - N_1)$. While for the scenario of $t \in [T_d - N_1, T_d + N_2]$, the event $\gamma_i(t) = 1$ corresponds to the statement that the control process (3.1) stops at or after the time instant t, which means that $T_i \geq t$. Thus,

$$\begin{aligned} \mathbf{P}[\gamma_i(t) = 1] &= \mathbf{P}[T_i \geq t] \\ &= 1 - \mathbf{P}[T_i < t] \\ &= 1 - \mathbf{P}[T_i < t] - \mathbf{P}[T_i = t] \\ &= 1 - \mathbf{P}[T_i \leq t] = 1 - F_{T_i}(t), \end{aligned} \tag{3.5}$$

where $\mathbf{P}[T_i = t] = 0$ is applied. Thus, it follows that

$$q(t) = 1 - F_{T_i}(t) = \begin{cases} 1, & t \in [0, T_d - N_1), \\ 1 - p(t), & t \in [T_d - N_1, T_d + N_2], \\ 0, & t > T_d + N_2 \end{cases} \tag{3.6}$$

Since $\gamma_i(t)$ satisfies Bernoulli distribution, the expectation $\mathbf{E}\{\gamma_i(t)\} = 1 \cdot q(t) + 0 \cdot (1 - q(t)) = q(t)$.

(3) Define a modified tracking error.

Denote

$$e_i^*(t) \triangleq \gamma_i(t) e_i(t), \ \ t \in [0, T_d] \tag{3.7}$$

as a modified tracking error, and

$$\dot{e}_i^*(t) \triangleq \gamma_i(t) \dot{e}_i(t), \ \ t \in [0, T_d], \tag{3.8}$$

which renders to

$$\dot{e}_i^*(t) = \begin{cases} \dot{e}_i(t), & t \in [0, T_i], \\ 0, & t \in (T_i, T_d], \end{cases} \tag{3.9}$$

when $T_i < T_d$, and

$$\dot{e}_i^*(t) = \dot{e}_i(t), \ \ t \in [0, T_d], \tag{3.10}$$

when $T_i \geq T_d$.

(4) The ILC scheme.

Different from Chapter 2, an iteratively-moving-average operator is introduced,

$$\mathbf{A}\{f_i(\cdot)\} \triangleq \frac{1}{m+1} \sum_{j=0}^{m} f_{i-j}(\cdot), \tag{3.11}$$

for a sequence $f_{i-m}(\cdot), f_{i-m+1}(\cdot), \ldots, f_i(\cdot)$ with $m \geq 1$ being the size of the moving window, which includes only the last $m+1$ trials since the recent trials could provide more accurate control information for learning. The ILC scheme is given as follows,

$$u_{i+1}(t) = \mathbf{A}\{u_i(t)\} + \sum_{j=0}^{m} \beta_j \dot{e}_{i-j}^*(t), \ t \in [0, T_d], \tag{3.12}$$

for all $i \in \mathscr{N}$, where the learning gains $\beta_j \in \mathbf{R}$, $j = 0, 1, \ldots, m$, will be determined in the following and $u_{-1}(t) = u_{-2}(t) = \cdots = u_{-m}(t) = 0$.

The following theorem presents the first main result of this chapter.

Theorem 3.1 *For the nonlinear system (3.1) and the ILC scheme (3.12), choose the learning gains β_j, $j = 0, 1, 2, \ldots, m$, such that, for any constant $0 \leq \rho < 1$,*

$$\sum_{j=0}^{m} \eta_j \leq \rho, \tag{3.13}$$

where

$$\eta_j \triangleq \sup_{t \in [0, T_d]} \left\{ \left| \frac{1}{m+1} - \beta_j \mathbf{c}^T \mathbf{b} \right| q(t) + \frac{1 - q(t)}{m+1} \right\},$$

then the tracking error $e_i(t)$, $t \in [0, T_i]$, will converge to zero asymptotically as $i \to \infty$.

Remark 3.1 *In practice, the probability distribution of the trial length T_i could be estimated in advance based on previous multiple experiments or by experience. In consequence, the probability distribution function $F_{T_i}(t)$ in Assumption 3.1 is known. Thus, $q(t)$ is available for controller design and can be calculated by (3.6).*

Proof. Denote $\triangle u_i(t) \triangleq u_d(t) - u_i(t)$ and $\triangle \mathbf{x}_i(t) \triangleq \mathbf{x}_d(t) - \mathbf{x}_i(t)$ the input and state errors, respectively, then there has

$$\begin{aligned} \dot{e}_i(t) &= \dot{y}_d(t) - \dot{y}_i(t) \\ &= \mathbf{c}^T(\dot{\mathbf{x}}_d(t) - \dot{\mathbf{x}}_i(t)) \\ &= \mathbf{c}^T(\mathbf{f}(\mathbf{x}_d(t),t) - \mathbf{f}(\mathbf{x}_i(t),t)) + \mathbf{c}^T\mathbf{b}\triangle u_i(t). \end{aligned} \tag{3.14}$$

From (3.12), the following relationship can be obtained

$$\begin{aligned} \triangle u_{i+1}(t) &= \mathbf{A}\{\triangle u_i(t)\} - \sum_{j=0}^{m} \beta_j \dot{e}^*_{i-j}(t) \\ &= \mathbf{A}\{\triangle u_i(t)\} - \sum_{j=0}^{m} \beta_j \gamma_{i-j}(t) \dot{e}_{i-j}(t) \\ &= \mathbf{A}\{\triangle u_i(t)\} - \mathbf{c}^T\mathbf{b} \sum_{j=0}^{m} \gamma_{i-j}(t)\beta_j \triangle u_{i-j}(t) \\ &\quad -\mathbf{c}^T \sum_{j=0}^{m} \gamma_{i-j}(t)\beta_j[\mathbf{f}(\mathbf{x}_d,t) - \mathbf{f}(\mathbf{x}_{i-j},t)] \\ &= \sum_{j=0}^{m} \left[\frac{1}{m+1} - \gamma_{i-j}(t)\beta_j\mathbf{c}^T\mathbf{b}\right] \triangle u_{i-j}(t) \\ &\quad -\mathbf{c}^T \sum_{j=0}^{m} \gamma_{i-j}(t)\beta_j[\mathbf{f}(\mathbf{x}_d,t) - \mathbf{f}(\mathbf{x}_{i-j},t)]. \end{aligned} \tag{3.15}$$

Taking norm on both sides of (3.15) yields

$$|\triangle u_{i+1}(t)| \leq \sum_{j=0}^{m} \left|\frac{1}{m+1} - \gamma_{i-j}(t)\beta_j\mathbf{c}^T\mathbf{b}\right| |\triangle u_{i-j}(t)| + cf_0 \sum_{j=0}^{m} \gamma_{i-j}(t)|\beta_j|\|\triangle \mathbf{x}_{i-j}\|, \tag{3.16}$$

where $c \geq \|\mathbf{c}^T\|$. According to Assumption 3.2, system (3.1) can be rewritten as

$$\triangle \mathbf{x}_i(t) = \int_0^t [\mathbf{f}(\mathbf{x}_d(\tau),\tau) - \mathbf{f}(\mathbf{x}_i(\tau),\tau) + \mathbf{b}\triangle u_i(\tau)]d\tau, \tag{3.17}$$

then

$$\|\triangle \mathbf{x}_i(t)\| \leq f_0 \int_0^t \|\triangle \mathbf{x}_i(\tau)\| dt + b \int_0^t |\triangle u_i(\tau)| d\tau, \tag{3.18}$$

where $b \geq \|\mathbf{b}\|$. By applying Gronwall Lemma, it gives

$$\begin{aligned} \|\triangle \mathbf{x}_i(t)\| &\leq be^{f_0 t} \int_0^t |\triangle u_i(\tau)| d\tau \\ &\leq be^{f_0 t} \int_0^t e^{\lambda \tau} d\tau |\triangle u_i(t)|_\lambda \\ &= be^{f_0 t} \frac{e^{\lambda t} - 1}{\lambda} |\triangle u_i(t)|_\lambda . \end{aligned} \tag{3.19}$$

Substituting (3.19) into (3.16) implies that

$$\begin{aligned} |\triangle u_{i+1}(t)| &\leq \sum_{j=0}^{m} \left| \frac{1}{m+1} - \gamma_{i-j}(t) \beta_j \mathbf{c}^T \mathbf{b} \right| |\triangle u_{i-j}(t)| \\ &\quad + bcf_0 e^{f_0 t} \frac{e^{\lambda t} - 1}{\lambda} \sum_{j=0}^{m} \gamma_{i-j}(t) |\beta_j| |\triangle u_{i-j}(t)|_\lambda . \end{aligned} \tag{3.20}$$

Applying the expectation operator $\mathbf{E}$ on both sides of (3.20) and noting that $\gamma_i(t)$ is the only stochastic variable, which is independent of $\triangle u_i(t)$, imply

$$\begin{aligned} |\triangle u_{i+1}(t)| &\leq \sum_{j=0}^{m} \mathbf{E}\left\{ \left| \frac{1}{m+1} - \gamma_{i-j}(t) \beta_j \mathbf{c}^T \mathbf{b} \right| \right\} |\triangle u_{i-j}(t)| \\ &\quad + bcf_0 e^{f_0 t} \frac{e^{\lambda t} - 1}{\lambda} \sum_{j=0}^{m} \mathbf{E}\{\gamma_{i-j}(t)\} |\beta_j| |\triangle u_{i-j}(t)|_\lambda . \end{aligned} \tag{3.21}$$

According to the definition of mathematical expectation, it follows

$$\begin{aligned} \mathbf{E}\left\{ \left| \frac{1}{m+1} - \gamma_{i-j}(t) \beta_j \mathbf{c}^T \mathbf{b} \right| \right\} &= \left| \frac{1}{m+1} - 1 \cdot \beta_j \mathbf{c}^T \mathbf{b} \right| q(t) \\ &\quad + \left| \frac{1}{m+1} - 0 \cdot \beta_j \mathbf{c}^T \mathbf{b} \right| (1 - q(t)) \\ &= \left| \frac{1}{m+1} - \beta_j \mathbf{c}^T \mathbf{b} \right| q(t) + \frac{1 - q(t)}{m+1} \end{aligned} \tag{3.22}$$

and

$$\begin{aligned} |\triangle u_{i+1}(t)| &\leq \sum_{j=0}^{m} \left[\left| \frac{1}{m+1} - \beta_j \mathbf{c}^T \mathbf{b} \right| q(t) + \frac{1 - q(t)}{m+1} \right] |\triangle u_{i-j}(t)| \\ &\quad + bcf_0 q(t) e^{f_0 t} \frac{e^{\lambda t} - 1}{\lambda} \sum_{j=0}^{m} |\beta_j| |\triangle u_{i-j}(t)|_\lambda . \end{aligned} \tag{3.23}$$

From (3.23) and the definition of λ-norm, there has

$$\begin{aligned} |\triangle u_{i+1}|_\lambda &\leq \sum_{j=0}^{m} \sup_{t\in[0,T_d]} \left\{ \left| \frac{1}{m+1} - \beta_j \mathbf{c}^T \mathbf{b} \right| q(t) + \frac{1-q(t)}{m+1} \right\} |\triangle u_{i-j}|_\lambda \\ &\quad + bcf_0 e^{f_0 T_d} \frac{1-e^{-\lambda T_d}}{\lambda} \sum_{j=0}^{m} |\beta_j| |\triangle u_{i-j}|_\lambda . \end{aligned} \tag{3.24}$$

Define

$$\eta_j \triangleq \sup_{t\in[0,T_d]} \left\{ \left| \frac{1}{m+1} - \beta_j \mathbf{c}^T \mathbf{b} \right| q(t) + \frac{1-q(t)}{m+1} \right\} \tag{3.25}$$

and

$$\delta \triangleq bcf_0 e^{f_0 T_d} \frac{1-e^{-\lambda T_d}}{\lambda} \sum_{j=0}^{m} |\beta_j|. \tag{3.26}$$

Then (3.24) can be rewritten as

$$|\triangle u_{i+1}|_\lambda \leq (\sum_{j=0}^{m} \eta_j + \delta) \max\{|\triangle u_i|_\lambda, |\triangle u_{i-1}|_\lambda, \ldots, |\triangle u_{i-m+1}|_\lambda\}, \tag{3.27}$$

where $0 < q(t) \leq 1$ is applied. Since δ can be made sufficiently small with a sufficiently large λ and is independent of i, noting that $\sum_{j=0}^{m} \eta_j \leq \rho < 1$, it follows that $\sum_{j=0}^{m} \eta_j + \delta \leq \rho + \delta < 1$. That is, as i goes to infinity, it has $\triangle u_i \to 0$, namely, $u_i \to u_d$.

According to the convergence of $\triangle u_i$ and the inequality (3.19), it is obvious that

$$\lim_{i\to\infty} \|\triangle \mathbf{x}_i(t)\| = 0. \tag{3.28}$$

Since

$$|e_i(t)| = |\mathbf{c}^T \triangle \mathbf{x}_i(t)| \leq \|\mathbf{c}^T\| \|\triangle \mathbf{x}_i(t)\| \leq c\|\triangle \mathbf{x}_i(t)\|, \tag{3.29}$$

it follows that $\lim_{i\to\infty} e_i(t) = 0$. ■

Remark 3.2 *In Assumption 3.1, it is assumed that the probability distribution is known and the expectation of $q(t)$ can be calculated directly. While, if $p(t)$ is unknown, but*

its lower and upper bounds $0 \le \alpha_1 \le p(t) \le \alpha_2 < 1$ *for* $t \in [T_d - N_1, T_d]$ *are available, where* α_1, α_2 *are known constants, then according to (3.6), there has*

$$1-\alpha_2 \le q(t) \le 1-\alpha_1,\ t \in [T_d - N_1, T_d].$$

Based on the lower and upper bounds of $q(t)$ *and convergence condition (3.13), the learning gains can be selected as follows.*

One sufficient condition of (3.13) is $\eta_j \le \frac{\rho}{m+1}$, $j = 0,1,2,\ldots,m$. *Since*

$$\begin{aligned}
\eta_j &= \sup_{t\in[0,T_d]} \left\{ \left| \frac{1}{m+1} - \beta_j \mathbf{c}^T\mathbf{b} \right| q(t) + \frac{1-q(t)}{m+1} \right\} \\
&= \sup_{t\in[0,T_d]} \left\{ \left(\left| \frac{1}{m+1} - \beta_j \mathbf{c}^T\mathbf{b} \right| - \frac{1}{m+1} \right) q(t) \right\} + \frac{1}{m+1} \\
&= \left(\left| \frac{1}{m+1} - \beta_j \mathbf{c}^T\mathbf{b} \right| - \frac{1}{m+1} \right) (1-\alpha_2) + \frac{1}{m+1}, \qquad (3.30)
\end{aligned}$$

the inequality $\eta_j \le \frac{\rho}{m+1}$ *yields*

$$\frac{1-\rho}{(m+1)(1-\alpha_2)} \le \beta_j \mathbf{c}^T\mathbf{b} \le \frac{1+\rho-2\alpha_2}{(m+1)(1-\alpha_2)}, \qquad (3.31)$$

where $\rho \ge \alpha_2$ *is required. Without loss of generality, it is assumed that* $\mathbf{c}^T\mathbf{b} > 0$. *From (3.31), the learning gain* β_j *satisfies*

$$\frac{1-\rho}{(m+1)(1-\alpha_2)(\mathbf{c}^T\mathbf{b})} \le \beta_j \le \frac{1+\rho-2\alpha_2}{(m+1)(1-\alpha_2)(\mathbf{c}^T\mathbf{b})}. \qquad (3.32)$$

Further, if $\mathbf{c}^T\mathbf{b}$ *is unknown, but its lower and upper bounds are known, i.e.,* $\underline{b} \le \mathbf{c}^T\mathbf{b} \le \overline{b}$, *then from (3.31), it gives*

$$\frac{1-\rho}{(m+1)(1-\alpha_2)} \le \beta_j \underline{b} \le \beta_j \mathbf{c}^T\mathbf{b} \le \beta_j \overline{b} \le \frac{1+\rho-2\alpha_2}{(m+1)(1-\alpha_2)}. \qquad (3.33)$$

Therefore, β_j *should be selected as*

$$\frac{1-\rho}{(m+1)(1-\alpha_2)\underline{b}} \le \beta_j \le \frac{1+\rho-2\alpha_2}{(m+1)(1-\alpha_2)\overline{b}}. \qquad (3.34)$$

In such case, ρ *should satisfy that*

$$\rho \ge \frac{\overline{b} + 2\alpha_2\underline{b} - \underline{b}}{\overline{b} + \underline{b}},$$

where

$$\frac{\overline{b}+2\alpha_2\underline{b}-\underline{b}}{\overline{b}+\underline{b}} < \frac{\overline{b}+2\underline{b}-\underline{b}}{\overline{b}+\underline{b}} = \frac{\overline{b}+\underline{b}}{\overline{b}+\underline{b}} = 1.$$

Remark 3.3 *The selection of m in the controller (3.12) is dependent on length of the random interval for the trial length T_i. If the random interval is long, it implies that the trial length T_i varies drastically in the iteration domain. In such case, increasing m in some ways will improve the control performance since some of the missing information can be made up by the average operator. While if the random interval is short, which means that the trial length in each iteration changes slightly and is close to the desired trial length, it is better to choose a small m. When the randomness is low, a large m may adversely weaken the learning effect because the large averaging operation would reduce the corrective action from the most recent trials.*

3.4 Extension to Nonlinear Non-affine Systems

In this section, the proposed ILC scheme is extended to nonlinear non-affine systems

$$\begin{cases} \dot{\mathbf{x}}_i(t) = \mathbf{f}(\mathbf{x}_i(t), u_i(t), t), \\ y_i(t) = \mathbf{c}^T(t)\mathbf{x}_i(t), \end{cases} \tag{3.35}$$

where $\mathbf{f}(\mathbf{x}_i(t), u_i(t), t)$ has at least second derivatives with respect to $\mathbf{x} \in \mathbf{R}^n$, $u \in \mathbf{R}$ and t, and satisfies $\|\mathbf{f}(\mathbf{x}_1(t), u_1(t), t) - \mathbf{f}(\mathbf{x}_2(t), u_2(t), t)\| \leq f_0(\|\mathbf{x}_1(t) - \mathbf{x}_2(t)\| + |u_1(t) - u_2(t)|)$, $\mathbf{c}(t) \in \mathbf{R}^n$ is a bounded vector-valued function, and $\mathbf{c}^T(t)\mathbf{f}_u \neq 0$, $\mathbf{f}_u \triangleq \partial\mathbf{f}/\partial\mathbf{u}$. The result is summarized in the following theorem.

Theorem 3.2 *For the nonlinear non-affine system (3.35) and the ILC algorithm (3.12),*

choose the learning gains $\beta_j(t)$ such that, for any constant $0 \leq \rho < 1$,

$$\sum_{j=0}^{m} \eta_j \leq \rho, \tag{3.36}$$

where

$$\eta_j \triangleq \sup_{t\in[0,T_d]} \left\{ \left| \frac{1}{m+1} - \beta_j(t)\mathbf{c}^T(t)\mathbf{f}_u^{i-j} \right| q(t) + \frac{1-q(t)}{m+1} \right\}, \tag{3.37}$$

then the tracking error $e_i(t)$, $t \in [0,T_i]$, will converge to zero asymptotically as $i \to \infty$.

Proof. The proof can be performed similarly as in the proof of Theorem 1.

The error dynamics corresponding to (3.35) is

$$\begin{aligned} \dot{e}_i(t) &= \mathbf{c}^T(t)(\mathbf{f}(\mathbf{x}_d(t),u_d(t),t) - \mathbf{f}(\mathbf{x}_i(t),u_i(t),t)) \\ &= \mathbf{c}^T(t)\mathbf{f}_{\mathbf{x}}^i \triangle\mathbf{x}_i(t) + \mathbf{c}^T(t)\mathbf{f}_u^i \triangle u_i(t) \end{aligned} \tag{3.38}$$

where the mean value theorem is applied, and $\mathbf{f}_{\mathbf{x}}^i \triangleq \mathbf{f}_{\mathbf{x}}(\mathbf{x}_d + \theta\triangle\mathbf{x}_i, u_d(t) + \theta\triangle u_i(t))$, $\mathbf{f}_u^i \triangleq \mathbf{f}_u(\mathbf{x}_d + \theta\triangle\mathbf{x}_i, u_d(t) + \theta\triangle u_i(t))$ and $0 < \theta < 1$. Similar as (3.16), there has

$$\begin{aligned} |\triangle u_{i+1}(t)| \leq & \sum_{j=0}^{m} \left| \frac{1}{m+1} - \gamma_{i-j}(t)\beta_j(t)\mathbf{c}^T(t)\mathbf{f}_u^{i-j} \right| |\triangle u_{i-j}(t)| \\ & + cf_0 \sum_{j=0}^{m} \gamma_{i-j}(t)|\beta_j(t)|\|\triangle\mathbf{x}_{i-j}\| \end{aligned} \tag{3.39}$$

where $c \geq \sup_{t\in[0,T_d]} \|\mathbf{c}^T(t)\|$. Now, replacing (3.14) and (3.16) in the proof of Theorem 3.1 with (3.38) and (3.39), respectively, it obtains that the inequality (3.27) holds, where η_j is defined by (3.37) and

$$\delta \triangleq c(f_0)^2 e^{f_0 T_d} \frac{1-e^{-\lambda T_d}}{\lambda} \sum_{j=1}^{m} \sup_{t\in[0,T_d]} |\beta_j(t)|.$$

By choosing a sufficient large λ and noticing the condition (3.36), it follows that $\sum_{j=0}^{m} \eta_j + \delta \leq \rho + \delta < 1$. Hence $\lim_{i\to\infty} |\triangle u_i|_\lambda = 0$ can be obtained similarly, which implies that $\lim_{i\to\infty} e_i(t) = 0$. ■

3.5 Illustrative Example

To show the effectiveness of the proposed ILC scheme, both numerical example and application are considered.

Example 1: Numerical example.

Consider the following non-affine dynamical system

$$\begin{aligned} \dot{x}_i(t) &= f(x_i(t),u_i(t),t), \\ y_i(t) &= x_i(t), \end{aligned}$$

where $f(x_i(t),u_i(t),t) \triangleq 0.5\cos(x_i(t)) + u_i(t) + 0.5\sin(u_i(t))$, $x_i(0) = 0$, $i \in \mathscr{N}$. Let the desired trajectory be $y_d(t) = \sin(2\pi t) + \sin(2\pi t/5) + \sin(5\pi t)$, $t \in [0,2]$, and thus, $T_d = 2$. Without loss of generality, set $u_0(t) = 0$, $t \in [0,2]$ in the first iteration. Assume that T_i satisfies the Gaussian distribution with mean 2 and standard deviation 0.25. Further, set $m = 4$ and choose the learning gain as $\beta_0 = \beta_1 = \beta_2 = \beta_3 = \beta_4 = 1/5$, which renders to $\eta_0 = \eta_1 = \eta_2 = \eta_3 = \eta_4 = 3/20$ in this example, it follows that $\sum_{j=0}^{4} \eta_j = 3/4 < 1$. The performance of the maximal tracking error $\|e_i\|_s \triangleq \sup_{t \in \mathscr{I}_d} \|e_i\|$ is presented in Fig. 3.1, where $\|e_i\|_s$ decreases from 2.351 to 0.003035 within 20 iterations. Moreover, Fig. 3.2 gives the tracking error profiles for 1st, 4th, 10th, 16th iterations, respectively. The ends of these trials are marked with the dots A, B, C and D, respectively.

Fig. 3.3 shows the control performance of the proposed ILC law with different choices of m in the controller (3.12). We can see that for $m = 0,1,2,3,4$, the larger the value of m, the faster the convergence rate. While for $m = 5$, the control performance is degraded. This indicates that for the systems with non-uniform trial lengths, the introducing of the iteratively-moving-average operator will improve the control performance of ILC. However, the size of moving window m cannot be increased arbitrarily. A large m may adversely weaken the learning effect because the large averaging opera-

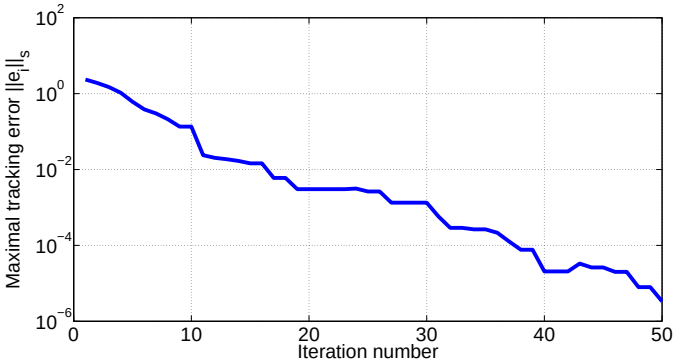

Figure 3.1: Maximal tracking error profile of ILC with trial length satisfying Gaussian distribution and m=4.

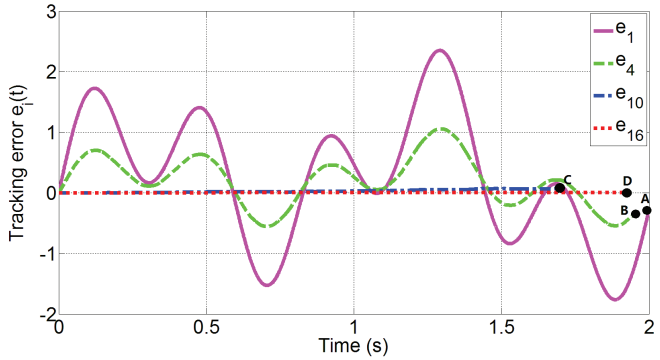

Figure 3.2: Tracking error profiles of ILC with trial length satisfying Gaussian distribution and m=4.

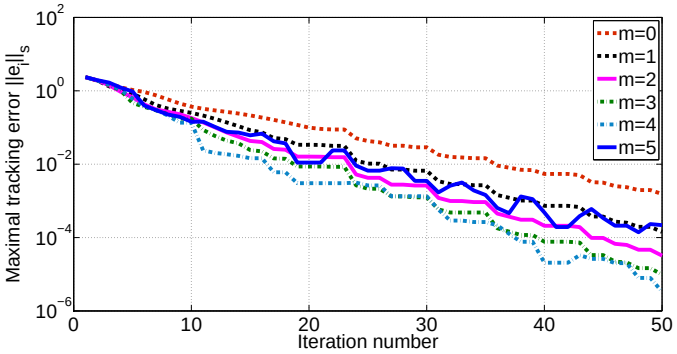

Figure 3.3: Maximal tracking error profiles of ILC with different choices of m.

tion would reduce the corrective action from the most recent trials.

Example 2: Application to robotic fish.

To show the applicability of the proposed ILC scheme, it is applied to the speed control of a two-link robotic fish. The mathematical model of the two-link robotic fish

in cruise motion is

$$\begin{cases} M\dot{v} = -\mu v^2 + F, \\ y = v \end{cases} \tag{3.40}$$

where M and v represent the mass and the velocity of the robotic fish, respectively, $\mu > 0$ is the water resistance coefficient, and F is the forward thrust generated by tail motion of the robotic fish. Dividing M on both sides of the first equation in (3.40), the system can be rewritten as

$$\begin{cases} \dot{v} = -\alpha v^2 + u, \\ y = v \end{cases} \tag{3.41}$$

where $\alpha \triangleq \mu/M > 0$ and by Least Square Method, its estimation value is $\alpha = 31.2485$. $u \triangleq F/M$ is viewed as the control input of the system. Because of the term $-\alpha v^2$, system (3.41) is local Lipschitz continuous. However, in real world the velocity of the robotic fish is bounded, namely, there exists a constant $\bar{v} > 0$ such that $|v| \leq \bar{v}$. As such, for any v_1, v_2, there has

$$\begin{aligned} |-\alpha v_1^2 - (-\alpha v_2^2)| &= \alpha |v_2^2 - v_1^2| \\ &= \alpha |v_2 + v_1||v_2 - v_1| \\ &\leq 2\alpha \bar{v} |v_2 - v_1|, \end{aligned} \tag{3.42}$$

which implies the global Lipschitz continuity of system (3.41) and the applicability of the proposed ILC scheme. Let the desired velocity trajectory be $v_d(t) = 48/50^5 t^2 (t - 50)^2$, $t \in [0, 50]$.

To improve the control performance, the following PD-type ILC is adopted

$$u_{i+1}(t) = \frac{1}{m+1} \sum_{j=0}^{m} u_{i-j}(t) + \left(\sum_{j=0}^{m} \beta_j \dot{e}_{i-j}^*(t) - L e_i^*(t) \right), \tag{3.43}$$

where $m = 2$, $\beta_0 = \beta_1 = \beta_2 = 1/3$, and $e_i^*(t) \triangleq \gamma_i(t) e_i(t)$. Based on the results in [66], the P-type learning gain L should be a negative value. Without loss of generality, set

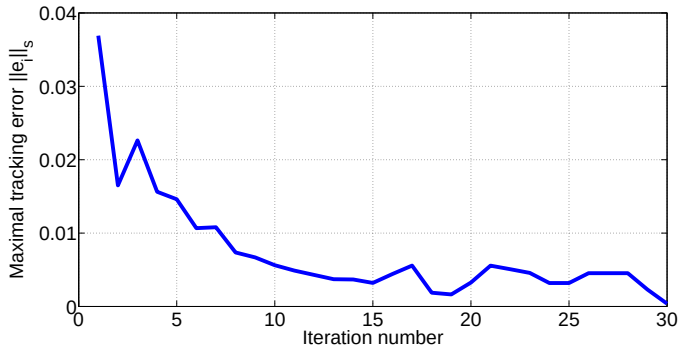

Figure 3.4: Maximal tracking error profile of ILC for speed control of robotic fish with $N_1 = 6$, $N_2 = 8$.

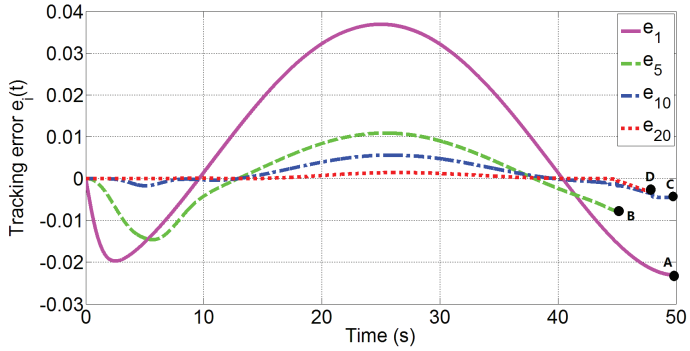

Figure 3.5: Tracking error profiles of ILC for speed control of robotic fish with $N_1 = 6$, $N_2 = 8$.

$L = -1$ and $u_0(t) = 0.05$, $t \in [0, 50]$. Moreover, due to the random disturbances in the external environment, the trial length T_i in each experiment is randomly varying. Based on multiple experiments and estimation, T_i approximately satisfies an uniform distribution $U(44, 58)$. Consequently, Fig. 3.4 presents the convergence of the maximal tracking error $\|e_i\|_s$, which shows that $\|e_i\|_s$ decreases more than 90 times within 30 iterations, and Fig. 3.5 gives the tracking error profiles for 1st, 5th, 10th, 20th iterations, respectively.

3.6 Conclusion

This chapter presents the ILC design and analysis results for nonlinear dynamic systems with non-uniform trial lengths. Due to the variation of the trial lengths, a modified

ILC scheme is developed by introducing an iteratively-moving-average operator. As such, the requirement on classic ILC that each trial must end in a fixed time of duration is mitigated. Moreover, the efficiency of the proposed ILC scheme is verified by both numerical example and practical application. The formulation of ILC with non-uniform trial lengths is novel and could be extended to other control problems that are perturbed by random factors, for instance, control systems with random factors in biomedical engineering.

Chapter 4

Adaptive ILC for Tracking Tasks with Different Magnitude and Time Scales

4.1 Introduction

In practice, a control system may implement different but highly correlated motion tasks. For instance, consider that a XY-table draws a number of circles in specified time periods [67]. There are three different kinds of operation specifications: 1) draw all the circles with the same radius but different periods; 2) draw all the circles with the same periods but different radii; 3) draw all the circles which differ one from another in both radii and periods. Obviously, those control signals are inherently correlated because: 1) they are generated by the same robotic dynamics and 2) each motion pattern is related (or proportional) to another either in spatial distribution or in time scale. Now, the control problem is whether a control system can learn consecutively from different but

highly correlated tracking tasks.

Different from Chapters 2 and 3 that randomly varying trial lengths are caused by external disturbance, this chapter considers ILC design for systems with non-uniform trial lengths which are aroused because of the variation of control tasks. In the existing literature, there are some works that have investigated learning control problems for iteration-varying control tasks. In [68], D-type, PD-type, and PID-type learning algorithms were presented for tracking trajectories "slowly" varying in the iteration domain. In that work, the difference between two consecutive iterations is assumed to be bounded by a small constant. Due to the presence of non-parametric system uncertainties, only a bounded tracking error is guaranteed if the target trajectory keeps changing in the iteration axis. In [67, 69–71], direct learning control and recursive direct learning control schemes were developed to make the use of previously obtained control information to generate control input for a new trajectory. However, a difficulty encountered in further expansion of these direct learning control schemes is the requirement for the perfect preceding control information and the open-loop control nature. In [72], the authors developed a new ILC method based on composite energy function, where the target trajectories of any two consecutive iterations can be different, but the dynamics must repeat in a fixed time interval. In a sense, it is a special case of control tasks in the same time scale but different magnitude scales. To the best of our knowledge, there are no works dealing with learning control problems for target trajectories that are different in both magnitude and time scales. For these kinds of non-repeatable learning control problems, in spite of the variations of the trajectory patterns, it should be noted that the underlying dynamic properties of the controlled system remain the same. We need to explore the inherent relations of different trajectory patterns and the learning scheme

could potentially be both plant-dependent and trajectory-dependent.

In this chapter, a new adaptive iterative learning control (AILC) scheme is designed by introducing a time-scaling factor to deal with control tasks with different magnitude and time scales. By adopting the time-scaling transformations, all the target trajectories are scaled into the same time scale, and the convergence of tracking errors for nonlinear systems with time-invariant and time-varying parametric uncertainties are proved based on Lyapunov theory. In this way, the learning control system is capable of fully utilizing all the learned knowledge to solve different but somehow correlated control problems. The main contribution of this chapter is to show that the limitations of traditional ILC, that the target trajectory must be identical in iteration domain and every trial must repeat in a fixed time duration, can be removed.

The chapter is organized as follows. In Section 4.2, learning control problem is formulated. In Section 4.3, the controller design and convergence analysis are presented. Further, the proposed AILC law is extended to nonlinear systems with time-varying parametric uncertainties in Section 4.4. Lastly, Section 4.5 gives two illustrative examples. Throughout this chapter, for a given vector $\mathbf{x} = [x_1, x_2, \ldots, x_n] \in \mathbf{R}^n$, $\|\mathbf{x}\|$ denotes the vector norm. For any matrix $A \in \mathbf{R}^{n\times n}$, $\|A\|$ is the induced matrix norm. For any function $\mathbf{h}(t), t \in [0,T]$, $\|\mathbf{h}(t)\|_{L^2} \triangleq \int_0^T \|\mathbf{h}(s)\|^2 ds$ represents the L^2-norm of $\mathbf{h}(t)$.

4.2 Problem Formulation

Consider the following nonlinear dynamic system

$$\frac{d\mathbf{x}}{dt} = \Theta\mathbf{f}(\mathbf{x}) + B(\mathbf{x},t)\mathbf{v}(t), \tag{4.1}$$

where $\mathbf{x} \in \mathbf{R}^m$ is the physically measurable state vector; $\mathbf{v} \in \mathbf{R}^m$ is the control input; $\Theta = \text{diag}(\theta_1^T, \theta_2^T, \ldots, \theta_m^T) \in \mathbf{R}^{m \times n}$ is an unknown constant parametric matrix,

$$\theta_j = [\theta_{j,1}, \theta_{j,2}, \ldots, \theta_{j,q_j}]^T \in \mathbf{R}^{q_j},\ j = 1,2,\ldots,m,\ \sum_{j=1}^{m} q_j = n, q_j \in \mathbf{Z}^+;$$

$\mathbf{f}(\mathbf{x}) = [f_1(\mathbf{x}), \ldots, f_n(\mathbf{x})]^T \in \mathbf{R}^n$ is a known vector valued function; $B(\mathbf{x},t) \in \mathbf{R}^{m \times m}$ is a known control input distribution matrix, which is invertible.

The target trajectory at the ith iteration is denoted as $\mathbf{x}_i^r(t_i) \in \mathbf{R}^m$, $t_i \in [0, T_i]$, that could be different from iteration to iteration, where t_i is the time scale and T_i is the trial length of ith iteration. Throughout this chapter, we assume that the given trajectories $\mathbf{x}_i^r(t_i)$ are at least continuously differentiable with respect to the time t_i.

Before addressing the non-repeatable learning control problem, let us provide some notations and definitions that would be useful in the derivation of our main result.

Definition 4.1 *[67] Trajectory $\mathbf{x}_i(t_i)$, $t_i \in [0, T_i]$ is said to be proportional to another trajectory $\mathbf{x}(t)$, $t \in [0, T]$ both in magnitude and time scales if and only if*

$$K_i^{-1}(t_i)\mathbf{x}_i(t_i) = \mathbf{x}(t)$$

where $K_i^{-1}(t_i)$ is the inverse matrix of the time-varying magnitude scaling factor $K_i(t_i) \triangleq diag(\kappa_{i,1}(t_i), \ldots, \kappa_{i,m}(t_i)) \in \mathbf{R}^{m \times m}$, and $\rho_i(t) = t_i$ is the time scaling factor, which is continuously differentiable and satisfies $\rho_i(0) = 0$ and $\rho_i(T) = T_i$.

Remark 4.1 *The definition "proportional both in magnitude and time scales" describes quite general inherent relations among different trajectories and includes the following one as a special case. When $\rho_i(t) = t$, from Definition 4.1, we have $\mathbf{x}(t) = K_i^{-1}(t_i)\mathbf{x}_i(t_i) = K_i^{-1}(\rho_i(t))\mathbf{x}_i(\rho_i(t)) = K_i^{-1}(t)\mathbf{x}_i(t)$, i.e., $\mathbf{x}_i(t) = K_i(t)\mathbf{x}(t)$, which means that the trajectory $\mathbf{x}_i(t_i)$ and $\mathbf{x}(t)$ are proportional in magnitude while the time scale are the same. For this case, it can be considered as a special case of the problem addressed in [72].*

Assumption 4.1 *$d\rho_i(t)/dt > 0$ and the inverse function $\rho_i^{-1}(t_i)$ of $\rho_i(t)$ exists and is known. The magnitude scaling matrix $K_i(t_i)$ is continuously differentiable.*

Remark 4.2 *$d\rho_i(t)/dt > 0$ implies that $\rho_i(t)$ is a monotonically increasing function with respect to the time t. The conditions $\rho_i(0) = 0$ and $\rho_i(T) = T_i$ are satisfied for this kind of monotonically increasing function.*

Assume that $\mathbf{x}_i^r(t_i)$, $i = 1,2,3,\ldots$ are proportional to a trajectory $\mathbf{x}^r(t)$, $t \in [0,T]$. According to the Definition 4.1, there has $K_i^{-1}(t_i)\mathbf{x}_i^r(t_i) = \mathbf{x}^r(t)$. Premultiply $K_i(t_i)$ on both sides, we can obtain $\mathbf{x}_i^r(t_i) = K_i(t_i)\mathbf{x}^r(t) = K_i(\rho_i(t))\mathbf{x}^r(t)$. Denote $\mathbf{x}_i^d(t) = K_i(\rho_i(t))\mathbf{x}^r(t)$, $i = 1,2,3,\ldots$, it shows that $\mathbf{x}_i^r(t_i) = \mathbf{x}_i^d(t)$, $i = 1,2,3,\ldots$.

Since the time scale at the ith iteration is $t_i \in [0,T_i]$, the dynamics at the ith iteration is

$$\frac{d\mathbf{x}_i}{dt_i} = \Theta\mathbf{f}(\mathbf{x}_i) + B(\mathbf{x}_i,t_i)\mathbf{v}_i(t_i), \quad t_i \in [0,T_i]. \tag{4.2}$$

By applying a time-scaling transformation $dt_i = \dot{\rho}_i(t)dt$, system (4.2) can be rewritten as

$$\begin{aligned}
\frac{d\mathbf{x}_i}{dt} &= \frac{d\mathbf{x}_i}{dt_i}\cdot\frac{dt_i}{dt} \\
&= (\Theta\mathbf{f}(\mathbf{x}_i) + B(\mathbf{x}_i,t_i)\mathbf{v}_i(t_i))\cdot\frac{dt_i}{dt} \\
&= (\Theta\mathbf{f}(\mathbf{x}_i) + B(\mathbf{x}_i,t_i)\mathbf{v}_i(t_i))\cdot\frac{d\rho_i(t)}{dt} \\
&= \dot{\rho}_i(t)\Theta\mathbf{f}(\mathbf{x}_i) + \dot{\rho}_i(t)B(\mathbf{x}_i,\rho_i(t))\mathbf{u}_i(t),
\end{aligned} \tag{4.3}$$

where $t \in [0,T]$ and $\mathbf{u}_i(t) \triangleq \mathbf{v}_i(\rho_i(t))$.

Denote $\mathbf{x}_i(t)$, $t \in [0,T]$ the solution of system (4.3) and $\mathbf{e}_i(t) \triangleq \mathbf{x}_i(t) - \mathbf{x}_i^d(t)$, $t \in [0,T]$ the tracking error. The error dynamics at the ith iteration is

$$\begin{aligned}
\frac{d\mathbf{e}_i(t)}{dt} &= \frac{d\mathbf{x}_i(t)}{dt} - \frac{d\mathbf{x}_i^d(t)}{dt} \\
&= \dot{\rho}_i(t)\Theta\mathbf{f}(\mathbf{x}_i) + \dot{\rho}_i(t)B(\mathbf{x}_i,\rho_i(t))\mathbf{u}_i(t) - \dot{\mathbf{x}}_i^d(t).
\end{aligned} \tag{4.4}$$

The control objective is to tune $\mathbf{u}_i(t)$ such that the tracking error $\mathbf{e}_i(t)$ converges to zero as the iteration number $i \to \infty$.

As is common in ILC field, the following assumption is made.

Assumption 4.2 *Initial error satisfies the identical initialization condition* $\mathbf{e}_i(0) = 0$*,* $\forall i \in \mathbf{Z}^+$.

4.3 AILC Design and Convergence Analysis

In this section, based on the assumptions and notations that were given in Section 4.2, AILC law design and convergence analysis are addressed, respectively.

The proposed controller is

$$\mathbf{u}_i(t) = B_i^{-1}(t)(-\Gamma \mathbf{e}_i(t) + \dot{\mathbf{x}}_i^d(t)/\dot{\rho}_i(t) - \hat{\Theta}_i(t)\mathbf{f}(\mathbf{x}_i)),\ t \in [0,T] \tag{4.5}$$

with the updating law

$$\begin{aligned} \hat{\Theta}_i(t) &= \hat{\Theta}_{i-1}(t) + \dot{\rho}_i(t)\mathbf{e}_i(t)\mathbf{f}^T(\mathbf{x}_i), \\ \hat{\Theta}_0(t) &= 0,\ t \in [0,T], \end{aligned} \tag{4.6}$$

where $\Gamma = \mathrm{diag}(\gamma_1, \ldots, \gamma_m)$ is the feedback gain, $\gamma_j > 0,\ j = 1,2,\ldots,m$, $\hat{\Theta}_i(t)$ is the estimation of Θ at the ith iteration and $B_i^{-1}(t)$ is the matrix such that $B(\mathbf{x}_i, \rho_i(t))B_i^{-1}(t) = I_{m\times m}$. Then, our main result is presented in the following theorem.

Theorem 4.1 *For the nonlinear system (4.3), under the Assumption 4.2, the AILC scheme (4.5) with (4.6) guarantees that the tracking error converges to zero pointwisely over* $[0,T]$*, i.e.,* $\lim_{i\to\infty} \mathbf{e}_i(t) = 0,\ \ \forall t \in [0,T]$*, which leads to* $\mathbf{x}_i(t_i) \to \mathbf{x}_i^r(t_i),\ \ as\ \ i \to \infty$*, where* $\mathbf{x}_i(t_i)$ *is solutions of system (4.2).*

Proof. See *Appendix A.2.* ■

Remark 4.3 *ILC design in Chapters 2 and 3 is based on the contraction mapping (CM) method. A limitation of CM-based ILC is that it is only applicable to systems with global Lipschitz continuous nonlinear factors. As a complementary part of CM-based ILC, adaptive ILC is developed to handle broader classes of system nonlinearities, such as local Lipschitz continuous ones, and system uncertainties, such as time-varying parametric and non-parametric uncertainties.*

Remark 4.4 *The key idea in this chapter to deal with the iteration-varying trial lengths is to map the iteration-varying time intervals to a fixed time interval by a class of time-scaling maps, and then analyze the convergence of tracking error on the fixed time scale* $t \in [0,T]$. *After that by making the inverse transformation, the convergence of tracking error on the iteration-varying time scale* $t_i \in [0,T_i]$ *can be obtained. The last part of Theorem 4.1 shows that the convergence on the fixed time scale implies the convergence on the iteration-varying time scales.*

Remark 4.5 *From (4.5) and* $\mathbf{v}_i(t_i) = \mathbf{v}_i(\rho_i(t)) = \mathbf{u}_i(t)$, *the control input at the ith iteration is*

$$\begin{aligned}\mathbf{v}_i(t_i) &= \mathbf{u}_i(\rho_i^{-1}(t_i)) \\ &= B_i^{-1}(\rho_i^{-1}(t_i))\{-\Gamma\mathbf{e}_i(\rho_i^{-1}(t_i)) + \frac{d\mathbf{x}_i^r(t_i)}{dt_i} - \hat{\Theta}_i^T(\rho_i^{-1}(t_i))\mathbf{f}(\mathbf{x}_i(\rho_i^{-1}(t_i)))\}.\end{aligned}$$

4.4 Extension to Systems with Time-varying Parameter

In this section, the proposed AILC scheme is extended to nonlinear systems with time-varying parameter

$$\frac{d\mathbf{x}}{dt} = \Theta(t)\mathbf{f}(\mathbf{x}) + B(\mathbf{x},t)\mathbf{v}(t),\ t \in [0,T], \tag{4.7}$$

where $\mathbf{x} \in \mathbf{R}^m$ is the physically measurable state vector; $\mathbf{v} \in \mathbf{R}^m$ is the control input; $\Theta(t) = \text{diag}(\theta_1^T(t), \theta_2^T(t), \ldots, \theta_m^T(t)) \in \mathbf{R}^{m\times n}$ is the unknown time-varying parameter matrix, $\theta_j(t) = [\theta_{j,1}(t), \theta_{j,2}(t), \ldots, \theta_{j,q_j}(t)]^T \in \mathbf{R}^{q_j}$, $j = 1,2,\ldots,m$, $\sum_{j=1}^m q_j = n$, $q_j \in \mathbf{Z}^+$; $\mathbf{f}(\mathbf{x}) = [f_1(\mathbf{x}), f_2(\mathbf{x}), \ldots, f_n(\mathbf{x})]^T \in \mathbf{R}^n$ is a known vector-valued function; and $B(\mathbf{x},t) \in \mathbf{R}^{m\times m}$ is a known invertible input distribution matrix. In addition, there exists a known continuous function $g(\mathbf{x}) > 0$ such that $\|\mathbf{f}(\mathbf{x})\| \leq g(\mathbf{x})$.

The dynamics at the ith iteration is

$$\frac{d\mathbf{x}_i}{dt_i} = \Theta(t_i)\mathbf{f}(\mathbf{x}) + B(\mathbf{x}_i, t_i)\mathbf{v}_i(t_i),\ t_i \in [0, T_i], \tag{4.8}$$

It is worth noting that if we apply the time-scaling transformation $dt_i = \dot{\rho}_i(t)dt$ directly to the system (4.8), the system can be rewritten as

$$\frac{d\mathbf{x}_i}{dt} = \dot{\rho}_i(t)\zeta_i(t)\mathbf{f}(\mathbf{x}_i) + \dot{\rho}_i(t)B(\mathbf{x}_i, \rho_i(t))\mathbf{u}_i(t),\ t \in [0, T], \tag{4.9}$$

where $\mathbf{u}_i(t) \triangleq \mathbf{v}_i(\rho_i(t))$ and $\zeta_i(t) \triangleq \Theta(\rho_i(t))$ is iteration-time-varying. To solve the learning problem for system (4.9) with iteration-time-varying uncertainties $\zeta_i(t)$, we present the following assumption firstly.

Assumption 4.3 *Assume that the time-varying parameters $\theta_{j,k}(t)$, $j = 1,2,\ldots,m$, $k = 1,2,\ldots,q_j$, are smooth and can be approximated as:*

$$\theta_{j,k}(t) = \Pi_{j,k}^T(t)\eta_{j,k} + \varepsilon_{j,k}(t)$$

in a sufficiently large interval $[0, \overline{T}]$, where $\overline{T} \geq \max_{i\geq 1}\{T, T_i\}$, $\Pi_{j,k}(t) \in \mathbf{R}^{h_{j,k}}$, $h_{j,k} \in \mathbf{Z}^+$, is a known vector-valued function, which is an orthonormal basis, $\eta_{j,k} \in \mathbf{R}^{h_{j,k}}$ is the unknown constant coefficient and $\varepsilon_{j,k}(t)$ is the approximation error.

Due to the boundedness of $\theta_{j,k}(t)$ for $t \in [0, \overline{T}]$, there exists a constant $\overline{\lambda}_{j,k} > 0$ such

that $|\varepsilon_{j,k}(t)| \leq \overline{\lambda}_{j,k}$, $t \in [0, \overline{T}]$. Let

$$\begin{aligned}
\Pi_j(t) &= \text{diag}(\Pi_{j,1}(t), \Pi_{j,2}(t), \ldots, \Pi_{j,q_j}(t)) \in \mathbf{R}^{(\Sigma_{k=1}^{q_j} h_{j,k}) \times q_j}, \\
\eta_j &= [\eta_{j,1}^T, \eta_{j,2}^T, \ldots, \eta_{j,q_j}^T]^T \in \mathbf{R}^{\Sigma_{k=1}^{q_j} h_{j,k}}, \\
\varepsilon_j(t) &= [\varepsilon_{j,1}(t), \varepsilon_{j,2}(t), \ldots, \varepsilon_{j,q_j}(t)]^T \in \mathbf{R}^{q_j},
\end{aligned}$$

then we have

$$\theta_j(t) = \Pi_j^T(t)\eta_j + \varepsilon_j(t), \ j = 1, 2, \ldots, m.$$

It is obvious that $\Theta(t)$ can be rewritten in the matrix form

$$\Theta(t) = \eta^T \Pi(t) + \varepsilon(t), \tag{4.10}$$

where

$$\begin{aligned}
\Pi(t) &= \text{diag}(\Pi_1(t), \Pi_2(t), \ldots, \Pi_m(t)) \in \mathbf{R}^{(\Sigma_{j=1}^{m} \Sigma_{k=1}^{q_j} h_{j,k}) \times n}, \\
\eta &= \text{diag}(\eta_1, \eta_2, \ldots, \eta_m) \in \mathbf{R}^{(\Sigma_{j=1}^{m} \Sigma_{k=1}^{q_j} h_{j,k}) \times m}, \\
\varepsilon(t) &= \text{diag}(\varepsilon_1^T(t), \varepsilon_2^T(t), \ldots, \varepsilon_m^T(t)) \in \mathbf{R}^{m \times n},
\end{aligned}$$

Further, according to $|\varepsilon_{j,k}(t)| \leq \overline{\lambda}_{j,k}$, $t \in [0, \overline{T}]$, there exists a constant $\lambda > 0$ such that $\|\varepsilon(t)\| \leq \lambda$ for $t \in [0, \overline{T}]$.

From (4.10), we have

$$\Theta(t_i) = \eta^T \Pi(t_i) + \varepsilon(t_i), \ t_i \in [0, T_i]. \tag{4.11}$$

Substituting (4.11) into the system (4.8) yields

$$\frac{d\mathbf{x}_i}{dt_i} = \eta^T \Pi(t_i)\mathbf{f}(\mathbf{x}_i) + \varepsilon(t_i)\mathbf{f}(\mathbf{x}_i) + B(\mathbf{x}_i, t_i)\mathbf{v}_i(t_i). \tag{4.12}$$

Similarly as the previous case with time-invariant parameters, apply the time-scaling transformation $dt_i = \dot{\rho}_i(t)dt$, $t \in [0, T]$ to system (4.12), we can obtain

$$\frac{d\mathbf{x}_i}{dt} = \dot{\rho}_i(t)\eta^T \Xi_i(t)\mathbf{f}(\mathbf{x}_i) + \dot{\rho}_i(t)\xi_i(t)\mathbf{f}(\mathbf{x}_i) + \dot{\rho}_i(t)B(\mathbf{x}, \rho_i(t))\mathbf{u}_i(t), \tag{4.13}$$

where $\Xi_i(t) \triangleq \Pi(\rho_i(t))$, $\xi_i(t) \triangleq \varepsilon(\rho_i(t))$ and $\mathbf{u}_i(t) = \mathbf{v}_i(\rho_i(t))$. Since $\|\varepsilon(t)\| \leq \lambda$ for $t \in [0, \overline{T}]$ and $\|\mathbf{f}(\mathbf{x})\| \leq g(\mathbf{x})$, we have

$$\|\varepsilon(t)\mathbf{f}(\mathbf{x})\| \leq \lambda g(\mathbf{x}), t \in [0, \overline{T}].$$

Further, according to $[0, T_i] \subseteq [0, \overline{T}]$, it is obvious that

$$\|\xi_i(t)\mathbf{f}(\mathbf{x}_i)\| = \|\varepsilon(\rho_i(t))\mathbf{f}(\mathbf{x}_i)\| = \|\varepsilon(t_i)\mathbf{f}(\mathbf{x}_i)\| \leq \lambda g(\mathbf{x}_i). \tag{4.14}$$

Denote $\hat{\eta}_i(t)$ and $\hat{\lambda}_i(t)$ the estimation of η and λ at the ith iteration, respectively. The new AILC law is proposed as

$$\mathbf{u}_i(t) = B_i^{-1}(t)(-\Gamma\mathbf{e}_i(t) + \dot{\mathbf{x}}_i^d(t)/\dot{\rho}_i(t) - \hat{\eta}_i^T(t)\Xi_i(t)\mathbf{f}(\mathbf{x}_i) - \hat{\lambda}_i(t)g(\mathbf{x}_i)\mathrm{sgn}(\mathbf{e}_i(t))), \tag{4.15}$$

where $\Gamma = \mathrm{diag}(\gamma_1, \ldots, \gamma_m)$ is the feedback gain, $\gamma_j > 0$, $j = 1, 2, \ldots, m$; $B_i^{-1}(t)$ is the matrix such that $B(\mathbf{x}_i, \rho_i(t))B_i^{-1}(t) = I_{m\times m}$; and $\mathrm{sgn}(\mathbf{e}_i(t)) \triangleq [\mathrm{sgn}(e_{i,1}(t)), \ldots, \mathrm{sgn}(e_{i,m}(t))]^T$. The updating laws for $\hat{\eta}_i(t)$ and $\hat{\lambda}_i(t)$ are

$$\begin{aligned} \hat{\eta}_i(t) &= \hat{\eta}_{i-1}(t) + \dot{\rho}_i(t)\Xi_i(t)\mathbf{f}(\mathbf{x}_i)\mathbf{e}_i^T(t), \\ \hat{\eta}_0(t) &= 0,\ t \in [0, T], \end{aligned} \tag{4.16}$$

and

$$\begin{aligned} \hat{\lambda}_i(t) &= \hat{\lambda}_{i-1}(t) + \dot{\rho}_i(t)g(\mathbf{x}_i)\sum_{j=1}^{m}|e_{i,j}(t)|, \\ \hat{\lambda}_0(t) &= 0,\ t \in [0, T], \end{aligned} \tag{4.17}$$

respectively.

The convergence property of the proposed learning controller is derived in the following theorem.

Theorem 4.2 *For the nonlinear system (4.13), under the Assumptions 4.2, 4.3, the AILC scheme (4.15) with (4.16) and (4.17) guarantees that the tracking error con-*

verges to zero pointwisely over $[0,T]$*, i.e.,* $\lim_{i\to\infty}\mathbf{e}_i(t)=0,\ \ \forall t\in[0,T]$*, which implies* $\mathbf{x}_i(t_i)\to\mathbf{x}_i^r(t_i),\ \ as\ \ i\to\infty$*, where* $\mathbf{x}_i(t_i)$ *is solutions of system (4.8).*

Proof. See *Appendix A.3.* ■

In general, the discontinuous control scheme (4.15) should be avoided, since it causes not only the problem of existence and uniqueness of solutions ([73, 74]), but also chattering ([75]) that may excite high-frequency unmodeled dynamics ([76]). This motivates us to seek an appropriate smooth approximation of (4.15) that can guarantee the boundedness of the parameter estimations $\hat{\eta}_i(t)$ and $\hat{\lambda}_i(t)$, as well as the convergence of $\mathbf{e}_i(t)$ to a reasonably small neighborhood of the origin.

Let $\overline{\varepsilon}>0$ be a constant and consider the following smooth learning scheme

$$\mathbf{u}_i(t)=B_i^{-1}(t)(-K\mathbf{e}_i(t)+\dot{\mathbf{x}}_i^d(t)/\dot{\rho}_i(t)-\hat{\eta}_i^T(t)\Xi_i(t)\mathbf{f}(\mathbf{x}_i)-\hat{\lambda}_i(t)\omega(\mathbf{x}_i,\mathbf{e}_i)), \tag{4.18}$$

with the updating laws

$$\begin{aligned}\hat{\eta}_i(t) &= \hat{\eta}_{i-1}(t)+\dot{\rho}_i(t)\Xi_i(t)\mathbf{f}(x_i)\mathbf{e}_i^T(t)-\mu_1\hat{\eta}_i(t), \\ \hat{\eta}_0(t) &= 0,\ t\in[0,T],\end{aligned} \tag{4.19}$$

and

$$\begin{aligned}\hat{\lambda}_i(t) &= \hat{\lambda}_{i-1}(t)+\dot{\rho}_i(t)\mathbf{e}_i^T(t)\omega(\mathbf{x}_i,\mathbf{e}_i)-\mu_2\hat{\lambda}_i(t), \\ \hat{\lambda}_0(t) &= 0,\ t\in[0,T],\end{aligned} \tag{4.20}$$

where

$$\omega(\mathbf{x}_i,\mathbf{e}_i)\triangleq\begin{bmatrix} g(\mathbf{x}_i)\tanh(\dot{\rho}_i(t)g(\mathbf{x}_i)e_{i,1}(t)/\overline{\varepsilon}) \\ g(\mathbf{x}_i)\tanh(\dot{\rho}_i(t)g(\mathbf{x}_i)e_{i,2}(t)/\overline{\varepsilon}) \\ \vdots \\ g(\mathbf{x}_i)\tanh(\dot{\rho}_i(t)g(\mathbf{x}_i)e_{i,m}(t)/\overline{\varepsilon}) \end{bmatrix}\in\mathbf{R}^m,$$

$\mu_1, \mu_2 > 0$ are design constants. The updating laws (4.19) and (4.20) incorporate a leakage term based on a variant of σ modification [77, 78]. By applying the smooth controller (4.18) with the updating laws (4.19) and (4.20), the convergence property can be summarized in the following theorem.

Theorem 4.3 *For the nonlinear system (4.13), under the Assumptions 4.2, 4.3, the AILC scheme (4.18) with (4.19) and (4.20) guarantees that the tracking error* $\mathbf{e}_i(t)$ *will converge to the* $\sqrt{2\zeta}$*-neighborhood of zero asymptotically within finite iterations, where*

$$\zeta \triangleq \frac{m}{2}\lambda\overline{\varepsilon} + \frac{T}{2}\mu_1 trace(\eta^T\eta) + \frac{T}{2}\mu_2\lambda^2. \tag{4.21}$$

Proof. See *Appendix A.4*. ■

Remark 4.6 *From the expression of* ζ *in (4.21), any prespecified non-zero bound of tracking error can be obtained by tuning the design parameters* $\overline{\varepsilon}$*,* μ_1 *and* μ_2 *appropriately. More clearly, since the magnitude of* ζ *is proportional to* $\overline{\varepsilon}$*,* μ_1 *and* μ_2*, a tighter bound can be achieved by reducing* $\overline{\varepsilon}$*,* μ_1 *and* μ_2*, if possible.*

4.5 Illustrative Example

To show the effectiveness of the proposed AILC scheme, two examples are considered.

Example 1: system with time-invariant parameter

Consider the following nonlinear system

$$\frac{d\mathbf{x}_i}{dt_i} = \Theta\mathbf{f}(\mathbf{x}_i) + B\mathbf{v}_i(t_i),$$

where

$$\Theta = \begin{bmatrix} \theta_1 & 0 \\ 0 & \theta_2 \end{bmatrix} = \begin{bmatrix} 3 & 0 \\ 0 & 2 \end{bmatrix}, \mathbf{f}(\mathbf{x}_i) = \begin{bmatrix} x_{i,1}^3 \\ \sin(x_{i,1}+x_{i,2}) \end{bmatrix}, B = \begin{bmatrix} 2 & 0 \\ 0 & 1 \end{bmatrix}.$$

Let the reference trajectory in the ith iteration be

$$\mathbf{x}_i^r(t_i) \triangleq \begin{bmatrix} \kappa_{i,1}(t_i) & 0 \\ 0 & \kappa_{i,2}(t_i) \end{bmatrix} \begin{bmatrix} \sin(\lambda_i t_i) \\ 1-\cos(\lambda_i t_i) \end{bmatrix}, t_i \in [0, 2\pi/\lambda_i], \tag{4.22}$$

where $\lambda_i = |\sin(i)| + 1/2$, $\kappa_{i,1}(t_i) = \cos(t_i) + 3/2$ and $\kappa_{i,2}(t_i) = \sin(t_i) + 3/2$. Obviously, $\mathbf{x}_i^r(t_i), t_i \in [0, 2\pi/\lambda_i]$ is proportional to $\mathbf{x}^r(t) \triangleq [\sin(t), 1-\cos(t)]^T, t \in [0, 2\pi]$, as defined in Definition 4.1, if $t_i = \rho_i(t) = t/\lambda_i$.

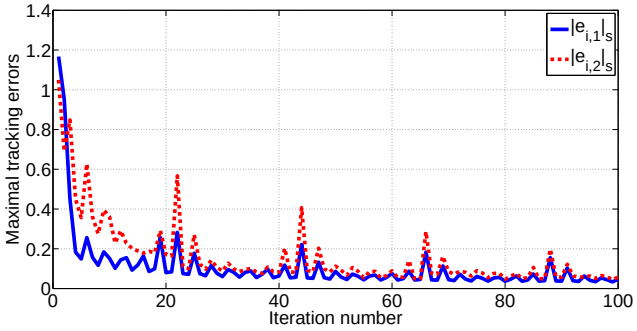

Figure 4.1: Maximal tracking errors for system with time-invariant parameter.

Set the feedback gain $\Gamma = \text{diag}(2,1)$ in the controller (4.5) with (4.6) and $\mathbf{x}_i(0) = 0$. The performance of the maximal tracking errors, $|e_{i,j}|_s \triangleq \sup_{t\in[0,2\pi]} |e_{i,j}(t)|$, $j = 1,2$ are given in Fig. 4.1.

Moreover, Figs. 4.2 and 4.3 give the references and output profiles for the 1st and 100th iterations, respectively. Observing the output tracking profile in the 100th iteration in Figs. 4.2 and 4.3, the difference between $\mathbf{x}_{100}$ and $\mathbf{x}_{100}^r$ is almost invisible.

Example 2: system with time-varying parameters

In order to show effectiveness of our proposed AILC algorithm for system with time-

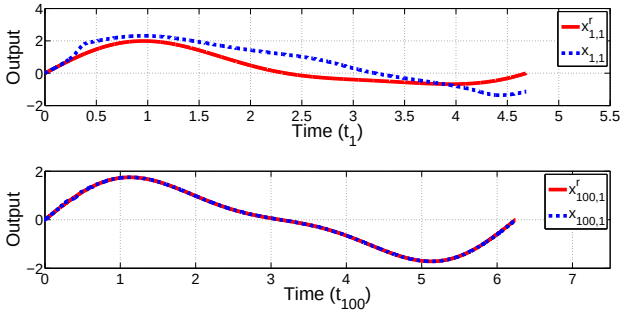

Figure 4.2: Output tracking profiles of x_1 at the 1st and 100th iterations for system with time-invariant parameter.

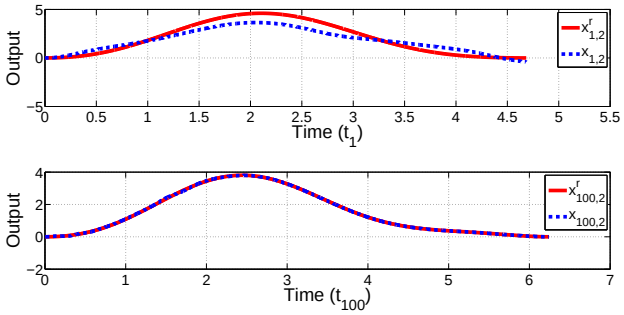

Figure 4.3: Output tracking profiles of x_2 at the 1st and 100th iterations for system with time-invariant parameter.

varying parameters, we consider the following nonlinear system

$$\frac{d\mathbf{x}_i}{dt_i} = \Theta(t_i)\mathbf{f}(\mathbf{x}_i) + B\mathbf{v}_i(t_i),$$

where

$$\Theta(t_i) = \begin{bmatrix} \theta_1(t_i) & 0 \\ 0 & \theta_2(t_i) \end{bmatrix}, \mathbf{f}(\mathbf{x}_i) = \begin{bmatrix} x_{i,1} + \sin(x_{i,2}) \\ \sin(x_{i,1} + x_{i,2}) \end{bmatrix}, B = \begin{bmatrix} 2 & 0 \\ 0 & 1 \end{bmatrix},$$

$\theta_1(t_i) = e^{\sin(t_i)} + 2\sin(\cos(t_i))$, and $\theta_2(t_i) = \sin^2(t_i)$. The same as example 1, let the reference trajectory in the ith iteration be (4.22). Assume

$$\begin{aligned} \theta_1(t_i) &= \eta_1^T \Pi_1(t_i) + \varepsilon_1(t_i), \\ \theta_2(t_i) &= \eta_2^T \Pi_2(t_i) + \varepsilon_2(t_i), \end{aligned}$$

where

$$\begin{aligned}\Pi_1(t_i) &= [1, \sin(t_i), \cos(t_i), \sin(2t_i), \cos(2t_i)]^T, \\ \Pi_2(t_i) &= [1, \sin(t_i), \cos(t_i), \sin(2t_i), \cos(2t_i)]^T, \\ \eta_1 &= [\eta_{1,1}, \eta_{1,2}, \eta_{1,3}, \eta_{1,4}, \eta_{1,5}]^T, \\ \eta_2 &= [\eta_{2,1}, \eta_{2,2}, \eta_{2,3}, \eta_{2,4}, \eta_{2,5}]^T.\end{aligned}$$

Then

$$\Theta(t_i) = \begin{bmatrix} \eta_1^T & 0 \\ 0 & \eta_2^T \end{bmatrix} \begin{bmatrix} \Pi_1(t_i) & 0 \\ 0 & \Pi_2(t_i) \end{bmatrix} + \begin{bmatrix} \varepsilon_1(t_i) & 0 \\ 0 & \varepsilon_2(t_i) \end{bmatrix}$$

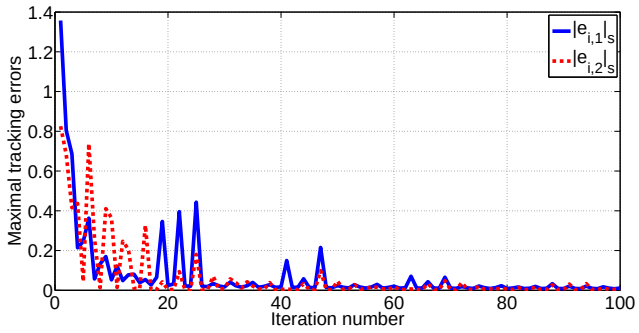

Figure 4.4: Maximal tracking errors for controller with sign function.

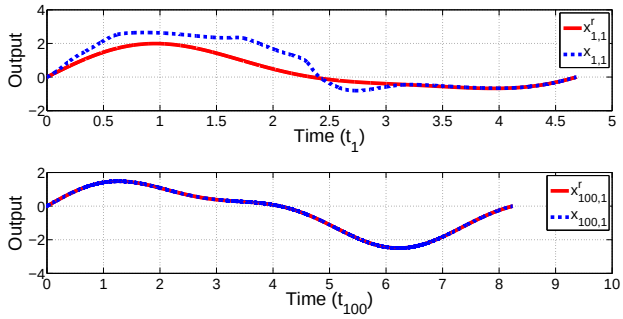

Figure 4.5: Output tracking profiles of x_1 at the 1st and 100th iterations for controller with sign function.

Set the feedback gain $\Gamma = \text{diag}(2,1)$, $g(\mathbf{x}_i) = 0.5[|x_{i,1} + \sin(x_{i,2})| + 2|\sin(x_{i,1} + x_{i,2})|]$ and $\mathbf{x}_i(0) = 0$ in the controller (4.15) with (4.16) and (4.17). The performance of the

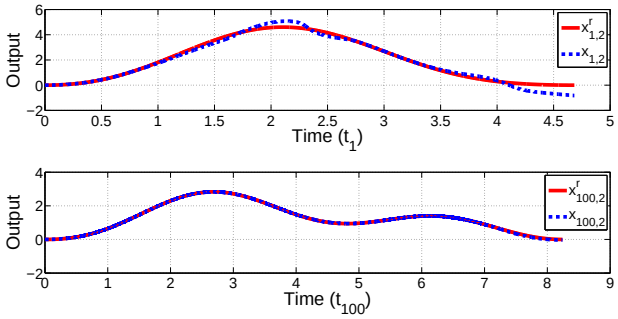

Figure 4.6: Output tracking profiles of x_2 at the 1st and 100th iterations for controller with sign function.

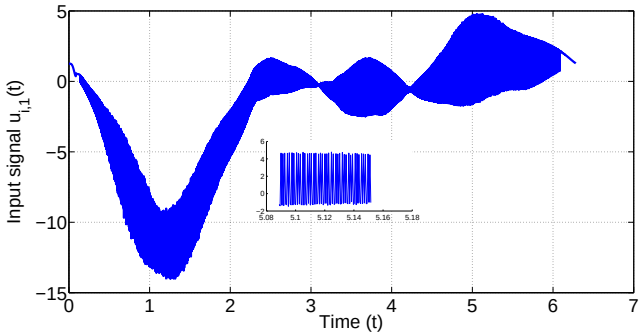

Figure 4.7: Input signal u_1 at the 100th iteration for controller with sign function.

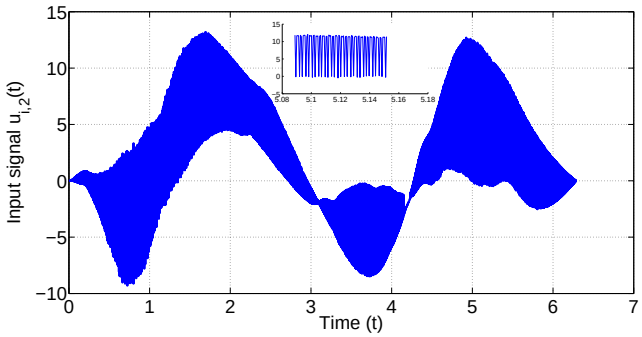

Figure 4.8: Input signal u_2 at the 100th iteration for controller with sign function.

maximal tracking errors and the tracking performance for 1st and 100th iterations are presented in Figs. 4.4, 4.5 and 4.6, respectively. In addition, Figs. 4.7 and 4.8 give the control input signals at the 100th iteration. It can be seen that since the sign function is used in the controller (4.15), the input signals oscillate at high frequencies.

To avoid the chattering phenomena and demonstrate the effect of the function $\tanh(\bullet)$, we fix the feedback gain $K = \mathrm{diag}(2,1)$, $g(\mathbf{x}_i) = 0.5[|x_{i,1} + \sin(x_{i,2})| + 2|\sin(x_{i,1} + x_{i,2})|]$

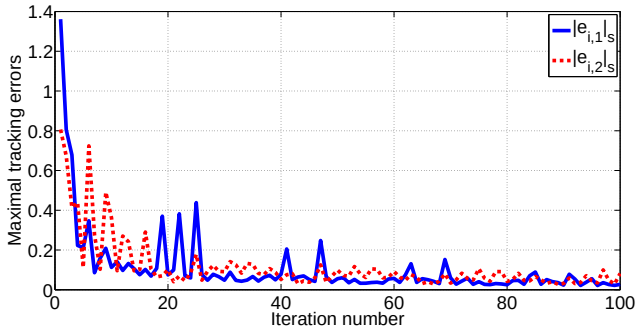

Figure 4.9: Maximal tracking errors for smoothed controller.

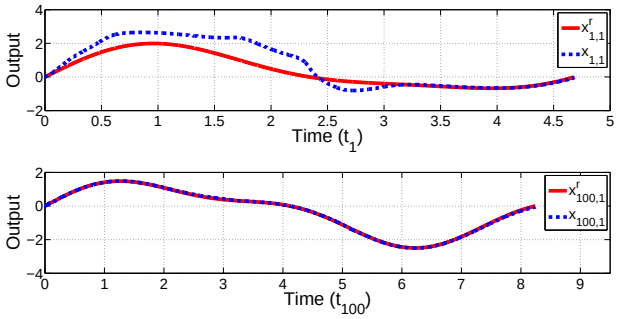

Figure 4.10: Output tracking profiles of x_1 at the 1st and 100th iterations for smoothed controller.

and $\mathbf{x}_i(0) = 0$ in the controller with tanh(•) and set $\overline{\varepsilon} = 0.1$. In addition, we choose $\mu_1 = 10^{-3}$, $\mu_2 = 10^{-2}$ in the updating laws (4.19) and (4.20). The simulation results are shown in Figs. 4.9, 4.10, 4.11, 4.12 and 4.13. Although the convergence speed by applying the controller with tanh(•) is slower than that of the controller with sign(•), control signals with tanh(•), as shown in Figs. 4.12 and 4.13, are smooth. It implies that the controller with tanh(•) is more applicable to practical systems.

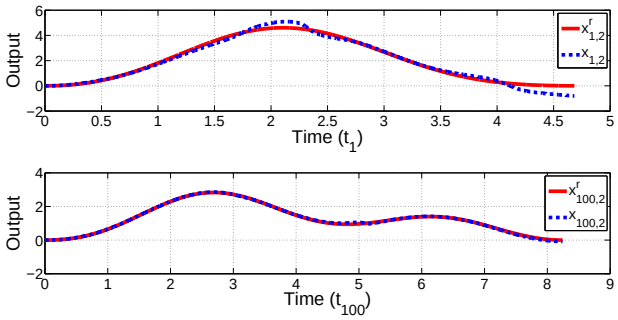

Figure 4.11: Output tracking profiles of x_2 at the 1st and 100th iterations for smoothed controller.

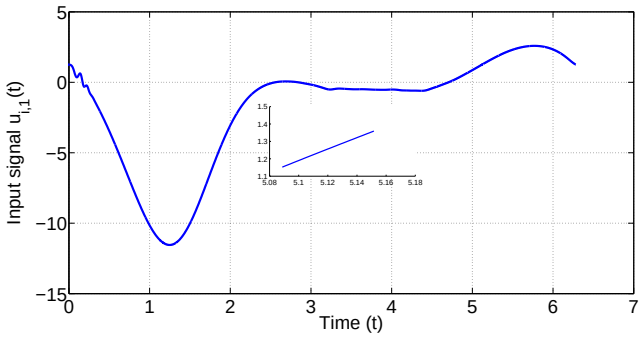

Figure 4.12: Input signal u_1 at the 100th iteration for smoothed controller.

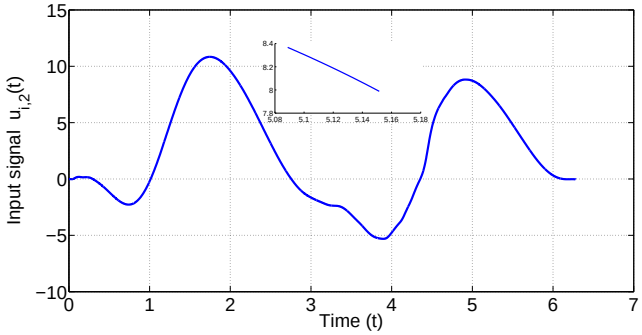

Figure 4.13: Input signal u_2 at the 100th iteration for smoothed controller.

4.6 Conclusion

This chapter presents the AILC law design and analysis results for trajectories with different magnitude and time scales. Due to the variation of the magnitude and time scales, a new AILC scheme is developed by introducing time-scaling transformations and the convergence of tracking error is derived based on Lyapunov theory. The proposed AILC scheme overcomes the limitation of traditional ILC that the target trajectory must be identical in all iterations. In addition, the requirement on classic ILC that every trial must repeat in a fixed time duration is absolutely removed. The design method is novel and it is shown that the learning control system is capable of fully utilizing all the learned knowledge despite the iteratively varying tracking tasks.

Chapter 5

Robust ILC for Systems with Norm-bounded Uncertainties

5.1 Introduction

In the research field of ILC, two categories of uncertainties are considered, namely, parametric ones and non-parametric/unstructured ones. For the former class, the system model is assumed to be linear in parameters, and adaptive ILC scheme is developed to learn the unknown system parameters pointwisely in the iteration domain [27–30]. For the latter class, there are mainly three types of unstructured uncertainties [31]: (1) the uncertainty itself is norm-bounded by a known function $\rho(\mathbf{x},t)$: $\|\eta(\mathbf{x},t)\|_2 \leq \rho(\mathbf{x},t)$, (2) the variation of uncertainty is norm-bounded by a known function $\rho(\mathbf{x}_1,\mathbf{x}_2,t)$: $\|\eta(\mathbf{x}_1,t) - \eta(\mathbf{x}_2,t)\|_2 \leq \rho(\mathbf{x}_1,\mathbf{x}_2,t)\|\mathbf{x}_1 - \mathbf{x}_2\|_2$, and (3) the uncertainty itself is norm-bounded but with unknown coefficient θ: $\|\eta(\mathbf{x},t)\|_2 \leq \theta\rho(\mathbf{x},t)$. Much effort has been made to address ILC design for the second type of non-parametric uncertainties, which may be globally Lipschitz continuous (GLC) [5] or locally Lipschitz continuous (LLC) [32, 33].

When the system is GLC, the popular methodology for convergence analysis is based on contraction mapping. However, for LLC systems, the contraction mapping methodology is not globally applicable any more, and as an alternative, composite energy function (CEF) based ILC design has been well exploited, e.g., [28], [5, 30, 31]. Except for ILC, many other control approaches also consider the second type of non-parametric uncertainties, such as adaptive fuzzy output feedback control [79, 80], sliding mode control [81], etc.

Relatively, there are few works that focus on learning controller design for systems with the other two types of non-parametric uncertainties. In [82], a robust adaptive learning controller is designed for uncertain nonlinear systems, in which the non-parametric uncertainty is simply bounded by a constant. In [83], a repetitive learning control scheme is proposed for nonlinear systems with structured periodic and unstructured aperiodic uncertainties, where the unstructured uncertainties are confined by differentiable bounding functions. Further, in [84], a robust ILC (RILC) law is developed for uncertain systems with the first type unstructured uncertainties. Notice that all the systems considered in [82–84] are single-input single-output (SISO). It would be meaningful to extend those learning type controllers to more general multi-input multi-output (MIMO) systems, especially with more general unstructured uncertainties.

In this chapter, a new RILC scheme is developed for a class of nonlinear MIMO systems under the alignment condition [33]. The involved unstructured uncertainties include the first type or the third type of unstructured uncertainties as a special case, and the bounding function $\rho(\mathbf{x},t)$ could be any LLC function. Notice that the two types of unstructured uncertainties can be unified by setting $\theta = 1$ in the first type. Hence, the idea behind the proposed controller is to parameterize the bounding functions, and then

learn those parametric uncertainties pointwisely in the iteration domain. In such sense, ILC of systems with non-parametric uncertainties is fulfilled by a parametric adaptation method. The main contributions of this chapter can be summarized as follows: (1) robust iterative learning controller design and analysis are presented for nonlinear systems that possess the first or third-type of unstructured uncertainties; (2) input distribution uncertainties are addressed in the new controller design; (3) the classical resetting condition of iterative learning control is removed and replaced with more practical alignment condition; (4) effort is also made to solve the discontinuity issue of control input profile, and to extend the considered systems to more general scenarios.

The rest of this chapter is organized as follows. In Section 5.2, RILC with the alignment condition is investigated for MIMO nonlinear system. A more generic formulation of problem is considered in Section 5.3 with uncertainties in input distribution matrix. At last, an illustrative example is presented in Section 5.4 to demonstrate the effectiveness of the proposed control scheme. Throughout this chapter, denote $\mathbf{R}$ the set of real numbers. For a given vector $\mathbf{x} = [x_1, x_2, \ldots, x_n] \in \mathbf{R}^n$, $\|\mathbf{x}\|_2$ denotes the l_2 vector norm. For any matrix $A \in \mathbf{R}^{n\times n}$, $\|A\|$ is the induced matrix norm. For any function $\mathbf{h}(t)$, $t \in [0,T]$, $\int_0^T \|\mathbf{h}(s)\|_2^2 ds$ represents the L^2-norm of $\mathbf{h}(t)$. Denote $|\cdot|$ the absolute value.

5.2 RILC of systems with non-parametric uncertainties

5.2.1 Problem formulation

Consider the following MIMO nonlinear system

$$\dot{\mathbf{x}}_i = \mathbf{f}_i + \mathbf{w}^r + B_i \mathbf{u}_i(t), \tag{5.1}$$

where i is the iteration index; $t \in [0,T]$, T is the trial length; $\mathbf{x}_i \triangleq \mathbf{x}_i(t) \in \mathbf{R}^n$ are the physically measurable vector valued system states; $\mathbf{w}^r \triangleq \mathbf{w}(\mathbf{x}^r,t) \in \mathbf{R}^n$ is a known vector valued function; $B_i \triangleq B(\mathbf{x}_i,t) \in \mathbf{R}^{n\times n}$ is a known control input distribution matrix, which is invertible; $\mathbf{u}_i(t) \in \mathbf{R}^n$ is the system input; $\mathbf{f}_i \triangleq \mathbf{f}(\mathbf{x}_i,t) \in \mathbf{R}^n$ is a lumped uncertainty, which is norm-bounded

$$\|\mathbf{f}(\mathbf{x}_i,t)\|_2 \leq \rho(\mathbf{x}_i,t), \tag{5.2}$$

with $\rho(\mathbf{x}_i,t) > 0$ being a known LLC function.

The desired state is generated by the following reference model

$$\dot{\mathbf{x}}^r(t) = \mathbf{w}^r \triangleq \mathbf{w}(\mathbf{x}^r,t),\ t \in [0,T], \tag{5.3}$$

where $\mathbf{x}^r \in \mathbf{R}^n$ is the target trajectory, and $\mathbf{w}^r$ is continuous with respect to all its arguments. Define the tracking error $\mathbf{e}_i(t) \triangleq \mathbf{x}_i(t) - \mathbf{x}^r(t)$. The error dynamics at the ith iteration is

$$\dot{\mathbf{e}}_i = \mathbf{f}_i + B_i\mathbf{u}_i(t). \tag{5.4}$$

The control objective is to track the desired trajectory $\mathbf{x}^r(t)$, $t \in [0,T]$ by determining a sequence of control inputs $\mathbf{u}_i(t)$, such that the tracking converges as the iteration number i increases.

For a smooth transfer during the update of iterations, the following alignment condition is assumed.

Assumption 5.1 *In each iteration of ILC, the initial states of the system (5.1) and its desired correspondence (5.3) satisfy the alignment condition, namely,* $\mathbf{x}_{i-1}(T) = \mathbf{x}_i(0)$ *and* $\mathbf{x}^r(0) = \mathbf{x}^r(T)$. *As such,* $\mathbf{e}_{i-1}(T) = \mathbf{e}_i(0)$, $\forall i \in \mathbf{Z}^+ \triangleq \{1,2,3,\cdots\}$.

Remark 5.1 *Most practical systems operate continuously in time. Hence, resetting them to the identical initial condition (i.i.c.) before proceeding to the next iteration, as*

requested in traditional ILC, might be difficult or even impossible. In such case, the alignment condition would be more rational.

5.2.2 RILC design and convergence analysis

The proposed controller is

$$\mathscr{I}_1: \quad \mathbf{u}_i(t) = B_i^{-1}[-\Gamma \mathbf{e}_i(t) - \hat{\theta}_i(t)\rho(\mathbf{x}_i,t)\mathrm{sgn}(\mathbf{e}_i(t))], \quad t \in [0,T], \tag{5.5}$$

where $\Gamma \in \mathbf{R}^{n\times n}$ is a control gain matrix that is symmetric and positive definite; $B_i^{-1} \triangleq B(\mathbf{x}_i,t)^{-1}$ is the inverse of $B(\mathbf{x}_i,t)$; and $\mathrm{sgn}(\mathbf{e}_i(t)) \triangleq [\mathrm{sgn}(e_{1,i}(t)), \mathrm{sgn}(e_{2,i}(t)), \ldots, \mathrm{sgn}(e_{n,i}(t))]^T$ with $\mathbf{e}_i(t) \triangleq [e_{1,i}(t), e_{2,i}(t), \ldots, e_{n,i}(t)]^T$. The updating law for $\hat{\theta}_i(t) \in \mathbf{R}$ is

$$\begin{aligned} \hat{\theta}_i(t) &= \hat{\theta}_{i-1}(t) + \gamma\rho(\mathbf{x}_i,t)\sum_{k=1}^{n}|e_{k,i}(t)|, \\ \hat{\theta}_0(t) &= 0, \ t \in [0,T], \end{aligned} \tag{5.6}$$

where $\gamma > 0$ is the learning gain and $|\cdot|$ represents absolute value. It can be seen that (5.5) consists of a robust feedback part and a parametric learning part.

In order to facilitate the analysis of the proposed RILC, the following CEF is introduced

$$E_i(t) = \frac{1}{2}\mathbf{e}_i^T(t)\mathbf{e}_i(t) + \frac{1}{2\gamma}\int_0^t \phi_i^2 ds, \tag{5.7}$$

where $\phi_i \triangleq \hat{\theta}_i(t) - 1$ is the virtual estimation error. The convergence property of the proposed RILC scheme is summarized in the following theorem.

Theorem 5.1 *For the nonlinear system (5.1) under the alignment condition, the RILC scheme (5.5)-(5.6) guarantees that the tracking error $\mathbf{e}_i(t)$, $t \in [0,T]$ converges to zero asymptotically in the sense of L^2-norm as $i \to \infty$.*

Proof. See *Appendix A.5.* ■

In general, the discontinuous control scheme (5.5) should be avoided, since it causes not only the problem of existence and uniqueness of solutions ([73, 74], but also chattering ([75]) that might excite high-frequency unmodeled dynamics ([76]). This motivates us to seek an appropriate smooth approximation of (5.5) that can guarantee the boundedness of the parameter estimation $\hat{\theta}_i(t)$ as well as the convergence of $\mathbf{e}_i(t)$ to a prespecified small neighborhood of the origin.

Let $\overline{\varepsilon} > 0$ be a constant and consider the following smooth learning scheme

$$\mathscr{I}_2: \quad \mathbf{u}_i(t) = B_i^{-1}(-\Gamma \mathbf{e}_i(t) - \hat{\theta}_i(t)\omega(\mathbf{x}_i, \mathbf{e}_i)),\ t \in [0,T], \tag{5.8}$$

with the updating law

$$\begin{aligned} \hat{\theta}_i(t) &= \hat{\theta}_{i-1}(t) + \gamma \mathbf{e}_i^T(t)\omega(\mathbf{x}_i, \mathbf{e}_i) - \mu \hat{\theta}_i(t), \\ \hat{\theta}_0(t) &= 0,\ t \in [0,T], \end{aligned} \tag{5.9}$$

where

$$\omega(\mathbf{x}_i, \mathbf{e}_i) \triangleq \begin{bmatrix} \rho(\mathbf{x}_i,t)\tanh(\rho(\mathbf{x}_i,t)e_{1,i}(t)/\overline{\varepsilon}) \\ \rho(\mathbf{x}_i,t)\tanh(\rho(\mathbf{x}_i,t)e_{2,i}(t)/\overline{\varepsilon}) \\ \vdots \\ \rho(\mathbf{x}_i,t)\tanh(\rho(\mathbf{x}_i,t)e_{n,i}(t)/\overline{\varepsilon}) \end{bmatrix} \in \mathbf{R}^n,$$

and $\mu > 0$ is a constant. From (5.8), it can be seen that the sign function in the control law (5.5) is smoothed by the hyperbolic tangent function. Based on a variant of σ-modification [77, 78], the updating law (5.9) incorporates a leakage term $-\mu\hat{\theta}_i(t)$ to increase the robustness of the learning algorithm. By applying the smooth controller (5.8) with the updating law (5.9), the convergence property is summarized as follows.

Theorem 5.2 *For the nonlinear system (5.1) under the alignment condition, the modified RILC scheme (5.8)-(5.9) guarantees that the tracking error* $\mathbf{e}_i(t)$ *will converge to the*

ζ-neighborhood of zero asymptotically in the sense of L^2-norm within finite iterations, where

$$\zeta \triangleq \frac{n\overline{\varepsilon}}{2\lambda_{min}} + \frac{\mu T}{2\lambda_{min}\gamma} + \varepsilon, \tag{5.10}$$

with λ_{min}, n, T, μ being the minimal eigenvalue of feedback gain Γ, the dimension of system state $\mathbf{x}$, the trial length of process in each iteration, and the leakage gain, respectively, and $\varepsilon > 0$ being a sufficiently small constant.

Proof. See *Appendix A.6.* ■

Remark 5.2 *From the expression of ζ in (5.10), any prespecified non-zero bound of tracking error can be obtained by tuning the design parameters $\overline{\varepsilon}$, μ, γ, and λ_{min} appropriately. More clearly, since the magnitude of ζ is proportional to μ as well as the inverses of γ and λ_{min}, a tighter bound can be achieved by using a high-gain feedback, a high-gain learning, and less robustness concern, if possible.*

5.2.3 RILC for systems with the third type of unstructured uncertainties

Note that in Subsection 5.2.2, the bounding function $\rho(\mathbf{x}_i, t)$ is assumed to be fully known. If the unstructured uncertainty is the third type one, namely, $\|\mathbf{f}(\mathbf{x}_i, t)\|_2 \leq \theta\rho(\mathbf{x}_i, t)$, where θ is an unknown constant or continuous function of t, our approach still applies and the result is summarized as follows.

Theorem 5.3 *For the nonlinear system (5.1) with $\|\mathbf{f}(\mathbf{x}_i, t)\|_2 \leq \theta\rho(\mathbf{x}_i, t)$ under the alignment condition, the RILC scheme (5.5)-(5.6) guarantees that the tracking error $\mathbf{e}_i(t)$, $t \in [0, T]$ converges to zero asymptotically in the sense of L^2-norm as $i \to \infty$.*

Stimulated by (5.7), the following CEF is built to analyze the convergence of system tracking,

$$E_i(t) = \frac{1}{2}\mathbf{e}_i^T(t)\mathbf{e}_i(t) + \frac{1}{2\gamma}\int_0^t \phi_i^2 ds,$$

where $\phi_i \triangleq \hat{\theta}_i(t) - \theta$ is the estimation error of parametric uncertainty embedded in the bounding function. More details in proving Theorem 5.3 are given in *Appendix A.7*.

5.3 Extension to more generic systems

To show the generality of the proposed RILC scheme, consider a more general class of deterministic uncertain dynamic systems,

$$\dot{\mathbf{x}}_i = \mathbf{f}_i + \mathbf{w}^r + B_i[(I + H_i)\mathbf{u}_i(t) + \mathbf{d}_i],\ \forall t \in [0, T], \tag{5.11}$$

where $\mathbf{x}_i, \mathbf{f}_i, \mathbf{w}^r, B_i$, and $\mathbf{u}_i$ are same as in (5.1), while $H_i \triangleq H(\mathbf{x}_i, t) \in \mathbf{R}^{n\times n}$ represents the additional uncertainties in the input distribution matrix and $\mathbf{d}_i \triangleq \mathbf{d}(\mathbf{x}_i, t) \in \mathbf{R}^n$ is the state-dependent input disturbance. In (5.11), I denotes the identity matrix of appropriate dimension. Further, $\mathbf{f}_i$, $\mathbf{d}_i$ and H_i are norm-bounded, namely, for any $\mathbf{x}_i \in \mathbf{R}^n$,

$$\|\mathbf{f}(\mathbf{x}_i, t)\|_2 \leq \alpha_i,\ \|\mathbf{d}(\mathbf{x}_i, t)\|_2 \leq \beta_i,\ \|H(\mathbf{x}_i, t)\| \leq \kappa_i,$$

where $\alpha_i \triangleq \alpha(\mathbf{x}_i, t) > 0$ and $\beta_i \triangleq \beta(\mathbf{x}_i, t) > 0$ are known LLC functions, and $\kappa_i \triangleq \kappa(\mathbf{x}_i, t) > 0$ is a known bounded function. Moreover, it is assumed that a constant $\xi \in (0, 1)$ can be found such that $\mathbf{x}^T(\xi I + H_i)\mathbf{x} \geq 0$, $\forall \mathbf{x} \in \mathbf{R}^n$, implying that the control direction is certain.

The dynamics of state tracking error will be

$$\dot{\mathbf{e}}_i = \dot{\mathbf{x}}_i - \dot{\mathbf{x}}_i^r = \mathbf{f}_i + B_i[(I + H_i)\mathbf{u}_i(t) + \mathbf{d}_i]. \tag{5.12}$$

Under the alignment condition described in Assumption 5.1, there has $\mathbf{e}_i(0) = \mathbf{e}_{i-1}(T)$. The new RILC law is proposed as

$$\begin{aligned}\mathscr{I}_3: \ \mathbf{u}_i(t) &= B_i^{-1}[-\Gamma\mathbf{e}_i(t) - \hat{\theta}_i(t)\alpha(\mathbf{x}_i,t)\mathrm{sgn}(\mathbf{e}_i)] - \hat{\eta}_i(t)\beta(\mathbf{x}_i,t)\frac{B_i^T\mathbf{e}_i}{\|B_i^T\mathbf{e}_i\|_2} \\ &\quad -\frac{B_i^T\mathbf{e}_i}{(1-\xi)\|\mathbf{e}_i^TB_i\|_2}\left[\frac{\kappa(\mathbf{x}_i,t)\|\Gamma\|\|\mathbf{e}_i\|_2}{\|B_i\|} + \frac{\sqrt{n}\kappa(\mathbf{x}_i,t)\alpha_i|\hat{\theta}_i(t)|}{\|B_i\|}\right. \\ &\quad \left.+\kappa(\mathbf{x}_i,t)\beta(\mathbf{x}_i,t)|\hat{\eta}_i(t)|\right] \qquad (5.13)\end{aligned}$$

with the updating laws

$$\begin{aligned}\hat{\theta}_i(t) &= \hat{\theta}_{i-1}(t) + \gamma_1\alpha(\mathbf{x}_i,t)\sum_{k=1}^{n}|e_{k,i}|, \qquad (5.14)\\ \hat{\theta}_0(t) &= 0,\ t\in[0,T],\end{aligned}$$

and

$$\begin{aligned}\hat{\eta}_i(t) &= \hat{\eta}_{i-1}(t) + \gamma_2\beta(\mathbf{x}_i,t)\|\mathbf{e}_i^TB_i\|_2, \qquad (5.15)\\ \hat{\eta}_0(t) &= 0,\ t\in[0,T],\end{aligned}$$

where $\Gamma\in\mathbf{R}^{n\times n}, \gamma_1>0, \gamma_2>0$ are the feedback and learning gains respecitvely, $\hat{\theta}_i(t)\in\mathbf{R}$ and $\hat{\eta}_i(t)\in\mathbf{R}$ are two virtual parametric estimations at the ith iteration.

In order to analyze the convergence of tracking error, the following CEF is introduced

$$E_i(t) = \frac{1}{2}\mathbf{e}_i^T(t)\mathbf{e}_i(t) + \frac{1}{2\gamma_1}\int_0^t\phi_i^2ds + \frac{1}{2\gamma_2}\int_0^t\psi_i^2ds, \qquad (5.16)$$

where $\phi_i \triangleq \hat{\theta}_i(t)-1$ and $\psi_i \triangleq \hat{\eta}_i(t)-1$. The fourth main result of this chapter is presented in the following.

Theorem 5.4 *For the nonlinear system (5.11) under the alignment condition, the RILC scheme (5.13)-(5.15) guarantees that the tracking error $\mathbf{e}_i(t)$, $t\in[0,T]$ converges to zero asymptotically in the sense of L^2-norm as $i\to\infty$.*

Proof. See *Appendix A.8.* ■

Remark 5.3 *The RILC law (5.13) consists of four terms: the first term is a robust feedback term that is same as in $\mathscr{I}_1$ and $\mathscr{I}_2$, the second and third terms are used to learn the unstructured uncertainties $\mathbf{f}_i$ and $\mathbf{d}_i$ respectively, and the last term is an additional part to compensate for the uncertainties in input distribution.*

Remark 5.4 *The smoothing procedure proposed in Subsection 2.2 is still applicable for the RILC law $\mathscr{I}_3$ and the smooth control law corresponding to $\mathscr{I}_3$ can be given as follows:*

$$\begin{aligned}\mathbf{u}_i(t) &= B_i^{-1}[-\Gamma\mathbf{e}_i(t)-\hat{\theta}_i(t)\omega(\mathbf{x}_i,\mathbf{e}_i)]-\hat{\eta}_i(t)\beta(\mathbf{x}_i,t)\frac{B_i^T\mathbf{e}_i}{\|B_i^T\mathbf{e}_i\|_2} \\ &\quad -\frac{B_i^T\mathbf{e}_i}{(1-\xi)\|\mathbf{e}_i^TB_i\|_2}\left[\frac{\kappa(\mathbf{x}_i,t)\|\Gamma\|\|\mathbf{e}_i\|_2}{\|B_i\|}+\frac{\sqrt{n}\kappa(\mathbf{x}_i,t)\alpha(\mathbf{x}_i,t)\hat{\theta}_i(t)\tanh(\hat{\theta}_i(t))}{\|B_i\|}\right. \\ &\quad \left.+\kappa(\mathbf{x}_i,t)\beta(\mathbf{x}_i,t)\hat{\eta}_i(t)\tanh(\hat{\eta}_i(t))\right].\end{aligned} \tag{5.17}$$

Moreover, only the first type of unstructured uncertainties is considered here. Parallel to Subsection 2.3, similar RILC scheme can be designed for system (5.11) when the third type of unstructured uncertainties is considered.

5.4 An illustrative example

To demonstrate the efficacy of the proposed RILC scheme, the nonlinear system (5.11) with

$$\mathbf{f}_i = \begin{bmatrix} x_{1,i}+\sin(x_{2,i}) \\ 2\sin(x_{1,i}+x_{2,i}) \end{bmatrix},\ \mathbf{w}^r = \begin{bmatrix} 4\pi\cos(8\pi t) \\ 4\pi\sin(16\pi t) \end{bmatrix},$$

$$B_i = \begin{bmatrix} 2+\sin(x_{1,i})+0.1\sin(2\pi t) & 0 \\ 0 & 1+\sin(x_{2,i})+0.1\sin(4\pi t) \end{bmatrix}$$

is considered. Let the target trajectory be

$$\mathbf{x}^r(t) \triangleq \begin{bmatrix} 0.5\sin(8\pi t)+1 \\ -0.25\cos(16\pi t)-0.5 \end{bmatrix}, \quad t \in [0,0.5]. \tag{5.18}$$

In order to show the effectiveness of the proposed controllers $\mathscr{I}_i, i = 1,\cdots,3$, simulations were performed in two cases: (1) apply the controllers $\mathscr{I}_1$ and $\mathscr{I}_2$ to the system by assuming $H_i = 0$ and $\mathbf{d}_i = 0$; (2) adopt the controller $\mathscr{I}_3$ to the system for non-zero H_i and $\mathbf{d}_i$.

Case 1: $H_i = 0$ and $\mathbf{d}_i = 0$.

Set the feedback gain $\Gamma = \mathrm{diag}(3,2)$ in the controllers $\mathscr{I}_1$ and $\mathscr{I}_2$, as well as $\gamma = 1$ in the updating laws (5.6) and (5.9) with $\mu = 0$. Moreover, let $\overline{\varepsilon} = 0.1$, $\mathbf{x}_1(0) = [1.5,-0.4]^T$, and $\hat{\theta}_0(t) = 0$, $t \in [0,0.5]$. The performance of the maximal tracking errors, $|e_{i,j}|_s \triangleq \sup_{t\in[0,0.5]} |e_{i,j}(t)|$, $j = 1,2$ and input signals of the RILC scheme $\mathscr{I}_1$ are illustrated in Fig. 5.1 and Fig. 5.2, respectively, and those of $\mathscr{I}_2$ are presented in Fig. 5.3 and Fig. 5.4, respectively. It can be seen from Fig. 5.1 and Fig. 5.3 that the convergence performance of $\mathscr{I}_1$ is superior to that of $\mathscr{I}_2$. However, the discontinuity in the input signals of $\mathscr{I}_1$ in Fig. 5.2 is smoothed by the hyperbolic tangent function in $\mathscr{I}_2$, which is shown in Fig. 5.4. These observations are consistent with our analysis in the controller design parts.

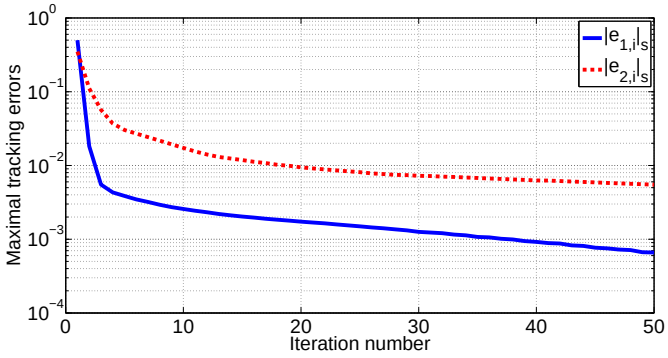

Figure 5.1: Maximal tracking error profiles when the RILC law $\mathscr{I}_1$ is applied, and the tracking errors will converge to zero asymptotically as $i \to \infty$.

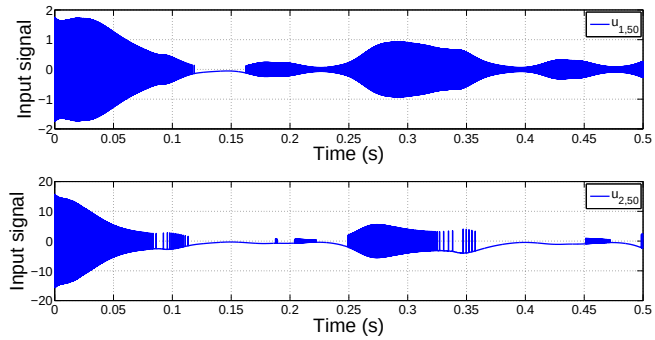

Figure 5.2: Input signals at 50th iteration when the RILC law $\mathscr{I}_1$ is applied. Due to the sign function in $\mathscr{I}_1$, the input signals have high amount of chattering phenomenon.

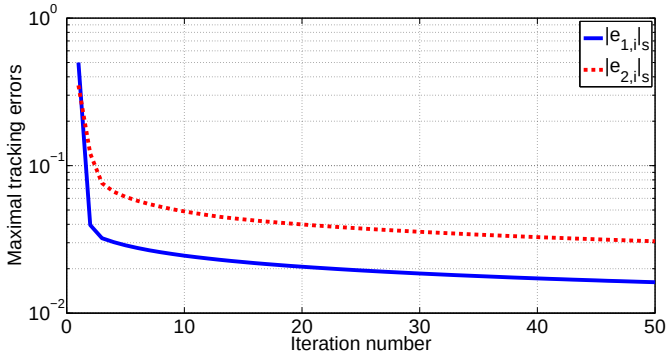

Figure 5.3: Maximal tracking error profiles when the RILC law $\mathscr{I}_2$ is applied. By virtue of the use of the hyperbolic tangent function, the tracking errors will converge to a neighborhood of zero asymptotically.

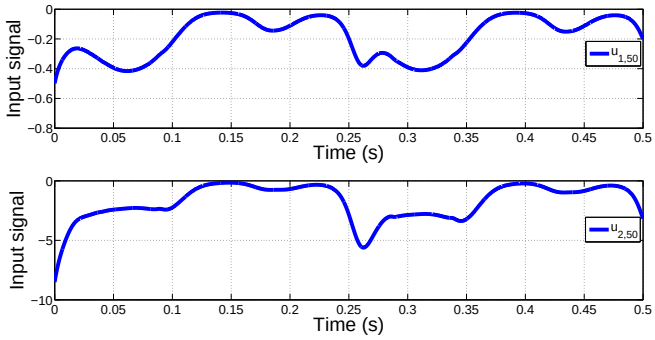

Figure 5.4: Input signals at 50th iteration when the RILC law $\mathscr{I}_2$ is applied. Benefit from the hyperbolic tangent function, the discontinuity in the input signals of $\mathscr{I}_1$ is smoothed.

Case 2: $H_i \neq 0$ and $\mathbf{d}_i \neq 0$.

Assume that

$$H_i = -0.1\sin(x_{1,i}), \quad \mathbf{d}_i = \begin{bmatrix} 0.1\sin(x_{1,i}) \\ 0.2\sin(x_{2,i}) \end{bmatrix}.$$

The RILC law adopted here is the smoothed $\mathscr{I}_3$, namely,

$$\begin{aligned}
\mathbf{u}_i(t) &= B_i^{-1}[-\Gamma \mathbf{e}_i(t) - \hat{\theta}_i(t)\omega(\mathbf{x}_i,\mathbf{e}_i)] - \hat{\eta}_i(t)\beta_i \frac{B_i^T \mathbf{e}_i}{\|B_i^T \mathbf{e}_i\|_2} \qquad (5.19)\\
&\quad - \frac{B_i^T \mathbf{e}_i}{(1-\xi)\|\mathbf{e}_i^T B_i\|_2}\left[\frac{\kappa_i \|\Gamma\|\|\mathbf{e}_i\|_2}{\|B_i\|} + \frac{\sqrt{2}\kappa_i\alpha_i\hat{\theta}_i(t)\tanh(\hat{\theta}_i(t))}{\|B_i\|} + \kappa_i\beta_i\hat{\eta}_i(t)\tanh(\hat{\eta}_i(t))\right]\\
\hat{\theta}_i(t) &= \hat{\theta}_{i-1}(t) + \gamma_1 \mathbf{e}_i^T(t)\omega(\mathbf{x}_i,\mathbf{e}_i), \qquad (5.20)\\
\hat{\eta}_i(t) &= \hat{\eta}_{i-1}(t) + \gamma_2\beta_i\|\mathbf{e}_i^T B_i\|_2, \qquad (5.21)
\end{aligned}$$

and

$$\omega(\mathbf{x}_i,\mathbf{e}_i) = \begin{bmatrix} \alpha_i \tanh(\alpha_i e_{1,i}(t)/\overline{\varepsilon}) \\ \alpha_i \tanh(\alpha_i e_{2,i}(t)/\overline{\varepsilon}) \end{bmatrix} \in \mathbf{R}^2,$$

$$\begin{aligned}
\alpha_i &= 2[(x_{1,i} + \sin(x_{2,i}))^2 + 4\sin^2(x_{1,i} + x_{2,i})]^{1/2},\\
\beta_i &= 0.2[\sin^2(x_{1,i}) + 4\sin^4(x_{2,i})]^{1/2},\\
\kappa_i &= 0.1|\sin(x_{1,i})|.
\end{aligned}$$

Similar to Case 1, the feedback gain is set as $\Gamma = \mathrm{diag}(3,2)$, $\overline{\varepsilon} = 0.1$, $\mathbf{x}_1(0) = [1.5, -0.4]^T$, and $\hat{\theta}_0(t) = 0$, $t \in [0, 0.5]$. Furthermore, let $\gamma_1 = 1$, $\gamma_2 = 4$, $\xi = 0.1$, and $\hat{\eta}_0(t) = 0$, $t \in [0, 0.5]$.

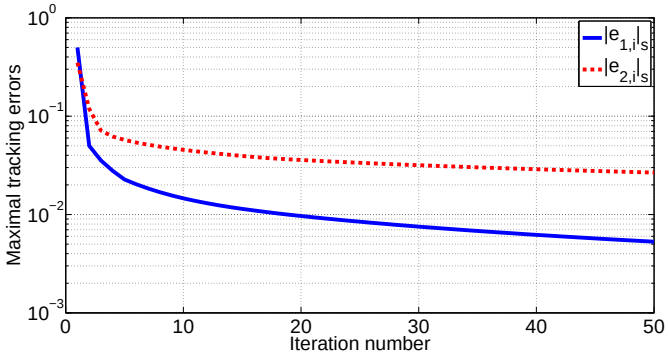

Figure 5.5: Maximal tracking error profile when the RILC law (5.19)-(5.21) is applied. The tracking errors will converge to a neighborhood of zero asymptotically because of the proposed smoothing procedure.

The performance of the maximal tracking errors is given in Fig. 5.5. It can be seen that the errors are decreased dramatically after a few iterations, and ultimately enter into

the prespecified bound $\overline{\varepsilon}$ after 10 iterations' learning. In addition, as shown in Fig. 5.6, the discontinuity of control input is avoided due to the proposed smoothing procedure.

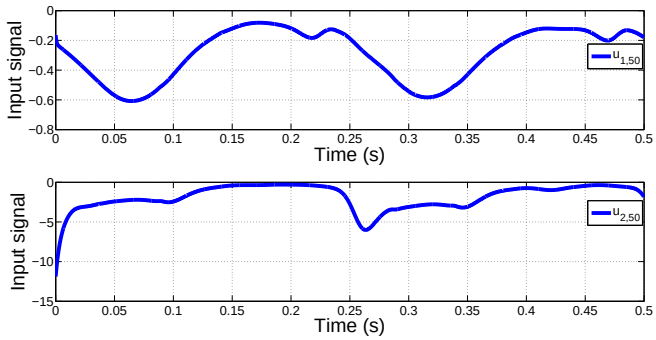

Figure 5.6: Control input profile when the RILC law (5.19)-(5.21) is applied, and the discontinuity of control input is avoided due to the use of the hyperbolic tangent function.

5.5 Conclusion

A new RILC scheme is developed for a class of nonlinear MIMO systems with non-parametric uncertainties under the alignment condition. To deal with the norm-bounded uncertainties, a composite energy function is introduced to prove the asymptotical convergence of the tracking error. In addition, general problem formulation with uncertain input distribution matrix is also investigated. The efficiency of the proposed RILC scheme is verified by a simulated example. Under the framework of ILC, our idea could be extended along the following directions: (1) extension to systems with non-square uncertain input distribution matrix, (2) extension to output tracking control or state tracking control but with input or state constraints, (3) extension to systems whose nonlinear part does not belong to any of the three types of uncertainties defined in this chapter, which would be addressed in the next research phase.

Chapter 6

ILC for Linear Inhomogeneous Distributed Parameter Systems

6.1 Introduction

Different from the previous four chapters that focus on ILC design of discrete-time or ODE systems, this thesis starts to discuss the applicability of ILC approach to PDE systems in this chapter.

Currently, the vast majority of the work reported on ILC considers finite-dimensional systems but there has been some work reported on ILC of distributed parameter systems (DPSs) governed by partial differential equations (PDEs). In [34], an iterative learning approach is applied for the constrained digital regulation of a class of linear hyperbolic PDE systems, where the plant model is first reduced to ordinary differential equation (ODE) systems and then approximated by the discrete-time equivalence. In [35], ILC scheme is presented for more general spatio-temporal dynamics using nD discrete linear system models. Without any discretization of system, [36] considers the

design of P-type and D-Type ILC laws for a class of infinite-dimensional linear systems using semigroup theory. It is worthy of noticing that the aforementioned three works all adopt distributed control structure, namely, the number of control actuators is more than one and they are uniformly distributed along the spatial domain. Further, to address the application of ILC for some specific DPSs, [37] considers ILC of flow rate in a center pivot irrigator used in dry-land farming, which can be modeled as a spatial-temporal diffusion process in three spatial dimensions coupled with flow in one dimension. In [38], based on Lyapunov theory, differential-difference type ILC is augmented with proportional controller to attenuate the unknown periodic speed variation for a stretched string system on a transporter. In [39], the similar ILC scheme is combined with proportional-derivative controller to compensate for the unknown periodic motion on the right end for a class of axially moving material systems. In [38] and [39], ILC is mainly designed for the stability maintainence of mechanical processes. Recently, under the framework of ILC, velocity boundary control of a quasi-linear PDE process is considered in [40], where the convergence of output regulation is guaranteed in the steady-state stage. In addition, [85–88] extend the idea of ILC to active control of fluid flows in wind turbine, combustor, etc. Investigating all the available results in this field, ILC for infinite-dimensional processes demonstrates clear differences to ILC for finite-dimensional processes in design and analysis, e.g., the infinite-dimensional characteristic of system, the interweave of 3D dynamics in the time, space, and iteration domains, and the absence of universal analysis tools in convergence analysis [20].

The study of this chapter is motivated by the following facts. First, up to the present, all the references that address ILC of linear and nonlinear PDEs are focusing on some specific processes, where the controller design highly depends on the properties of sys-

tem model. Second, many industrial and engineering processes can be described by linear or linearized PDE models, although nonlinear PDEs would have been of interest from a practical viewpoint [89]. Meanwhile, the involved system parameters or even inhomogeneous source terms may change with operating conditions. Third, parametric or non-parametric uncertainties can be dealt with by ILC easily under repetitive control environment, owing to the model-free nature in the design process of learning controller [90]. In association with the above observations, this chapter aims at ILC design and analysis for general linear inhomogeneous distributed parameter systems (LIDPSs) that may be hyperbolic, parabolic, or elliptic, and include many important physical processes such as diffusion, vibration, heat conduction and wave propagation as special cases. In order to overcome the difficulties that are associated with ILC of LIDPSs, the system equations are first reformulated into a matrix form in the Laplace transform domain. Through determination of a fundamental matrix, the system transfer function is then precisely evaluated in a closed form. The transfer function of a LIDPS contains all information required to predict the system spectrum, the system response under any initial and external disturbances, and the stability of the system response. Meanwhile, the derived transfer function clearly demonstrates the input-output relationship of system, and thus facilitates the consequent ILC design and convergence analysis in the frequency domain. As a result, one can iteratively tune the boundary input condition such that the output at the concerned position can track the desired reference pointwisely. Owing to the fact that ILC is a feedforward control, the proposed scheme not only makes anticipatory compensation possible to overcome the time delay in boundary output tracking, but also eliminates the gain margin limitation encountered in feedback control.

The main contributions of this chapter can be summarized as follows.

(i) A uniform design and analysis framework is presented for ILC of LIDPSs in the frequency domain. Nevertheless, [20, 34–40] consider the ILC of LIDPSs or DPSs all in the time domain.

(ii) Instead of simplifying the infinite-dimensional PDEs to finite-dimensional ODEs and/or replacing them by the discrete-time equivalences as in [34, 35, 37], the model approximation problem is avoided in controller design. Thus the often physically motivated model is advantageously maintained throughout the entire control design process. In doing so, non-physically motivated parameters, like discretization parameters are avoided [91].

(iii) Different from [34–36] that use a distributed control structure, LIDPSs with point (boundary) control is considered, namely, both the input actuator and the output sensor are unique. Such scenario is more practical and implementable in certain applications [92–94].

(iv) Instead of considering the stability or set-point problem as in [34, 38–40], more general output tracking problem is considered.

This chapter is organized as follows. In Section 6.2, problem formulation is first given. In Section 6.3, the details for calculating the input-output transfer functions for the considered LIDPSs is presented. In consequence, based on the derivation in Section 6.3, ILC design and convergence analysis are given in Section 6.4. Then, Section 6.5 addresses the robustness problem of the ILC scheme. At last, an illustrative example is presented in Section 6.6.

6.2 Problem Formulation

Consider the one-dimensional, nth-order, linear inhomogeneous PDE under a repeatable process environment

$$\left(A\frac{\partial^2}{\partial t^2}+B\frac{\partial}{\partial t}+C\right)w^i(x,t)=f(x,t)+g^i(x,t), \tag{6.1}$$

where the time $t\in(0,T]$ for any fixed $T>0$, the spatial coordinate $x\in(0,1)$, $i\in\mathscr{Z}\triangleq\{0,1,2,\cdots\}$ is the trial or iteration number, and $w^i(x,t)$ represents the system state at the ith iteration that may be interpreted as temperature in a heat transfer process or pollutant concentration in a wastewater treatment process. Meanwhile, the *unknown* nonlinear functions $f(x,t)$ and $g^i(x,t)$ denote the iteration-independent and iteration-dependent external disturbances, respectively. Moreover, A, B and C are spatial differential operators of the form $A=\sum_{k=0}^{n}a_k\frac{\partial^k}{\partial x^k}$, $B=\sum_{k=0}^{n}b_k\frac{\partial^k}{\partial x^k}$, $C=\sum_{k=0}^{n}c_k\frac{\partial^k}{\partial x^k}$ with a_k, b_k and c_k being constants and satisfying $|a_k|^2+|b_k|^2+|c_k|^2\neq 0$ as $k=n$. For the system (6.1), the boundary conditions are set as, for $t\in[0,T], i\in\mathscr{Z}, 1\leq j\leq n$,

$$\begin{cases} M_jw^i(0,t)+N_jw^i(1,t) &= \gamma_j(t),\ \ j\neq j_0,\\ M_jw^i(0,t)+N_jw^i(1,t) &= u^i(t),\ \ j=j_0, \end{cases} \tag{6.2}$$

where $1\leq j_0\leq n$ is a fixed integer, and M_j,N_j are temporal-spatial, linear differential operators of proper order. The functions $\gamma_j(t), j\neq j_0$ are unknown but iteration-invariant, while u^i is the tunable system control input. Meanwhile, the initial conditions of system (6.1) for all $x\in(0,1)$ are specified as

$$w(x,t)|_{t=0}=v_0(x),\ \ \frac{\partial}{\partial t}w(x,t)|_{t=0}=v_1(x), \tag{6.3}$$

where $v_0(x)$ and $v_1(x)$ are given continuous functions. To validate our consequent ILC design and analysis, it is assumed that the boundary value problem (6.1)-(6.3) is well posed, and always has one and only one solution.

It is worth highlighting that the system (6.1) may be hyperbolic, parabolic, or elliptic, and describes many important physical processes such as diffusion, heat transfer, vibration, wave propagation, etc. For instance, in describing vibration of a continuum, (6.1) is of hyperbolic type, the operator $A\partial^2/\partial t^2$ is associated with the inertia properties of the continuum, the operator $B\partial/\partial t$ evolves from damping, Coriolis acceleration, and mass transport, and the operator C is relevant to stiffness, centrifugal forces, and circulatory effects [95].

Consider a point control problem for the system (6.1), namely, iteratively tuning the boundary input condition $u^i(t)$ such that the output $y^i(t) = w^i(x^*,t),\ t \in [0,T]$ can track the given reference trajectory $y^d(t),\ t \in [0,T]$, where $0 \leq x^* \leq 1$ is the spatial position of the measurement output. Clearly, when $x^* = 0$ or $x^* = 1$, the control problem is a typical boundary-input boundary-output problem. Due to the well posedness of the boundary value problem (6.1)-(6.3), there must exists a desired control input profile $u^d(t),\ t \in [0,T]$ such that $y^i(t) = y^d(t)$ if and only if $u^i(t) = u^d(t)$. Under the framework of ILC, exploiting the input-output relationship that has been embedded in the boundary value problem (6.1)-(6.3) is always crucial, which can be done in the time or frequency domain. Considering the linear structure of the model in system state and the fact that the transfer function of the LIDPS contains all information required to predict the system spectrum, the system response under any initial and external disturbances, and the stability of the system response, the ILC design and analysis in the frequency domain will be addressed in the next section.

6.3 Input-Output Transfer Function

In terms of determining the input-output transfer function of system (6.1)-(6.3), classical methods lead to an eigenfunction expansion, i.e., the transfer function expressed by an infinite series of the system eigenfunctions. The eigenfunction expansion, while useful in some theoretical analysis, has some disadvantages in control analysis. On the one hand, the method requires exact eigensolutions, which may be difficult to obtain particularly for some uncertain systems. On the other hand, in general, truncation of the series has to be made in deriving the control convergence. Since the series truncation reduces the order of the system model, which leads to loss of information about the system dynamics of high-frequency modes, the resultant controller might not achieve the desirable control performance as expected. Next, following the idea proposed in [95], an evaluation scheme for the input-output transfer function of the LIDPS (6.1) will be developed.

First, define the Laplace transform of time-varying function $m(t)$ as $\mathscr{M}(s) \triangleq L[m(t)] = \int_0^\infty m(t)e^{-st}dt$, where s is the complex variable. For the nth order derivative of function $m(t)$, denoted by $m^{(n)}(t)$, it follows that

$$L[m^{(n)}(t)] = s^n\mathscr{M}(s) - s^{n-1}m(0) - s^{n-2}m^{(1)}(0) - \cdots - m^{(n-1)}(0).$$

Using the above property, Laplace transform of system (6.1) renders to

$$\begin{aligned} & \left(s^2A + sB + C\right)\mathscr{W}^i(x,s) \\ = \;& \mathscr{F}(x,s) + \mathscr{G}^i(x,s) + (sA+B)v_0(x) + Av_1(x) \\ = \;& \Theta(x,s) + \mathscr{G}^i(x,s), \end{aligned} \tag{6.4}$$

where $\Theta(x,s) \triangleq \mathscr{F}(x,s) + (sA+B)v_0(x) + Av_1(x)$. In (6.4), $\mathscr{W}^i(x,s), \mathscr{F}(x,s)$ and $\mathscr{G}^i(x,s)$ are the Laplace transforms of functions w^i, f, and g^i, respectively. Further, Laplace

transform of the boundary conditions (6.2) gives for $1 \leq j \leq n$,

$$\begin{cases} \mathscr{M}_j \mathscr{W}^i(0,s) + \mathscr{N}_j \mathscr{W}^i(1,s) &= \Gamma_j(s) + \mathscr{S}_j(s), \quad j \neq j_0, \\ \mathscr{M}_j \mathscr{W}^i(0,s) + \mathscr{N}_j \mathscr{W}^i(1,s) &= U^i(s) + \mathscr{S}_j(s), \quad j = j_0, \end{cases} \tag{6.5}$$

where $\mathscr{M}_j$ and $\mathscr{N}_j$ are the operators M_j and N_j with the time-derivative operators $\partial/\partial t$ and $\partial^2/\partial t^2$ replaced by s and s^2, respectively, $\Gamma_j(s)$ and $U^i(s)$ are the Laplace transform of $\gamma_j(t)$ and $u^i(t)$, respectively, and $\mathscr{S}_j(s)$ is a polynomial of s representing the initial conditions at the boundaries $x = 0$ and $x = 1$. It is easy to see that $\mathscr{S}_j(s) = 0$ when both M_j and N_j are time-invariant.

Define

$$\eta^i(x,s) = \left(\mathscr{W}^i \ \frac{\partial}{\partial x}\mathscr{W}^i \ \ldots \ \frac{\partial^{n-1}}{\partial x^{n-1}}\mathscr{W}^i \right)^T, \tag{6.6}$$

$$\mathbf{p}^i(x,s) = \left(0\,0 \ \ldots \ 0 \ \frac{\Theta(x,s) + \mathscr{G}^i(x,s)}{a_n s^2 + b_n s + c_n} \right)^T, \tag{6.7}$$

$$\mathbf{r}^i(s) = \begin{pmatrix} \Gamma_1(s) + \mathscr{S}_1(s) \\ \vdots \\ \Gamma_{j_0-1}(s) + \mathscr{S}_{j_0-1}(s) \\ U^i(s) + \mathscr{S}_{j_0}(s) \\ \Gamma_{j_0+1}(s) + \mathscr{S}_{j_0+1}(s) \\ \vdots \\ \Gamma_n(s) + \mathscr{S}_n(s) \end{pmatrix}, \tag{6.8}$$

$$F(s) = \begin{pmatrix} 0 & 1 & 0 & \cdots & 0 \\ 0 & 0 & 1 & \cdots & 0 \\ \vdots & \vdots & \vdots & \ddots & \vdots \\ 0 & 0 & 0 & \cdots & 1 \\ -d_0(s) & -d_1(s) & -d_2(s) & \cdots & -d_{n-1}(s) \end{pmatrix}, \tag{6.9}$$

where $d_k(s) = (a_k s^2 + b_k s + c_k)/(a_n s^2 + b_n s + c_n)$, $k = 0, 1, \ldots, n-1$, with a_k, b_k and c_k given in the operators A, B, and C. Note that the matrix $F(s)$ is not a function of x. By (6.6)-(6.9), equations (6.4)-(6.5) are reformulated into a matrix form in the Laplace transform domain

$$\frac{\partial}{\partial x}\eta^i(x,s) = F(s)\eta^i(x,s) + \mathbf{p}^i(x,s), \quad x \in (0,1), \tag{6.10}$$

$$\mathscr{M}(s)\eta^i(0,s) + \mathscr{N}(s)\eta^i(1,s) = \mathbf{r}^i(s), \tag{6.11}$$

where $\mathscr{M}(s)$ and $\mathscr{N}(s)$ are $n \times n$ complex matrices, consisting of the coefficients of the operators $\mathscr{M}_j$ and $\mathscr{N}_j$, $j = 1, 2, \ldots, n$.

System (6.10) with the boundary condition (6.11) defines a one-dimensional boundary value problem. The following lemma, which is directly from [95], gives the structure of the solution for $\eta^i(x,s)$.

Lemma 6.1 *Suppose the system (6.10) with $\mathbf{p}^i = 0$ and $\mathbf{r}^i = 0$ has only the null solution. Then there exists a unique solution of system (6.10) with the boundary condition (6.11),*

$$\eta^i(x,s) = \int_0^1 G(x,\xi,s)\mathbf{p}^i(\xi,s)d\xi + H(x,s)\mathbf{r}^i(s), \tag{6.12}$$

where $x \in (0,1)$, the matrix Green's function is

$$G(x,\xi,s) \triangleq \begin{cases} e^{F(s)x}\left(\mathscr{M}(s) + \mathscr{N}(s)e^{F(s)}\right)^{-1}\mathscr{M}(s)e^{-F(s)\xi}, & \xi < x, \\ -e^{F(s)x}\left(\mathscr{M}(s) + \mathscr{N}(s)e^{F(s)}\right)^{-1}\mathscr{N}(s)e^{F(s)(1-\xi)}, & \xi > x, \end{cases}$$

and the transfer matrix between $\mathbf{r}^i(s)$ and $\eta^i(x,s)$ is $H(x,s) \triangleq e^{F(s)x}\left(\mathscr{M}(s) + \mathscr{N}(s)e^{F(s)}\right)^{-1}$, with $e^{F(s)x}$ being the fundamental matrix of system (6.10).

In detail, since the process model (6.1) has order of n, we write

$$G(x,\xi,s)=\begin{pmatrix} g_{11}(x,\xi,s) & \cdots & g_{1n}(x,\xi,s) \\ \vdots & \ddots & \vdots \\ g_{n1}(x,\xi,s) & \cdots & g_{nn}(x,\xi,s) \end{pmatrix}, \tag{6.13}$$

$$H(x,s)=\begin{pmatrix} h_{11}(x,s) & \cdots & h_{1n}(x,s) \\ \vdots & \ddots & \vdots \\ h_{n1}(x,s) & \cdots & h_{nn}(x,s) \end{pmatrix}. \tag{6.14}$$

From (6.12), the unique solution of system (6.10) with the boundary condition (6.11), it follows that

$$\begin{aligned} \mathscr{W}^i(x,s) &= h_{1j_0}(x,s)U^i(s) \\ &\quad + \int_0^1 \frac{g_{1n}(x,\xi,s)}{a_n s^2+b_n s+c_n}\mathscr{G}^i(\xi,s)d\xi + \Xi(x,s), \end{aligned} \tag{6.15}$$

where

$$\begin{aligned} \Xi(x,s) &\triangleq \int_0^1 \frac{g_{1n}(x,\xi,s)}{a_n s^2+b_n s+c_n}\Theta(\xi,s)d\xi \\ &\quad + \sum_{j=1,j\neq j_0}^{n} h_{1j}(x,s)(\Gamma_j(s)+\mathscr{S}_j(s)) + h_{1j_0}(x,s)\mathscr{S}_{j_0}(s) \end{aligned}$$

denotes all the iteration-independent terms on the right hand side of (6.15). Considering the concerned output $y^i(t)=w^i(x^*,t)$, it follows from (6.15) that

$$Y^i(s) = h_{1j_0}(x^*,s)U^i(s) + \int_0^1 \frac{g_{1n}(x^*,\xi,s)}{a_n s^2+b_n s+c_n}\mathscr{G}^i(\xi,s)d\xi + \Xi(x^*,s), \tag{6.16}$$

where $Y^i(s)$ is the Laplace transform of $y^i(t)$. Noticing the fact that the function $\mathscr{G}^i$ is state-independent and Ξ is iteration-independent, the output $Y^i(s)$ is only manipulated by the input $U^i(s)$ through the transfer function $h_{1j_0}(x^*,s)$.

Remark 6.1 *For a given LIDPS (6.1), a flowchart has been presented above to calculate (6.16). Although tedious matrix operations might be involved, e.g., performing*

matrix diagonalization to derive $e^{F(s)x}$, the introduced method still shows some clear advantages: it is exact, and no approximation has been made; it does not require a knowledge of the system eigensolutions; the system type, differential operators, and boundary conditions are treated uniformly; and the method can be easily extended to LIDPSs with parameters as functions of the spatial coordinate x, e.g., $a_k = a_k(x), b_k = b_k(x)$, and $c_k = c_k(x)$.

Next, ILC design and convergence analysis are addressed based on the input-output relationship (6.16).

6.4 ILC Design and Convergence Analysis

In order to demonstrate our idea clearly, a simple scenario: there is no iteration-dependent external disturbance in (6.1), namely, $g^i(x,t) \equiv 0$ in (6.1), is first considered.

6.4.1 LIDPSs Without Iteration-dependent External Disturbance

In the absence of iteration-dependent external disturbance ($g^i(x,t) = 0$), (6.16) becomes

$$Y^i(s) = h_{1j_0}(x^*,s)U^i(s) + \Xi(x^*,s). \tag{6.17}$$

Denote by $Y_d(s)$ and $U_d(s)$ the Laplace transforms of $y_d(t)$ and $u_d(t)$, respectively. The uniqueness of solution of LIDPS (6.1) implies that

$$Y^d(s) = h_{1j_0}(x^*,s)U^d(s) + \Xi(x^*,s). \tag{6.18}$$

The expressions of (6.17) and (6.18) mean that the dynamics of the LIDPS is absolutely repeatable, i.e., same control input profiles always lead to identical system outputs. Let $E^i(s) \triangleq Y^d(s) - Y^i(s)$ be the Laplace transform of tracking error in the ith iteration.

Then, the central task of ILC is to iteratively tune $U^i(s)$ such that $\lim_{i\to\infty} E^i(s) = 0$ or equivalently $\lim_{i\to\infty} U^i(s) = U^d(s)$ for the concerned frequency range.

Define the ILC updating law as follows,

$$U^{i+1}(s) = U^i(s) + \rho(s)E^i(s), \;\; i \in \mathscr{Z}, \tag{6.19}$$

where the learning gain function $\rho(s)$ is to be determined. From (6.19), it can be seen that the control input in the $(i+1)$th iteration consists of two parts: the first part is the control input profile in the previous iteration and the second part is relevant to the tracking error profile in the previous iteration. Since both $U^i(s)$ and $E^i(s)$ are available before implementing control in the $(i+1)$th iteration, the ILC law (6.19) is obviously a feedforward control scheme. It is also worth noticing that different choices of the learning function $\rho(s)$ will induce different categories of ILC schemes, for instance, $\rho(s) = \rho_0$ corresponds to a pure P-type ILC, $\rho(s) = \rho_0 s$ to a D-type ILC, and $\rho(s) = \rho_0 s^2$ to a D^2-type ILC, where ρ_0 is a constant.

Theorem 6.1 *Let Ω be the concerned frequency range. If there exists a constant ζ such that*

$$\sup_{\omega\in\Omega} \left|1 - \rho(j\omega)h_{1j_0}(x^*, j\omega)\right| \leq \zeta < 1, \tag{6.20}$$

where $j = \sqrt{-1}$ is the imaginary unit, then $E_i(j\omega), \omega \in \Omega$ will converge to zero asymptotically when $i \to \infty$.

Proof. Observing the input-output relationship (6.17), the term $\Xi(x^*, s)$ is iteration-independent. As such, in any two consecutive iterations,

$$Y^{i+1}(s) - Y^i(s) = h_{1j_0}(x^*, s)(U^{i+1}(s) - U^i(s)).$$

Further, applying the ILC law (6.19) leads to

$$Y^{i+1}(s) - Y^i(s) = \rho(s)h_{1j_0}(x^*, s)E^i(s). \tag{6.21}$$

Now, the relationship between $E^{i+1}(s)$ and $E^i(s)$ can be evaluated as follows,

$$\begin{aligned} E_{i+1}(s) &= Y_d(s) - Y_{i+1}(s) = Y_d(s) - Y_i(s) - [Y_{i+1}(s) - Y_i(s)] \\ &= E_i(s) - \rho(s) h_{1j_0}(x^*, s) E_i(s) \\ &= [1 - \rho(s) h_{1j_0}(x^*, s)] E_i(s), \end{aligned} \tag{6.22}$$

where the equality (6.21) is used. Then, for any $\omega \in \Omega$, there has

$$\begin{aligned} |E^{i+1}(j\omega)| &= |[1 - \rho(j\omega) h_{1j_0}(x^*, j\omega)] E_i(j\omega)| \\ &\leq |1 - \rho(j\omega) h_{1j_0}(x^*, j\omega)| |E^i(j\omega)| \\ &\leq \sup_{\omega \in \Omega} |1 - \rho(j\omega) h_{1j_0}(x^*, j\omega)| |E^i(j\omega)| \\ &\leq \zeta |E^i(j\omega)|. \end{aligned} \tag{6.23}$$

Applying the inequality (6.23) repeatedly yields $\forall \omega \in \Omega$,

$$|E^{i+1}(j\omega)| \leq \zeta |E^i(j\omega)| \leq \zeta^2 |E^{i-1}(j\omega)| \leq \cdots \leq \zeta^{i+1} |E^0(j\omega)|.$$

Since $0 \leq \zeta < 1$, $\lim_{i \to \infty} \zeta^{i+1} = 0$, thus $\lim_{i \to \infty} |E^{i+1}(j\omega)| = 0$, $\forall \omega \in \Omega$. ■

Remark 6.2 *For any real implementations, the ILC law can be designed as follows.*

(1) *Calculate the input-output transfer function $h_{1j_0}(x^*, s)$ from the LIDPS (6.1).*

(2) *Determine the concerned frequency range Ω, and solve the learning function $\rho(s)$ from the inequality (6.20).*

(3) *Perform the inverse Laplace transform for (6.19) and implement the induced ILC law in the time domain.*

Remark 6.3 *The convergence condition for the ILC law (6.19) is given in (6.20), where the pre-determination of the concerned frequency range Ω is obviously crucial. First,*

at least, Ω includes the set of reference frequencies as a subset. Second, since many other frequency components, e.g., external disturbance and measurement noise, are involved in the system simultaneously, Ω has to be expanded to cover these frequencies. In practice, (6.20) can be solved numerically, where the transfer function h_{1j_0} is approximated by sampled-data system. When the reference contains only a finite number of frequencies up to ω_b rad/s that are below the Nyquist frequency ω_s rad/s, the concerned frequency range can be chosen as $\Omega = [0, \omega_c]$, where ω_c is a cutoff frequency chosen for the used Q-filter in the range $\omega_s > \omega_c > \omega_b$.

Next, the effect of non-repeatable inhomogeneous disturbance to the control performance of the proposed method will be considered.

6.4.2 LIDPSs With Iteration-dependent External Disturbance

The main idea of ILC is to compensate for repeatable tracking error via iterative learning. When nonrepeatable source terms are presented in the process, the ILC performance might be degraded in the sense that the tracking error would not fully vanish but may be kept within an acceptable error bound.

In this case, we have $g^i(x,t) \neq 0$ in system (6.1), and the main result can be summarized as follows.

Theorem 6.2 *Let Ω be the concerned frequency range. If there exist constants ζ and ε such that (6.20) and*

$$\sup_{x\in(0,1),\omega\in\Omega} \left|\mathscr{G}^i(x, j\omega)\right| \leq \varepsilon < \infty \tag{6.24}$$

hold, then $Y^i(j\omega),\ \omega \in \Omega$ will converge to a neighborhood of $Y^d(j\omega)$ that is given in

(6.18) asymptotically with maximum possible error $\varepsilon_1/(1-\zeta)$ *when* $i \to \infty$*, where*

$$\varepsilon_1 \triangleq 2\varepsilon \sup_{\omega\in\Omega} \left| \int_0^1 \frac{g_{1n}(x^*,\xi,j\omega)}{a_n(j\omega)^2 + b_n(j\omega) + c_n} d\xi \right|. \tag{6.25}$$

Proof. In any two consecutive iterations, the inhomogeneous term $\Xi(x^*,s)$ in (6.16) is iteration-independent or repeatable, thus

$$\begin{aligned} Y^{i+1}(s) - Y^i(s) &= h_{1j_0}(x^*,s)(U^{i+1}(s) - U^i(s)) \\ &\quad + \int_0^1 \frac{g_{1n}(x^*,\xi,s)}{a_n s^2 + b_n s + c_n} \left(\mathscr{G}^{i+1}(\xi,s) - \mathscr{G}^i(\xi,s)\right) d\xi. \end{aligned} \tag{6.26}$$

Further, applying the ILC law (6.19) in (6.26) leads to

$$\begin{aligned} Y^{i+1}(s) - Y^i(s) &= \rho(s) h_{1j_0}(x^*,s) E^i(s) \\ &\quad + \int_0^1 \frac{g_{1n}(x^*,\xi,s)}{a_n s^2 + b_n s + c_n} \left(\mathscr{G}^{i+1}(\xi,s) - \mathscr{G}^i(\xi,s)\right) d\xi. \end{aligned} \tag{6.27}$$

In consequence, the relationship between $E^{i+1}(s)$ and $E^i(s)$ can be evaluated as follows,

$$\begin{aligned} E_{i+1}(s) &= Y_d(s) - Y_{i+1}(s) = Y_d(s) - Y_i(s) - [Y_{i+1}(s) - Y_i(s)] \\ &= [1 - \rho(s) h_{1j_0}(x^*,s)] E_i(s) \\ &\quad - \int_0^1 \frac{g_{1n}(x^*,\xi,s)}{a_n s^2 + b_n s + c_n} \left(\mathscr{G}^{i+1}(\xi,s) - \mathscr{G}^i(\xi,s)\right) d\xi \end{aligned} \tag{6.28}$$

where the equality (6.27) is used. Considering the bound information (6.24), it gives

$$\begin{aligned} |E^{i+1}(j\omega)| &\leq |1 - \rho(j\omega) h_{1j_0}(x^*,j\omega)||E^i(j\omega)| \\ &\quad + \left| \int_0^1 \frac{g_{1n}(x^*,\xi,j\omega)}{a_n(j\omega)^2 + b_n(j\omega) + c_n} \left(\mathscr{G}^{i+1} - \mathscr{G}^i\right)(\xi,j\omega) d\xi \right| \\ &\leq \sup_{\omega\in\Omega} |1 - \rho(j\omega) h_{1j_0}(x^*,j\omega)||E^i(j\omega)| \\ &\quad + 2\varepsilon \sup_{\omega\in\Omega} \left| \int_0^1 \frac{g_{1n}(x^*,\xi,j\omega)}{a_n(j\omega)^2 + b_n(j\omega) + c_n} d\xi \right| \leq \zeta |E^i(j\omega)| + \varepsilon_1, \end{aligned} \tag{6.29}$$

where ε_1 is defined in (6.25) and the condition (6.20) is used. Applying (6.29) repeatedly leads to

$$\begin{aligned} |E^{i+1}(j\omega)| &\leq \zeta(\zeta|E^{i-1}(j\omega)|+\varepsilon_1)+\varepsilon_1 \\ &\vdots \\ &\leq \zeta^{i+1}|E^0(j\omega)|+\varepsilon_1\zeta^i+\cdots+\varepsilon_1 \\ &= \zeta^{i+1}|E^0(j\omega)|+\frac{1-\zeta^{i+1}}{1-\zeta}\varepsilon_1. \end{aligned} \tag{6.30}$$

Due to the boundedness of $|E^0(j\omega)|$, and the fact $0 \leq \zeta < 1$, $\lim_{i\to\infty}|E^{i+1}(j\omega)| \leq \lim_{i\to\infty}\zeta^{i+1}|E^0(j\omega)|+\lim_{i\to\infty}\frac{1-\zeta^{i+1}}{1-\zeta}\cdot\varepsilon_1 = \frac{\varepsilon_1}{1-\zeta}$. The proof is complete. ■

Remark 6.4 *Theorem 6.2 reveals that the ultimate bound of tracking error is proportional to the maximum magnitude of nonrepeatable external disturbances, which is obviously rational. In practice, a possible way to reduce the effect of nonrepeatable components to ILC performance is to incorporate robust feedback control such as the proportional-integral controller.*

6.5 Robustness Concern

For practical applications, many engineering or industrial systems are nonlinear distributed parameter systems. Though linearization can be carried out, the linearized model parameters will change with operating conditions. Fortunately, ILC is a kind of model-free control method in the sense that it is still efficient in the presence of certain model uncertainties or modeling error. Denote $P_e(s)$ the estimation of the actual input-output transfer function model $h_{1j_0}(x^*,s)$, which is obtained by conducting model identification from real processes. When $P_e(s)$ is minimum phase and proper, the learning function $\rho(s)$ can be chosen to be $1/P_e(s)$ straightforwardly, which leads to the

fastest possible learning convergence. Taking the condition (6.20) into account for the proposed ILC scheme, the convergence of ILC is achieved if

$$\sup_{\omega\in\Omega}\left|1-h_{1j_0}(x^*,j\omega)/P_e(j\omega)\right|<1.$$

When $P_e(s)$ is proper but nonminimum phase, the learning filter $\rho(s)$ can be designed accordingly based on pole-zero cancelation [96].

Further, in stand ILC, a low-pass zero-phase Q filter is essentially utilized to enhance the system robustness against model uncertainties and modeling error, and to suppress the noise transmission in the learning process [96]. As such, the ILC law is revised to

$$U^{i+1}(s)=Q(s)(U^i(s)+\rho(s)E^i(s)),\ \ i\in\mathscr{Z}. \tag{6.31}$$

The corresponding convergence result can be summarized as follows.

Theorem 6.3 *Let Ω be the concerned frequency range. If there exists a constant ζ such that*

$$\sup_{\omega\in\Omega}\left|Q(j\omega)(1-\rho(j\omega)h_{1j_0}(x^*,j\omega))\right|\le\zeta<1, \tag{6.32}$$

then $E_i(j\omega),\omega\in\Omega$ will converge to a neighborhood of zero asymptotically when $i\to\infty$.

The convergence analysis can be performed similarly as Theorem 6.1 and Theorem 6.2 based on contraction mapping method.

The inequality (6.32) means that Nyquist plot of $Q(1-\rho h_{1j_0})$ should be within a unit circle centered at the origin of the complex plane. This learning condition can be

satisfied by the proper designs of $Q(s)$ and $\rho(s)$. Noticing that

$$\begin{aligned} E^{i+1}(s) &= Q(s)(1-\rho(s)h_{1j_0}(x^*,s))E^i(s)+(1-Q(s))(Y_d(s)-\Xi(x^*,s)) \\ &\quad -\int_0^1 \frac{g_{1n}(x^*,\xi,s)}{a_n s^2+b_n s+c_n}\mathscr{G}^{i+1}(\xi,s)d\xi \\ &\quad +Q(s)\int_0^1 \frac{g_{1n}(x^*,\xi,s)}{a_n s^2+b_n s+c_n}\mathscr{G}^{i}(\xi,s)d\xi, \end{aligned} \tag{6.33}$$

the tracking error $E(s)$ is also affected by $Y_d(s)-\Xi(x^*,s)$ modulated through the factor $1-Q(s)$, and by $\int_0^1 \frac{g_{1n}(x^*,\xi,s)}{a_n s^2+b_n s+c_n}\mathscr{G}^i(\xi,s)d\xi$ modulated through the factor $Q(s)$. Since $Y_d(s)-\Xi(x^*,s)$ is usually much larger than the iteration-dependent factor, the design of filter $Q(s)$ must take into account that

$$\sup_{\omega\in\Omega}|1-Q(j\omega)| \ll 1. \tag{6.34}$$

Although a steady-state error may occur by using filter $Q(s)$, a remarkable advantage is that the stability region for certain frequencies can be increased if $Q(s)$ is a filter with a gain less than one for those frequencies. This can be seen from (6.32) or equivalently, the condition

$$\left|1-\rho(j\omega)h_{1j_0}(x^*,j\omega)\right| < \frac{1}{|Q(j\omega)|}, \quad \omega\in\Omega.$$

For the point-tracking control of nonlinear PDE processes, especially those that cannot be linearized, transfer function based analysis is obviously not applicable. Also, it is impossible to find a general ILC design framework for them. However, the work [20] reveals that simple (D-type) ILC scheme still demonstrates its efficacy for some highly nonlinear systems. The extension of ILC from linear PDEs to nonlinear PDEs will be addressed in the next chapter.

6.6 Illustrative Example with Analysis and Design

Consider the parabolic heat conduction equation

$$\begin{cases} C_p\nu\frac{\partial w^i}{\partial t} = K_0\frac{\partial^2 w^i}{\partial x^2} + f(x,t), \ \ x\in(0,1), \ \ t\in(0,T], \\ \frac{\partial}{\partial x}w^i(0,t) = 0, \ \ t\in[0,T], \\ K_0\frac{\partial}{\partial x}w^i(1,t) = u^i(t), \ t\in[0,T], \\ w^i(x,0) = 0, \ \ x\in[0,1], \end{cases} \tag{6.35}$$

where $T>0$ is the time length in each iteration, K_0, C_p, and ν are constant thermal conductivity, specific heat, and mass density, respectively [89]. The source term $f(x,t) = 2xt + x^2$ behaves as the system uncertainty. In addition, the heat flux $u^i(t) = K_0\partial w^i(1,t)/\partial x$ is the control input, and the temperature state $y^i(t) \triangleq w^i(0,t)$ is the system output.

First calculate the input-output transfer function of the system (6.35). Comparing (6.35) with the general LIDPS (6.1), there has that $a_0 = a_1 = a_2 = 0$, $b_0 = C_p\nu$, $b_1 = b_2 = 0$, $c_0 = c_1 = 0, c_2 = -K_0$, and the matrix F in (6.9) is

$$F(s) = \begin{pmatrix} 0 & 1 \\ \alpha s & 0 \end{pmatrix}, \tag{6.36}$$

where $\alpha \triangleq C_p\nu/K_0$. The eigenvalues of $F(s)$ are $\lambda_{1,2}(s) = \pm\sqrt{\alpha s}$. Hence, $e^{F(s)x}$ can be computed by performing matrix diagonalization,

$$\begin{aligned} e^{F(s)x} &= Q(s)e^{J(s)x}Q^{-1}(s) \\ &= \begin{pmatrix} \cosh(\sqrt{\alpha s}x) & \frac{1}{\sqrt{\alpha s}}\sinh(\sqrt{\alpha s}x) \\ \sqrt{\alpha s}\sinh(\sqrt{\alpha s}x) & \sinh(\sqrt{\alpha s}x) \end{pmatrix} \end{aligned}$$

where $Q(s) = \begin{pmatrix} 1 & 1 \\ \sqrt{\alpha s} & -\sqrt{\alpha s} \end{pmatrix}$, $e^{J(s)x} = \begin{pmatrix} e^{\sqrt{\alpha s}x} & 0 \\ 0 & e^{-\sqrt{\alpha s}x} \end{pmatrix}$. Meanwhile, it is

easy to see $\mathscr{M}(s)=\begin{pmatrix} 0 & 1 \\ 0 & 0 \end{pmatrix}$, $\mathscr{N}(s)=\begin{pmatrix} 0 & 0 \\ 0 & K_0 \end{pmatrix}$. Since both $\mathscr{M}(s)$ and $\mathscr{N}(s)$ are constant matrices, $\mathscr{S}_1(s)=\mathscr{S}_2(s)=0$ in (6.5). Further,

$$\begin{aligned} H(x,s) &= e^{F(s)x}\left(M(s)+N(s)e^{F(s)}\right)^{-1} \\ &= \begin{pmatrix} h_{11}(x,s) & h_{12}(x,s) \\ 0 & h_{22}(x,s) \end{pmatrix}, \end{aligned}$$

can be calculated, where $h_{11}=-\frac{1}{\sqrt{\alpha s}}e^{-\sqrt{\alpha s}x}$, $h_{12}=\frac{\cosh(\sqrt{\alpha s}x)}{K_0\sqrt{\alpha s}\sinh(\sqrt{\alpha s})}$, $h_{22}=\frac{\sinh(\sqrt{\alpha s}x)}{K_0\sinh(\sqrt{\alpha s})}$, and

$$G(x,\xi,s)=\begin{cases} \begin{pmatrix} g_{11}(x,\xi,s) & g_{12}(x,\xi,s) \\ 0 & 0 \end{pmatrix}, & \xi<x \\ \begin{pmatrix} h_{12}(x,s)\phi(\xi,s) & h_{12}(x,s)\varphi(\xi,s) \\ h_{22}(x,s)\phi(\xi,s) & h_{22}(x,s)\varphi(\xi,s) \end{pmatrix}, & \xi>x, \end{cases}$$

where $g_{11}=\sqrt{\alpha s}g_{12}(x,\xi,s), g_{12}=-h_{11}(x,s)\sinh(\sqrt{\alpha s}\xi)$, $\phi=-K_0\sqrt{\alpha s}\sinh(\sqrt{\alpha s}(1-\xi)), \varphi=-K_0\sinh(\sqrt{\alpha s}(1-\xi))$. As such, it immediately gives that

$$H(0,s)=\begin{pmatrix} h_{11}(0,s) & h_{12}(0,s) \\ 0 & h_{22}(0,s) \end{pmatrix}, \tag{6.37}$$

and that

$$G(0,\xi,s)=\begin{pmatrix} h_{12}(0,s)\phi(\xi,s) & h_{12}(0,s)\varphi(\xi,s) \\ h_{22}(0,s)\phi(\xi,s) & h_{22}(0,s)\varphi(\xi,s) \end{pmatrix}. \tag{6.38}$$

Immediately, from (6.16) the relationship between the input $U(s)$ and the output $Y(s)$ in the ith iteration can be derived

$$\begin{aligned} Y^i(s) &= h_{12}(0,s)U^i(s)+\int_0^1 \frac{h_{12}(0,s)\varphi(\xi,s)}{-K_0}\mathscr{F}(\xi,s)d\xi \\ &= \frac{1}{K_0\sqrt{\alpha s}\sinh(\sqrt{\alpha s})}U^i(s)+\int_0^1 \frac{\sinh(\sqrt{\alpha s}(1-\xi))}{K_0\sqrt{\alpha s}\sinh(\sqrt{\alpha s})}\mathscr{F}(\xi,s)d\xi, \end{aligned} \tag{6.39}$$

where $\mathscr{F}(x,s)$ is the Laplace transform of the inhomogeneous function $f(x,t) = 2xt + x^2$.

The poles of $h_{12}(0,s)$ are the zeros of its denominator and are the real non-positive numbers $-k^2\pi^2/\alpha, k \in \mathscr{Z}$, while the zeros are the zeros of the numerator and are the real negative numbers $-(k\pi+\pi/2)^2/\alpha$. Note that, owing to the pole at 0, $h_{12}(0,s)$ is not stable, but it is well-posed, and positive real [89]. The considered heat conduction process demonstrates complicated input-output dynamics in the sense that the infinite dimensional linear operator $\sqrt{s}$ is involved. It is hard to solve the inequality (6.20) analytically to determine the convergence condition for the learning function $\rho(s)$. Alternatively, it may be solved numerically by adopting some approximation schemes of transfer functions.

Recall that, in (6.35), the heat flux at the boundary $x = 1$ is adopted as control input to perform the temperature output tracking at the other boundary $x = 0$. This stimulates us to consider D-type ILC for (6.35), namely, $\rho(s) = \rho_0 s$ with ρ_0 being the constant learning gain. Then, (6.20) becomes

$$\left|1 - \rho_0 \frac{\sqrt{s}}{K_0\sqrt{\alpha}\sinh(\sqrt{\alpha s})}\right| \leq \zeta < 1, \;\; s = j\omega, \;\; \omega \in \Omega. \tag{6.40}$$

Employing the Oustaloup-Recursive-Approximation method [97], for the prespecified sampling period $T_s = 0.01$ s, the operator $\sqrt{s}$ in (6.40) can be approximated by

$$\mathscr{A}(z) = \frac{14.14z^5 - 7.07z^4 + 1.414z^3 - 2.475z^2 + 0.707z - 1.414}{z^5 + 0.5z^4 + 0.1z^3 + 0.175z^2 + 0.05z + 0.1}.$$

Substituting $\sqrt{s}$ by $\mathscr{A}(z)$ in (6.40), it follows that

$$\left|1 - \rho_0 \frac{\mathscr{A}(z)}{K_0\sqrt{\alpha}\sinh(\sqrt{\alpha}\mathscr{A}(z))}\right| \leq \zeta < 1, \; z = e^{j\omega T_s}, \; \omega \in \Omega,$$

from which the feasible range of ρ_0 can be solved numerically.

When the concerned frequency set Ω contains more than one frequency component, it is rational to address the optimal learning gain design by solving the following min-max problem:

$$\begin{aligned} J &= \min_{\rho_0} \max_{\omega\in\Omega} \left| 1-\rho_0 \tfrac{\mathscr{A}(e^{j\omega T_s})}{\sinh(\mathscr{A}(e^{j\omega T_s}))} \right|, \\ \text{s.t.} \quad & \left| 1-\rho_0 \tfrac{\mathscr{A}(e^{j\omega T_s})}{\sinh(\mathscr{A}(e^{j\omega T_s}))} \right| < 1, \ \forall \omega \in \Omega, \end{aligned} \tag{6.41}$$

where the constraint comes from the convergence condition of ILC.

Assume that $C_p = 1, \nu = 1, K_0 = 1$ in simulation, yielding $\alpha = C_p \nu / K_0 = 1$. Further, let the output reference be $y^d(t) = t^3(10-t)^3/1000$°C, $t \in [0,10]$ mins. Then, the corresponding reference frequency is at $\omega_b = 0.01$ rad/s, and $\rho_0 = 2.839$ is optimal when the single reference frequency is involved in the system. Nevertheless, when ILC is performed for any LIDPSs, the measured signals are usually corrupted by other frequency parts and noise. These components may degrade the performance of ILC in practice, especially when high-order ILC is applied. For the considered D-type ILC, a Q-filter is then adopted to filter them out from the measured signals, namely,

$$Q(z) = H(z)H(z^{-1}), \quad H(z) = \frac{1+z^{-1}+\cdots+z^{-(N_0-1)}}{N_0}. \tag{6.42}$$

Note that, on the one hand, the filter $Q(z)$ given in (6.42) is a zero-phase filter, which does not incur any phase delay. On the other hand, such a filter is non-causal in the time domain, which can only be implemented off-line in general. From the ILC law (6.19), however, it can be seen that causality is not an issue for ILC implementation, because the current input U_{i+1} only uses the signals of previous iteration, namely, E_i and U_i. For implementation, choose $N_0 = 20$ in (6.42) that yields a cut-off frequency of $\omega_c = 10$ rad/s. As such, the concerned frequency range is $\Omega = [0, \omega_c]$, and solving (6.41) renders to $\rho_0 = 0.7444$.

Now, set $\rho(s) = 0.7444s$, and the initial heat flux input $u^0(t) = 0\,W/m^2$. The system (6.35) is simulated using the Matlab solver *'pdepe'* with sampling period 0.6 s in the temporal domain and 0.01 m in the spatial domain, respectively. Since ILC is a feed-forward control scheme, the control input boundary condition can be calculated offline and updated directly in *'@pdex1bc'* by defining the input variable as a global variable. Figs. 6.1 to 6.3 give the simulation results. As can be seen from Fig. 6.1, the maximal tracking error $|e^i|_s \triangleq \sup_{t\in[0,\ 10]} \min |e^i(t)|$ decreases drastically from 13.20 to 0.0371 within 7 iterations. Observing the output tracking profile of the 7th iteration in Fig. 6.2, the difference between y^7 and y^d is almost invisible. Meanwhile, by inputting the learned heat flux control profile in the 7th iteration, the induced temperature variation versus time and space are shown in Fig. 6.3. All the simulation results demonstrate the efficacy of D-type ILC to the boundary control of system (6.35).

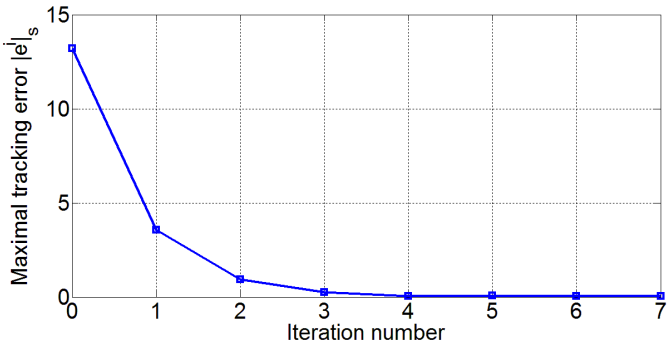

Figure 6.1: Maximal tracking error profile using D-type ILC for the heat conduction process (6.35).

Remark 6.5 *D-type ILC scheme has been considered for the above parabolic example. In practice, the structure of ILC can be chosen by evaluating the characteristics of controlled LIDPS, the availability of output data, and the complexity of control algorithm, etc. Probably, low-order ILC takes a relatively simpler structure than high-order ILC, thus is more implementable. However, since high-order learning filter approximates the*

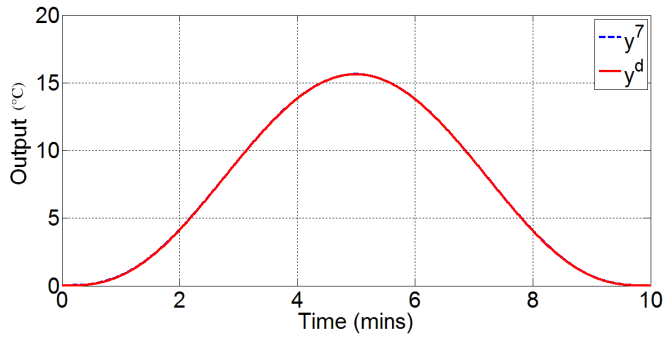

Figure 6.2: Output temperature tracking profile in the 7th iteration, where the difference between y^7 and y^d is almost invisible.

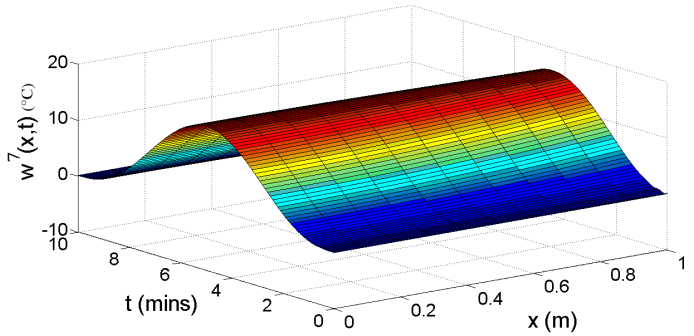

Figure 6.3: Temperature variation versus time and space, generated by the learned input profile in the 7th iteration of ILC.

inverse of the input-output transfer function of LIDPS more closely, the corresponding high-order ILC could achieve faster convergence speed.

6.7 Conclusion

This chapter presents the ILC design and analysis result for the boundary control of LIDPSs. Due to the generality of the structure of LIDPS, many well-known processes, e.g., the heat conduction and the wave propagation, are integrated together. Noticing the linear characteristic of systems and that the system transfer function can be derived in a closed form, the ILC design and convergence analysis are performed in the frequency domain. The proposed control scheme is simple in structure, able to deal with parametric and non-parametric uncertainties, and makes full use of the process repetition.

Chapter 7

ILC for Nonlinear Inhomogeneous Heat Equations

7.1 Introduction

As an extension of Chapter 6, this chapter investigates ILC design for a class of nonlinear inhomogeneous heat equations. Because of the nonlinearity of the system, the techniques based on Laplace transformation in Chapter 6 are no longer applicable and new analysis methods have to be developed.

Heat control problem has been frequently encountered in many industrial or chemical processes, e.g., indirect heating of liquids and polymers, single-fluid batch processing, pipeline tracing, energy recovery, low pressure cogeneration, drying and heating of bulk materials, gas processing, and ebullient cooling. In the control of heat transfer equations or more general parabolic PDE systems, repetition and correction mechanisms are as common as in lumped parameter systems modelled by ordinary differential equations (ODEs). Examples include batch heat treatment furnace [98], tubular

heat exchangers [99], batch thermal sterilization processes [100], temperature control of tokamak plasmas [36], and many other batch processes. In [101–105], the boundary control problem for heat processes was studied under strict assumptions on the admitted uncertainties and perturbations. Moreover, the most important characteristic of processes, i.e., the repetitiveness, will be ignored, when the control schemes proposed in [101–105] are applied for batch processes.

In this chapter, a D-type anticipatory ILC scheme is applied to the boundary control of a class of nonlinear inhomogeneous heat equations, where the nonlinear heat source is state-independent or state-dependent. Under repeatable process environment, the heat flux at one side is considered as the control input while the temperature measurement at the other side is considered as the control output. First, the heat conduction equation is transformed into its integral form, based on which the input-output error dynamics are presented clearly. Then, rigorous analysis is performed to exploit the properties of the embedded Jacobi Theta functions in the error dynamics. With practical assumption on the uncertainties of heat equations, these properties facilitate the consequent ILC design and convergence analysis. As a result, by iteratively tune the heat flux boundary condition on one side, the boundary output at the other side can track the desired reference pointwisely.

It is worthy of noticing that we neither simplify the infinite-dimensional heat equations to finite-dimensional ODE systems as in [40] nor replace them by the discrete-time equivalences as in [35]. On the one hand, in [40], the infinite-dimensional heat equation is simplified as a finite-dimensional ODE system at steady-state stage, which is only applicable for set-point control task. If tracking control is considered as in our work, model simplification has the disadvantage of not taking relevant heat conduction

issues into account, namely, the distributed parameter characteristic of heat conduction process is neglected, thus is ineffective here. On the other hand, in [35], explicit discretization is conducted for a class of linear heat equations to derive a multidimensional discrete linear system, based on which the ILC law is designed. The models obtained by the approach are of the local type and hence the state-space dimension is low and finite. It is obviously necessary to ensure that they adequately capture the dynamics of the defining PDEs. Since this problem has not been addressed in [35], there is much further research to be done on this approach to ensure that an adequate discrete model for design is produced in the most efficient way. Meanwhile, numerical instability must be prevented by imposing limits on the time and space discretization periods. Although it can be calculated by means of some numerical analysis methods or software tools, it also hinders us to apply the proposed ILC scheme conveniently, which might be a disadvantage of ILC with model discretization. In particular, when the heat equation is nonlinear and/or possesses some structural uncertainties, the analysis method proposed for linear systems in [35] will lose its efficacy. In our work, the ILC design and analysis is performed for the original heat conduction equation, thus a class of "real" distributed parameter systems. Without checking the numerical stability or the adequate approximation property of the reduced plant, the proposed control scheme is applicable directly for the boundary tracking control of nonlinear heat equations.

Moreover, owing to the fact that ILC is a feedforward control, the proposed scheme not only makes anticipatory compensation possible to overcome the heat conduction delay in boundary output tracking, but also eliminates the gain margin limitation encountered in feedback control.

Throughout this chapter, denote $\mathbf{R}$ the set of real numbers, $\mathscr{N}$ the set of nonnega-

tive integers, Q the set of $\{(x,t)|0<x<1,0<t\leq T\}$, $\overline{Q}$ the closed set of Q, namely, $\{(x,t)|0\leq x\leq 1,0\leq t\leq T\}$, $C^n([l_1,l_2],\mathbf{R})$ the set of scalar continuous functions as $n=0$ or continuously differentiable functions as $n=1$ in the interval $[l_1,l_2]$, and $\mathscr{H}(E,\mathbf{R})$ an infinite-dimensional Hilbert space of scalar functions defined on a domain E. For the function $v(x,t)\in\mathscr{H}(\overline{Q},\mathbf{R})$, v_z denotes its partial derivative with respect to variable z, e.g., $v_t=\partial v/\partial t$ and $v_{xx}=\partial^2 v/\partial x^2$. For simplicity, sometimes the abbreviation v is used instead of $v(x,t)$ below. For a time-related function $f(t)\in\mathbf{R}$, $|f(t)|$ takes its absolute value, and $|f|_\lambda \stackrel{\triangle}{=} \sup_{\tau\in[0,T]} e^{-\lambda\tau}|f(\tau)|$ denotes its λ-norm, where λ is a positive constant.

7.2 System Description and Problem Statement

Consider the heat flux boundary control of the following one-dimensional inhomogeneous heat equation under repeatable environment[106]

$$\begin{cases} v_t^i(x,t) &= v_{xx}^i(x,t)+F(x,t,v^i(x,t),v_x^i(x,t)),\ (x,t)\in Q,\\ v^i(x,0) &= f(x),\quad x\in(0,1),\\ v_x^i(0,t) &= u^i(t),\quad t\in[0,T],\\ v_x^i(1,t) &= g(t),\quad t\in[0,T], \end{cases} \tag{7.1}$$

where $t\in[0,T]$ is the time, $x\in[0,1]$ is the spatial coordinate, $v^i(x,t)\in\mathscr{H}(\overline{Q},\mathbf{R})$ is the temperature measurement at the time t and the position x, and $i\in\mathscr{N}$ is the iteration number. Moreover, $u^i\in C^0([0,T],\mathbf{R})$, $g\in C^0([0,T],\mathbf{R})$, and $f\in C^1((0,1),\mathbf{R})$ such that f and f_x are bounded. The unknown function $F(x,t,v^i,v_x^i)$ is defined on the set $\Theta=\{(x,t,v^i,v_x^i)\mid(x,t)\in\overline{Q},-\infty<v^i,v_x^i<\infty\}$. Assuming the finiteness of $|v^i|$ and $|v_x^i|$, the function $F(x,t,v^i,v_x^i)$ is uniformly Hölder continuous [1] in x and t for each compact

[1] A real or complex-valued function χ on d-dimensional Euclidean space is Hölder continuous when there are nonnegative real constants C and α such that $|\chi(x)-\chi(y)|\leq C|x-y|^\alpha$ for all x and y in the

subset of Q. In addition, there exists an unknown constant C_F such that

$$|F(x,t,p_1,q_1)-F(x,t,p_2,q_2)| \leq C_F\{|p_1-p_2|+|q_1-q_2|\}, \quad (x,t) \in \overline{Q} \tag{7.2}$$

holds for all $(p_i,q_i),\ i=1,2$, namely, $F(x,t,v^i,v^i_x)$ is Lipschitz continuous in the state-dependent variables v^i and v^i_x. It is easy to write down examples of such functions, for example, $F(x,t,p,q)=\sin(xt)\cos(p)+\cos(xt)\sin(q)$. In the context of heat conduction or diffusion, the uncertainty function F can be interpreted as a heat source or sink. For most applications, the nonlinear source or sink F may be extended linearly for p and q beyond the range of physical reality [106]. Due to the generality of F, (7.1) denotes a wide range of heat conduction processes [108]. Further, noticing that the PDE model (7.1) generally describes the diffusion-convection phenomena in open-loop processes, many other important industrial processes can also be formulated within this modelling framework, e.g., industrial chemical reactors [109], biochemical reactors [110], and biofilters for air and water pollution control [111]. Much effort has been put to solve the so-called inverse problems for (7.1) to determine the unknown source term or the boundary heat flux [112].

In this chapter, instead of performing identification for the uncertainties in (7.1), the ILC of the process is considered directly, where the heat flux condition $v^i_x(0,t)=u^i(t)\in C^0([0,T],\mathbf{R})$ is the control input and the boundary temperature $y^i(t)=v^i(1,t)\in C^1([0,T],\mathbf{R})$ is the controlled output. The control objective is to iteratively tune the heat flux condition at one side such that the boundary output at the other side can track the designated continuous differentiable reference $y^d(t)$ as $i\to\infty$. The reference $y^d(t),t\in[0,T]$ is generated by (7.1) with the desired unknown control input $u^d(t),t\in[0,T]$. The magnitude of u^d is assumed to be always less than the maximum heat flux input

domain of χ [107]. The number α is called the exponent of the Hölder condition. If $\alpha=1$, then the function satisfies a Lipschitz condition. If $\alpha=0$, then the function is bounded.

magnitude that is acceptable in the concerned heat conduction process.

Remark 7.1 *To validate our consequent ILC design and analysis, the well-posedness of heat equation (7.1) is always assumed, i.e., the solution of (7.1) exists, is unique, and depends continuously on the problem data consisting of the coefficients in (7.1), the functions appearing in boundary and initial conditions, as well as the region on which (7.1) is required to hold. Actually, according to Theorem 20.3.4 in [106], under the above problem setting, there exists a unique, bounded classic solution $v^i = v^i(x,t)$ for the system (7.1). Thus, given the desired control output y^d, the corresponding control input u^d exists and is unique. It is worthy of highlighting that, by the Banach fixed-point theorem, without the uniqueness of desired control input profile, any contraction mapping based ILC is meaningless.*

Remark 7.2 *For concise presentation, the thermal diffusivity, i.e., the coefficient of the term v^i_{xx} is set as unity in (7.1). Heat equations with non-unity thermal diffusivities can be converted to (7.1) via some transformations. For instance, equations of the form $v_t = \mu v_{xx} + F(x,t,v,v_x)$ can be reduced to the form of (7.1) by the time-scaling transformation $\tau = \mu t$; and the nonlinear equation $\mu(v)v_t = (\mu(v)v_x)_x + F(x,t,v,v_x), \mu(\cdot) > 0$ can be reduced to (7.1) via the change in dependent variable $v_1 = \int_0^v \mu(\zeta)d\zeta$.*

7.3 ILC for Systems with State-Independent Uncertainties

In order to clearly present the main idea on ILC of the heat equation (7.1), a simple scenario is first considered in this section, namely, the uncertainty function F is state-

independent. In consequence, (7.1) is

$$\begin{cases} v_t^i(x,t) &= v_{xx}^i(x,t)+F(x,t), \quad (x,t)\in Q, \\ v^i(x,0) &= f(x), \quad x\in(0,1), \\ v_x^i(0,t) &= u^i(t), \quad t\in(0,T], \\ v_x^i(1,t) &= g(t), \quad t\in(0,T], \end{cases} \tag{7.3}$$

where F is continuous in x and t, respectively. Before presenting the ILC design and convergence analysis, (7.3) can be written into the following integral form [106],

$$\begin{aligned} v^i(x,t) &= \int_0^1 \{\theta(x-\xi,t)+\theta(x+\xi,t)\}f(\xi)d\xi - 2\int_0^t \theta(x,t-\tau)u^i(\tau)d\tau \\ &\quad +2\int_0^t \theta(x-1,t-\tau)g(\tau)d\tau \\ &\quad +\int_0^t\int_0^1 \{\theta(x-\xi,t-\tau)+\theta(x+\xi,t-\tau)\}\times F(\xi,\tau)d\xi d\tau, \end{aligned} \tag{7.4}$$

where the Jacobi Theta function is defined as [113]

$$\theta(x,t)=\sum_{m=-\infty}^{\infty} K(x+2m,t), \quad t>0, \tag{7.5}$$

with

$$K(x,t)=\frac{1}{\sqrt{4\pi t}}\exp\left\{\frac{-x^2}{4t}\right\}, \quad t>0. \tag{7.6}$$

Explicitly, (7.4) gives the unique, bounded continuous solution of the direct problem (7.3). According to the uniqueness of solution of (7.3), given the desired reference output y^d, u^d is also unique and satisfies

$$\begin{aligned} y^d(t) &= \lim_{x\to 1} v^d(x,t) \\ &\triangleq \int_0^1 \{\theta(1-\xi,t)+\theta(1+\xi,t)\}f(\xi)d\xi - 2\int_0^t \theta(1,t-\tau)u^d(\tau)d\tau \\ &\quad +2\int_0^t \theta(0,t-\tau)g(\tau)d\tau \\ &\quad +\int_0^t\int_0^1 \{\theta(1-\xi,t-\tau)+\theta(1+\xi,t-\tau)\}\times F(\xi,\tau)d\xi d\tau. \end{aligned} \tag{7.7}$$

In the ith iteration, similar relation can be derived for y^i and u^i, which is in the form of (7.7) with y^d and u^d replaced by y^i and u^i, respectively.

Define the boundary output error and input error as $e^i(t) = y^d(t) - y^i(t)$ and $\Delta u^i(t) = u^d(t) - u^i(t)$, respectively. From now onwards, augments of functions may be dropped for concise presentation, if no confusions occur. Owing to the iteration-independent properties of functions f, g, and F, it follows that

$$e^i = -2\int_0^t \theta(1, t-\tau)\Delta u^i(\tau)d\tau. \tag{7.8}$$

As can be seen from (7.8), e^i is expressed as a convolution of Δu^i and the Jacobi Theta function θ, namely, the tracking error at the time instant t is relevant to the control input profile from the time instant 0 to t. In principle, when the relative degree of input-output mapping is zero, P-type ILC is sufficient, and the output error information is directly used to update input profile of the next iteration pointwisely. When the relative degree of input-output mapping is non-zero but finite n, D-type ILC should be adopted where the information on the nth-order derivative of output error is supposed to be available. In all the scenarios of finite relative degree, due to the existence of direct transmission term between input and output or its derivative, the additional convolution part is usually discarded in convergence analysis by introducing λ-norm [5]. Since there is no direct transmission term between input and output in (7.8), one natural way to circumvent this difficulty is to produce the direct transmission term by persistent differentiation [114]. However, it is not hard to prove that $\theta(1,t)$ and all its finite-order derivatives vanish at $t \downarrow 0$, where $t \downarrow 0$ means that t decreases from positive and converges to 0 ultimately. This implies that the relative degree of (7.8) is infinite and the persistent differentiation is infeasible. Moreover, in such a state-independent case, (7.8) consists of the convolution part only, thus cannot be discarded using λ-norm. The following

analysis reveals that the infinite relative degree between input and output in (7.8) is caused by the spatial heat conduction delay from one boundary to another boundary, and D-type anticipatory ILC can be selected to achieve the learning convergence under practical system properties.

To facilitate the consequent ILC design and convergence analysis for the input-output error dynamics (7.8), some properties of the kernel function θ are first given.

By the definition of θ function, namely, (7.5) and (7.6),

$$\begin{aligned}\theta(x,t) &= \frac{1}{\sqrt{4\pi t}}\sum_{m=-\infty}^{\infty}\exp\left(\frac{-(x+2m)^2}{4t}\right)\\ &= \frac{1}{2\sqrt{\pi t}}\sum_{m=-\infty}^{\infty}\exp\left(-\frac{\left(\frac{x}{2}+m\right)^2}{t}\right), \quad t>0. \end{aligned} \tag{7.9}$$

Considering the Jacobi Theta function identity [115], it follows from (7.9) that

$$\begin{aligned}\theta(x,t) &= \frac{1}{2}\sum_{n=-\infty}^{\infty}\cos(n\pi x)\exp\left(-n^2\pi^2 t\right)\\ &= \frac{1}{2}\left(1+2\sum_{n=1}^{\infty}\cos(n\pi x)\exp\left(-n^2\pi^2 t\right)\right)\\ &= \frac{1}{2}\theta_3\left(\frac{\pi x}{2},\exp\left(-\pi^2 t\right)\right),\end{aligned}$$

where $\theta_3(z,q)\stackrel{\triangle}{=}1+2\sum_{n=1}^{\infty}q^{n^2}\cos(2nz)$ is the third class of Jacobi Theta function [116].

According to the analysis on Jacobi Theta function in [106] and the well-known results for θ_3 [116], several main properties of $\theta(x,t)$ are presented in the following, without any verification.

(1) For $t>0$, the series for $\theta(x,t)$ and its partial derivatives are uniformly absolutely convergent and continuous.

(2) For $t>0$, $\theta(x,t)$ is periodic in x with periodicity of 2. Thus, the initial space for the involved $\theta(x,t)$ is $x\in(0,2)$.

(3) The singularities of $\theta(x,t)$ occur at $t=0, x=\pm 2n, n\in\mathcal{N}$.

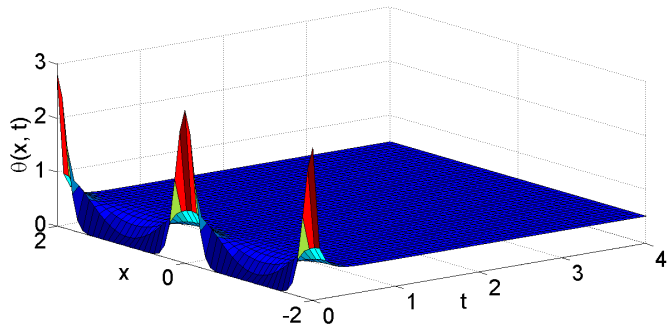

Figure 7.1: Variation of $\theta(x,t)$ in the spatiotemporal domain.

(4) For $t>0$, $\lim_{x\downarrow 0} -2\int_0^t \frac{\partial\theta}{\partial x}(x,t-\tau)g(\tau)d\tau = g(t)$ at each point of continuity of g.

(5) For $t>0$, $\lim_{x\uparrow 1} \frac{\partial\theta}{\partial x}(x,t) = 0$.

(6) For $t>0$, $\lim_{x\uparrow 1} -2\int_0^t \frac{\partial\theta}{\partial x}(x,t-\tau)g(\tau)d\tau = 0$ for any Lebesgue-integrable g. Moreover, this limit is taken on uniformly with respect to t contained in compact sets.

For illustration, Fig. 7.1 shows the variation of $\theta(x,t)$ in the spatiotemporal domain.

Observing the expression of solution (7.4), $\theta(x\pm\xi,t-\tau), 0<\xi<1, 0<\tau<t$ are involved, where $(x,t)\in Q$. Thus, it suffices to consider θ in the domain of $\{(x,t)|-1\leq x\leq 2, 0<t\leq T\}$. Applying the continuity and periodicity properties of the Jacobi Theta function $\theta(x,t)$ as well as its partial derivatives, the following result is derived immediately.

Lemma 7.1 *For all $t\in[\delta,T]$, $0<\delta\ll T$, there exist constants $\kappa_i, i=1,\cdots,4$ such that (1) $\sup_{-1\leq x\leq 2}|\theta(x,t)|\leq\kappa_1$, (2) $\sup_{-1\leq x\leq 2}|\theta_t(x,t)|\leq\kappa_2$, (3) $\sup_{-1\leq x\leq 2}|\theta_x(x,t)|\leq\kappa_3$, and (4) $\sup_{-1\leq x\leq 2}|\theta_{tx}(x,t)|\leq\kappa_4$.*

More clearly, Fig. 7.2 simulates the varying $\theta(1,t), 0<t\leq 1$, which clearly shows that there exists a constant $0<\delta\ll T$ such that $\theta(1,t), 0<t\leq\delta$ is sufficiently small. Recalling the convolution relationship (7.8) between input/output errors, it reveals that

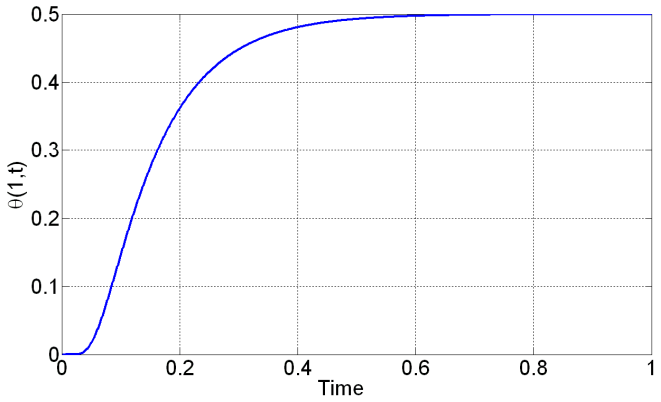

Figure 7.2: Variation of $\theta(1,t)$ in the time domain.

at the current time instant t, any bounded control input $u(\tau), \max\{0,t-\delta\} \leq \tau \leq t$ has infinitesimal effect on the current boundary output $y(t)$. In other words, the system (7.3) is uncontrollable as $t \leq \delta$. This obviously meets the actual scenario of boundary control of heat conduction equations, where δ refers to the input reaction delay in the time domain that is induced by the heat conduction from the input boundary to the output boundary.

Design a D-type anticipatory ILC law as [117]

$$u^{i+1}(t) = \begin{cases} u^i(t) + \rho \dot{e}^i(t+\delta), & 0 \leq t \leq T-\delta, \\ & i \in \mathcal{N}, \\ u^i(T-\delta), & T-\delta < t \leq T, \end{cases} \tag{7.10}$$

where $\dot{e} \triangleq de/dt$ and ρ is the learning gain to be determined. In the first iteration, u^0 can be set as 0 directly or generated by any prespecified feedback controller that leads to bounded tracking error e^0.

Remark 7.3 *When ILC is performed for the heat conduction process (7.3), the measured signals are usually corrupted by noise. A reasonable estimate of derivative term $\dot{e}^i(t+\delta)$ in (7.10) can be obtained by filtered differentiation [76]. For instance, one can*

use a filtered differentiation of the form

$$\frac{\alpha s}{\alpha+s}=\alpha\left(1-\frac{\alpha}{s+\alpha}\right) \tag{7.11}$$

where s is the Laplace variable and $\alpha \gg 1$. Clearly, this operation is causal because $e^i(t+\delta)$ is available at the $(i+1)$th iteration.

Remark 7.4 *The ILC law (7.10) is designed without considering any potential input saturation problem, namely, it is assumed that*

$$|u^i| \le \overline{u},\ i \in \mathscr{N}, \tag{7.12}$$

with $\overline{u}$ being the maximum heat flux input magnitude that is acceptable in the concerned heat conduction process. Although the control process becomes nonlinear with the effect of input saturation, the convergence analysis can be performed similarly by taking [40, Property 2] into account, namely $|u^d - Proj(u^i)| \le |u^d - u^i|$, where $Proj(\cdot)$ is a projection operator and $|u^d| \le \overline{u}$.

The next theorem summarizes the performance of ILC for the system (7.3).

Theorem 7.1 *Consider the PDE process (7.3) under the ILC law (7.10). If*

$$\frac{-\gamma-1}{2\theta(1,\delta)} \le \rho \le \frac{\gamma-1}{2\theta(1,\delta)},\quad 0 \le \gamma < 1, \tag{7.13}$$

then $e^i(t),\ t \in [0,T]$ will converge to the $((1+\rho_1)\ell/(1-\gamma))$-neighborhood of zero asymptotically in the sense of λ-norm as $i \to \infty$, where

$$\ell \triangleq 4\overline{u}\int_0^\delta \theta(1,\tau)d\tau,\quad \rho_1 = 2|\rho| \sup_{t\in[0,T]} |\theta(1,t)|. \tag{7.14}$$

Proof. See *Appendix A.9.* ■

Observing (7.13) and (A.94), ILC achieves the fastest possible convergence speed when $\gamma = 0$ or equivalently $\rho = -1/2\theta(1,\delta)$.

A prior evaluation of δ is compulsory when implementing the ILC law (7.10). Before determining δ, it is worthy to analyze how it is relevant to the ILC performance. Recall the tracking error bound that is guaranteed in Theorem 7.1,

$$b_{max} \triangleq \frac{(1+\rho_1)\ell}{1-\gamma}.$$

By substituting (7.14),

$$b_{max} = \frac{\left(1+2|\rho|\sup_{t\in[0,T]}|\theta(1,t)|\right)4\overline{u}\int_0^\delta \theta(1,\tau)d\tau}{1-\gamma}, \tag{7.15}$$

where the infinite series $\theta(1,t)$, $t \in [0,T]$ is involved.

Fig. 7.2 has demonstrated the monotonicity of $\theta(1,t)$ with respect to the time t. Further, it is easy to verify that $\sup_{t\in[0,T]}|\theta(1,t)| \leq 1/2$ numerically. In detail, define $\theta_N(x,t) = \sum_{m=-N}^{N} K(x+2m,t)$, and then $\theta(x,t) = \lim_{N\to\infty}|\theta_N(1,t)|$. Fig. 7.3 simulates the variation of $\sup_{t\in[0,T]}|\theta_N(1,t)|$ in N, from which it has that $\sup_{t\in[0,T]}|\theta_N(1,t)| \leq 1/2$ when $N \leq 200$, and the magnitude change is invisible as N is sufficiently large. Hence, it is rational to claim that

$$\begin{aligned}\sup_{t\in[0,T]}|\theta(1,t)| &= \sup_{t\in[0,T]}\lim_{N\to\infty}|\theta_N(1,t)| \\ &= \lim_{N\to\infty}\sup_{t\in[0,T]}|\theta_N(1,t)| \leq \frac{1}{2}.\end{aligned} \tag{7.16}$$

As such, there has $\sup_{t\in[0,\delta]}|\theta(1,t)| = \theta(1,\delta) \leq 1/2$ and

$$\begin{aligned}b_{max} &\leq \frac{4\overline{u}\left(1+\frac{(1+\gamma)\sup_{t\in[0,T]}|\theta(1,t)|}{\theta(1,\delta)}\right)\sup_{t\in[0,\delta]}|\theta(1,t)|\delta}{1-\gamma} \\ &\leq \frac{4\overline{u}\left(1+\frac{1+\gamma}{2\theta(1,\delta)}\right)\theta(1,\delta)\delta}{1-\gamma} \\ &= \frac{2\overline{u}(2\theta(1,\delta)+1+\gamma)\delta}{1-\gamma} \leq \frac{2\overline{u}\delta(2+\gamma)}{1-\gamma}.\end{aligned} \tag{7.17}$$

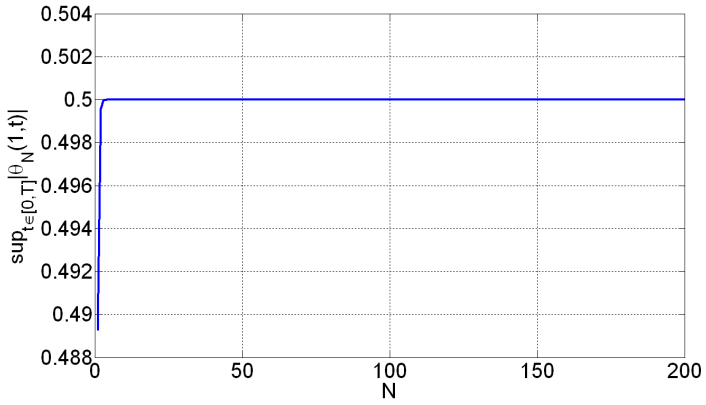

Figure 7.3: $\sup_{t\in[0,T]}|\theta_N(1,t)|$. To bring the simulation here into correspondence with the simulations in Section 5, $T = 10$ minutes is used.

Qualitatively, (7.17) reveals that the utilization of a smaller δ in (7.10) would result in a higher tracking precision or a smaller maximal tracking error in ILC. Moreover, given the prespecified tracking accuracy $\varepsilon > 0$, the parameter δ in the anticipatory ILC law (7.10) can be decided by solving $2\overline{u}\delta(2+\gamma)/(1-\gamma) \leq \varepsilon$. In the sequel,

$$\delta \leq \frac{1-\gamma}{2\overline{u}(2+\gamma)}\varepsilon. \tag{7.18}$$

As shown in (7.17), the condition (7.18) is derived by applying the properties of Jacobi Theta function, namely, (7.16) and

$$\int_0^\delta \theta(1,\tau)d\tau \leq \sup_{t\in[0,\delta]}|\theta(1,t)|\delta \leq \theta(1,\delta)\delta.$$

Due to the amplification of inequalities, the choice of δ in (7.18) is obviously conservative. As such, ILC with larger δ might also be applicable to achieve the desired tracking accuracy.

To further investigate how the choice of δ affects the learning rate of the proposed

ILC scheme, it can be seen from (7.13), (7.14), (7.17), and (A.95) that

$$\begin{aligned}
|e^{i+1}|_\lambda &\leq \gamma^{i+1}|e^0|_\lambda + \frac{1-\gamma^{i+1}}{1-\gamma}(1+\rho_1)\ell \\
&\leq \gamma^{i+1}M + \frac{1-\gamma^{i+1}}{1-\gamma}4\bar{u}\delta\theta(1,\delta)(1+|\rho|) \\
&\leq \gamma^{i+1}M + \frac{1-\gamma^{i+1}}{1-\gamma}4\bar{u}\delta\theta(1,\delta)\left(1+\frac{1+\gamma}{2\theta(1,\delta)}\right) \\
&\leq \gamma^{i+1}M + \frac{1-\gamma^{i+1}}{1-\gamma}2\bar{u}\delta(2+\gamma),
\end{aligned}$$

where the constant $M > \varepsilon$ is an upper bound estimation for the tracking error e^0. Then, the learning rate can be estimated by solving the iteration index i from the inequality

$$\gamma^{i+1}M + \frac{1-\gamma^{i+1}}{1-\gamma}2\bar{u}\delta(2+\gamma) < \varepsilon,$$

yielding

$$i > \frac{\log\frac{\varepsilon(1-\gamma)-2\bar{u}\delta(2+\gamma)}{M(1-\gamma)-2\bar{u}\delta(2+\gamma)}}{\log\gamma} - 1. \tag{7.19}$$

Thus, the output y^i will converge to the ε-neighborhood of the desired output y^d with a finite number of iterations no more than

$$\mathscr{I}(\delta) \triangleq \frac{\log\frac{\varepsilon(1-\gamma)-2\bar{u}\delta(2+\gamma)}{M(1-\gamma)-2\bar{u}\delta(2+\gamma)}}{\log\gamma},$$

in the sense of λ-norm. Calculating the derivative of $\mathscr{I}$ with respect to δ and noticing the relationship $2\bar{u}\delta(2+\gamma)/(1-\gamma) < \varepsilon < M$ give

$$\frac{d\mathscr{I}}{d\delta} = \frac{-2\bar{u}(2+\gamma)(M-\varepsilon)(1-\gamma)}{(2\bar{u}\delta(2+\gamma)-(1-\gamma)\varepsilon)(2\bar{u}\delta(2+\gamma)-(1-\gamma)M)\log\gamma} > 0. \tag{7.20}$$

Hence, a smaller δ will lead to a smaller $\mathscr{I}$, thus expedite the learning rate of the proposed ILC scheme.

Remark 7.5 *The iterative convergence derived in Theorem 7.1 is based on the strict repeatable assumption for processes, such as the same initial condition and iteration-independent boundary conditions. From the practical point of view, these conditions*

may not be satisfied. In such cases, the convergence and performance of ILC can be similarly analyzed as in [118] and [119].

7.4 Extension to Systems with State-Dependent Uncertainties

In this section, the proposed ILC scheme in Section 3 will be extended to the boundary control of (7.1), where the nonlinear uncertainty function F is state-dependent but satisfies the Lipschitz continuous condition (7.2).

The input-to-state equation of (7.1) can be written into the following integral form [106],

$$\begin{aligned} v^i &= \int_0^1 \{\theta(x-\xi,t)+\theta(x+\xi,t)\}f(\xi)d\xi - 2\int_0^t \theta(x,t-\tau)u^i(\tau)d\tau \\ &\quad +2\int_0^t \theta(x-1,t-\tau)g(\tau)d\tau \\ &\quad +\int_0^t\int_0^1 \{\theta(x-\xi,t-\tau)+\theta(x+\xi,t-\tau)\}\times F(\xi,\tau,v^i(\xi,\tau),v^i_\xi(\xi,\tau))d\xi d\tau, \end{aligned} \tag{7.21}$$

where $(x,t)\in Q$. Comparing (7.21) with (7.4), the state-dependent uncertainties in the heat equation induce more complex expression of temperature state. Since F is state-dependent and thus iteration-varying, it cannot be compensated or cancelled simply in the input-output error dynamics by the corresponding term of process equations in two consecutive iterations. Nevertheless, it will show that the proposed anticipatory D-type ILC scheme is still effective in such scenario.

Looking into (7.21), the temperature state v^i is relevant to the control input u^i in the second and fourth terms only. Analogous to the state-independent scenario, the infinitesimal effect of control input $u^i(\tau),\tau\in[\max\{0,t-\delta\},t]$ to the temperature state v^i at position $x>0$ and current time instant t will be first quantified as follows.

Assumption 7.1 *For a given δ, there exist two positive constants ℓ_1 and ℓ_2 such that*

for any input u^i *satisfying* $|u^i| < \overline{u}$,

$$|\Xi^i(x,t)| < \frac{\ell_1}{2}, \quad |\Xi^i_x(x,t)| < \frac{\ell_2}{2}, \ \ i \in \mathscr{N}, \ (x,t) \in Q, \tag{7.22}$$

where

$$\begin{aligned} \Xi^i(x,t) &= -2\int_{\max\{0,t-\delta\}}^{t} \theta(x,t-\tau)u^i(\tau)d\tau \\ &\quad + \int_{\max\{0,t-\delta\}}^{t}\int_0^1 \{\theta(x-\xi,t-\tau)+\theta(x+\xi,t-\tau)\} \times F^i d\xi d\tau \end{aligned} \tag{7.23}$$

Remark 7.6 *(7.23) is an improper double integral with singularity at* (x,t)*, owing to that* $\theta(x-\xi,t-\tau)|_{\xi=x,\tau=t} = \theta(0,0) = \infty$*. However, the boundedness of solution of (7.1), which has been addressed in Remark 7.1, implies that* $\Xi^i(x,t)$ *is convergent and bounded. Thus, by (7.23), both* Ξ^i *and* Ξ^i_x *vanish when* $\delta \to 0$*, and the existence of* $\ell_i, i = 1,2$ *is obvious.*

Having (7.21) in mind, the input-output relationship is implicitly given by letting $x \to 1$. Considering the uniqueness of solution of (7.1), the output tracking error profile of the *i*th iteration can be evaluated as follows,

$$\begin{aligned} e^i &= \lim_{x\to 1}\Big(v^d(x,t) - v^i(x,t)\Big) \\ &= -2\int_0^t \theta(1,t-\tau)\Delta u^i(\tau)d\tau \\ &\quad + \int_0^t\int_0^1 \{\theta(1-\xi,t-\tau)+\theta(1+\xi,t-\tau)\} \times \Big(F^d - F^i\Big)d\xi d\tau, \end{aligned} \tag{7.24}$$

where $F^d \triangleq F(\xi,\tau,v^d(\xi,\tau),v^d_\xi(\xi,\tau)), F^i \triangleq F(\xi,\tau,v^i(\xi,\tau),\, v^i_\xi(\xi,\tau))$ when no confusions occur. Using (7.24) in two adjacent iterations, there has

$$\begin{aligned} e^{i+1} - e^i &= 2\int_0^{t-\delta} \theta(1,t-\tau)(u^{i+1}(\tau) - u^i(\tau))d\tau \\ &\quad - \int_0^{t-\delta}\int_0^1 \{\theta(1-\xi,t-\tau)+\theta(1+\xi,t-\tau)\} \times (F^{i+1} - F^i)d\xi d\tau \\ &\quad - \Xi^{i+1}(1,t) + \Xi^i(1,t), \end{aligned} \tag{7.25}$$

where Ξ^i is given in (7.23). Clearly, the output tracking convergence in such scenario is highly depending on how the involved uncertain term F affects the output tracking. Noticing the Lipschitz continuous condition for F, it has

$$|F^{i+1} - F^i| \leq C_F\{|v^{i+1} - v^i| + |v_x^{i+1} - v_x^i|\}, \quad (x,t) \in \overline{Q}. \tag{7.26}$$

The right hand side of (7.26) can be further bounded by functions of e^i from the above, as demonstrated in the following.

Lemma 7.2 *Applying the ILC law (7.10) in the PDE process (7.1), there exist finite constants $\kappa_j, j = 5, \cdots, 7$ for all $t \in [\delta,\ T]$ such that*

$$\sup_{0\leq x\leq 1} \left\{|v^{i+1} - v^i| + |v_x^{i+1} - v_x^i|\right\} < \kappa_5|e^i(t)| + \kappa_6 \int_\delta^t |e^i(\tau)|d\tau + \kappa_7.$$

Proof. See *Appendix A.10.* ■

By applying Lemma 7.2, the second main result in this chapter is derived.

Theorem 7.2 *Consider the PDE process (7.1) under the ILC law (7.10) and Assumption 7.1. If the learning gain ρ is selected such that the inequality (7.13) holds, then $e^i(t), t \in [0,T]$, will converge to the $((1+\rho_1)\ell_1/(1-\gamma))$-neighborhood of zero asymptotically in the sense of λ-norm as $i \to \infty$, where γ, ρ_1, and ℓ_1 are defined in (7.13), (7.14), and (7.22), respectively.*

Proof. See *Appendix A.11.* ■

Comparing with the state-independent case, ILC achieves the similar convergence performance under the same gain condition (7.13) in the state-dependent case. For instance, in the expressions of upper bound of tracking error, the only difference is that the quantity ℓ is replaced by ℓ_1 in Theorem 7.2. This is owing to the fact that the proposed

ILC design method is contraction mapping based, thus needs less system structure information than other design techniques in boundary control of PDE processes, e.g., the Lyapunov-functional-based method [92].

However, since the state-dependent nonlinearities F are involved in ℓ_1, the choice of anticipatory time δ cannot be confined simply as in the state-independent scenario. In order to explore how ℓ_1 is relevant to δ, we perform a simple time-scaling transformation in (7.23) and take absolute value on other sides of the induced equation,

$$\begin{aligned} |\Xi^i(x,t)| \quad \leq \quad & \left| 2\int_0^\delta \theta(x,s)u^i(t-s)ds \right| \\ & + \left| \int_0^\delta \int_0^1 \{\theta(x-\xi,s)+\theta(x+\xi,s)\} \right. \\ & \left. \times F(\xi,t-s,v^i(\xi,t-s),v^i_\xi(\xi,t-s))d\xi ds \right|. \end{aligned} \tag{7.27}$$

Recalling the proof of Theorem 7.2, ℓ_1 is employed to quantify Ξ^i at the boundary $x=1$. Thus, substituting $x=1$ into (7.27) leads to

$$\begin{aligned} |\Xi^i(1,t)| \quad \leq \quad & \left| 2\int_0^\delta \theta(1,s)u^i(t-s)ds \right| \\ & + \left| \int_0^\delta \int_0^1 \{\theta(1-\xi,s)+\theta(1+\xi,s)\} \right. \\ & \left. \times F(\xi,t-s,v^i(\xi,t-s),v^i_\xi(\xi,t-s))d\xi ds \right| \\ \leq \quad & 2\overline{u}\int_0^\delta \theta(1,s)ds + \overline{F}\int_0^\delta \int_0^1 \{\theta(1-\xi,s)+\theta(1+\xi,s)\}d\xi ds, \end{aligned} \tag{7.28}$$

where the constant $\overline{F}$ is assumed to satisfy

$$|F(x,t,v,v_x)| < \overline{F}, (x,t) \in Q \tag{7.29}$$

for all $|u| \leq \overline{u}$. In practice, the effect of nonlinear source or sink F is always finite for any bounded heat flux input u. Thus, the existence of $\overline{F}$ is clear. By the Lipschitz

continuous property of F,

$$\begin{aligned} |F(x,t,v,v_x)| &= |F(x,t,0,0)| + |F(x,t,v,v_x) - F(x,t,0,0)| \\ &\leq \sup_{(x,t)\in Q} |F(x,t,0,0)| + C_F \sup_{(x,t)\in Q} (|v| + |v_x|), \end{aligned}$$

implying that the estimation of $\overline{F}$ is highly relevant to the prior information on $|F(x,t,0,0)|$, the Lipschitz constant C_F, and the maximal possible magnitudes of system states $|v|$ and $|v_x|$, when $|u| \leq \overline{u}$ and $(x,t) \in Q$.

Now, by (7.28), set

$$\ell_1 = 4\overline{u}\int_0^\delta \theta(1,s)ds + 2\overline{F}\int_0^\delta \int_0^1 \{\theta(1-\xi,s) + \theta(1+\xi,s)\}d\xi ds.$$

Similar to the state-independent case, the ultimate tracking error bound can be estimated as follows when choosing $\gamma = 0$ or $\rho = -1/2\theta(1,\delta)$.

$$\begin{aligned} b'_{max} &\triangleq \frac{(1+\rho_1)\ell_1}{(1-\gamma)} \\ &\leq 2\left(1 + \frac{\sup_{t\in[0,T]} |\theta(1,t)|}{\theta(1,\delta)}\right)\left(2\overline{u}\int_0^\delta \theta(1,s)ds \right. \\ &\quad \left. + \overline{F}\int_0^\delta \int_0^1 \{\theta(1-\xi,s) + \theta(1+\xi,s)\}d\xi ds\right) \\ &\leq 2\left(1 + \frac{1}{2\theta(1,\delta)}\right)(2\delta\overline{u}\theta(1,\delta) \\ &\quad \left. + \overline{F}\int_0^\delta \int_0^1 \{\theta(1-\xi,s) + \theta(1+\xi,s)\}d\xi ds\right) \\ &\triangleq \Theta(\delta). \end{aligned} \tag{7.30}$$

Given the prespecified tracking accuracy $\varepsilon > 0$, the parameter δ in the anticipatory ILC law (7.10) can be decided by numerically solving $\Theta(\delta) \leq \varepsilon$.

Alternatively, in order to simplify the design procedure for δ in (7.10), we still recommend to initially choose δ as in (7.18), i.e., $\delta \leq \varepsilon/4\overline{u}$. This is mainly due to the following two points: (1) since $b_{max} \leq b'_{max}$, a smaller δ is preferable in the state-dependent scenario than in the state-independent scenario, and (2) the choice of δ that meets the condition (7.18) is probably conservative for the state-independent scenario.

Remark 7.7 *The proposed ILC is a feedforward control scheme that makes full use of process repetition. Since it mainly deals with repeatable tracking error, those non-repeatable components cannot be effectively compensated by ILC. A possible way to suppress non-repeatable components is to incorporate additional feedback control [120]. Depending on the bandwidth requirement, characteristics of disturbance and noise in system, etc, feedback loop can be specified using all kinds of feedback controller design techniques, e.g., PID control, H_∞ optimal control, or other robust control. In particular, the bandwidth of a closed-loop system gives a measure of the transient response properties, in that a large bandwidth corresponds to a faster response. Conversely, for a small bandwidth, the time response will generally be slow and sluggish. Together with the cut-off rate, bandwidth indicates the noise-filtering characteristics and the robustness of the system. In practice, the bandwidth of the closed-loop system, which may impose limits on the control signals at each point along the system, can be determined by considering the control task to be performed, the location of resonant modes in system, and the precision of hardware components, e.g., system repeatability, resolutions of feedback sensor, digital-to-analog converter channel as well as analog-to-digital converter channel, etc.*

7.5 Illustrative Example

In this section, the ILC for the following heat conduction equation will be simulated

$$v_t^i = v_{xx}^i - \varsigma(c(x,t)v^i)_x + \varphi(v^i), \quad t,x \in Q, \tag{7.31}$$

where the constant ς is relevant to advection average velocity, $c(x,t) = xt + x^2/2$ denotes the variation of flow rate in thermal convection, and the source term $\varphi(v^i)$ behaves as the nonlinear Monod function, namely, $\varphi(v^i) = -\mu_{max} v^i/(K_s + v^i)$ with constant μ_{max}

and K_s. The distributed parameter structure of (7.31) is also used to depict anaerobic digestion process for wastewater treatment in [40] and [121]. Writing (7.31) into the form of (7.1) yields

$$\begin{aligned} F(x,t,v^i,v^i_x) &= -\varsigma(c(x,t)v^i)_x+\varphi(v^i) \\ &= -\varsigma(t+x)v^i+\varphi(v^i)-\varsigma(xt+x^2/2)v^i_x, \end{aligned}$$

which is assumed to be unknown when designing the ILC law. To check the Lipschitz continuous property of function F, it is noted that $|d\varphi(v)/dv| = |-\mu_{max}K_s/(K_s+v)^2| \leq \mu_{max}/K_s$. Then, it follows that

$$\begin{aligned} & |F(x,t,p_1,q_1)-F(x,t,p_2,q_2)| \\ \leq & \left(\varsigma(t+x)+\frac{\mu_{max}}{K_s}\right)|p_1-p_2|+\varsigma\left(xt+\frac{x^2}{2}\right)|q_1-q_2| \\ \leq & \max\left\{\varsigma(t+x)+\frac{\mu_{max}}{K_s},\varsigma\left(xt+\frac{x^2}{2}\right)\right\}\times(|p_1-p_2|+|q_1-q_2|). \quad (7.32) \end{aligned}$$

Since $0\leq x\leq 1$ and $0\leq t\leq T<\infty$, the quantity $\max\left\{\varsigma(t+x)+\mu_{max}/K_s,\varsigma(xt+x^2/2)\right\}$ is finite, implying that the nonlinear source function F is Lipschitz continuous.

In the simulation, let $T=10\ min, \varsigma=2$, $\mu_{max}=3.2$, and $K_s=1$. The initial condition is set as $v^i(x,0)=f(x)=0$°C, the boundary condition at $x=1$ m is set as $v^i_x(1,t)=g(t)=1\ W/m^2$, and the initial control input is set as $u^0(t)=0\ W/m^2, t\in[0,T]$. The desired boundary output profile is generated by the polynomial $t^3(1-t/T)^3$°C, $t=[0,T]$. The acceptable tracking accuracy is within ± 1°C, i.e., $\varepsilon=1$°C. In order to check the effect of anticipatory time δ to the tracking control performance, set $\delta=0.25,0.15,0.10,0.05,0.02$ min, respectively, in the ILC law (7.10). Meanwhile, the learning gain is fixed to be $\rho=-1/2\theta(1,0.25)=-1.2041$, which avoids the utilization of high gain learning in (7.10) when δ is small.

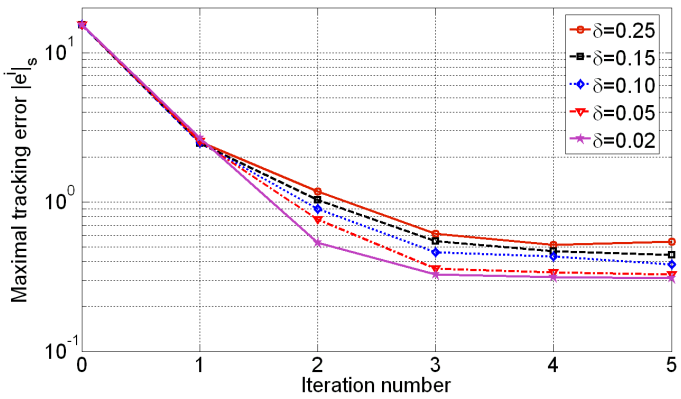

Figure 7.4: Maximal tracking error profile, derived by applying (7.10) with $\delta = 0.25, 0.15, 0.10, 0.05, 0.02$ min, respectively.

The heat conduction equation (7.31) is solved using the Matlab solver *'pdepe'* with sampling period 0.01 in the temporal and spatial domains, respectively. Since ILC is a feedforward control scheme, the control input boundary condition can be calculated offline and updated directly in *'@pdex1bc'* by defining the input variable as a global variable.

Define $|e^i|_s = \sup_{t\in[0,T]} |e^i|$. Fig. 7.4 shows the maximal tracking error profiles by choosing different δ in (7.10). The results reveal that

(i) The desired tracking accuracy is achieved via ILC in all the scenarios, namely, $|e^i|_s < 1$°C after 5 iterations' learning.

(ii) Although the considered heat conduction process is perturbed by some state-dependent nonlinearities, smaller δ still renders to better ultimate tracking accuracy.

(iii) For different δ, the tracking error is reduced by at least 96%. More simulations show that the tracking accuracy can be further improved by reducing the sampling periods in the time and spatial domains.

Figs. 7.5-7.7 show the input profile, the output profile, and the temperature varia-

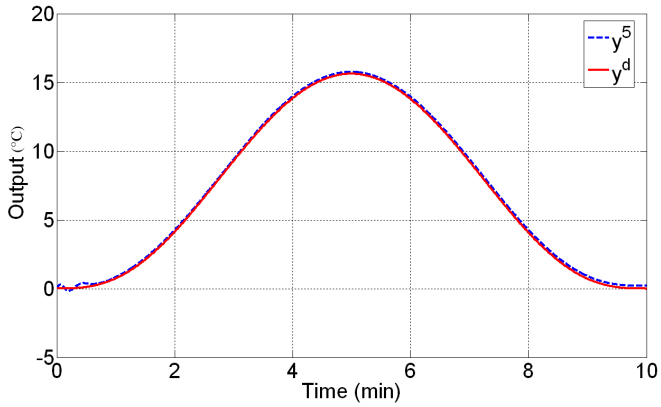

Figure 7.5: The system output profile y^5, which is generated by the learned heat flux input $u^5(t), t \in [0,T]$ for $\delta = 0.02$ min. The desired reference output y^d is given for comparison.

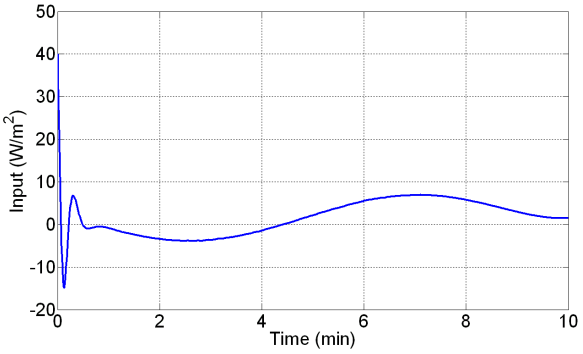

Figure 7.6: The control input profile in the 5th iteration, derived by the anticipatory D-type ILC law (7.10) with $\delta = 0.02$ min.

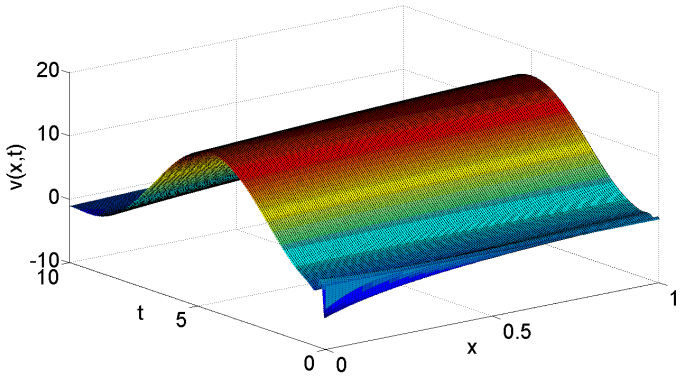

Figure 7.7: Temperature variation versus time and space, generated by the learned input profile in the 5th iteration of ILC with $\delta = 0.02$ min.

tion in the spatiotemporal domain, respectively, by applying the learned heat flux input in the last iteration of ILC with $\delta = 0.02$ min. These simulation results demonstrate the efficacy of ILC law (7.10) in boundary output tracking of the inhomogeneous heat equations (7.31).

7.6 Conclusion

This chapter addresses the boundary control problem of heat equations under the framework of ILC. To the best of our knowledge, this is the first work to extend ILC to the tracking control of nonlinear parabolic distributed parameter systems, without any model simplification or discretization. The difficulties are overcome by transforming the PDE system into its integral form and exploiting the properties of the embedded Jacobi Theta functions. A class of D-type anticipatory ILC scheme is proposed to iteratively tune the heat flux at one side such that the temperature measurement at the other side can track the designated reference. The advantages of the proposed control scheme are: (1) it makes full use of process repetition; (2) it can deal with input reaction delay efficiently; (3) it eliminates the gain margin limitation encountered in feedback control; and (4) its convergence analysis avoids any simplification or discretization of the 3D dynamics in the time, space as well as iteration domains. Our next research phase is to consider iterative boundary control for more distributed parameter systems and implementation issues, e.g., the initial resetting problem in each iteration.

Chapter 8

Precise Speed Tracking Control of A Robotic Fish via ILC

8.1 Introduction

As a real-time application, the objective of this chapter is to apply ILC approach to precise speed tracking problem of a biomimetic robotic fish.

Currently, there are tremendous interests in the use of autonomous underwater vehicles (AUVs) for ocean exploration, scientific research and commercial missions. Among different kinds of AUVs, robotic fish is generally regarded as the most remarkable one because of its high efficiency, high maneuverability and low noise. In order to develop robotic fish as agile as real fish, many efforts have been made [122–128]. Although a lot of impressive results have been achieved, such as the works in propulsion mechanism of fish swimming [129, 130], actuators [131, 132] and mechanical structures [133], the results are not sufficient to develop an autonomous robotic fish that can swim freely in an unstructured environment as how a real fish does. One of the main challenges lies

in the difficulty of robotic fish motion control.

Previous works on motion control of robotic fish mainly concern two aspects: (1) generate fish-like swimming gait in a robot; (2) drive a robotic fish to achieve a desired motion. The former explores producing coordinated movements of actuation components of a robotic fish, and the latter focuses on controlling the motion of whole body of a robot. From the perspective of cybernetics, approaches for swimming gait generation can be categorized as: kinematics-based and bio-inspired. The kinematics-based approach aims to replicate body motion of swimming fish with discrete mechanical multiple links connected by rotating joints [47–50], and the bio-inspired approach adopts the central pattern generator (CPG) to translate fish undulatory body motion into robotic joint movement [51–55]. Although the swimming gait generation approaches can be used to generate fish-like swimming locomotion in robotic fish, these approaches are not able to help the robots to achieve a desired motion since they are open-loop methods. To control a robotic fish to achieve a given target, several feedback control algorithms have been developed [56–60, 134, 135].

In [56], to implement a point-to-point (PTP) control of a four-link biomimetic robotic fish, a classic proportional-integral-derivative (PID) controller and a fuzzy logic controller (FLC) are designed for speed and orientation control respectively, where a vision-based feedback system is employed. In [134], the author develops several fuzzy control laws for a pectoral-fin-driven robotic fish. The proposed fuzzy control not only works well to deal with the complexity of swimming hydrodynamics, but also enables the fish robot to perform rendezvous and docking with an underwater post in water currents. Different from [56, 134] that focus on set-point or PTP control, [57] investigates efficient swimming control of a Carangiform robotic fish under the framework of fuzzy

logic control. By comparing the thrust performance of the robotic fish with different control methods via simulations, it turns out that the fuzzy controller is able to achieve faster acceleration and smaller steady-state error than what could be achieved by an open-loop and classic PID controller. Furthermore, there are some works addressing trajectory tracking problems of robotic fish. In [58], a neural-network-based sliding mode control algorithm is developed for cooperative trajectory tracking task of multiple biomimetic robotic fish. In [59], a target-tracking and collision-avoidance task for two autonomous robotic fish is designed and implemented by a situated-behavior-based decentralized control approach. According to the quasi-steady fluid flow theory, [60] presents a mathematical model for a Carangiform robotic fish. Based on the constructed model, nonlinear control methods are applied to generate forward propulsion and turning gaits for the robotic fish, and trajectory tracking tasks are implemented in experiments simultaneously. In addition, authors in [135] develop a local control law for coordinating joint angles in Carangiform swimming and a global control law for solving the waypoint tracking problem of biomimetic AUVs.

The objective of this chapter is to address a precise speed tracking problem of a biomimetic robotic fish via ILC, which is essential to both motion control and motion planning. In fact, due to the appealing features and its simplicity in implementation, ILC has been widely applied in practice, such as robotic manipulators, chemical batch reactors, electric motors, as well as motion control of robotic fish. For instance, in [136, 137] an ILC-approach-based motion control is proposed to improve the present propulsion performance of the the bionic undulating fin-*RoboGnilos*, in which a denoising filter and the curve fitting component are incorporated into the anticipant ILC algorithm for satisfying undulatory propulsion. Besides, to tackle the phase lagging

problem, a modified ILC algorithm is presented for the *RoboGnilos* in [138], where a memory clearing operator is also introduced to guarantee the Lipschitz condition. The experimental results in [138] show that the developed ILC scheme enables the undulating fish robot to perform the fin-ray undulation kinematics similar to that of real fish. However, one common characteristic of the above works involving ILC is that they only focus on fish-like swimming gait generation of the robot. Different from the above works, this chapter mainly considers the precise speed tracking control problem of robotic fish via ILC, which belongs to the scenario of driving a robotic fish to achieve a desired motion. In practice, many applications might require robotic fish to swim along prespecified speed trajectories and perform the tasks repeatedly. For instance, a robotic fish, used for transportation between two wharfs, is expected to swim with a pre-determined speed trajectory. The task is repeatable, and the formation fits perfectly in the ILC framework. Another example is rendezvous and docking of a robotic fish with an underwater post. In such kind of task implementations, the robot has to move with a given speed trajectory. Besides, pipe cleaning or pipeline leakage detection performed by robotic fish also falls in this category. These observations motivate the study of speed tracking of robotic fish from the perspective of ILC.

In this chapter, an ILC method is applied to a two-link Carangiform robotic fish in real time and achieves precise speed tracking performance. The main contributions of this chapter can be summarized as follows: (1) A dynamical model for the two-link Carangiform robotic fish is constructed by utilizing Newton's second law. The robotic fish model is highly nonlinear and non-affine in control input, which hinders the applicability of most control methods that require affine-in-input. (2) A P-type ILC scheme with input saturation is proposed for speed tracking of the robotic fish. It

is worth noting that the controller can be designed without using the accurate model and only the bounded gradient information of the system is required for convergence analysis. (3) The rigorous convergence analysis of the developed ILC scheme is derived by applying composite energy function (CEF). (4) Both simulations and experiments are conducted to illustrate the effectiveness of ILC, and excellent speed tracking is achieved for the robotic fish.

This chapter is organized as follows. Section 8.2 introduces the biomimetic robotic fish prototype and hardware configuration. In Section 8.3, the dynamical model of the robotic fish is established by using Lagrangian mechanics method. Section 8.4 presents the ILC law design and its convergence analysis. Further, the efficiency of the proposed ILC scheme is verified by both simulations and experiments in Section 8.5. Section 8.6 gives a brief conclusion.

8.2 Robotic Fish Prototype and Hardware Configuration

Most of fish in nature generate thrust principally via body and/or caudal fin, namely, body and caudal fin (BCF) swimmers, and some of the most impressive BCF swimmers, such as carps or trout, propel themselves by Carangiform swimming mode. Since Carangiform movement is easy to be replicated from the mechanical design perspective, this chapter focus on Carangiform fish. In Carangiform swimming, the front two-thirds of the fish's body moves in a largely rigid way, and the propulsive body movements are confined to the rear third of the body - primarily the tail. According to the morphology of Carangiform fish, many multi-link robotic fish have been developed [56, 139, 140], which are able to generate various swimming modes via undulating their tails as a real Carangiform fish does. Generally, the more links the robotic fish have, the more

complex fish-like maneuvers they are able to generate. However, it is extremely hard to construct a dynamical model for a multi-joint robotic fish due to the complexity of hydrodynamics and interactions between the fish body and water. For the benefit of mathematical modelling, many researchers try to simplify robotic fish into two-link models, such as [141–143]. In this chapter, since the speed tracking of the robotic fish swimming at "cruise" will be explored which is a basic Carangiform swimming mode, a two-link one-joint robotic fish prototype is thus developed for investigation.

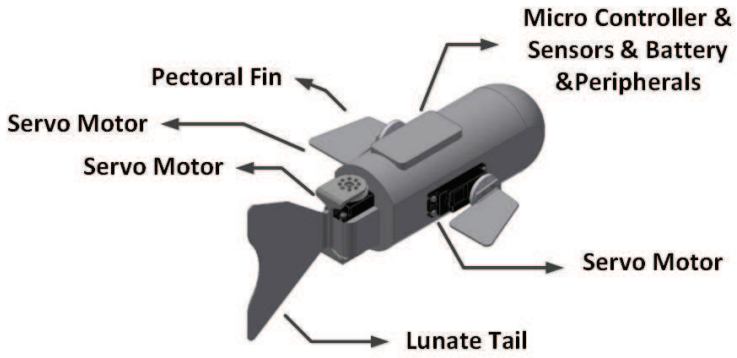

Figure 8.1: Schematic structure of the robotic fish.

Figure 1 shows the schematic structure of the robotic fish. The length of the robotic fish is approximately 36 cm. It consists of two links which are connected by a high-torque servo motor (JR DS R8801). Due to mechanical restriction, the angle range for the servomotor is about -60° to 60°. Basically, the shape of the middle part of the fish body is a cylinder, and the shape of the fish head is a cone with a round nose for the purpose of reducing drag force. The lunate tail is made of perspex with chord length 12 cm and span 17 cm. The first link of the robotic body has a sealed compartment composed of plastic side or top panel wrapped with waterproof tap. The compartment contains a micro controller (ATMEL ATSAM3X8E), an inertial measurement unit (VN-100), a Bluetooth wireless communication module and a lithium battery. The micro controller is responsible for controlling the servo motors, transferring diagnostic information via

the wireless link, processing sensor data and making decisions. The wireless communication module is used to receive command from a host computer. The lithium battery is applied to provide power for the servomotors, and a toggle switch is used to switch on/off the battery. The frequency of the control signal is 1Hz in this chapter. In addition, in this chapter, an overhead camera is used to record the trajectories of the robotic fish, and the frame rate of the camera is 25 frames per second. After processing a series of images at different time instants, the average speed of the robot with respect to time can be obtained.

8.3 Modelling

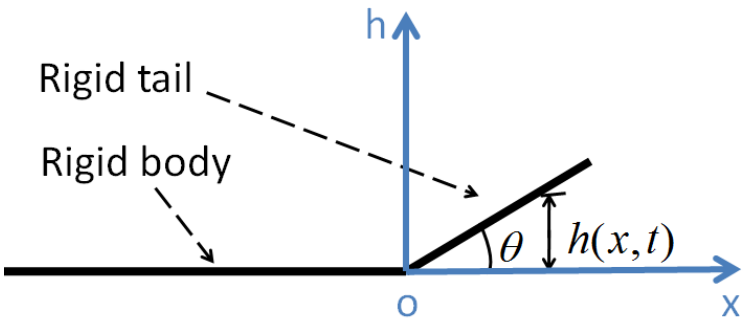

Figure 8.2: The top-view geometry of the two-link robotic fish.

Figure 8.2 shows the top-view geometry of the two-link robotic fish. Without loss of generality, it is assumed that both the body center of mass and the central line locate at the center of the fish body. The length of the robotic fish is l and that of the tail is $l/3$.

8.3.1 Caudal Fin Thrust Modelling

As shown in Fig. 8.2, the robotic fish prototype in this chapter has two links. The front two-thirds of the robotic fish is rigid and the rear third moves symmetrically to its

central line. The displacement $h(x,t)$ at the position x can be calculated as follows

$$h(x,t) = x\tan(\theta), \tag{8.1}$$

where θ in radians is the angle between the tail and the central line of the robotic fish. The angle θ is directly proportional to the motor rotation, and it is used as the driving term as a function of time. If $\theta(t)$ is driven sinusoidally, i.e., $\theta(t) = \theta_m \sin(2\pi ft)$, as used in [141], the displacement $h(x,t)$ can be written as

$$h(x,t) = x\tan(\theta_m \sin(2\pi ft)), \tag{8.2}$$

where θ_m is the amplitude and f is the frequency of the sinusoidal motion. Now, taking the derivative with respect to time t on both side of (8.2), it follows that

$$\left(\frac{\partial h(x,t)}{\partial t}\right)_{x=\frac{l}{3}} = \frac{2}{3}\pi f\theta_m l \sec^2(\theta_m \sin(2\pi ft))\cos(2\pi ft). \tag{8.3}$$

In addition, the spatial derivative of $h(x,t)$ at $x = l/3$ is

$$\left(\frac{\partial h(x,t)}{\partial x}\right)_{x=\frac{l}{3}} = \tan(\theta_m \sin(2\pi ft)). \tag{8.4}$$

According to the small displacement model developed in [129], the average thrust F generated by the fish is given as follows

$$F = \frac{\rho A(l)}{2}\left[\left(\frac{\partial h}{\partial t}\right)^2 - v^2\left(\frac{\partial h}{\partial x}\right)^2\right], \tag{8.5}$$

where ρ is the density of water, v is the velocity of fish, $A(l)$ is the area of a circle computed by using the overall dimension of the tail as a diameter, and the squares of the derivative values are averages over a typical cycle, namely,

$$\left(\frac{\partial h}{\partial t}\right)^2 \triangleq \frac{1}{T}\int_0^T \left(\frac{\partial h}{\partial t}\right)^2_{x=\frac{l}{3}} dt, \tag{8.6}$$

$$\left(\frac{\partial h}{\partial x}\right)^2 \triangleq \frac{1}{T}\int_0^T \left(\frac{\partial h}{\partial x}\right)^2_{x=\frac{l}{3}} dt, \tag{8.7}$$

where $T = 1/f$ is the period of sinusoidal motion. Further, the time-averaged values for these derivatives can be found numerically for various amplitudes and frequencies, and the results are shown in Figs. 8.3 and 8.4, respectively. The values $f = 1$Hz and $\theta_m = \pi/6$ in Figs. 8.3 and 8.4 are only illustrative examples. If other values for f and θ_m are adopted in the simulation, similar variation tendencies for $\left(\frac{\partial h}{\partial t}\right)^2$ and $\left(\frac{\partial h}{\partial x}\right)^2$ will be presented.

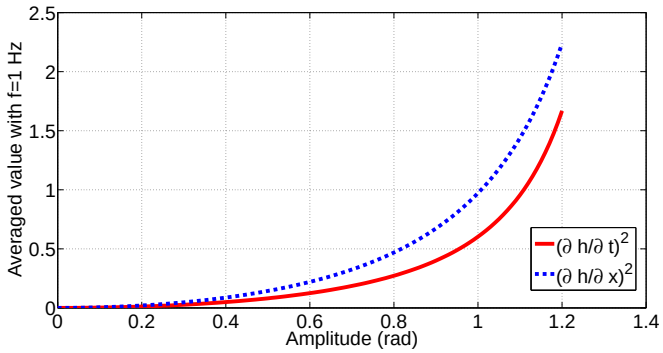

Figure 8.3: The integrated square of the slope and velocity of the tail over one cycle vs. Amplitude.

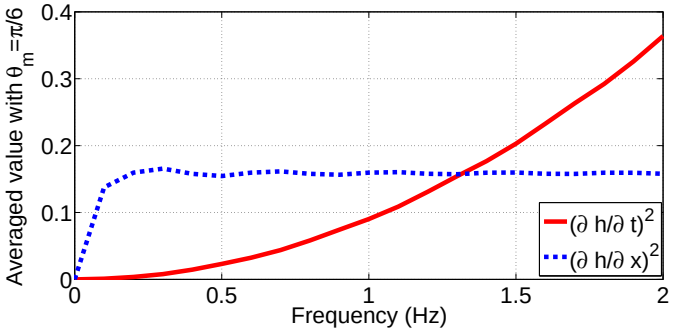

Figure 8.4: The integrated square of the slope and velocity of the tail over one cycle vs. Frequency.

Let $H_1(\theta_m, f)$ and $H_2(\theta_m, f, v)$ be defined as follows

$$H_1(\theta_m, f) \triangleq \frac{\rho A(l)}{2}\left(\frac{\partial h}{\partial t}\right)^2 \tag{8.8}$$

and

$$H_2(\theta_m, f, v) \triangleq \frac{\rho A(l) v^2}{2}\left(\frac{\partial h}{\partial x}\right)^2. \tag{8.9}$$

The thrust F can be rewritten as

$$F = H_1(\theta_m, f) - H_2(\theta_m, f, v). \tag{8.10}$$

8.3.2 Drag Force

Besides the thrust generated by caudal fin undulations, the robot body also experiences drag force. Similar as [133, 143, 144], the drag on the body of the robot is assumed to be generated in steady or quasi-steady flow, and it takes the form

$$D = \alpha v^2 \tag{8.11}$$

where $\alpha \triangleq \frac{1}{2}\rho S C_D$ is a positive constant. ρ is the density of water, S is a suitably defined reference surface area for the robot body, and C_D is the drag coefficient. The coefficient α will be estimated numerically later. In addition, the drag acts parallel to the direction of motion.

8.3.3 Dynamical Model

By applying Newton's second law, the dynamics model of the two-link robotic fish at "cruise" swimming mode can be given as follows

$$M\dot{v} = F - D, \tag{8.12}$$

where M is the mass of the robotic fish, and F is highly nonlinear with respect to the amplitude θ_m and the frequency f.

8.4 Controller Design and Convergence Analysis

From the view of biomimetics, present works and progresses in robotic fish are still located at shape-similarity mechanism design, namely, fish-like swimming gait generation. However, few works investigate the speed tracking problem for the robotic fish,

which is an indispensable research step in motion control and motion planning of the robotic fish.

There is substantial evidence from ichthyology suggesting that symmetric body and fin kinematics usually lead to powered translational maneuvers, whereas asymmetrical kinematics may bring on rotational maneuvers [145, 146]. Hence at "cruise" swimming mode, the caudal fin of the robotic fish should undulate symmetrically. Therefore, if the undulatory frequency or amplitude of the caudal fin is fixed, the speed of the robotic fish can be adjusted by the other one. Without loss of generality, this chapter fixes the undulatory frequency as 1Hz, and the amplitude of undulation will be used to manipulate the speed of the robotic fish.

Due to the hardware limitation, the magnitude of the tail motion is bounded. That is, there exists an input saturation. Assume that the amplitude satisfies $0 \leq \theta_m \leq \theta_m^* < \pi/2$. Consider system

$$M\dot{v}_i = -\alpha v_i^2 + F_i, \tag{8.13}$$

where $i \in \mathbb{Z}^+$ is the experiment or iteration number, and $F_i = H_1(\tilde{\theta}_{m,i}, 1) - H_2(\tilde{\theta}_{m,i}, 1, v_i)$ with

$$\tilde{\theta}_{m,i} \triangleq \text{sat}(\theta_{m,i}, \theta_m^*) = \begin{cases} 0, & \theta_{m,i} \leq 0, \\ \theta_{m,i}, & 0 < \theta_{m,i} < \theta_m^*, \\ \theta_m^*, & \theta_{m,i} > \theta_m^*. \end{cases}$$

Let the target speed trajectory be $v_d(t) \in C^1[0,T]$. For any given $v_d(t)$ to be realizable, it is assumed that there exists θ_m^d such that the following dynamics holds,

$$M\dot{v}_d = -\alpha v_d^2 + F_d, \tag{8.14}$$

where $F_d \triangleq H_1(\theta_m^d, 1) - H_2(\theta_m^d, 1, v_d)$, and $0 \leq \theta_m^d \leq \theta_m^*$. Denote $e_i(t) \triangleq v_d(t) - v_i(t)$ the tracking error at the ith iteration. From (8.13) and (8.14), the error dynamics can be

written as

$$\dot{e}_i = -\frac{\alpha}{M}(v_d^2 - v_i^2) + \frac{1}{M}(F_d - F_i). \tag{8.15}$$

The control objective is to tune $\theta_{m,i}$ such that the tracking error $e_i(t)$ converges to zero as the iteration number increases.

Considering the constraints of hardware, a P-type ILC scheme with a saturator is designed as follows

$$\theta_{m,i+1} = \tilde{\theta}_{m,i} + \gamma e_i(t), \tag{8.16a}$$

$$\tilde{\theta}_{m,i} = \text{sat}(\theta_{m,i}, \theta_m^*), \tag{8.16b}$$

where $\gamma > 0$ is the learning gain to be determined.

Remark 8.1 *The initial input $\theta_{m,0}$ can be set to zero directly or generated by any pre-specified feedback controller that leads to bounded tracking error e_0.*

As common in ILC theory, the following assumption is made.

Assumption 8.1 *The initial state is reset to the desired initial state at each iteration, i.e., $e_i(0) = 0$.*

The main result of this chapter can be summarized as follows.

Theorem 8.1 *For system (8.13), under the Assumption 8.1, the proposed ILC law (8.16) guarantees that the tracking error $e_i(t)$, $t \in [0, T]$ converges to zero uniformly as $i \to \infty$.*

To facilitate the proof of Theorem 8.1, a lemma for the thrust F and a property regarding to the saturation function given in [147] are first presented.

Lemma 8.1 *For system (8.12), $\frac{\partial F}{\partial v}$ is non-positive, and there exists a constant $\vartheta > 0$ such that $0 < \frac{\partial F}{\partial \theta_m} \leq \vartheta$.*

Proof. See *Appendix A.12*.

Property 1. For a given $\theta_m^d(t)$ satisfying $\sup_{t\in[0,T]} |\theta_m^d(t)| \leq \theta_m^*$, the following inequality holds:

$$[\theta_m^d - \text{sat}(\theta_{m,i}, \theta_m^*)]^2 \leq [\theta_m^d - \theta_{m,i}]^2.$$

Proof of Theorem 8.1. Let $\Delta\theta_{m,i} = \theta_m^d - \theta_{m,i}$. Consider the CEF at the ith iteration

$$E_i(t) = \frac{1}{2}e^{-\lambda t}e_i^2 + \frac{1}{2\gamma M}\int_0^t e^{-\lambda s}\frac{\partial F}{\partial \theta_m}\Delta\theta_{m,i+1}^2 ds,$$

where $\lambda > \frac{\gamma\vartheta}{M}$, $\frac{\partial F}{\partial \theta_m} \triangleq \frac{\partial F}{\partial \theta_m}(\hat{v}_i, \hat{\theta}_{m,i})$, $\hat{v}_i \triangleq v_i + \mu(v_d - v_i)$, $\hat{\theta}_{m,i} \triangleq \tilde{\theta}_{m,i} + \mu(\theta_m^d - \tilde{\theta}_{m,i})$ and $\mu \in (0,1)$. The proof consists of two parts, which address the non-increasing property of the CEF along the iteration axis and the uniform convergence of the tracking error, respectively.

Part I. Difference of $E_i(t)$. Let $\delta\theta_{m,i+1}^2 \triangleq \Delta\theta_{m,i+1}^2 - \Delta\theta_{m,i}^2$. Then the difference of $E_i(t)$ is

$$\begin{aligned}\Delta E_i(t) &\triangleq E_i(t) - E_{i-1}(t) \\ &= \frac{1}{2}e^{-\lambda t}e_i^2 + \frac{1}{2\gamma M}\int_0^t e^{-\lambda s}\frac{\partial F}{\partial \theta_m}\delta\theta_{m,i+1}^2 ds - \frac{1}{2}e^{-\lambda t}e_{i-1}^2.\end{aligned} \tag{8.17}$$

The first term on the right-hand side of (8.17), with the identical initial condition, can be expressed as

$$\frac{1}{2}e^{-\lambda t}e_i^2 = -\frac{\lambda}{2}\int_0^t e^{-\lambda s}e_i^2 ds + \int_0^t e^{-\lambda s}e_i\dot{e}_i ds. \tag{8.18}$$

According to the error dynamics (8.15), (8.18) can be rewritten as

$$\begin{aligned}\frac{1}{2}e^{-\lambda t}e_i^2 &= -\frac{\lambda}{2}\int_0^t e^{-\lambda s}e_i^2 ds \\ &\quad + \int_0^t e^{-\lambda s}e_i[-\frac{\alpha}{M}(v_d^2 - v_i^2) + \frac{1}{M}(F_d - F_i)]ds \\ &= -\frac{\lambda}{2}\int_0^t e^{-\lambda s}e_i^2 ds - \frac{\alpha}{M}\int_0^t e^{-\lambda s}(v_d + v_i)e_i^2 ds + \frac{1}{M}\int_0^t e^{-\lambda s}e_i(F_d - F_i)ds \\ &\leq -\frac{\lambda}{2}\int_0^t e^{-\lambda s}e_i^2 ds + \frac{1}{M}\int_0^t e^{-\lambda s}e_i(F_d - F_i)ds \end{aligned} \tag{8.19}$$

where $\alpha\int_0^t e^{-\lambda s}(v_d + v_i)e_i^2 ds \geq 0$ is applied since both the desired speed v_d and the actual speed v_i are non-negative, i.e., always moving ahead. By applying the Mean Value Theorem, there has

$$F_d - F_i = \frac{\partial F}{\partial v}(v_d - v_i) + \frac{\partial F}{\partial \theta_m}(\theta_m^d - \tilde{\theta}_{m,i}), \tag{8.20}$$

where $\frac{\partial F}{\partial v} \triangleq \frac{\partial F}{\partial v}(\hat{v}_i, \hat{\theta}_{m,i})$. By combining (8.19) and (8.20), it is obvious that

$$\begin{aligned}\frac{1}{2}e^{-\lambda t}e_i^2 &\leq -\frac{\lambda}{2}\int_0^t e^{-\lambda s}e_i^2 ds + \frac{1}{M}\int_0^t e^{-\lambda s}\frac{\partial F}{\partial v}e_i^2 ds \\ &\quad + \frac{1}{M}\int_0^t e^{-\lambda s}\frac{\partial F}{\partial \theta_m}(\theta_m^d - \tilde{\theta}_{m,i})e_i ds \\ &\leq -\frac{\lambda}{2}\int_0^t e^{-\lambda s}e_i^2 ds + \frac{1}{M}\int_0^t e^{-\lambda s}\frac{\partial F}{\partial \theta_m}(\theta_m^d - \tilde{\theta}_{m,i})e_i ds \end{aligned} \tag{8.21}$$

where the property $\frac{\partial F}{\partial v} \leq 0$ in Lemma 8.1 is used.

Now looking into the second term on the right-hand side of (8.17), it follows that

$$\begin{aligned}&\frac{1}{2\gamma M}\int_0^t e^{-\lambda s}\frac{\partial F}{\partial \theta_m}\delta\theta_{m,i+1}^2 ds \\ =\ &\frac{1}{2\gamma M}\int_0^t e^{-\lambda s}\frac{\partial F}{\partial \theta_m}[(\theta_m^d - \theta_{m,i+1})^2 - (\theta_m^d - \theta_{m,i})^2]ds \\ \leq\ &\frac{1}{2\gamma M}\int_0^t e^{-\lambda s}\frac{\partial F}{\partial \theta_m}[(\theta_m^d - \theta_{m,i+1})^2 - (\theta_m^d - \tilde{\theta}_{m,i})^2]ds \\ =\ &\frac{1}{2\gamma M}\int_0^t e^{-\lambda s}\frac{\partial F}{\partial \theta_m}[(\theta_{m,i+1} - \tilde{\theta}_{m,i})(\theta_{m,i+1} + \tilde{\theta}_{m,i} - 2\theta_m^d)]ds, \end{aligned} \tag{8.22}$$

where Property 1 is applied. Substitute the ILC law (8.16) into (8.22), it gives

$$\begin{aligned} & \frac{1}{2\gamma M}\int_0^t e^{-\lambda s}\frac{\partial F}{\partial \theta_m}\delta\theta_{m,i+1}^2 ds \qquad (8.23)\\ \leq\ & \frac{1}{2\gamma M}\int_0^t e^{-\lambda s}\frac{\partial F}{\partial \theta_m}\gamma e_i(2\theta_{m,i+1}-\gamma e_i-2\theta_m^d)ds \\ =\ & -\frac{1}{M}\int_0^t e^{-\lambda s}\frac{\partial F}{\partial \theta_m}(\theta_m^d-\theta_{m,i+1})e_i ds-\frac{\gamma}{2M}\int_0^t e^{-\lambda s}\frac{\partial F}{\partial \theta_m}e_i^2 ds \end{aligned}$$

Then combining (8.21) and (8.23) with (8.17) yields

$$\begin{aligned} \Delta E_i(t) \leq\ & -\frac{\lambda}{2}\int_0^t e^{-\lambda s}e_i^2 ds-\frac{\gamma}{2M}\int_0^t e^{-\lambda s}\frac{\partial F}{\partial \theta_m}e_i^2 ds \\ & -\frac{1}{2}e^{-\lambda t}e_{i-1}^2+\frac{1}{M}\int_0^t e^{-\lambda s}\frac{\partial F}{\partial \theta_m}(\theta_{m,i+1}-\tilde{\theta}_{m,i})e_i ds \\ =\ & -\frac{\lambda}{2}\int_0^t e^{-\lambda s}e_i^2 ds-\frac{\gamma}{2M}\int_0^t e^{-\lambda s}\frac{\partial F}{\partial \theta_m}e_i^2 ds \\ & -\frac{1}{2}e^{-\lambda t}e_{i-1}^2+\frac{\gamma}{M}\int_0^t e^{-\lambda s}\frac{\partial F}{\partial \theta_m}e_i^2 ds \\ =\ & -\frac{\lambda}{2}\int_0^t e^{-\lambda s}e_i^2 ds+\frac{\gamma}{2M}\int_0^t e^{-\lambda s}\frac{\partial F}{\partial \theta_m}e_i^2 ds-\frac{1}{2}e^{-\lambda t}e_{i-1}^2. \qquad (8.24) \end{aligned}$$

By using the property $0<\frac{\partial F}{\partial \theta_m}\leq\vartheta$ in Lemma 8.1, (8.24) yields that

$$\Delta E_i(t) \leq -\frac{1}{2}(\lambda-\frac{\gamma\vartheta}{M})\int_0^t e^{-\lambda s}e_i^2 ds-\frac{1}{2}e^{-\lambda t}e_{i-1}^2. \qquad (8.25)$$

Since $\lambda>\frac{\gamma\vartheta}{M}$, the term $-\frac{1}{2}(\lambda-\frac{\gamma\vartheta}{M})$ is negative. Consequently, from (8.25) it follows that

$$\Delta E_i(t)\leq -\frac{1}{2}e^{-\lambda t}e_{i-1}^2<0. \qquad (8.26)$$

Part II. Convergence property. From (8.26), there has

$$\sum_{j=1}^{i}\Delta E_j(t)\leq -\frac{1}{2}e^{-\lambda t}\sum_{j=1}^{i}e_{j-1}^2\leq -\frac{1}{2}e^{-\lambda T}\sum_{j=1}^{i}e_{j-1}^2. \qquad (8.27)$$

Then it follows that

$$E_i(t)\leq E_0(t)-\frac{1}{2}e^{-\lambda T}\sum_{j=1}^{i}e_{j-1}^2. \qquad (8.28)$$

Note that $E_i(t)$ is positive, and $E_0(t)$ is finite since both $e_0(t)$ and $\theta_{m,1}$ are finite. Therefore, we can obtain from (8.28) that the tracking error $e_i(t)$ converges to zero pointwisely as $i \to \infty$.

Further, from (8.3)-(8.4) and (8.6)-(8.7), it follows that

$$\left(\frac{\partial h}{\partial t}\right)^2 \leq \frac{4}{9}\pi^2 f^2 l^2 \theta_m^{*2} \sec^4(\theta_m^*), \tag{8.29}$$

$$\left(\frac{\partial h}{\partial x}\right)^2 \leq \tan^2(\theta_m^*). \tag{8.30}$$

Therefore, the boundedness of F_i can be obtained from (8.10), which implies that $\dot{v}_i$ is bounded by (8.13). Consequently, since both $v_d \in C^1[0,T]$ and $\dot{v}_d \in C[0,T]$ are bounded, it obtains the boundedness of $\dot{e}_i(t)$, which guarantees the uniform continuity of $e_i(t)$ in the interval $[0,T]$. In the sequel, by applying Barbalat lemma, the uniform convergence of $e_i(t)$ can be obtained. ■

Remark 8.2 *In the updating law (8.16), the convergence of tracking error can be guaranteed as long as the learning gain γ is positive. Generally, an appropriate learning gain is desired for practical applications. With a small learning gain, more iterations may be needed before reaching a preset accuracy. With an overly large learning gain, overshoot may occur, leading to an oscillatory response along the iteration axis.*

8.5 Simulation and Experiment

In order to illustrate the efficiency of the proposed ILC scheme, both simulations and experiments are conducted in this section.

8.5.1 Parametric Estimations

The parameters used in the simulation have been selected based on the two-link robotic fish prototype: $M = 0.4kg$, $l = 0.36m$, $\rho = 1000\text{kg}/m^3$, $A(l) = 0.165^2\pi/4m^2$ and $\theta_m^* = \pi/4$. Furthermore, in order to estimate the water resistance coefficient three experiments are conducted firstly. In the experiments, the robotic fish swims at "cruise" swimming mode and the overhead camera is used to record the trajectories of the fish, by which the speed of the robot can be estimated. The undulatory amplitudes of the tail, and the corresponding average speeds are presented in the following table.

Table 8.1: Experimental Results for Parameter Estimations

Amplitude (rad)	$\frac{\pi}{4}$	$\frac{7}{36}\pi$	$\frac{5}{36}\pi$
Speed (m/s)	0.12762	0.09282	0.05117

By utilizing Least Square Method, the water resistance coefficient α can be estimated as $\alpha = 165.7056\ kg/m$, which will be utilized for simulation.

8.5.2 Simulations

Consider the dynamical model (8.13), and let the target speed trajectory be

$$v_d(t) = \begin{cases} 2.25t^2(t-40)^2/40^4, & t \in [0,10]\bigcup[30,40]s, \\ 0.0791, & t \in (10,30)s, \end{cases} \tag{8.31}$$

which is shown in Fig. 8.5.

In such desired motion, it is expected that the robotic fish should accelerate from 0 m/s to 0.0791 m/s within 10 seconds and holds the speed for the next 20 seconds. After that, it begins to decelerate to 0 m/s within 10 seconds.

Set the input signal at the zeroth iteration as $\theta_{m,0}(t) = 0$ for simplicity, and thus

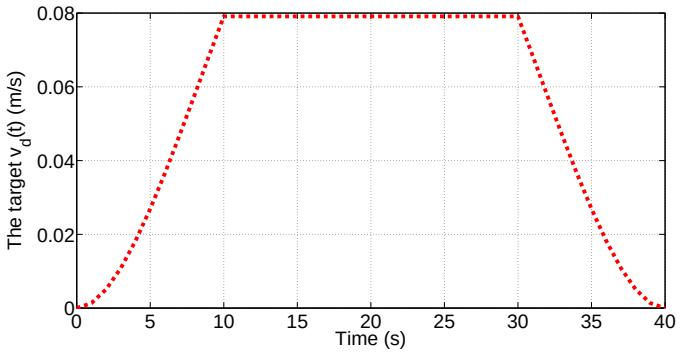

Figure 8.5: The target speed trajectory.

the corresponding speed of the robot is $v_0(t) = 0$. As such, the control input at the first iteration is generated by the product of the target and the learning gain. In such case, if the selected learning gain is too small, the learning process will be very slow. If the learning gain is too large, overshot will occur, and thus the convergence rate will be adversely affected. In this part, three different learning gains are implemented, namely, $\gamma = 4$, $\gamma = 7$, and $\gamma = 10$. Figure 8.6 presents the maximal tracking errors, $|e_i|_s \triangleq \sup_{t\in[0,40]} |e_i(t)|$, in three cases. It shows numerically that $\gamma = 7$ leads to the fastest convergence rate. For the learning gain $\gamma = 4$, more iterations are needed to reach the same convergence accuracy as $\gamma = 7$, and the learning gain $\gamma = 10$ slows the learning process down due to the occurrence of overshot which is shown in Fig. 8.7. To show the effect of saturation function, the input signals at different iterations for the learning gain $\gamma = 10$ is presented in Fig. 8.8, where the input signal at the first iteration is saturated by $\theta_m^* = \pi/4$, and those at the 2nd, 4th, 6th iterations do not reach the saturation value $\theta_m^* = \pi/4$. Moreover, Fig. 8.9 gives the reference and output profiles for $\gamma = 4$ at the 1st, 2nd, 4th, 6th iterations, respectively. Observing the output profiles in Fig. 8.9, the speed trajectories approach the target gradually as the iteration number increases, and the difference between v_6 and v_d is almost invisible.

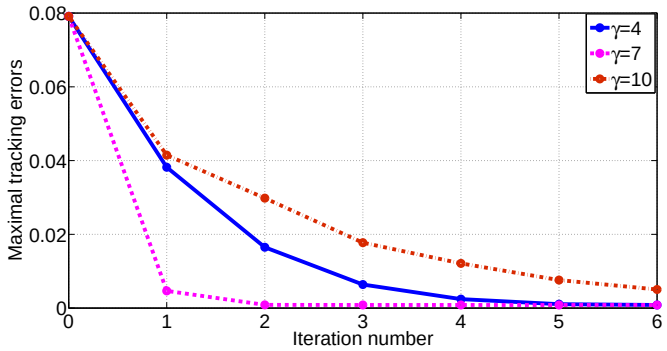

Figure 8.6: Maximal tracking error profiles for different learning gains.

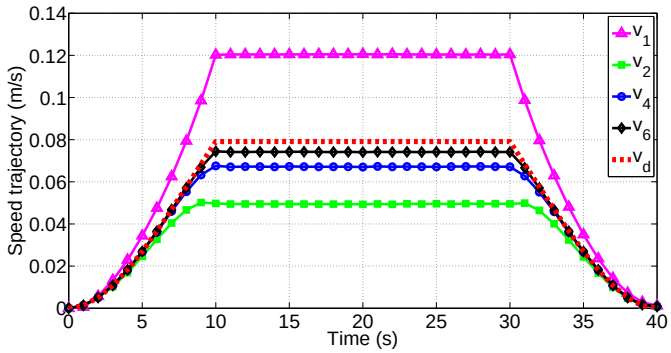

Figure 8.7: Speed profiles at different iterations for $\gamma = 10$.

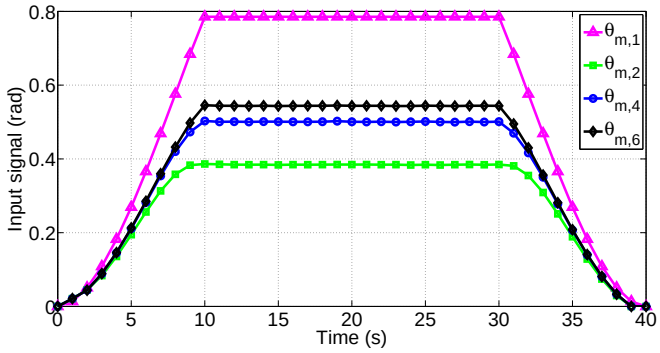

Figure 8.8: Control input signals at different iterations for $\gamma = 10$.

8.5.3 Experiments

To verify the feasibility and reliability of the proposed P-type ILC algorithm, experiments for speed tracking are conducted in a water tank of the size about $3 \times 1.8\ m^2$ with still water of 0.5m in depth. The frequency of the tail undulation is fixed at 1 Hz and the amplitude signals is sent to the robotic fish from the host computer. After receiving

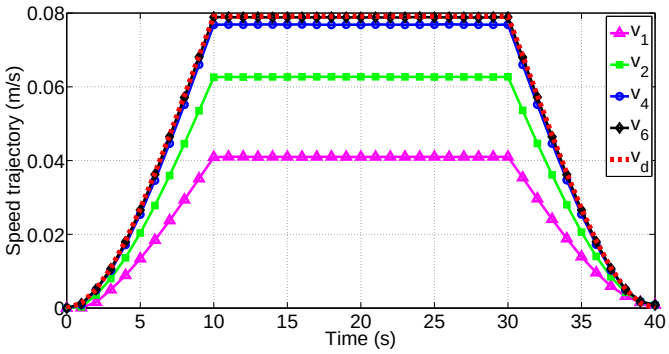

Figure 8.9: Speed profiles at different iterations for $\gamma = 4$.

the signals of amplitude through the wireless module, the processor transform them to pulse width modulation (PWM) signals to drive the servomotor. Then, the motor begins to work and the corresponding swimming gait will be performed by the fish according to the received signals. In these experiments, the amplitude signals are symmetric and the robotic fish swims at the "cruise" swimming mode, which is shown in Fig. 8.10.

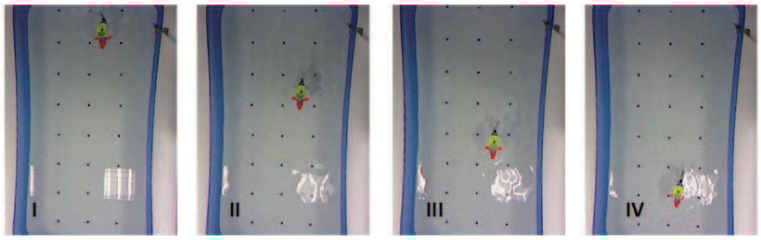

Figure 8.10: The robotic fish swims at "cruise" swimming mode in experiments.

Similar as the simulation part, the desired speed trajectory is given as (8.31), namely, the robot performs acceleration, constant speed and deceleration process in sequence. It is worthwhile to note that the reset condition in Assumption 8.1 can be met since it only requires a zero initial speed. To ensure the stability of experiments, the modest learning gain $\gamma = 4$ is selected. The control input at the first iteration is the same as that in simulation.

Figure 8.11 gives the variation of the maximal tracking error $|e_i|_s$. It shows that $|e_i|_s$ has been decreased by more than 80% within 6 iterations. Figure 8.12 presents the

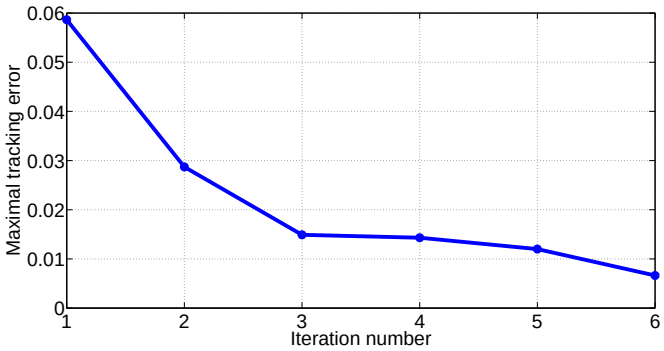

Figure 8.11: Maximal tracking error profile in experiments.

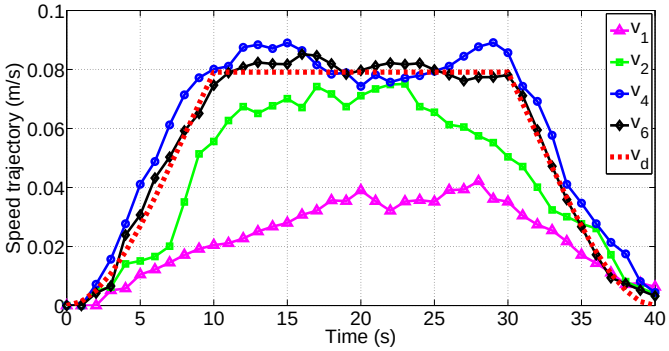

Figure 8.12: Speed profiles in different experiments.

learning performance in each experiment. At the 1st experiment, the speed trajectory has very large deviations from the desired one. The maximal tracking error is gradually reduced by the learning controller, and is almost eliminated at 6th iteration. It is noted that in Fig. 8.12, the speed of the robotic fish is actually not 0 m/s when $t = 40$s, which is due to the inertia of the robot and the fluid characteristics. Furthermore, since the feedback information providing by ILC is off-line, it is difficult for the robot to achieve a steady state within a short time. Therefore, oscillations in the speed trajectory during the time interval $[10, 30]$s are unavoidable but acceptable. The results reveal that the proposed ILC scheme is an effective control approach for the speed tracking of robotic fish.

8.6 Conclusion

This chapter presents an ILC approach for precise speed tracking control of a two-link robotic fish. ILC can significantly improve the tracking performance by iteratively learning the desired control profile from previous control executions despite the high nonlinearity in fish model. It is shown, from both theoretical analysis and real-time experiments, that ILC is an appropriate and powerful motion control method for robotic fish because of its almost model-free property and the simplicity of the control algorithm. Motivated by its effectiveness in the speed tracking control, the applicability of ILC in turning control of robotic fish will be investigated in the next research phase.

Chapter 9

Conclusion and Future Works

9.1 Conclusion

This thesis aims to apply ILC to solve new control problems. The main contribution of this research work is to extend learning control theory and then facilitate the real-time applications of learning control. The summary of the thesis is as follows.

In Chapter 2, ILC design for discrete-time linear systems with randomly varying trial lengths is presented. By introducing a stochastic variable and an iteration-average operator, a unified expression of ILC scheme for systems with non-unified trial lengths is proposed. Because of the stochastic property of trial lengths, the convergence of tracking error is derived in the sense of mathematical expectation.

In Chapter 3, a class of continuous-time nonlinear dynamical systems with randomly varying trial lengths is considered under the framework of ILC. Different from Chapter 2, an iteratively-moving-average operator is adopted in the ILC law due to the fact that the latest trials could provide more accurate control information than those 'older' trials. Based on the contraction mapping methodology, it is shown that the proposed learning algorithm works effectively to nullify the tracking error for both nonlinear

affine and non-affine systems.

In Chapter 4, an AILC scheme with a scaling function is proposed for control tasks with different magnitude and time scales. The major advantage of the proposed AILC algorithm is the ability to utilize all the learned knowledge despite the iteratively varying tracking tasks for nonlinear systems with time-invariant and time-varying parametric uncertainties. The convergence is derived through Lyapunov-like theory.

In Chapter 5, a RILC scheme is presented for state tracking control of nonlinear MIMO systems with non-parametric uncertainties under the alignment condition. To deal with the norm-bounded uncertainties, a CEF is introduced to prove the asymptotical convergence of the tracking error. In addition, the proposed RILC approach is also extended to systems with uncertain input distribution matrix.

In Chapters 6 and 7, the ILC approaches are extended from ODE systems to PDE systems, where ILC for linear and nonlinear PDE systems are investigated, respectively. In Chapter 6, owning to the linear property of the system model, the LIDPSs are first reformulated into a matrix form in the frequency domain. Then, through the determination of a fundamental matrix, the transfer function of LIDPS from input to output is precisely evaluated, which thus facilitates the consequent ILC design and convergence analysis in the frequency domain. The proposed control design scheme is able to deal with parametric and non-parametric uncertainties and make full use of the process repetition, while avoid any simplification or discretization for the 3D dynamics of LIDPS in the time, space, and iteration domains. In Chapter 7, a D-type anticipatory ILC scheme is applied to the boundary control of nonlinear inhomogeneous heat equations. By transforming the inhomogeneous heat equation into its integral form and exploiting the properties of the embedded Jacobi Theta function, the learning conver-

gence of ILC is guaranteed based on contraction mapping methodology. Meanwhile, due to the feedforward characteristic of ILC, the proposed scheme not only makes anticipatory compensation possible to overcome the heat conduction delay in boundary output tracking, but also eliminates the gain margin limitation encountered in feedback control.

At last, Chapter 8 considers a real-time application of ILC, that is, ILC for precise speed tracking of a robotic fish. The mathematical model for the robotic fish is first constructed by virtue of Newton's second law, which is highly nonlinear and non-affine in control input. Then based on the constructed model, a P-type ILC algorithm is proposed for speed tracking tasks of the robotic fish, and the convergence analysis is conducted under the framework of CEF method. Due to its partial model-free property, ILC is shown to be an appropriate and powerful motion control method for robotic fish from both theoretical analysis and real-time experiments.

9.2 Future Works

This section provides potential future research directions in continuation of this research.

1. In Chapters 2 and 3, ILC for systems with randomly varying trial lengths are investigated based on contraction mapping methodology, where the global Lipschitz continuous property of the systems is required. For local Lipschitz continuous systems, how to formulate and deal with non-uniform trial lengths under the framework of CEF-based ILC is of interest and challenge. Besides, the novel formulation of ILC with non-uniform trial lengths could be extended to more control problems that are perturbed by random factors.

2. In Chapter 5, a RILC scheme is developed for nonlinear MIMO systems with non-parametric uncertainties under alignment condition. Under the framework of ILC, our idea could be extended along the following directions: (1) extension to systems with non-square uncertain input distribution matrix, (2) extension to output tracking control or state tracking control but with input or state constraints, (3) extension to systems whose nonlinear part does not belong to any of the three types of uncertainties defined in the chapter.

3. Chapters 6 and 7 address ILC design problems for boundary tracking control of some particular PDE systems. In the future work, extensions should be done for more general systems, such as PDE systems with nonlinear uncertainties, high order PDE systems, etc. Meanwhile, it is also desirable to explore more advanced ILC schemes for PDE processes.

4. Many control issues in traditional ILC, such as initial resetting problem, non-uniform trial length problem, iteration-varying target trajectories, etc, should be considered correspondingly in ILC design of PDE systems.

5. In Chapter 8, a P-type ILC algorithm is developed for precise speed tracking control of a two-link robotic fish. Because of its almost model-free property and the simplicity of the control algorithm, ILC is proved to be an powerful motion control method for robotic fish. Motivated by its effectiveness in the speed tracking control, the applicability of ILC in turning control of robotic fish will be investigated in the near future. In addition, applicability of ILC to other real-time systems with repetitiveness is worthy of study.

6. The convergence of ILC in the thesis is based on L_2-norm or λ-norm. Whether

the monotonic convergence of ILC in vector norm can be guaranteed for generic systems is still an open and challenging problem.

Bibliography

[1] Suguru Arimoto, Sadao Kawamura, and Fumio Miyazaki. Bettering operation of robots by learning. *Journal of Robotic Systems*, 1(2):123–140, 1984.

[2] Kevin L. Moore. *Iterative Learning Control for Deterministic Systems*. Springer-Verlag, London, 1993.

[3] Richard W. Longman. Iterative learning control and repetitive control for engineering practice. *International Journal of Control*, 73(10):930–954, 2000.

[4] Mikael Norrlof and Svante Gunnarsson. Time and frequency domain convergence properties in iterative learning control. *International Journal of Control*, 75(14):1114–1126, 2002.

[5] Jian-Xin Xu and Ying Tan. *Linear and Nonlinear Iterative Learning Control*. Springer-Verlag, Germany, 2003. In series of Lecture Notes in Control and Information Sciences.

[6] D. A. Bristow, M. Tharayil, and A. G. Alleyne. A survey of iterative learning control. *IEEE Control Systems*, 26(3):96–114, 2006.

[7] Kevin L. Moore, Yangquan Chen, and Hyo-Sung Ahn. Iterative learning con-

trol: A tutorial and big picture. In *Proceedings of the 45th IEEE Conference on Decision and Control*, pages 2352–2357, 2006.

[8] Youqing Wang, Furong Gao, and Francis J. Doyle. Survey on iterative learning control, repetitive control, and run-to-run control. *Journal of Process Control*, 19(10):1589–1600, 2009.

[9] Hyo-Sung Ahn, Yangquan Chen, and Kevin L. Moore. Iterative learning control: Brief survey and categorization. *IEEE Transactions on Systems, Man, and Cybernetics - Part C: Applications and Reviews*, 37(6):1099–1121, 2007.

[10] Hyo-Sung Ahn, Kevin L. Moore, and Yangquan Chen. Trajectory-keeping in satellite formation flying via robust periodic learning control. *International Journal of Robust and Nonlinear Control*, 20(14):1655–1666, 2010.

[11] Abdelhamid Tayebi. Adaptive iterative learning control of robot manipulators. *Automatica*, 40:1195–1203, 2004.

[12] Abdelhamid Tayebi and S. Islam. Adaptive iterative learning control of robot manipulators: Experimental results. *Control Engineering Practice*, 14:843–851, 2006.

[13] Mingxuan Sun, Shuzhi Sam Ge, and Iven M Y Mareels. Adaptive repetitive learning control of robotic manipulators without the requirement for initial repositioning. *IEEE Transactions on Robotics*, 22(3):563–568, 2006.

[14] YangQuan Chen, Kevin L. Moore, Jie Yu, and Tao Zhang. Iterative learning control and repetitive control in hard disk drive industry–a tutorial. *International Journal of Adaptive Control and Signal Processing*, 22(4):325–343, 2008.

[15] Mingxuan Sun, Xiongxiong He, and Bingyu Chen. Repetitive learning control for time-varying robotic systems: A hybrid learning scheme. *Acta Automatica Sinica*, 33(11):1189 – 1195, 2007.

[16] Toshiharu Sugie and Fumitoshi Sakai. Noise tolerant iterative learning control for a class of continuous-time systems. *Automatica*, 43(10):1766–1771, 2007.

[17] Abdelhamid Tayebi, S. Abdul, M. B. Zaremba, and Y. Ye. Robust iterative learning control design: Application to a robot manipulator. *IEEE/ASME Transactions on Mechatronics*, 13(5):608–613, 2008.

[18] Xuhui Bu, Zhongsheng Hou, Fashan Yu, and Ziyi Fu. Iterative learning control for a class of non-linear switched systems. *IET Control Theory & Applications*, 7(3):470–481, 2013.

[19] Xiaoe Ruan and Jianyong Zhao. Convergence monotonicity and speed comparison of iterative learning control algorithms for nonlinear systems. *IMA Journal of Mathematical Control and Information*, 30(4):473–486, 2013.

[20] Deqing Huang, Jian-Xin Xu, Xuefang Li, Chao Xu, and Miao Yu. D-type anticipatory iterative learning control for a class of inhomogeneous heat equations. *Automatica*, 49(8):2397–2408, 2013.

[21] Chiang-Ju Chien. A discrete iterative learning control for a class of nonlinear time-varying systems. *IEEE Transactions on Automatic Control*, 43(5):748–752, 1998.

[22] Kwang-Hyun Park. An average operator-based pd-type iterative learning control for variable initial state error. *IEEE Transactions on Automatic Control*, 50(6):865–869, 2005.

[23] Hyo-Sung Ahn, Yang Quan Chen, and Kevin L. Moore. Iterative learning control: Brief survey and categorization. *IEEE Transactions on Systems, Man, and Cybernetics, Part C: Applications and Reviews*, 37(6):1099–1121, 2007.

[24] Thomas Seel, Thomas Schauer, and Jörg Raisch. Iterative learning control for variable pass length systems. In *Proceedings of the 18th World Congress, International Federation of Automatic Control (IFAC11)*, pages 4880–4885, 2011.

[25] Richard W. Longman and K. D. Mombaur. Investigating the use of iterative learning control and repetitive control to implement periodic gaits. In *Fast Motions in Biomechanics and Robotics*, pages 189–218. Springer, 2006.

[26] Mickaël Guth, Thomas Seel, and Jörg Raisch. Iterative learning control with variable pass length applied to trajectory tracking on a crane with output constraints. In *Proceedings of the 52nd IEEE Conference on Decision and Control*, pages 6676–6681, 2013.

[27] M. French and E. Rogers. Non-linear iterative learning by an adaptive Lyapunov technique. *International Journal of Control*, 73(10):840–850, 2000.

[28] Jian-Xin Xu and Ying Tan. A composite energy function-based learning control approach for nonlinear systems with time-varying parametric uncertainties. *IEEE Transactions on Automatic Control*, 47(11):1940–1945, 2002.

[29] Ying-Chung Wang, Chiang-Ju Chien, and Ching-Cheng Teng. Direct adaptive iterative learning control of nonlinear systems using an output-recurrent fuzzy neural network. *IEEE Transactions on Systems, Man, and Cybernetics, Part B: Cybernetics*, 34(3):1348–1359, 2004.

[30] Abdelhamid Tayebi and Chiang-Ju Chien. A unified adaptive iterative learning control framework for uncertain nonlinear systems. *IEEE Transactions on Automatic Control*, 52(10):1907–1913, 2007.

[31] Jian-Xin Xu. A survey on iterative learning control for nonlinear systems. *International Journal of Control*, 84(7):1275–1294, 2011.

[32] Jian-Xin Xu and Rui Yan. On repetitive learning control for periodic tracking tasks. *IEEE Transactions on Automatic Control*, 51(11):1842–1848, 2006.

[33] Jian-Xin Xu, Xu Jin, and Deqing Huang. Composite energy function-based iterative learning control for systems with nonparametric uncertainties. *International Journal of Adaptive Control and Signal Processing*, 28(1):1–13, 2014.

[34] Jinhoon Choi, Beom Joon Seo, and Kwang Soon Lee. Constrained digital regulation of hyperbolic pde systems: A learning control approach. *Korean Journal of Chemical Engineering*, 18(5):606–611, 2001.

[35] B. Cichy, K. Galkowski, E. Rogers, and A. Kummert. An approach to iterative learning control for spatio-temporal dynamics using nd discrete linear systems models. *Multidimensional Systems and Signal Processing*, 22(1-3):83–96, 2011.

[36] Chao Xu, R. Arastoo, and E. Schuster. On iterative learning control of parabolic distributed parameter systems. In *Proceedings of the 17th Mediterranean Conference on Control and Automation*, pages 510–515, 2009.

[37] Kevin L. Moore and Yang Quan Chen. Iterative learning control approach to a diffusion control problem in an irrigation application. In *Proceedings of the 2006 IEEE International Conference on Mechatronics and Automation*, pages 1329–1334, 2006.

[38] Zhihua Qu. An iterative learning algorithm for boundary control of a stretched moving string. *Automatica*, 38(5):821 – 827, 2002.

[39] Haiyu Zhao and Christopher D. Rahn. Iterative learning velocity and tension control for single span axially moving materials. *Journal of Dynamic Systems, Measurement, and Control*, 130(5):051003, 2008.

[40] Deqing Huang and Jian-Xin Xu. Steady-state iterative learning control for a class of nonlinear pde processes. *Journal of Process Control*, 21(8):1155 – 1163, 2011.

[41] Jingli Kang. A newton-type iterative learning algorithm of output tracking control for uncertain nonlinear distributed parameter systems. In *Proceedings of the 33rd Chinese Control Conference (CCC)*, pages 8901–8905, 2014.

[42] Jianxiang Zhang, Xisheng Dai, and Senping Tian. Iterative learning control for distributed parameter switched systems. In *Proceedings of the 27th ChineseControl and Decision Conference (CCDC)*, pages 1105–1110, 2015.

[43] Xisheng Dai, Senping Tian, Yunjian Peng, and Wenguang Luo. Closed-loop p-type iterative learning control of uncertain linear distributed parameter systems. *IEEE/CAA Journal of Automatica Sinica*, 1(3):267–273, 2014.

[44] Qian Qiu, Wenguang Luo, Xisheng Dai, and Chuang Lin. Iterative learning control for nonlinear distributed parameter system with state time delay. In *Proceedings of the 2013 IEEE International Conference on Information and Automation (ICIA)*, pages 478–482, 2013.

[45] Xisheng Dai, Chao Xu, Senping Tian, and Zhenglin Li. Iterative learning control for mimo second-order hyperbolic distributed parameter systems with uncertainties. *Advances in Difference Equations*, 2016(1):1–13, 2016.

[46] Xisheng Dai, Sen-Ping Tian, and Ya-Jun Guo. Iterative learning control for discrete parabolic distributed parameter systems. *International Journal of Automation and Computing*, 12(3):316–322, 2015.

[47] Junzhi Yu, Long Wang, and Min Tan. Geometric optimization of relative link lengths for biomimetic robotic fish. *IEEE Transactions on Robotics*, 23(2):382–386, 2007.

[48] Junzhi Yu, Lizhong Liu, Long Wang, Min Tan, and De Xu. Turning control of a multilink biomimetic robotic fish. *IEEE Transactions on Robotics*, 24(1):201–206, 2008.

[49] M. S. Triantafyllou, A. H. Techet, and F. S. Hover. Review of experimental work in biomimetic foils. *IEEE Journal of Oceanic Engineering*, 29(3):585–594, 2004.

[50] K. A. Harper, M.D. Berkemeier, and S. Grace. Modeling the dynamics of spring-driven oscillating-foil propulsion. *IEEE Journal of Oceanic Engineering*, 23(3):285–296, 1998.

[51] W. Zhao, Y. Hu, L. Zhang, and L. Wang. Design and cpg-based control of biomimetic robotic fish. *IET Control Theory & Applications*, 3(3):281–293, 2009.

[52] Wei Wang, Jiajie Guo, Zijian Wang, and Guangming Xie. Neural controller for swimming modes and gait transition on an ostraciiform fish robot. In *Proceedings of the 2013 IEEE/ASME International Conference on Advanced Intelligent Mechatronics (AIM)*, pages 1564–1569, 2013.

[53] Yonghui Hu, Jianhong Liang, and Tianmiao Wang. Parameter synthesis of coupled nonlinear oscillators for cpg-based robotic locomotion. *IEEE Transactions on Industrial Electronics*, 61(11):6183–6191, 2014.

[54] Yonghui Hu, Weicheng Tian, Jianhong Liang, and Tianmiao Wang. Learning fish-like swimming with a cpg-based locomotion controller. In *Proceedings of the 2011 IEEE/RSJ International Conference on Intelligent Robots and Systems (IROS)*, pages 1863–1868, 2011.

[55] Xuelei Niu, Jianxin Xu, Qinyuan Ren, and Qingguo Wang. Locomotion learning for an anguilliform robotic fish using central pattern generator approach. *IEEE Transactions on Industrial Electronics*, 61(9):4780–4787, 2014.

[56] Junzhi Yu, Min Tan, Shuo Wang, and Erkui Chen. Development of a biomimetic robotic fish and its control algorithm. *IEEE Transactions on Systems, Man, and Cybernetics, Part B: Cybernetics*, 34(4):1798–1810, 2004.

[57] Li Wen, Tianmiao Wang, Guanhao Wu, Jianhong Liang, and Chaolei Wang. Novel method for the modeling and control investigation of efficient swimming for robotic fish. *IEEE Transactions on Industrial Electronics*, 59(8):3176–3188, 2012.

[58] Kexu Zou, Chen Wang, Guangming Xie, Tianguang Chu, Long Wang, and Yingmin Jia. Cooperative control for trajectory tracking of robotic fish. In *Proceedings of the 2009 American Control Conference*, pages 5504–5509, 2009.

[59] Yonghui Hu, Wei Zhao, and Long Wang. Vision-based target tracking and collision avoidance for two autonomous robotic fish. *IEEE Transactions on Industrial Electronics*, 56(5):1401–1410, 2009.

[60] K. A. Morgansen, V. Duidam, R. J. Mason, J. W. Burdick, and R. M. Murray. Nonlinear control methods for planar carangiform robot fish locomotion. In *Proceedings of the 2001 IEEE International Conference on Robotics and Automation*, volume 1, pages 427–434, 2001.

[61] Kevin L. Moore. A non-standard iterative learning control approach to tracking periodic signals in discrete-time non-linear systems. *International Journal of Control*, 73(10):955–967, 2000.

[62] Greg Heinzinger, D. Fenwick, B. Paden, and F. Miyazaki. Stability of learning control with disturbances and uncertain initial conditions. *IEEE Transactions on Automatic Control*, 37(1):110–114, 1992.

[63] Kwang-Hyun Park and Zeungnam Bien. A generalized iterative learning controller against initial state error. *International Journal of Control*, 73(10):871–881, 2000.

[64] Yangquan Chen, Changyun Wen, Zhiming Gong, and Mingxuan Sun. An iterative learning controller with initial state learning. *IEEE Transactions on Automatic Control*, 44(2):371–376, 1999.

[65] Zeungnam Bien and Jian-Xin Xu. *Iterative learning control: analysis, design, integration and applications*. Kluwer Academic Publishers, 1998.

[66] Hak-Sung Lee and Zeungnam Bien. Study on robustness of iterative learning control with non-zero initial error. *International Journal of Control*, 64(3):345–359, 1996.

[67] Jian-Xin Xu and Tao Zhu. Dual-scale direct learning control of trajectory track-

ing for a class of nonlinear uncertain systems. *IEEE Transactions on Automatic Control*, 44(10):1884–1888, 1999.

[68] Samer S. Saab, William G. Vogt, and Marlin H. Mickle. Learning control algorithms for tracking slowly varying trajectories. *IEEE Transactions on Systems, Man, and Cybernetics, Part B: Cybernetics*, 27(4):657–670, 1997.

[69] Jian-Xin Xu. Direct learning of control efforts for trajectories with different magnitude scales. *Automatica*, 33(12):2191–2195, 1997.

[70] Jian-Xin Xu. Direct learning of control efforts for trajectories with different time scales. *IEEE Transactions on Automatic Control*, 43(7):1027–1030, 1998.

[71] Jian-Xin Xu, Jing Xu, and Badrinath Viswanathan. Recursive direct learning of control efforts for trajectories with different magnitude scales. *Asian Journal of Control*, 4(1):49–59, 2002.

[72] Jian-Xin Xu and Jing Xu. On iterative learning from different tracking tasks in the presence of time-varying uncertainties. *IEEE Transactions on Systems, Man, and Cybernetics, Part B: Cybernetics*, 34(1):589–597, 2004.

[73] Otomar Hájek. Discontinuous differential equations. I. *Journal of Differential Equations*, 32(2):149–170, 1979.

[74] M. M. Polycarpou and P. A. Ioannou. On the existence and uniqueness of solutions in adaptive control systems. *IEEE Transactions on Automatic Control*, 38(3):474–479, 1993.

[75] Vadim Ivanovich Utkin. *Sliding modes and their application in variable structure systems*. Mir Publishers, 1978.

[76] Jean-Jacques E. Slotine and Weiping Li. *Applied nonlinear control*, volume 199. Prentice-hall Englewood Cliffs, NJ, 1991.

[77] P. A. Ioannou and A. Datta. Robust adaptive control: a unified approach. *Proceedings of the IEEE*, 79(12):1736–1768, 1991.

[78] Petros A. Ioannou and Petar V. Kokotovic. Adaptive systems with reduced models. *Lecture notes in control and information sciences*, 1983.

[79] Shaocheng Tong, Yongming Li, and Peng Shi. Observer-based adaptive fuzzy backstepping output feedback control of uncertain mimo pure-feedback nonlinear systems. *IEEE Transactions on Fuzzy Systems*, 20(4):771–785, 2012.

[80] Shaocheng Tong and Yongming Li. Adaptive fuzzy output feedback control of mimo nonlinear systems with unknown dead-zone inputs. *IEEE Transactions on Fuzzy Systems*, 21(1):134–146, 2013.

[81] Fanglai Zhu, Jian Xu, and Maoyin Chen. The combination of high-gain sliding mode observers used as receivers in secure communication. *IEEE Transactions on Circuits and Systems I: Regular Papers*, 59(11):2702–2712, 2012.

[82] Weisheng Chen, Junmin Li, and Jing Li. Practical adaptive iterative learning control framework based on robust adaptive approach. *Asian Journal of Control*, 13(1):85–93, 2011.

[83] Yu-Ping Tian and Xinghuo Yu. Robust learning control for a class of nonlinear systems with periodic and aperiodic uncertainties. *Automatica*, 39(11):1957–1966, 2003.

[84] Ying Tan and Jian-Xin Xu. Learning based nonlinear internal model control. In

Proceedings of the 2003 American Control Conference, volume 4, pages 3009–3013, 2003.

[85] Zhonglun Cai, David Angland, Xin Zhang, and Peng Chen. Iterative learning control for trailing-edge flap lift enhancement with pulsed blowing. *AIAA Journal*, 53(7):1969–1979, 2015.

[86] Mark W. Blackwell, Owen R. Tutty, E. Rogers, and Richard D. Sandberg. Iterative learning control applied to a non-linear vortex panel model for improved aerodynamic load performance of wind turbines with smart rotors. *International Journal of Control*, 89(1):55–68, 2016.

[87] Owen Tutty, Mark Blackwell, Eric Rogers, and Richard Sandberg. Iterative learning control for improved aerodynamic load performance of wind turbines with smart rotors. *IEEE Transactions on Control Systems Technology*, 22(3):967–979, 2014.

[88] Simon J. Steinberg, Marcel Staats, Wolfgang Nitsche, and Rudibert King. Iterative learning active flow control applied to a compressor stator cascade with periodic disturbances. *Journal of Turbomachinery*, 137(11):111003, 2015.

[89] Ruth Curtain and Kirsten Morris. Transfer functions of distributed parameter systems: a tutorial. *Automatica*, 45(5):1101–1116, 2009.

[90] Youqing Wang, Furong Gao, and Francis J. Doyle. Survey on iterative learning control, repetitive control, and run-to-run control. *Journal of Process Control*, 19(10):1589 – 1600, 2009.

[91] F. Malchow and O. Sawodny. Feedforward control of inhomogeneous linear

first order distributed parameter systems. In *Proceedings of the 2011 American Control Conference (ACC)*, pages 3597–3602, 2011.

[92] Wei He, Shuzhi Sam Ge, Bernard Voon Ee How, Yoo Sang Choo, and Keum-Shik Hong. Robust adaptive boundary control of a flexible marine riser with vessel dynamics. *Automatica*, 47(4):722–732, 2011.

[93] Wei He, Shuzhi Sam Ge, Bernard Voon Ee How, and Yoo Sang Choo. *Dynamics and control of mechanical systems in offshore engineering*. Springer, 2014.

[94] Wei He and Shuzhi Sam Ge. Robust adaptive boundary control of a vibrating string under unknown time-varying disturbance. *IEEE Transactions on Control Systems Technology*, 20(1):48–58, 2012.

[95] B. Yang and C. A. Tan. Transfer functions of one-dimensional distributed parameter systems. *Transactions of the ASME. Journal of Applied Mechanics*, 59(4):1009–1014, 1992.

[96] Deqing Huang, Jian-Xin Xu, Venkatakrishnan Venkataramanan, and The Cat Tuong Huynh. High-performance tracking of piezoelectric positioning stage using current-cycle iterative learning control with gain scheduling. *IEEE Transactions on Industrial Electronics*, 61(2):1085–1098, 2014.

[97] Yang Quan Chen and Kevin L. Moore. On d^{α}-type iterative learning control. In *Proceedings of the 40th IEEE Conference on Decision and Control*, volume 5, pages 4451–4456, 2001.

[98] Manish Kumar Tiwari, Achintya Mukhopadhyay, and Dipankar Sanyal. Process modeling for control of a batch heat treatment furnace with low no_x radiant tube burner. *Energy Conversion and Management*, 46(13-14):2093 – 2113, 2005.

[99] J. D. Alvarez, L. J. Yebra, and M. Berenguel. Repetitive control of tubular heat exchangers. *Journal of Process Control*, 17(9):689 – 701, 2007.

[100] Stepan G. Akterian. On-line control strategy for compensating for arbitrary deviations in heating-medium temperature during batch thermal sterilization processes. *Journal of Food Engineering*, 39(1):1 – 7, 1999.

[101] Alessandro Pisano and Yury Orlov. Boundary second-order sliding-mode control of an uncertain heat process with unbounded matched perturbation. *Automatica*, 48(8):1768 – 1775, 2012.

[102] D. M. Boskovic, M. Krstic, and Weijiu Liu. Boundary control of an unstable heat equation via measurement of domain-averaged temperature. *IEEE Transactions on Automatic Control*, 46(12):2022–2028, 2001.

[103] Emilia Fridman and Yury Orlov. An lmi approach to boundary control of semilinear parabolic and hyperbolic systems. *Automatica*, 45(9):2060 – 2066, 2009.

[104] M. Krstic and A. Smyshlyaev. Adaptive boundary control for unstable parabolic pdes. part i: Lyapunov design. *IEEE Transactions on Automatic Control*, 53(7):1575–1591, 2008.

[105] H. Jiang, T. H. Nguyen, and M. Prud'homme. Control of the boundary heat flux during the heating process of a solid material. *International Communications in Heat and Mass Transfer*, 32(6):728–738, 2005.

[106] John Rozier Cannon. *The one-dimensional heat equation*. Number 23. Cambridge University Press, 1984.

[107] Lawrence C. Evans. *Partial differential equations*. Providence, 1998.

[108] W. H. Ray. Some recent applications of distributed parameter systems theory- a survey. *Automatica*, 14(3):281 – 287, 1978.

[109] Gilbert F. Froment, Kenneth B. Bischoff, and Juray De Wilde. *Chemical reactor analysis and design*, volume 2. Wiley New York, 1990.

[110] D. Dochain, J. P. Babary, and N. Tali-Maamar. Modelling and adaptive control of nonlinear distributed parameter bioreactors via orthogonal collocation. *Automatica*, 28(5):873 – 883, 1992.

[111] Zarook Shareefdeen and Basil C. Baltzis. Biofiltration of toluene vapor under steady-state and transient conditions: Theory and experimental results. *Chemical Engineering Science*, 49(24, Part A):4347 – 4360, 1994.

[112] A. Shidfar, G. R. Karamali, and J. Damirchi. An inverse heat conduction problem with a nonlinear source term. *Nonlinear Analysis*, 65(3):615–621, 2006.

[113] I. S. Gradshteyn and I. M. Ryzhik. *Table of integrals, series, and products*. Academic Press, Inc., San Diego, CA, fifth edition, 1996.

[114] Toshiharu Sugie and Toshiro Ono. An iterative learning control law for dynamical systems. *Automatica*, 27(4):729 – 732, 1991.

[115] Philippe Biane, Jim Pitman, and Marc Yor. Probability laws related to the Jacobi theta and Riemann zeta functions, and Brownian excursions. *American Mathematical Society. Bulletin. New Series*, 38(4):435–465, 2001.

[116] Richard Bellman. *A brief introduction to theta functions*. Athena Series: Selected Topics in Mathematics. Holt, Rinehart and Winston, New York, 1961.

[117] Mingxuan Sun and Danwei Wang. Anticipatory iterative learning control for nonlinear systems with arbitrary relative degree. *IEEE Transactions on Automatic Control*, 46(5):783–788, 2001.

[118] Mingxuan Sun and Danwei Wang. Iterative learning control with initial rectifying action. *Automatica*, 38(8):1177–1182, 2002.

[119] Jian-Xin Xu and Rui Yan. On initial conditions in iterative learning control. *IEEE Transactions on Automatic Control*, 50(9):1349–1354, 2005.

[120] Khalid Abidi and Jian-Xin Xu. Iterative learning control for sampled-data systems: From theory to practice. *IEEE Transactions on Industrial Electronics*, 58(7):3002–3015, 2011.

[121] Jose Alvarez-Ramirez, Hector Puebla, and J. Alberto Ochoa-Tapia. Linear boundary control for a class of nonlinear PDE processes. *Systems & Control Letters*, 44(5):395–403, 2001.

[122] Huosheng Hu, Jindong Liu, I. Dukes, and G. Francis. Design of 3d swim patterns for autonomous robotic fish. In *Proceedings of the 2006 IEEE/RSJ International Conference on Intelligent Robots and Systems*, pages 2406–2411, 2006.

[123] Koichi Hirata et al. Development of experimental fish robot. In *Proceedings of the 6th International Symposium on Marine Engineering*, pages 235–240, 2000.

[124] Michael Sfakiotakis, D. M. Lane, and J. B. C. Davies. Review of fish swimming modes for aquatic locomotion. *IEEE Journal of Oceanic Engineering*, 24(2):237–252, 1999.

[125] Junzhi Yu, Shuo Wang, and Min Tan. Design of a free-swimming biomimetic

robot fish. In *Proceedings of the 2003 IEEE/ASME International Conference on Advanced Intelligent Mechatronics*, volume 1, pages 95–100, 2003.

[126] Shuo Wang, Zhigang Zhang, and Haiquan Sang. Analysis of velocity control algorithms for biomimetic robot fish. In *Proceedings of the 2004 IEEE International Conference on Robotics and Biomimetics*, pages 972–976, 2004.

[127] Wei Wang and Guangming Xie. Online high-precision probabilistic localization of robotic fish using visual and inertial cues. *IEEE Transactions on Industrial Electronics*, 62(2):1113–1124, 2015.

[128] K. A. Morgansen, B. I. Triplett, and D. J. Klein. Geometric methods for modeling and control of free-swimming fin-actuated underwater vehicles. *IEEE Transactions on Robotics*, 23(6):1184–1199, 2007.

[129] M. J. Lighthill. Note on the swimming of slender fish. *Journal of Fluid Mechanics*, 9(02):305–317, 1960.

[130] M. J. Lighthill. Large-amplitude elongated-body theory of fish locomotion. *Proceedings of the Royal Society of London B: Biological Sciences*, 179(1055):125–138, 1971.

[131] Iain A. Anderson, Milan Kelch, Shumeng Sun, Casey Jowers, Daniel Xu, and Mark M. Murray. Artificial muscle actuators for a robotic fish. 8064:350–352, 2013.

[132] Zhenlong Wang, Guanrong Hang, Jian Li, Yangwei Wang, and Kai Xiao. A micro-robot fish with embedded {SMA} wire actuated flexible biomimetic fin. *Sensors and Actuators A: Physical*, 144(2):354 – 360, 2008.

[133] J. E. Colgate and K. M. Lynch. Mechanics and control of swimming: a review. *IEEE Journal of Oceanic Engineering*, 29(3):660–673, 2004.

[134] N. Kato. Control performance in the horizontal plane of a fish robot with mechanical pectoral fins. *IEEE Journal of Oceanic Engineering*, 25(1):121–129, 2000.

[135] Jenhwa Guo and Yung-Jyi Joeng. Guidance and control of a biomimetic autonomous underwater vehicle using body-fin propulsion. *Proceedings of the Institution of Mechanical Engineers, Part M: Journal of Engineering for the Maritime Environment*, 218(2):93–111, 2004.

[136] Tianjiang Hu, Longxin Lin, Daibing Zhang, Danwei Wang, and Lincheng Shen. Effective motion control of the biomimetic undulating fin via iterative learning. In *Proceedings of the 2009 IEEE International Conference onRobotics and Biomimetics (ROBIO)*, pages 627–632, 2009.

[137] Jing Chen, Tianjiang Hu, Longxin Lin, Haibin Xie, and Lincheng Shen. Learning control for biomimetic undulating fins: An experimental study. *Journal of Bionic Engineering*, 7, Supplement:S191 – S198, 2010.

[138] Tianjiang Hu, K.H. Low, Lincheng Shen, and Xin Xu. Effective phase tracking for bioinspired undulations of robotic fish models: A learning control approach. *IEEE/ASME Transactions on Mechatronics*, 19(1):191–200, 2014.

[139] Jindong Liu and Huosheng Hu. Biological inspiration: From carangiform fish to multi-joint robotic fish. *Journal of Bionic Engineering*, 7(1):35 – 48, 2010.

[140] Qinyuan Ren, Jianxin Xu, Lupeng Fan, and Xuelei Niu. A gim-based biomimetic

learning approach for motion generation of a multi-joint robotic fish. *Journal of Bionic Engineering*, 10(4):423 – 433, 2013.

[141] Robert L. McMasters, Casey P. Grey, John M. Sollock, Ranjan Mukherjee, Andre Benard, and Alejandro R. Diaz. Comparing the mathematical models of lighthill to the performance of a biomimetic fish. *Bioinspiration & Biomimetics*, 3(1):016002, 2008.

[142] Wei Wang, Guangming Xie, and Hong Shi. Dynamic modeling of an ostraciiform robotic fish based on angle of attack theory. In *Proceedings of the 2014 International Joint Conference on Neural Networks (IJCNN)*, pages 3944–3949, 2014.

[143] Jianxun Wang and Xiaobo Tan. A dynamic model for tail-actuated robotic fish with drag coefficient adaptation. *Mechatronics*, 23(6):659 – 668, 2013.

[144] Matteo Aureli, V. Kopman, and Maurizio Porfiri. Free-locomotion of underwater vehicles actuated by ionic polymer metal composites. *IEEE/ASME Transactions on Mechatronics*, 15(4):603–614, 2010.

[145] M. Sfakiotakis and D. P. Tsakiris. Neuromuscular control of reactive behaviors for undulatory robots. *Neurocomputing*, 70(10-12):1907 – 1913, 2007.

[146] James M. Wakeling and Ian A. Johnston. Body bending during fast-starts in fish can be explained in terms of muscle torque and hydrodynamic resistance. *Journal of experimental biology*, 202(6):675–682, 1999.

[147] Jian-Xin Xu, Ying Tan, and Tong-Heng Lee. Iterative learning control design based on composite energy function with input saturation. *Automatica*, 40(8):1371 – 1377, 2004.

[148] M. M. Polycarpou and P. A. Ioannou. A robust adaptive nonlinear control design. *Automatica*, 32(3):423–427, 1996.

Appendix A

Detailed Proofs

A.1 Convergence Analysis of ILC law (2.3)

Let $\triangle \mathbf{u}_i(t) \triangleq \mathbf{u}_d(t) - \mathbf{u}_i(t)$ and $\triangle \mathbf{x}_i(t) \triangleq \mathbf{x}_d(t) - \mathbf{x}_i(t)$ be the input and state errors, respectively. From the reference system (2.2) and the system (2.1), there have

$$\begin{cases} \triangle \mathbf{x}_i(t+1) = A\triangle \mathbf{x}_i(t) + B\triangle \mathbf{u}_i(t), \\ \mathbf{e}_i(t) = C\triangle \mathbf{x}_i(t). \end{cases} \tag{A.1}$$

According to the ILC law (2.3) and the error dynamics (A.1), we can obtain that

$$\begin{aligned} \triangle \mathbf{u}_{i+1}(t) &= \triangle \mathbf{u}_i(t) - L\mathbf{e}_i(t+1) \\ &= (I - LCB)\triangle \mathbf{u}_i(t) - LCA\triangle \mathbf{x}_i(t). \end{aligned} \tag{A.2}$$

In addition, the solution of (A.1) can be expressed as

$$\triangle \mathbf{x}_i(t) = \sum_{k=0}^{t-1} A^{t-1-k} B\triangle \mathbf{u}_i(k), \tag{A.3}$$

where the identical initial condition $\mathbf{x}_d(0) = \mathbf{x}_i(0)$ is applied. By substituting (A.3) into (A.2), it gives

$$\begin{aligned} \triangle\mathbf{u}_{i+1}(t) &= \triangle\mathbf{u}_i(t) - L\mathbf{e}_i(t+1) \\ &= (I - LCB)\triangle\mathbf{u}_i(t) - LC\sum_{k=0}^{t-1} A^{t-k}B\triangle\mathbf{u}_i(k). \end{aligned} \tag{A.4}$$

Taking the norm $\|\cdot\|$ on both sides of (A.4) leads to

$$\|\triangle\mathbf{u}_{i+1}(t)\| \leq \|I - LCB\|\|\triangle\mathbf{u}_i(t)\| + \beta\sum_{k=0}^{t-1}\alpha^{t-k}\|\triangle\mathbf{u}_i(k)\|, \tag{A.5}$$

where the parameter α satisfies $\alpha \geq \|A\|$ and $\beta \triangleq \sup_{t\in[0,T]}\|LC\|\|B\|$. Multiplying both sides of (A.5) by $\alpha^{-\lambda t}$, and taking the supremum over $[0,T]$, there have

$$\sup_{t\in[0,T]}\alpha^{-\lambda t}\|\triangle\mathbf{u}_{i+1}(t)\| \leq \rho\sup_{t\in[0,T]}\alpha^{-\lambda t}\|\triangle\mathbf{u}_i(t)\| + \beta\sup_{t\in[0,T]}\alpha^{-\lambda t}\sum_{k=0}^{t-1}\alpha^{t-k}\|\triangle\mathbf{u}_i(k)\| \tag{A.6}$$

where the constant ρ is chosen such that $\|I - LCB\| \leq \rho < 1$. From the definition of λ-norm, it follows that

$$\begin{aligned} \sup_{t\in[0,T]}\alpha^{-\lambda t}\sum_{k=0}^{t-1}\alpha^{t-k}\|\triangle\mathbf{u}_i(k)\| &= \sup_{t\in[0,T]}\alpha^{-(\lambda-1)t}\sum_{k=0}^{t-1}\alpha^{-\lambda k}\|\triangle\mathbf{u}_i(k)\|\alpha^{(\lambda-1)k} \\ &\leq \|\triangle\mathbf{u}_i(t)\|_\lambda \sup_{t\in[0,T]}\alpha^{-(\lambda-1)t}\sum_{k=0}^{t-1}\alpha^{(\lambda-1)k} \\ &\leq \frac{1-\alpha^{-(\lambda-1)T_d}}{\alpha^{\lambda-1}-1}\|\triangle\mathbf{u}_i(t)\|_\lambda. \end{aligned} \tag{A.7}$$

Then, combining (A.6) and (A.7), there finally have

$$\|\mathbf{E}\{\mathbf{A}\{\triangle\mathbf{u}_{i+1}(t)\}\}\|_\lambda \leq \rho_0\|\mathbf{E}\{\mathbf{A}\{\triangle\mathbf{u}_i(t)\}\}\|_\lambda, \tag{A.8}$$

where $\rho_0 \triangleq \rho + \beta\frac{1-\alpha^{-(\lambda-1)T_d}}{\alpha^{\lambda-1}-1}$. Since $0 \leq \rho < 1$ by the condition (2.11), it is possible to choose a sufficiently large λ such that $\rho_0 < 1$. Therefore, (A.8) implies that

$$\lim_{i\to\infty}\|\triangle\mathbf{u}_i(t)\}\}\|_\lambda = 0. \tag{A.9}$$

Finally, we can obtain the convergence of $\triangle\mathbf{u}_i(t)$ from (A.9), which implies that $\lim_{i\to\infty}\mathbf{e}_i(t) = 0$ for $\forall t \in [0,T]$. ■

A.2 Proof of Theorem 4.1

Denote $\Phi_i \triangleq \hat{\Theta}_i(t) - \Theta$ the estimation error. Define the CEF at the ith iteration

$$E_i(t) = \frac{1}{2}\mathbf{e}_i^T(t)\mathbf{e}_i(t) + \frac{1}{2}\int_0^t \text{trace}(\Phi_i^T\Phi_i)ds, \;\; i \in \mathbf{Z}^+,$$

which is composed by tracking error and the estimation error for basis function. The proof consists of three parts. In the first part, the negative definite difference of CEF is derived. In the second part, the convergence of $\mathbf{e}_i(t)$ for $i \geq 2$ is proved. In the third part, the boundedness of $E_1(t)$ is derived.

Part I. The difference of E_i: The difference of E_i for $i \geq 2$, defined between two consecutive iterations, is

$$\begin{aligned}
\Delta E_i(t) &\triangleq E_i(t) - E_{i-1}(t) \\
&= \frac{1}{2}\mathbf{e}_i^T(t)\mathbf{e}_i(t) + \frac{1}{2}\int_0^t \text{trace}(\Phi_i^T\Phi_i - \Phi_{i-1}^T\Phi_{i-1})ds \\
&\quad -\frac{1}{2}\mathbf{e}_{i-1}^T(t)\mathbf{e}_{i-1}(t).
\end{aligned} \tag{A.10}$$

Substituting the controller (4.5) into the error dynamics (4.4), we have

$$\begin{aligned}
\dot{\mathbf{e}}_i(t) &= \dot{\rho}_i(t)\Theta\mathbf{f}(\mathbf{x}_i) + \dot{\rho}_i(t)B(\mathbf{x}_i,t_i)\mathbf{u}_i(t) - \dot{\mathbf{x}}_i^d(t) \\
&= -\Gamma\dot{\rho}_i(t)\mathbf{e}_i(t) - \dot{\rho}_i(t)(\hat{\Theta}_i(t) - \Theta)\mathbf{f}(\mathbf{x}_i) \\
&= -\Gamma\dot{\rho}_i(t)\mathbf{e}_i(t) - \dot{\rho}_i(t)\Phi_i\mathbf{f}(\mathbf{x}_i).
\end{aligned} \tag{A.11}$$

Applying the initial resetting condition and (A.11) yields

$$\begin{aligned}
\frac{1}{2}\mathbf{e}_i^T(t)\mathbf{e}_i(t) &= \int_0^t \mathbf{e}_i^T(s)\dot{\mathbf{e}}_i(s)ds \qquad (A.12) \\
&= \int_0^t \mathbf{e}_i^T(s)[-\Gamma\dot{\rho}_i(s)\mathbf{e}_i(s) - \dot{\rho}_i(s)\Phi_i\mathbf{f}(\mathbf{x}_i)]ds \\
&= -\int_0^t \dot{\rho}_i(s)\mathbf{e}_i^T(s)\Gamma\mathbf{e}_i(s)ds - \int_0^t \dot{\rho}_i(s)\mathbf{e}_i^T(s)\Phi_i\mathbf{f}(\mathbf{x}_i)ds.
\end{aligned}$$

Noticing the definition of Φ_i and the trace property $\text{trace}((A-B)^T(A-B)-(C-B)^T(C-B)) = \text{trace}([2(B-A)+(A-C)]^T(C-A))$, we obtain

$$\begin{aligned}&\frac{1}{2}\int_0^t \text{trace}(\Phi_i^T\Phi_i - \Phi_{i-1}^T\Phi_{i-1})ds \\ &= \frac{1}{2}\int_0^t \text{trace}([2(\Theta-\hat{\Theta}_i(s))+(\hat{\Theta}_i(s)-\hat{\Theta}_{i-1}(s))]^T(\hat{\Theta}_{i-1}(s)-\hat{\Theta}_i(s)))ds\end{aligned} \tag{A.13}$$

Substituting the parametric updating law (4.6) into (A.13), we have

$$\begin{aligned}&\frac{1}{2}\int_0^t \text{trace}(\Phi_i^T\Phi_i - \Phi_{i-1}^T\Phi_{i-1})ds \\ &= \int_0^t \dot{\rho}_i(s)\text{trace}(\Phi_i^T\mathbf{e}_i(s)\mathbf{f}^T(\mathbf{x}_i))ds \\ &-\frac{1}{2}\int_0^t \text{trace}[(\hat{\Theta}_i(s)-\hat{\Theta}_{i-1}(s))^T(\hat{\Theta}_i(s)-\hat{\Theta}_{i-1}(s))]ds \\ &= \int_0^t \dot{\rho}_i(s)\mathbf{e}_i^T(s)\Phi_i\mathbf{f}(\mathbf{x}_i)ds - \frac{1}{2}\int_0^t \text{trace}[(\hat{\Theta}_i(s)-\hat{\Theta}_{i-1}(s))^T(\hat{\Theta}_i(s)-\hat{\Theta}_{i-1}(s))]ds,\end{aligned} \tag{A.14}$$

where

$$\text{trace}(\Phi_i^T\mathbf{e}_i(s)\mathbf{f}^T(\mathbf{x}_i)) = \text{trace}(\mathbf{f}(\mathbf{x}_i)\mathbf{e}_i^T(s)\Phi_i) = \text{trace}(\mathbf{e}_i^T(s)\Phi_i\mathbf{f}(\mathbf{x}_i)) = \mathbf{e}_i^T(s)\Phi_i\mathbf{f}(\mathbf{x}_i)$$

is applied. Combining (A.12) and (A.15) with (A.10), the difference $\Delta E_i(t)$ becomes

$$\begin{aligned}\Delta E_i(t) &= -\int_0^t \dot{\rho}_i(s)\mathbf{e}_i^T(s)\Gamma\mathbf{e}_i(s)ds - \frac{1}{2}\mathbf{e}_{i-1}^T(t)\mathbf{e}_{i-1}(t) \\ &\quad -\frac{1}{2}\int_0^t \text{trace}[(\hat{\Theta}_i(s)-\hat{\Theta}_{i-1}(s))^T(\hat{\Theta}_i(s)-\hat{\Theta}_{i-1}(s))]ds,\end{aligned}$$

which is negative definite.

Part II. Asymptotical Convergence: Note that the non-increasing property of $E_i(t)$ in the iteration domain holds for all $t \in [0,T]$

$$\Delta E_i(t) \leq -\frac{1}{2}\mathbf{e}_{i-1}^T(t)\mathbf{e}_{i-1}(t), \;\; i > 1. \tag{A.15}$$

Consider a finite sum of $\Delta E_i(t)$,

$$\sum_{j=2}^{i}\Delta E_j(t) = \sum_{j=2}^{i}(E_j(t)-E_{j-1}(t)) = E_i(t)-E_1(t),$$

and use the relationship (A.15), we have

$$E_i(t) \leq E_1(t) - \frac{1}{2}\sum_{j=2}^{i} \mathbf{e}_{i-1}^T(t)\mathbf{e}_{i-1}(t). \tag{A.16}$$

Note that $E_i(t)$ is positive. If $\sup_{t\in[0,T]} E_1(t)$ is finite, the inequality (A.16) implies asymptotical and pointwise convergence property $\lim_{i\to\infty} \mathbf{e}_i^T(t)\mathbf{e}_i(t) = 0$, $\forall t \in [0,T]$. So does $\mathbf{e}_i(t)$.

Part III. Boundedness of $E_1(t)$: The derivative of $E_1(t)$ is

$$\begin{aligned}
\dot{E}_1(t) &= \mathbf{e}_1^T(t)\dot{\mathbf{e}}_1(t) + \frac{1}{2}\text{trace}(\Phi_1^T\Phi_1) \\
&= \mathbf{e}_1^T(t)(-\Gamma\dot{\rho}_1(t)\mathbf{e}_1(t) - \dot{\rho}_1(t)\Phi_1\mathbf{f}(\mathbf{x}_1)) + \frac{1}{2}\text{trace}(\Phi_1^T\Phi_1) \\
&= -\dot{\rho}_1(t)\mathbf{e}_1^T(t)\Gamma\mathbf{e}_1(t) - \dot{\rho}_1(t)\mathbf{e}_1^T(t)\Phi_1\mathbf{f}(\mathbf{x}_1) + \frac{1}{2}\text{trace}(\Phi_1^T\Phi_1) \\
&= -\dot{\rho}_1(t)\mathbf{e}_1^T(t)\Gamma\mathbf{e}_1(t) - \text{trace}(\dot{\rho}_1(t)\Phi_1^T\mathbf{e}_1(t)\mathbf{f}^T(\mathbf{x}_1)) \\
&\quad + \frac{1}{2}\text{trace}(\Phi_1^T\Phi_1)
\end{aligned} \tag{A.17}$$

where the error dynamics in the 1st iteration is used. Since $\hat{\Theta}_0(t) = 0$, we have

$$\hat{\Theta}_1(t) = \dot{\rho}_1(t)\mathbf{e}_1(t)\mathbf{f}^T(x_1). \tag{A.18}$$

By substituting (A.18) into (A.17), we can get

$$\begin{aligned}
\dot{E}_1(t) &= -\dot{\rho}_1(t)\mathbf{e}_1^T(t)\Gamma\mathbf{e}_1(t) - \text{trace}(\Phi_1^T\hat{\Theta}_1(t)) + \frac{1}{2}\text{trace}(\Phi_1^T\Phi_1) \\
&= -\dot{\rho}_1(t)\mathbf{e}_1^T(t)\Gamma\mathbf{e}_1(t) - \frac{1}{2}\text{trace}(\Phi_1^T\Phi_1) - \text{trace}(\Phi_1^T\Theta).
\end{aligned}$$

Since there exists a constant $c > 0$ such that $-\Phi_1^T\Theta \leq c\Phi_1^T\Phi_1 + \frac{1}{4c}\Theta^T\Theta$, then let $0 < c < \frac{1}{2}$, we have

$$\dot{E}_1(t) \leq -\dot{\rho}_1(t)\mathbf{e}_1^T(t)\Gamma\mathbf{e}_1(t) - (\frac{1}{2} - c)\text{trace}(\Phi_1^T\Phi_1) + \frac{1}{4c}\text{trace}(\Theta^T\Theta).$$

Considering the boundedness of Θ, there exists a finite bound Θ_m such that $\Theta^T\Theta \leq \Theta_m^T\Theta_m$. As a result, whenever $\dot{\rho}_1(t)\mathbf{e}_1^T(t)\Gamma\mathbf{e}_1(t) + (\frac{1}{2} - c)\text{trace}(\Phi_1^T\Phi_1) \geq \frac{1}{4c}\text{trace}(\Theta_m^T\Theta_m)$, $\dot{E}_1$ becomes negative, which implies the boundedness of $E_1(t)$. ■

A.3 *Proof of Theorem 4.2*

The proof can be performed similarly as in the proof of Theorem 4.1. Denote $\Psi_i \triangleq \hat{\eta}_i(t) - \eta$ and $\psi_i \triangleq \hat{\lambda}_i(t) - \lambda$ the estimation errors and consider the CEF at the ith iteration

$$E_i(t) = \frac{1}{2}\mathbf{e}_i^T(t)\mathbf{e}_i(t) + \frac{1}{2}\int_0^t \text{trace}(\Psi_i^T\Psi_i)ds + \frac{1}{2}\int_0^t \psi_i^2 ds. \tag{A.19}$$

Part I. The difference of E_i: The difference of E_i between two consecutive iterations is

$$\begin{aligned}
\Delta E_i(t) &\triangleq E_i(t) - E_{i-1}(t) \\
&= \frac{1}{2}\mathbf{e}_i^T(t)\mathbf{e}_i(t) + \frac{1}{2}\int_0^t \text{trace}(\Psi_i^T\Psi_i - \Psi_{i-1}^T\Psi_{i-1})ds \\
&\quad + \frac{1}{2}\int_0^t (\psi_i^2 - \psi_{i-1}^2)ds - \frac{1}{2}\mathbf{e}_{i-1}^T(t)\mathbf{e}_{i-1}(t).
\end{aligned} \tag{A.20}$$

The error dynamics is

$$\begin{aligned}
\dot{\mathbf{e}}_i(t) &= \frac{d\mathbf{x}_i(t)}{dt} - \frac{d\mathbf{x}_i^d(t)}{dt} \\
&= -\Gamma\dot{\rho}_i(t)\mathbf{e}_i(t) - \dot{\rho}_i(t)\Psi_i^T\Xi_i(t)\mathbf{f}(\mathbf{x}_i) + \dot{\rho}_i(t)\xi_i^T(t)\mathbf{f}(\mathbf{x}_i) \\
&\quad -\dot{\rho}_i(t)\hat{\lambda}_i(t)g(\mathbf{x}_i)\text{sgn}(\mathbf{e}_i(t)),
\end{aligned}$$

where the new AIL law (4.15) is applied. Then it is obvious that

$$\begin{aligned}
\frac{1}{2}\mathbf{e}_i^T(t)\mathbf{e}_i(t) &= -\int_0^t \dot{\rho}_i(s)\mathbf{e}_i^T(s)\Gamma\mathbf{e}_i(s)ds - \int_0^t \dot{\rho}_i(s)\mathbf{e}_i^T(s)\Psi_i^T\Xi_i(s)\mathbf{f}(\mathbf{x}_i)ds \\
&\quad + \int_0^t \dot{\rho}_i(s)\mathbf{e}_i^T(s)[\xi_i^T(s)\mathbf{f}(\mathbf{x}_i) - \hat{\lambda}_i(t)g(\mathbf{x}_i)\text{sgn}(\mathbf{e}_i(s))]ds.
\end{aligned} \tag{A.21}$$

In addition, we have

$$\begin{aligned}
&\frac{1}{2}\int_0^t \text{trace}(\Psi_i^T\Psi_i - \Psi_{i-1}^T\Psi_{i-1})ds \qquad (A.22)\\
&= \int_0^t \dot{\rho}_i(s)\text{trace}(\Psi_i^T\Xi_i(s)\mathbf{f}(\mathbf{x}_i)\mathbf{e}_i^T(s))ds\\
&\quad -\frac{1}{2}\int_0^t \text{trace}((\hat{\eta}_i(s)-\hat{\eta}_{i-1}(s))^T(\hat{\eta}_i(s)-\hat{\eta}_{i-1}(s)))ds\\
&= \int_0^t \dot{\rho}_i(s)\mathbf{e}_i^T(s)\Psi_i^T\Xi_i(s)\mathbf{f}(\mathbf{x}_i)ds\\
&\quad -\frac{1}{2}\int_0^t \text{trace}((\hat{\eta}_i(s)-\hat{\eta}_{i-1}(s))^T(\hat{\eta}_i(s)-\hat{\eta}_{i-1}(s)))ds
\end{aligned}$$

and

$$\begin{aligned}
\frac{1}{2}\int_0^t(\psi_i^2-\psi_{i-1}^2)ds &= \frac{1}{2}\int_0^t[2(\lambda-\hat{\lambda}_i(s))+(\hat{\lambda}_i(s)-\hat{\lambda}_{i-1}(s))](\hat{\lambda}_{i-1}(s)-\hat{\lambda}_i(s))ds\\
&= \int_0^t \dot{\rho}_i(s)\psi_i g(\mathbf{x}_i)\sum_{j=1}^m |e_{i,j}(s)|ds\\
&\quad -\frac{1}{2}\int_0^t(\hat{\lambda}_i(s)-\hat{\lambda}_{i-1}(s))^2ds. \qquad (A.23)
\end{aligned}$$

Combining (A.20), (A.21), (A.22) and (A.23) yields

$$\begin{aligned}
\Delta E_i(t) &= -\int_0^t \dot{\rho}_i(s)\mathbf{e}_i^T(s)\Gamma\mathbf{e}_i(s)ds - \frac{1}{2}\mathbf{e}_{i-1}^T(t)\mathbf{e}_{i-1}(t)\\
&\quad -\frac{1}{2}\int_0^t \text{trace}((\hat{\eta}_i(s)-\hat{\eta}_{i-1}(s))^T(\hat{\eta}_i(s)-\hat{\eta}_{i-1}(s)))ds\\
&\quad -\frac{1}{2}\int_0^t(\hat{\lambda}_i(s)-\hat{\lambda}_{i-1}(s))^2ds\\
&\quad +\int_0^t \dot{\rho}_i[\mathbf{e}_i^T(s)\xi_i^T(s)\mathbf{f}(\mathbf{x}_i)-\lambda g(\mathbf{x}_i)\sum_{j=1}^m |e_{i,j}(s)|ds \le 0,
\end{aligned}$$

since (4.14) implies $|\mathbf{e}_i^T(s)\xi_i^T(s)\mathbf{f}(\mathbf{x}_i)| \le \lambda g(\mathbf{x}_i)\sum_{j=1}^m |e_{i,j}(s)|$.

Part II. Asymptotical Convergence: Note that the non-increasing property of $E_i(t)$ in the iteration domain holds for all $t \in [0,T]$

$$\Delta E_i(t) \le -\frac{1}{2}\mathbf{e}_{i-1}^T(t)\mathbf{e}_{i-1}(t), \;\; i>1. \qquad (A.24)$$

Consider a finite sum of $\Delta E_i(t)$,

$$\sum_{j=2}^i \Delta E_j(t) = \sum_{j=2}^i (E_j(t)-E_{j-1}(t)) = E_i(t)-E_1(t),$$

and use the inequality (A.24), we have

$$E_i(t) \leq E_1(t) - \frac{1}{2}\sum_{j=2}^{i} \mathbf{e}_{i-1}^T(t)\mathbf{e}_{i-1}(t). \tag{A.25}$$

Note that $E_i(t)$ is positive. If $\sup_{t\in[0,T]} E_1(t)$ is finite, the inequality (A.25) implies asymptotical and pointwise convergence property $\lim_{i\to\infty} \mathbf{e}_i^T(t)\mathbf{e}_i(t) = 0$, $\forall t \in [0,T]$. So does $\mathbf{e}_i(t)$.

Part III. Boundedness of $E_1(t)$: The derivative of $E_1(t)$ is

$$\begin{aligned}
\dot{E}_1(t) &= \mathbf{e}_1^T(t)\dot{\mathbf{e}}_1(t) + \frac{1}{2}\text{trace}(\Psi_1^T\Psi_1) + \frac{1}{2}\psi_1^2 \\
&= \mathbf{e}_1^T(t)[-\Gamma\dot{\rho}_1(t)\mathbf{e}_1(t) - \dot{\rho}_1(t)\Psi_1^T\Xi_1(t)\mathbf{f}(\mathbf{x}_1) + \dot{\rho}_1(t)\xi_1^T(t)\mathbf{f}(\mathbf{x}_1) \\
&\quad -\dot{\rho}_1(t)\hat{\lambda}_1(t)g(\mathbf{x}_1)\text{sgn}(\mathbf{e}_1(t))] + \frac{1}{2}\text{trace}(\Psi_1^T\Psi_1) + \frac{1}{2}\psi_1^2 \\
&= -\dot{\rho}_1(t)\mathbf{e}_1^T(t)\Gamma\mathbf{e}_1(t) - \dot{\rho}_1(t)\mathbf{e}_1^T(t)\Psi_1^T\Xi_1(t)\mathbf{f}(\mathbf{x}_1) + \dot{\rho}_1(t)\mathbf{e}_1^T(t)\xi_1^T(t)\mathbf{f}(\mathbf{x}_1) \\
&\quad -\dot{\rho}_1(t)\hat{\lambda}_1(t)g(\mathbf{x}_1)\sum_{j=1}^{m}|e_{1,j}(t)| + \frac{1}{2}\text{trace}(\Psi_1^T\Psi_1) + \frac{1}{2}\psi_1^2,
\end{aligned}$$

where the error dynamics in the 1th iteration is applied. By using $\mathbf{e}_1^T(t)\xi_1^T(t)\mathbf{f}(\mathbf{x}_1) \leq \lambda g(\mathbf{x}_1)\sum_{j=1}^{m}|e_{1,j}(t)|$, it is obvious that

$$\begin{aligned}
\dot{E}_1(t) \leq\ & -\dot{\rho}_1(t)\mathbf{e}_1^T(t)\Gamma\mathbf{e}_1(t) - \dot{\rho}_1(t)\mathbf{e}_1^T(t)\Psi_1^T\Xi_1(t)\mathbf{f}(\mathbf{x}_1) + \dot{\rho}_1(t)\lambda g(\mathbf{x}_1)\sum_{j=1}^{m}|e_{1,j}(t)| \\
& -\dot{\rho}_1(t)\hat{\lambda}_1(t)g(\mathbf{x}_1)\sum_{j=1}^{m}|e_{1,j}(t)| + \frac{1}{2}\text{trace}(\Psi_1^T\Psi_1) + \frac{1}{2}\psi_1^2.
\end{aligned} \tag{A.26}$$

Since $\hat{\eta}_0(t) = 0$ and $\hat{\lambda}_0(t) = 0$, we have

$$\hat{\eta}_1(t) = \dot{\rho}_1(t)\Xi_1(t)\mathbf{f}(\mathbf{x}_1)\mathbf{e}_1^T(t) \tag{A.27}$$

and

$$\hat{\lambda}_1(t) = \dot{\rho}_1(t)g(\mathbf{x}_1)\sum_{j=1}^{m}|e_{1,j}(t)|. \tag{A.28}$$

By substituting (A.27) and (A.28) into (A.26), we can get

$$\begin{aligned}\dot{E}_1(t) &\leq -\dot{\rho}_1(t)\mathbf{e}_1^T(t)\Gamma\mathbf{e}_1(t) - \text{trace}(\Psi_1^T\hat{\eta}_1(t)) + \lambda\hat{\lambda}_1(t) - \hat{\lambda}_1^2(t) \\ &\quad + \frac{1}{2}\text{trace}(\Psi_1^T\Psi_1) + \frac{1}{2}\psi_1^2 \\ &= -\dot{\rho}_1(t)\mathbf{e}_1^T(t)\Gamma\mathbf{e}_1(t) - \frac{1}{2}\text{trace}(\Psi_1^T\Psi_1) - \text{trace}(\Psi_1^T\eta) - \frac{1}{2}\psi_1^2 - \psi_1\lambda.\end{aligned}$$

Since there exists a constant $c_1 > 0$ such that $-\Psi_1^T\eta \leq c_1\Psi_1^T\Psi_1 + \frac{1}{4c_1}\eta^T\eta$ and $-\psi_1\lambda \leq c_1\psi_1^2 + \frac{1}{4c_1}\lambda^2$, then let $0 < c_1 < \frac{1}{2}$, we have

$$\begin{aligned}\dot{E}_1(t) &\leq -\dot{\rho}_1(t)\mathbf{e}_1^T(t)\Gamma\mathbf{e}_1(t) - (\frac{1}{2} - c_1)\text{trace}(\Psi_1^T\Psi_1) - (\frac{1}{2} - c_1)\psi_1^2 \\ &\quad + \frac{1}{4c_1}\text{trace}(\eta^T\eta) + \frac{1}{4c_1}\lambda^2.\end{aligned}$$

Considering the boundedness of η and λ, there exists a finite bound μ_m such that for any $t \in [0,T]$, $\text{trace}(\eta^T\eta) + \lambda^2 \leq \mu_m^2$. As a result, whenever $\dot{\rho}_1(t)\mathbf{e}_1^T(t)\Gamma\mathbf{e}_1(t) + (\frac{1}{2} - c_1)\text{trace}(\Psi_1^T\Psi_1) + (\frac{1}{2} - c_1)\psi_1^2 \geq \frac{1}{4c_1}\mu_m^2\}$, $\dot{E}_1$ is negative. Hence, the boundedness of $E_1(t)$ over $[0,T]$ is obtained. ■

A.4 *Proof of Theorem 4.3*

Still consider the CEF (A.19), whose difference in two consecutive iterations is

$$\begin{aligned}\Delta E_i(t) &= -\int_0^t \dot{\rho}_i(s)\mathbf{e}_i^T(s)\Gamma\mathbf{e}_i(s)ds - \frac{1}{2}\mathbf{e}_{i-1}^T(t)\mathbf{e}_{i-1}(t) \\ &\quad -\mu_1\int_0^t \dot{\rho}_i(s)\text{trace}(\Psi_i^T\hat{\eta}_i(s))ds \\ &\quad -\frac{1}{2}\int_0^t \text{trace}((\hat{\eta}_i(s) - \hat{\eta}_{i-1}(s))^T(\hat{\eta}_i(s) - \hat{\eta}_{i-1}(s)))ds \\ &\quad -\mu_2\int_0^t \dot{\rho}_i(s)\psi_i\hat{\lambda}_i(s)ds - \frac{1}{2}\int_0^t (\hat{\lambda}_i(s) - \hat{\lambda}_{i-1}(s))^2 ds \\ &\quad +\int_0^t \dot{\rho}_i(s)\mathbf{e}_i^T(s)[\xi_i^T(s)\mathbf{f}(x_i) - \lambda\omega(\mathbf{x}_i,\mathbf{e}_i)]ds. \qquad \text{(A.29)}\end{aligned}$$

By completing the square, it can be shown that

$$-\mu_1 \Psi_i^T \hat{\eta}_i(t) = -\frac{1}{2}\mu_1 \Psi_i^T \Psi_i - \frac{1}{2}\mu_1 \hat{\eta}_i(t)^T \hat{\eta}_i(t) + \frac{1}{2}\mu_1 \eta^T \eta, \tag{A.30}$$

$$-\mu_2 \psi_i \hat{\lambda}_i(t) = -\frac{1}{2}\mu_2 \psi_i^2 - \frac{1}{2}\mu_2 \hat{\lambda}_i^2(t) + \frac{1}{2}\mu_2 \lambda^2. \tag{A.31}$$

Now, combining (A.29), (A.30), (A.31) and $|\mathbf{e}_i^T(t)\xi_i^T(t)\mathbf{f}(\mathbf{x}_i)| \leq \lambda g(\mathbf{x}_i)\sum_{j=1}^m |e_{i,j}(t)|$, $t \in [0,T]$, we can obtain

$$\begin{aligned}
\Delta E_i(t) \leq & -\int_0^t \dot{\rho}_i(s)\mathbf{e}_i^T(s)\Gamma\mathbf{e}_i(s)ds - \frac{1}{2}\mathbf{e}_{i-1}^T(t)\mathbf{e}_{i-1}(t) \\
& -\frac{1}{2}\int_0^t \text{trace}((\hat{\eta}_i(s)-\hat{\eta}_{i-1}(s))^T(\hat{\eta}_i(s)-\hat{\eta}_{i-1}(s)))ds \\
& -\frac{1}{2}\mu_1\int_0^t \dot{\rho}_i(s)\text{trace}(\Psi_i^T\Psi_i)ds - \frac{1}{2}\mu_1\int_0^t \dot{\rho}_i(s)\text{trace}(\hat{\eta}_i^T(s)\hat{\eta}_i(s))ds \\
& -\frac{1}{2}\mu_2\int_0^t \dot{\rho}_i(s)\psi_i^2 ds - \frac{1}{2}\mu_2\int_0^t \dot{\rho}_i(s)\hat{\lambda}_i^2(s)ds - \frac{1}{2}\int_0^t (\hat{\lambda}_i(s)-\hat{\lambda}_{i-1}(s))^2 ds \\
& +\int_0^t \lambda\dot{\rho}_i(s)[g(\mathbf{x}_i)\sum_{j=1}^m |e_{i,j}(s)| - \mathbf{e}_i^T(s)\omega(\mathbf{x}_i,\mathbf{e}_i)]ds + \frac{T}{2}\mu_1\text{trace}(\eta^T\eta) + \frac{T}{2}\mu_2\lambda^2.
\end{aligned} \tag{A.32}$$

Claim[74]: The following inequality holds for any $\varepsilon > 0$ and for any $u \in \mathbb{R}$

$$0 \leq |u| - u\tanh(\frac{u}{\varepsilon}) \leq \delta\varepsilon,$$

where δ is a constant that satisfies $\delta = e^{-(\delta+1)}$, i.e., $\delta = 0.2785$.

As stated in Assumption 4.1, $\dot{\rho}_i(t) > 0$ for $t \in [0,T]$. Now, using the claim, it gives

$$\begin{aligned}
& \lambda[\dot{\rho}_i(t)g(\mathbf{x}_i)\sum_{j=1}^m |e_{i,j}(t)| - \dot{\rho}_i(t)\mathbf{e}_i(t)\omega(x_i,\mathbf{e}_i)] \\
& = \lambda\sum_{j=1}^m [\dot{\rho}_i(t)g(\mathbf{x}_i)|e_{i,j}(t)| - \dot{\rho}_i(t)e_{i,j}(t)g(\mathbf{x}_i)\tanh(\frac{\dot{\rho}_i(t)g(\mathbf{x}_i)e_{i,j}(t)}{\overline{\varepsilon}})] \\
& \leq m\lambda\delta\overline{\varepsilon} \leq \frac{m}{2}\lambda\overline{\varepsilon}.
\end{aligned} \tag{A.33}$$

Therefore, (A.32) yields

$$\Delta E_i(t) \leq -\frac{1}{2}\mathbf{e}_{i-1}^T(t)\mathbf{e}_{i-1}(t) + \zeta, \tag{A.34}$$

where

$$\zeta \triangleq \frac{m}{2}\lambda\overline{\varepsilon} + \frac{T}{2}\mu_1\text{trace}(\eta^T\eta) + \frac{T}{2}\mu_2\lambda^2.$$

It can be seen that γ will definitely affect the learning performance. We are not able to derive a general relation such that $\Delta E_i(t)$ is negative definiteness for all iterations, as we did in the proofs of Theorems 4.1 and 4.2. Instead, we will try to show that the tracking error $\mathbf{e}_i(t)$ will enter the specified bound within a finite number of iterations.

Consider a finite sum of $\Delta E_i(t)$,

$$\sum_{j=2}^{i} \Delta E_j(t) = \sum_{j=2}^{i} (E_j(t) - E_{j-1}(t)) = E_i(t) - E_1(t),$$

and use the inequality (A.34), we have

$$E_i(t) = E_1(t) + \sum_{j=2}^{i} \Delta E_j(t) \leq E_1(t) - \frac{1}{2} \sum_{j=2}^{i} \mathbf{e}_{i-1}^T(t)\mathbf{e}_{i-1}(t) - 2\gamma). \tag{A.35}$$

In addition, the boundedness of $E_1(t), \forall t \in [0,T]$ can be derived similarly as the proof of Theorem 4.2. Due to the positive definiteness of $E_i(t)$, we can derive the boundedness of $\mathbf{e}_i(t)$ for any finite iteration directly from (A.35). If $\mathbf{e}_i(t)$ goes to infinity at the ith iteration, since ζ is finite, the right hand of (A.35) will diverge to infinity. This contradicts the positiveness of $E_i(t)$. For $\forall t \in [0,T]$, if $E_1(t)$ is bounded, according to the positive definiteness of $E_i(t)$, there will exist a finite integer $i_0 > 0$ such that $\mathbf{e}_i^T(t)\mathbf{e}_i(t) \leq 2\zeta$ for $i > i_0$. Otherwise, $\mathbf{e}_i^T(t)\mathbf{e}_i(t) > 2\zeta$ holds for $i \to \infty$. Then the right hand side of (A.35) will approach $-\infty$, which contradicts the positive definiteness of $E_i(t)$. Hence, the tracking error $\mathbf{e}_i(t)$ will enter the specified bound within a finite number of iterations.

■

A.5 Proof of Theorem 5.1

Define $\phi_i \triangleq \hat{\theta}_i(t) - 1$ and consider the CEF at the ith iteration

$$E_i(t) = \frac{1}{2}\mathbf{e}_i^T(t)\mathbf{e}_i(t) + \frac{1}{2\gamma}\int_0^t \phi_i^2 ds. \tag{A.36}$$

The proof consists of three parts. In the first part, the negative definite difference of CEF is derived. In the second part, the convergence of $\mathbf{e}_i(t)$ for $i \geq 2$ is proved. In the third part, the boundedness properties of the system state, the parametric estimation, and the control signal are addressed.

Part I. The difference of E_i: The difference of E_i for $i \geq 2$, defined between two consecutive iterations, is

$$\begin{aligned} \Delta E_i(T) &\triangleq E_i(T) - E_{i-1}(T) \\ &= \frac{1}{2}\mathbf{e}_i^T(T)\mathbf{e}_i(T) - \frac{1}{2}\mathbf{e}_{i-1}^T(T)\mathbf{e}_{i-1}(T) + \frac{1}{2\gamma}\int_0^T (\phi_i^2 - \phi_{i-1}^2)ds. \end{aligned} \quad \text{(A.37)}$$

First of all, there has

$$\begin{aligned} \frac{1}{2}(\mathbf{e}_i^T(T)\mathbf{e}_i(T) - \mathbf{e}_{i-1}^T(T)\mathbf{e}_{i-1}(T)) &= \frac{1}{2}(\mathbf{e}_i^T(0)\mathbf{e}_i(0) - \mathbf{e}_{i-1}^T(T)\mathbf{e}_{i-1}(T)) \\ &\quad + \int_0^T \mathbf{e}_i^T(s)\dot{\mathbf{e}}_i(s)ds. \end{aligned} \quad \text{(A.38)}$$

Applying Assumption 5.1, namely, the alignment condition, the first term of the right hand side (RHS) of (A.39) is zero, which renders to

$$\frac{1}{2}(\mathbf{e}_i^T(T)\mathbf{e}_i(T) - \mathbf{e}_{i-1}^T(T)\mathbf{e}_{i-1}(T)) = \int_0^T \mathbf{e}_i^T(s)\dot{\mathbf{e}}_i(s)ds. \quad \text{(A.39)}$$

Substituting the controller (5.5) into the error dynamics (5.4) yields

$$\dot{\mathbf{e}}_i(t) = -\Gamma\mathbf{e}_i - \hat{\theta}_i(t)\rho(\mathbf{x}_i,t)\text{sgn}(\mathbf{e}_i(t)) + \mathbf{f}(\mathbf{x}_i,t). \quad \text{(A.40)}$$

Consequently, the RHS of (A.39) can be further written as

$$\begin{aligned} \int_0^T \mathbf{e}_i^T(s)\dot{\mathbf{e}}_i(s)ds &= -\int_0^T \mathbf{e}_i^T(s)\Gamma\mathbf{e}_i(s)ds - \int_0^T \hat{\theta}_i(s)\rho(\mathbf{x}_i,s)\mathbf{e}_i^T\text{sgn}(\mathbf{e}_i(s))ds \\ &\quad + \int_0^T \mathbf{e}_i^T\mathbf{f}(\mathbf{x}_i,s)ds \\ &\leq -\int_0^T \mathbf{e}_i^T(s)\Gamma\mathbf{e}_i(s)ds - \int_0^T \phi_i\rho(\mathbf{x}_i,s)\sum_{k=1}^n |e_{k,i}(s)|ds, \end{aligned} \quad \text{(A.41)}$$

where the relationship $\mathbf{e}_i^T \mathbf{f}(\mathbf{x}_i,t) \leq \rho(\mathbf{x}_i,t)\sum_{k=1}^{n}|e_{k,i}(t)|$ is used. In addition,

$$\begin{aligned} & \frac{1}{2\gamma}\int_0^T (\phi_i^2 - \phi_{i-1}^2)ds \\ = & \frac{1}{2\gamma}\int_0^T [2(1-\hat{\theta}_i(s)) + (\hat{\theta}_i(s) - \hat{\theta}_{i-1}(s))] \times (\hat{\theta}_{i-1}(s) - \hat{\theta}_i(s))ds \\ = & \int_0^T \phi_i \rho(\mathbf{x}_i,t)\sum_{k=1}^{n}|e_{k,i}(s)|ds - \frac{1}{2\gamma}\int_0^T (\hat{\theta}_i(s) - \hat{\theta}_{i-1}(s))^2 ds. \end{aligned} \tag{A.42}$$

Combining (A.37), (A.41), and (A.42) yields

$$\Delta E_i(T) \leq -\int_0^T \mathbf{e}_i^T(s)\Gamma\mathbf{e}_i(s)ds - \frac{1}{2\gamma}\int_0^T (\hat{\theta}_i(s) - \hat{\theta}_{i-1}(s))^2 ds.$$

Part II. Convergence of the Tracking Error: Note that the non-increasing property of $E_i(T)$ in the iteration domain holds, namely,

$$\Delta E_i(T) \leq -\int_0^T \mathbf{e}_i^T(s)\Gamma\mathbf{e}_i(s)ds \leq -\lambda_{min}\int_0^T \|\mathbf{e}_i(s)\|_2^2 ds, \;\; i>1, \tag{A.43}$$

where λ_{min} is the minimal eigenvalue of Γ. According to (A.43), it can be derived that the finiteness of $E_i(T)$ is ensured for each iteration provided $E_1(T)$ is finite, which will be verified in the following.

The derivative of $E_1(t)$ is

$$\begin{aligned} \dot{E}_1(t) &= \mathbf{e}_1^T(t)\dot{\mathbf{e}}_1(t) + \frac{1}{2\gamma}\phi_1^2 \\ &= \mathbf{e}_1^T(t)[-\Gamma\mathbf{e}_1 - \hat{\theta}_1(t)\rho(\mathbf{x}_1,t)\mathrm{sgn}(\mathbf{e}_1(t)) + \mathbf{f}(\mathbf{x}_1,t)] + \frac{1}{2\gamma}\phi_1^2 \\ &= -\mathbf{e}_1^T\Gamma\mathbf{e}_1 - \hat{\theta}_1(t)\rho(\mathbf{x}_1,t)\sum_{k=1}^{n}|e_{k,1}(t)| + \mathbf{e}_1^T\mathbf{f}(\mathbf{x}_1,t) + \frac{1}{2\gamma}\phi_1^2 \\ &\leq -\mathbf{e}_1^T\Gamma\mathbf{e}_1 - \hat{\theta}_1(t)\rho(\mathbf{x}_1,t)\sum_{k=1}^{n}|e_{k,1}(t)| + \rho(\mathbf{x}_1,t)\sum_{k=1}^{n}|e_{k,1}(t)| \\ &\quad + \frac{1}{2\gamma}\phi_1^2, \end{aligned} \tag{A.44}$$

where the error dynamics in the first iteration and the relationship

$$\mathbf{e}_1^T\mathbf{f}(\mathbf{x}_1,t) \leq \rho(\mathbf{x}_1,t)\sum_{k=1}^{n}|e_{k,1}(t)|$$

are applied. Since $\hat{\theta}_0(t) = 0$, it has

$$\hat{\theta}_1(t) = \gamma\rho(\mathbf{x}_1, t)\sum_{k=1}^{n}|e_{k,1}(t)|. \tag{A.45}$$

By substituting (A.45) into (A.45), there has

$$\begin{aligned}\dot{E}_1(t) &\leq -\mathbf{e}_1^T\Gamma\mathbf{e}_1 - \frac{1}{\gamma}\hat{\theta}_1^2(t) + \frac{1}{\gamma}\hat{\theta}_1(t) + \frac{1}{2\gamma}\phi_1^2 \\ &= -\mathbf{e}_1^T\Gamma\mathbf{e}_1 - \frac{1}{\gamma}\phi_1\hat{\theta}_1(t) + \frac{1}{2\gamma}\phi_1^2 \\ &= -\mathbf{e}_1^T\Gamma\mathbf{e}_1 - \frac{1}{\gamma}\phi_1 - \frac{1}{2\gamma}\phi_1^2.\end{aligned}$$

Since by Young's inequality $-\phi_1 \leq |\phi_1| \leq c\phi_1^2 + 1/(4c), \forall c > 0$, there exists $0 < c < 1/2$ such that

$$\dot{E}_1(t) \leq -\lambda_{min}\|\mathbf{e}_1\|_2^2 - (\frac{1}{2} - c)\frac{1}{\gamma}\phi_1^2 + \frac{1}{4c\gamma}.$$

As a result, whenever the inequality $\lambda_{min}\|\mathbf{e}_1\|_2^2 + (\frac{1}{2} - c)\frac{1}{\gamma}\phi_1^2 \geq \frac{1}{4c\gamma}$ holds, $\dot{E}_1$ is negative. Hence, the boundedness of $E_1(t)$ over $[0, T]$ is obtained. In particular, when $t = T$, $E_1(T)$ is bounded.

By considering a finite sum of $\Delta E_i(T)$,

$$\sum_{j=2}^{i}\Delta E_j(T) = \sum_{j=2}^{i}(E_j(T) - E_{j-1}(T)) = E_i(T) - E_1(T),$$

and using the inequality (A.43), it follows

$$E_i(T) \leq E_1(T) - \lambda_{min}\sum_{j=2}^{i}\int_0^T \|\mathbf{e}_j(s)\|_2^2 ds. \tag{A.46}$$

Note that $E_i(T)$ is positive and $E_1(T)$ is finite, the inequality (A.46) implies the asymptotical convergence of $\mathbf{e}_i$ in the sense of L^2-norm, namely, $\lim_{i\to\infty}\int_0^T \|\mathbf{e}_i(s)\|_2^2 ds = 0$.

Part III. Boundedness of the involved quantities:

Now, we are in the position of checking the boundedness property of the system state $\mathbf{x}_i$, the parametric estimation $\hat{\theta}_i$, and the control signal $\mathbf{u}_i$ in each iteration.

First address $\mathbf{x}_i$ and $\hat{\theta}_i$, whose boundedness is guaranteed by the boundedness of $E_i(t), \forall t \in [0,T]$. According to the definition of $E_i(t)$ and the finiteness of $E_i(T)$, the boundedness of $\int_0^T \phi_i^2 ds$ and $\mathbf{e}_i^T(T)\mathbf{e}_i(T)$ are guaranteed for all iterations. Therefore, $\forall i \in \mathbf{Z}^+$, there exist finite constant $M_1 > 0$ and $M_2 > 0$ satisfying

$$\begin{aligned} \mathbf{e}_i^T(T)\mathbf{e}_i(T) &\leq M_1 < \infty, & \text{(A.47)} \\ \int_0^t \phi_i^2 ds &\leq \int_0^T \phi_i^2 ds \leq M_2 < \infty, & \text{(A.48)} \end{aligned}$$

Hence, from (A.36), it gives

$$E_i(t) \leq \frac{1}{2}\mathbf{e}_i^T(t)\mathbf{e}_i(t) + \frac{1}{2\gamma}M_2. \tag{A.49}$$

On the other hand, similarly as in (A.37), there has

$$\Delta E_i(t) = \frac{1}{2}\mathbf{e}_i^T(t)\mathbf{e}_i(t) - \frac{1}{2}\mathbf{e}_{i-1}^T(t)\mathbf{e}_{i-1}(t) + \frac{1}{2\gamma}\int_0^t (\phi_i^2 - \phi_{i-1}^2) ds. \tag{A.50}$$

From (A.41) and (A.42), it is obvious that

$$\begin{aligned} \frac{1}{2}\mathbf{e}_i^T(t)\mathbf{e}_i(t) &= \frac{1}{2}\mathbf{e}_i^T(0)\mathbf{e}_i(0) + \int_0^t \mathbf{e}_i^T(s)\dot{\mathbf{e}}_i(s) ds \\ &\leq \frac{1}{2}\mathbf{e}_i^T(0)\mathbf{e}_i(0) - \int_0^t \mathbf{e}_i^T(s)\Gamma\mathbf{e}_i(s) ds \\ &\quad - \int_0^t \phi_i \rho(\mathbf{x}_i, s) \sum_{k=1}^n |e_{k,i}(s)| ds \end{aligned} \tag{A.51}$$

and

$$\frac{1}{2\gamma}\int_0^t (\phi_i^2 - \phi_{i-1}^2) ds = \int_0^t \phi_i \rho(\mathbf{x}_i, t) \sum_{k=1}^n |e_{k,i}(s)| ds - \frac{1}{2\gamma}\int_0^t (\hat{\theta}_i(s) - \hat{\theta}_{i-1}(s))^2 ds. \tag{A.52}$$

Therefore, (A.50), (A.51) and (A.52) yield

$$\Delta E_i(t) \leq \frac{1}{2}\mathbf{e}_i^T(0)\mathbf{e}_i(0) - \frac{1}{2}\mathbf{e}_{i-1}^T(t)\mathbf{e}_{i-1}(t). \tag{A.53}$$

Then, from (A.53),

$$\begin{aligned} \Delta E_{i+1}(t) &\leq \frac{1}{2}\mathbf{e}_{i+1}^T(0)\mathbf{e}_{i+1}(0) - \frac{1}{2}\mathbf{e}_i^T(t)\mathbf{e}_i(t) \\ &= \frac{1}{2}\mathbf{e}_i^T(T)\mathbf{e}_i(T) - \frac{1}{2}\mathbf{e}_i^T(t)\mathbf{e}_i(t). \end{aligned} \tag{A.54}$$

Summation of (A.49) and (A.54) leads to

$$\begin{aligned} E_{i+1}(t) &= E_i(t) + \Delta E_{i+1}(t) \\ &\leq \frac{1}{2}\mathbf{e}_i^T(T)\mathbf{e}_i(T) + \frac{1}{2\gamma}M_2 \\ &\leq \frac{1}{2}M_1 + \frac{1}{2\gamma}M_2. \end{aligned} \tag{A.55}$$

As it has shown that $E_1(t)$ is bounded, it follows that $E_i(t)$ is finite for $\forall i \in \mathbf{Z}^+$, and so are $\mathbf{x}_i$ as well as $\int_0^t \hat{\theta}_i^2 ds$.

At last, the boundedness of input profile will be analyzed. Since $\rho(\mathbf{x}_i,t)$ is LLC with respect to $\mathbf{x}_i$, the boundedness of $\mathbf{x}_i$ implies the boundedness of $\rho(\mathbf{x}_i,t)$. Thus, according to the control law (5.5), the control signal $\mathbf{u}_i(t)$ is also bounded in L^2-norm.

■

A.6 Proof of Theorem 5.2

Still consider the CEF (A.36), whose difference in two consecutive iterations is

$$\begin{aligned} \Delta E_i(T) &= -\int_0^T \mathbf{e}_i^T(s)\Gamma\mathbf{e}_i(s)ds - \int_0^T \mathbf{e}_i^T(s)\omega(\mathbf{x}_i,\mathbf{e}_i)ds + \int_0^T \mathbf{e}_i^T(s)\mathbf{f}(\mathbf{x}_i,s)ds \\ &\quad -\frac{1}{2\gamma}\int_0^T (\hat{\theta}_i(s) - \hat{\theta}_{i-1}(s))^2 ds - \frac{\mu}{\gamma}\int_0^T \phi_i\hat{\theta}_i(s)ds. \end{aligned} \tag{A.56}$$

By completing the square,

$$-\phi_i\hat{\theta}_i = -\frac{1}{2}\phi_i^2 - \frac{1}{2}\hat{\theta}_i^2 + \frac{1}{2}. \tag{A.57}$$

Now, with the aid of (A.56), (A.57), and the inequality $\mathbf{e}_i^T\mathbf{f}(\mathbf{x}_i,t) \leq \rho(\mathbf{x}_i,t)\sum_{k=1}^n |e_{k,i}(t)|$, it gives

$$\begin{aligned} \Delta E_i(T) &= -\int_0^T \mathbf{e}_i^T(s)\Gamma\mathbf{e}_i(s)ds - \int_0^T [\rho(\mathbf{x}_i,s)\sum_{k=1}^n |e_{k,i}(s)| - \mathbf{e}_i^T(s)\omega(\mathbf{x}_i,\mathbf{e}_i)]ds \\ &\quad -\frac{1}{2\gamma}\int_0^T (\hat{\theta}_i(s) - \hat{\theta}_{i-1}(s))^2 ds \\ &\quad -\frac{\mu}{2\gamma}\int_0^T \phi_i^2 ds - \frac{\mu}{2\gamma}\int_0^T \hat{\theta}_i^2(s)ds + \frac{\mu T}{2\gamma}. \end{aligned} \tag{A.58}$$

Claim [148]: The following inequality holds for any $\varepsilon > 0$ and for any $u \in \mathbf{R}$

$$0 \leq |u| - u\tanh(\frac{u}{\varepsilon}) \leq \delta\varepsilon,$$

where δ is a constant that satisfies $\delta = e^{-(\delta+1)}$, i.e., $\delta = 0.2785$.

Now, using the claim, there has

$$\begin{aligned}
&\rho(\mathbf{x}_i,t)\sum_{k=1}^{n}|e_{k,i}(t)| - \mathbf{e}_i^T(t)\omega(\mathbf{x}_i,\mathbf{e}_i) \\
&= \sum_{k=1}^{n}[\rho(\mathbf{x}_i,t)|e_{k,i}(t)| - \rho(\mathbf{x}_i,t)e_{k,i}(t)\tanh(\frac{\rho(\mathbf{x}_i,t)e_{1,i}(t)}{\overline{\varepsilon}})] \leq n\delta\overline{\varepsilon} \leq \frac{n}{2}\overline{\varepsilon}.
\end{aligned}$$

Therefore, (A.58) gives

$$\Delta E_i(T) = -\int_0^T \mathbf{e}_i^T(s)\Gamma\mathbf{e}_i(s)ds + \sigma \leq -\lambda_{min}\int_0^T \|\mathbf{e}_i(s)\|_2^2 ds + \sigma, \tag{A.59}$$

where $\sigma \triangleq \frac{n}{2}\overline{\varepsilon} + \frac{\mu T}{2\gamma} > 0$. Due to the effect of σ, it is impossible to derive that $\Delta E_i(T)$ will be negative definite for all iterations. Instead, it is shown that the tracking error $\mathbf{e}_i(t)$ will enter a neighborhood of zero within finite iterations.

Considering a finite sum of $\Delta E_i(T)$,

$$\sum_{j=2}^{i}\Delta E_j(T) = \sum_{j=2}^{i}(E_j(T) - E_{j-1}(T)) = E_i(T) - E_1(T),$$

and using the inequality (A.59) imply

$$E_i(T) \leq E_1(T) - \lambda_{min}\sum_{j=2}^{i}\left[\int_0^T \|\mathbf{e}_j(s)\|_2^2 ds - \frac{\sigma}{\lambda_{min}}\right]. \tag{A.60}$$

In addition, the boundedness of $E_1(t), \forall t \in [0,T]$ can be derived similarly as the proof of Theorem 5.1. Due to the positive definiteness of $E_i(T)$, the boundedness of $\int_0^T \|\mathbf{e}_i(s)\|_2^2 ds$ for any finite i is obtained immediately from (A.60). If $\int_0^T \|\mathbf{e}_i(s)\|_2^2 ds$ goes to infinity at the ith iteration, then the RHS of (A.60) will diverge to infinity owing to the finiteness of σ/λ_{min}. This contradicts the positiveness of $E_i(T)$. Further, for any given $\varepsilon > 0$, there exists a finite integer $i_0 > 0$ such that $\int_0^T \|\mathbf{e}_i(s)\|_2^2 ds < \sigma/\lambda_{min} + \varepsilon$ for $i > i_0$. Otherwise,

$\int_0^T \|\mathbf{e}_i(s)\|_2^2 ds \geq \sigma/\lambda_{min} + \varepsilon$ holds for $i \to \infty$. Then the RHS of (A.60) will approach $-\infty$, which contradicts the positive definiteness of $E_i(T)$. Hence, the tracking error $\int_0^T \|\mathbf{e}_i(s)\|_2^2 ds$ will enter the specified bound $\sigma/\lambda_{min} + \varepsilon$ within finite iterations. ■

A.7 Proof of Theorem 5.3

Considering $\phi_i = \hat{\theta}_i(t) - \theta$, it is obvious that

$$\begin{aligned} & \frac{1}{2\gamma}\int_0^T (\phi_i^2 - \phi_{i-1}^2) ds \\ = \; & \frac{1}{2\gamma}\int_0^T [2(\theta - \hat{\theta}_i(s)) + (\hat{\theta}_i(s) - \hat{\theta}_{i-1}(s))](\hat{\theta}_{i-1}(s) - \hat{\theta}_i(s)) ds \\ = \; & \int_0^T \phi_i \rho(\mathbf{x}_i, t) \sum_{k=1}^n |e_{k,i}(s)| ds - \frac{1}{2\gamma}\int_0^T (\hat{\theta}_i(s) - \hat{\theta}_{i-1}(s))^2 ds. \end{aligned} \tag{A.61}$$

In addition, from the condition $\|\mathbf{f}(\mathbf{x}_i, t)\| \leq \theta \rho(\mathbf{x}_i, t)$, it follows

$$\mathbf{e}_i^T \mathbf{f}(\mathbf{x}_i, t) \leq \theta \rho(\mathbf{x}_i, t) \sum_{k=1}^n |e_{k,i}(t)|. \tag{A.62}$$

Now, substituting (A.62) into (A.41) and replacing (A.42) with (A.61) in the proof of Theorem 5.1, the negative definite difference of CEF can be obtained, i.e.,

$$\Delta E_i(T) \leq -\lambda_{min} \int_0^T \|\mathbf{e}_i(s)\|_2^2 ds, \;\; i > 1. \tag{A.63}$$

Further, by substituting (A.62) at $i = 1$ into (A.45), there has

$$\begin{aligned} \dot{E}_1(t) &\leq -\mathbf{e}_1^T \Gamma \mathbf{e}_1 - \frac{1}{\gamma}\phi_1 \theta - \frac{1}{2\gamma}\phi_1^2 \\ &\leq -\lambda_{min}\|\mathbf{e}_1\|_2^2 - (\frac{1}{2} - c)\frac{1}{\gamma}\phi_1^2 + \frac{1}{4\gamma c}\theta^2, \end{aligned}$$

where $0 < c < 1/2$. Considering the boundedness of θ, there exists a finite bound θ_m such that $\theta^2 \leq \theta_m^2$. As a result, whenever $\lambda_{min}\|\mathbf{e}_1\|_2^2 + (\frac{1}{2} - c)\frac{1}{\gamma}\phi_1^2 \geq \frac{1}{4\gamma c}\theta_m^2$, $\dot{E}_1$ becomes negative, which implies the boundedness of $E_1(t)$. Therefore, by using the boundedness of $E_1(T)$, the positiveness of $E_i(T)$, and the following inequality

$$E_i(T) \leq E_1(T) - \lambda_{min} \sum_{j=2}^{i} \int_0^T \|\mathbf{e}_j(s)\|_2^2 ds, \tag{A.64}$$

the convergence of the tracking error is proved. Further, the boundedness of the involved quantities in each iteration can be obtained similarly as in proof of Theorem 5.1. ■

A.8 Proof of Theorem 5.4

Denote by $\phi_i \triangleq \hat{\theta}_i(t) - 1$ and $\psi_i \triangleq \hat{\eta}_i(t) - 1$ the estimation errors. Define the CEF at the ith iteration

$$E_i(t) = \frac{1}{2}\mathbf{e}_i^T(t)\mathbf{e}_i(t) + \frac{1}{2\gamma_1}\int_0^t \phi_i^2 ds + \frac{1}{2\gamma_2}\int_0^t \psi_i^2 ds.$$

Again, the proof consists of three parts. Since the third part on deriving the boundedness of system quantities can be obtained similarly as in the preceding theorems, only the first two parts are given in the following.

Part I. The difference of E_i: The difference of E_i for $i \geq 2$, defined between two consecutive iterations, is

$$\begin{aligned}\Delta E_i(T) &= \frac{1}{2}\mathbf{e}_i^T(T)\mathbf{e}_i(T) - \frac{1}{2}\mathbf{e}_{i-1}^T(T)\mathbf{e}_{i-1}(T) \\ &\quad + \frac{1}{2\gamma_1}\int_0^T (\phi_i^2 - \phi_{i-1}^2) ds + \frac{1}{2\gamma_2}\int_0^t (\psi_i^2 - \psi_{i-1}^2) ds. \end{aligned} \tag{A.65}$$

For the first two terms on the RHS of (A.65), there has

$$\begin{aligned}&\frac{1}{2}\mathbf{e}_i^T(T)\mathbf{e}_i(T) - \frac{1}{2}\mathbf{e}_{i-1}^T(T)\mathbf{e}_{i-1}(T) \\ =\ &\frac{1}{2}(\mathbf{e}_i^T(0)\mathbf{e}_i(0) - \mathbf{e}_{i-1}^T(T)\mathbf{e}_{i-1}(T)) + \int_0^T \mathbf{e}_i^T(s)\dot{\mathbf{e}}_i(s) ds. \end{aligned} \tag{A.66}$$

Applying the alignment condition at $t = T$, namely (5.1), the first term on the RHS of (A.66) is zero. Then, (A.66) renders to

$$\frac{1}{2}\mathbf{e}_i^T(T)\mathbf{e}_i(T) - \frac{1}{2}\mathbf{e}_{i-1}^T(T)\mathbf{e}_{i-1}(T) = \int_0^T \mathbf{e}_i^T(s)\dot{\mathbf{e}}_i(s) ds. \tag{A.67}$$

Therefore, from the error dynamics (5.12), it gives

$$\begin{aligned}
&\frac{1}{2}\mathbf{e}_i^T(T)\mathbf{e}_i(T) - \frac{1}{2}\mathbf{e}_{i-1}^T(T)\mathbf{e}_{i-1}(T) \\
= &\int_0^T \mathbf{e}_i^T\{\mathbf{f}_i + B_i[(I+H_i)\mathbf{u}_i(s) + \mathbf{d}_i]\}\,ds \\
= &\int_0^T [\mathbf{e}_i^T\mathbf{f}_i + \mathbf{e}_i^T B_i(I+H_i)\mathbf{u}_i(s) + \mathbf{e}_i^T B_i\mathbf{d}_i]ds. \qquad \text{(A.68)}
\end{aligned}$$

Due to the relationships $I+H_i = (1-\xi)I + (\xi I + H_i)$ and $\mathbf{e}_i^T B_i(\xi I + H_i)B_i^T \operatorname{sgn}(\mathbf{e}_i) \geq 0$, the following inequality can be obtained:

$$\begin{aligned}
-\frac{\mathbf{e}_i^T B_i(I+H_i)B_i^T\mathbf{e}_i}{(1-\xi)\|\mathbf{e}_i^T B_i\|_2} &= -\frac{\mathbf{e}_i^T B_i(1-\xi)B_i^T\mathbf{e}_i}{(1-\xi)\|\mathbf{e}_i^T B_i\|_2} - \frac{\mathbf{e}_i^T B_i(\xi I + H_i)B_i^T\mathbf{e}_i}{(1-\xi)\|\mathbf{e}_i^T B_i\|_2} \\
&\leq -\frac{\mathbf{e}_i^T B_i(1-\xi)B_i^T\mathbf{e}_i}{(1-\xi)\|\mathbf{e}_i^T B_i\|_2} = -\|\mathbf{e}_i^T B_i\|_2. \qquad \text{(A.69)}
\end{aligned}$$

Hence, for the second term of (A.68), by substituting the control law (5.13) into the integrand, it follows

$$\begin{aligned}
\mathbf{e}_i^T B_i(I+H_i)\mathbf{u}_i(t) \leq\ & -\mathbf{e}_i^T B_i(I+H_i)B_i^{-1}[\Gamma\mathbf{e}_i + \hat{\theta}_i(t)\alpha_i\operatorname{sgn}(\mathbf{e}_i)] \\
& -\frac{\mathbf{e}_i^T B_i(I+H_i)B_i^T\mathbf{e}_i}{\|\mathbf{e}_i^T B_i\|_2}\hat{\eta}_i(t)\beta_i - \frac{\lambda_i\|\Gamma\|\|\mathbf{e}_i\|_2\|\mathbf{e}_i^T B_i\|_2}{\|B_i\|} \\
& -\frac{\sqrt{n}\lambda_i\alpha_i|\hat{\theta}_i(t)|\|\mathbf{e}_i^T B_i\|_2}{\|B_i\|} - \lambda_i\beta_i|\hat{\eta}_i(t)|\|\mathbf{e}_i^T B_i\|_2 \\
= & -\mathbf{e}_i^T\Gamma\mathbf{e}_i - \hat{\theta}_i(t)\alpha_i\sum_{k=1}^{n}|e_{k,i}| - \mathbf{e}_i^T B_i H_i B_i^{-1}\Gamma\mathbf{e}_i \\
& -\hat{\theta}_i(t)\alpha_i\mathbf{e}_i^T B_i H_i B_i^{-1}\operatorname{sgn}(\mathbf{e}_i) - \hat{\eta}_i\beta_i\|\mathbf{e}_i^T B_i\|_2 \qquad \text{(A.70)} \\
& -\hat{\eta}_i(t)\beta_i\frac{\mathbf{e}_i^T B_i H_i B_i^T\mathbf{e}_i}{\|\mathbf{e}_i^T B_i\|_2} - \frac{\lambda_i\|\Gamma\|\|\mathbf{e}_i\|_2\|\mathbf{e}_i^T B_i\|_2}{\|B_i\|} \\
& -\frac{\sqrt{n}\lambda_i\alpha_i|\hat{\theta}_i(t)|\|\mathbf{e}_i^T B_i\|_2}{\|B_i\|} - \lambda_i\beta_i|\hat{\eta}_i(t)|\|\mathbf{e}_i^T B_i\|_2,
\end{aligned}$$

where the inequality (A.69) is applied. Further, the following inequalities are clear,

$$-\mathbf{e}_i^T B_i H_i B_i^{-1}\Gamma\mathbf{e}_i \leq \frac{\lambda_i\|\mathbf{e}_i^T B_i\|_2\|\Gamma\|\|\mathbf{e}_i\|_2}{\|B_i\|}, \qquad \text{(A.71)}$$

$$-\hat{\theta}_i(t)\alpha_i\mathbf{e}_i^T B_i H_i B_i^{-1}\operatorname{sgn}(\mathbf{e}_i) \leq \frac{\sqrt{n}|\hat{\theta}_i(t)|\alpha_i\lambda_i\|\mathbf{e}_i^T B_i\|_2}{\|B_i\|} \qquad \text{(A.72)}$$

and

$$-\hat{\eta}_i(t)\beta_i\frac{\mathbf{e}_i^T B_i H_i B_i^T \mathbf{e}_i}{\|\mathbf{e}_i^T B_i\|_2} \leq \lambda_i\beta_i|\hat{\eta}_i(t)|\|\mathbf{e}_i^T B_i\|_2. \tag{A.73}$$

Consequently, (A.71)-(A.73) give

$$\mathbf{e}_i^T B_i(I+H_i)\mathbf{u}_i(t) \leq -\mathbf{e}_i^T\Gamma\mathbf{e}_i - \hat{\theta}_i(t)\alpha_i\sum_{k=1}^{n}|e_{k,i}| - \hat{\eta}_i(t)\beta_i\|\mathbf{e}_i^T B_i\|_2. \tag{A.74}$$

Thus, combining (A.71) with (A.68) results in

$$\begin{aligned}
&\frac{1}{2}\mathbf{e}_i^T(T)\mathbf{e}_i(T) - \frac{1}{2}\mathbf{e}_{i-1}^T(T)\mathbf{e}_{i-1}(T)\\
\leq\ & \int_0^T [\mathbf{e}_i^T\mathbf{f}_i - \mathbf{e}_i^T\Gamma\mathbf{e}_i - \hat{\theta}_i(s)\alpha_i\sum_{k=1}^{n}|e_{k,i}| - \hat{\eta}_i(s)\beta_i\|\mathbf{e}_i^T B_i\|_2 + \mathbf{e}_i^T B_i\mathbf{d}_i]ds\\
\leq\ & \int_0^T [-\mathbf{e}_i^T\Gamma\mathbf{e}_i - (\hat{\theta}_i(s)-1)\alpha_i\sum_{k=1}^{n}|e_{k,i}| - (\hat{\eta}_i(s)-1)\beta_i\|\mathbf{e}_i^T B_i\|_2]ds,
\end{aligned} \tag{A.75}$$

where the relationships $\mathbf{e}_i^T\mathbf{f}_i \leq \alpha_i\sum_{k=1}^{n}|e_{k,i}|$ and $\mathbf{e}_i^T B_i\mathbf{d}_i \leq \beta_i\|\mathbf{e}_i^T B_i\|_2$ are applied. In addition, it has

$$\begin{aligned}
&\frac{1}{2\gamma_1}\int_0^T(\phi_i^2 - \phi_{i-1}^2)ds\\
=\ & \frac{1}{2\gamma_1}\int_0^T[2(1-\hat{\theta}_i(s)) + (\hat{\theta}_i(s) - \hat{\theta}_{i-1}(s))](\hat{\theta}_{i-1}(s) - \hat{\theta}_i(s))ds\\
=\ & \int_0^T(\hat{\theta}_i(s)-1)\alpha_i\sum_{k=1}^{n}|e_{k,i}(s)|ds - \frac{1}{2\gamma_1}\int_0^t(\hat{\theta}_i(s) - \hat{\theta}_{i-1}(s))^2 ds
\end{aligned} \tag{A.76}$$

and

$$\begin{aligned}
&\frac{1}{2\gamma_2}\int_0^T(\psi_i^2 - \psi_{i-1}^2)ds\\
=\ & \frac{1}{2\gamma_2}\int_0^T[2(1-\hat{\eta}_i(s)) + (\hat{\eta}_i(s) - \hat{\eta}_{i-1}(s))](\hat{\eta}_{i-1}(s) - \hat{\eta}_i(s))ds\\
=\ & \int_0^T(\hat{\eta}_i(s)-1)\beta_i\|\mathbf{e}_i^T B_i\|_2 ds - \frac{1}{2\gamma_2}\int_0^t(\hat{\eta}_i(s) - \hat{\eta}_{i-1}(s))^2 ds.
\end{aligned} \tag{A.77}$$

Combining (A.65), (A.75), (A.76) and (A.77) yields

$$\Delta E_i(T) \leq -\int_0^T \mathbf{e}_i^T(s)\Gamma\mathbf{e}_i(s)ds \leq -\lambda_{min}\int_0^T\|\mathbf{e}_i(s)\|_2^2 ds, \tag{A.78}$$

where λ_{min} is the minimal eigenvalue of Γ.

Part II. Asymptotical Convergence of tracking error: First derive the boundedness of $E_1(T)$. The derivative of $E_1(t)$ is

$$\begin{aligned}\dot{E}_1(t) &\leq -\mathbf{e}_1^T\Gamma\mathbf{e}_1 - \hat{\theta}_1(t)\alpha_1\sum_{k=1}^{n}|e_{k,1}(t)| + \alpha_1\sum_{k=1}^{n}|e_{k,1}(t)| \\ &\quad +\eta(t)\beta_1\|\mathbf{e}_1^T B_1\|_2 - \hat{\eta}_1(t)\beta_1\|\mathbf{e}_1^T B_1\|_2 + \frac{1}{2\gamma_1}\phi_1^2 + \frac{1}{2\gamma_2}\psi_1^2. \quad \text{(A.79)}\end{aligned}$$

Since $\hat{\theta}_0(t) = 0$ and $\hat{\eta}_0(t) = 0$, there has

$$\hat{\theta}_1(t) = \gamma_1\alpha_1\sum_{k=1}^{n}|e_{k,1}(t)|, \quad \text{(A.80)}$$

$$\hat{\eta}_1(t) = \gamma_2\beta_1\|\mathbf{e}_1^T B_1\|_2. \quad \text{(A.81)}$$

Thus, (A.79) can be rewritten as

$$\begin{aligned}\dot{E}_1(t) &\leq -\mathbf{e}_1^T\Gamma\mathbf{e}_1 - \frac{1}{\gamma_1}\hat{\theta}_1^2(t) + \frac{1}{\gamma_1}\hat{\theta}_1(t) + \frac{1}{\gamma_2}\hat{\eta}_1(t) - \frac{1}{\gamma_2}\hat{\eta}_1^2(t) + \frac{1}{2\gamma_1}\phi_1^2 + \frac{1}{2\gamma_2}\psi_1^2 \\ &= -\mathbf{e}_1^T\Gamma\mathbf{e}_1 - \frac{1}{\gamma_1}\phi_1 - \frac{1}{2\gamma_1}\phi_1^2 - \frac{1}{\gamma_2}\psi_1 - \frac{1}{2\gamma_2}\psi_1^2.\end{aligned}$$

Since $-\phi_1 \leq |\phi_1| \leq c\phi_1^2 + \frac{1}{4c}$ and $-\psi_1 \leq |\psi_1| \leq c\psi_1^2 + \frac{1}{4c}, \forall c > 0$, there exists $0 < c < \frac{1}{2}$ such that

$$\dot{E}_1(t) \leq -\mathbf{e}_1^T\Gamma\mathbf{e}_1 - (\frac{1}{2} - c)\frac{1}{2\gamma_1}\phi_1^2 - (\frac{1}{2} - c)\frac{1}{2\gamma_2}\psi_1^2 + \frac{1}{4c}(\frac{1}{\gamma_1} + \frac{1}{\gamma_2}).$$

As a result, whenever the relationship $\mathbf{e}_1^T\Gamma\mathbf{e}_1 + (\frac{1}{2} - c)\frac{1}{2\gamma_1}\phi_1^2 + (\frac{1}{2} - c)\frac{1}{2\gamma_2}\psi_1^2 \geq \frac{1}{4c}(\frac{1}{\gamma_1} + \frac{1}{\gamma_2})$ holds, $\dot{E}_1$ is negative. Hence, the boundedness of $E_1(t)$ over $[0, T]$ is obtained. In particular, when $t = T$, $E_1(T)$ is bounded.

From (A.78), it follows

$$\begin{aligned}E_i(T) &= E_1(T) + \sum_{j=2}^{i}\Delta E_j(T) \\ &\leq E_1(t) - \lambda_{min}\sum_{j=2}^{i}\int_0^T \|\mathbf{e}_j(s)\|_2^2 ds. \quad \text{(A.82)}\end{aligned}$$

Note that $E_i(T)$ is positive and $E_1(T)$ is finite, the inequality (A.82) implies that $\mathbf{e}_i(t)$ tends to zero asymptotically in the sense of L^2-norm as $i \to \infty$, namely,

$$\lim_{i\to\infty}\int_0^T \|\mathbf{e}_i(s)\|_2^2 ds = 0.$$

■

A.9 Proof of Theorem 7.1

First consider the scenario $t > \delta$. Observing (7.8), it has

$$\begin{aligned} e^i &= -2\int_0^t \theta(1,t-\tau)\Delta u^i(\tau)d\tau \\ &= -2\int_0^{t-\delta} \theta(1,t-\tau)\Delta u^i(\tau)d\tau - 2\int_{t-\delta}^t \theta(1,t-\tau)u^d(\tau)d\tau - \Xi^i, \end{aligned} \quad (A.83)$$

where

$$\begin{aligned} \Xi^i(t) &\triangleq -2\int_{t-\delta}^t \theta(1,t-\tau)u^i(\tau)d\tau \\ &= -2\int_0^{\delta} \theta(1,s)u^i(t-s)ds. \end{aligned}$$

In the $(i+1)$th iteration, (A.83) gives

$$\begin{aligned} e^{i+1} &= -2\int_0^{t-\delta} \theta(1,t-\tau)\Delta u^{i+1}(\tau)d\tau \\ &\quad -2\int_{t-\delta}^t \theta(1,t-\tau)u^d(\tau)d\tau - \Xi^{i+1}. \end{aligned} \quad (A.84)$$

Then, (A.83) and (A.84) render to

$$e^{i+1} - e^i = 2\int_0^{t-\delta} \theta(1,t-\tau)(u^{i+1}(\tau) - u^i(\tau))d\tau - \Xi^{i+1} + \Xi^i. \quad (A.85)$$

By applying the anticipatory ILC law (7.10), (A.85) further gives

$$\begin{aligned} e^{i+1} - e^i &= 2\rho\int_0^{t-\delta} \theta(1,t-\tau)\dot{e}^i(\tau+\delta)d\tau - \Xi^{i+1} + \Xi^i \\ &= 2\rho\theta(1,t-\tau)e^i(\tau+\delta)|_{\tau=0}^{t-\delta} \\ &\quad -2\rho\int_0^{t-\delta} e^i(\tau+\delta)\frac{d\theta(1,t-\tau)}{d\tau}d\tau - \Xi^{i+1} + \Xi^i \\ &= 2\rho\theta(1,\delta)e^i - 2\rho\theta(1,t)e^i(\delta) - \Xi^{i+1} + \Xi^i \\ &\quad -2\rho\int_0^{t-\delta} e^i(\tau+\delta)\frac{d\theta(1,t-\tau)}{d\tau}d\tau. \end{aligned} \quad (A.86)$$

Thus, the relationship between the tracking errors in two consecutive iterations can be obtained as follows,

$$\begin{aligned} e^{i+1} &= (1+2\rho\theta(1,\delta))e^i - 2\rho\theta(1,t)e^i(\delta) - \Xi^{i+1} + \Xi^i \\ &\quad -2\rho\int_0^{t-\delta} e^i(\tau+\delta)\frac{d\theta(1,t-\tau)}{d\tau}d\tau. \end{aligned} \tag{A.87}$$

Taking absolute value on both sides of (A.87), it gives

$$\begin{aligned} |e^{i+1}| &\leq |1+2\rho\theta(1,\delta)|\,|e^i| + |2\rho\theta(1,t)e^i(\delta)| + |\Xi^{i+1}-\Xi^i| \\ &\quad + \left|2\rho\int_0^{t-\delta} e^i(\tau+\delta)\frac{d\theta(1,t-\tau)}{d\tau}d\tau\right|. \end{aligned} \tag{A.88}$$

Using the relationships (7.12) and (7.14), the second and third terms of (A.88) can be further evaluated as follows.

$$\begin{aligned} |2\rho\theta(1,t)e^i(\delta)| &\leq 2|\rho| \sup_{t\in[0,T]} |\theta(1,t)||e^i(\delta)| \\ &\leq 2|\rho| \sup_{t\in[0,T]} |\theta(1,t)| \left|2\int_0^{\delta} \theta(1,\delta-\tau)\Delta u^i(\tau)d\tau\right| \\ &\leq 8|\rho| \sup_{t\in[0,T]} |\theta(1,t)|\overline{u}\int_0^{\delta} \theta(1,\delta-\tau)d\tau \\ &= \rho_1\ell, \end{aligned} \tag{A.89}$$

where $\rho_1 \triangleq 2|\rho|\sup_{t\in[0,T]}|\theta(1,t)|$, and

$$\begin{aligned} |\Xi^{i+1}-\Xi^i| &\leq 2\int_0^{\delta} \theta(1,s)|u^{i+1}(t-s)-u^i(t-s)|ds \\ &\leq 4\overline{u}\int_0^{\delta}\theta(1,s)ds = \ell. \end{aligned} \tag{A.90}$$

For the last term on the right hand side of (A.88), since $\theta_t(1,t)$ is always bounded for $\delta \leq t \leq T$ by Lemma 7.1, it follows that

$$\begin{aligned} &\left|2\rho\int_0^{t-\delta} e^i(\tau+\delta)\frac{d\theta(1,t-\tau)}{d\tau}d\tau\right| \\ \leq\ & 2|\rho|\kappa_2\int_0^t \exp(\lambda\tau)\max_{\tau\in[0,T]}\exp(-\lambda\tau)|e^i(\tau)|d\tau \\ =\ & \frac{2|\rho|\kappa_2(\exp(\lambda t)-1)}{\lambda}|e^i|_\lambda. \end{aligned} \tag{A.91}$$

Finally, substituting (A.89)-(A.91) into (A.88) leads to

$$|e^{i+1}| \leq |1+2\rho\theta(1,\delta)|\,|e^i| + (1+\rho_1)\,\ell + \frac{2|\rho|\kappa_2(\exp(\lambda t)-1)}{\lambda}|e^i|_\lambda. \quad \text{(A.92)}$$

Consider the other scenario $t \in [0,\delta]$. Noticing the maximal input bound (7.12) and the monotonicity of $\theta(1,t)$, it can be seen from the error dynamics (7.8) that

$$\begin{aligned} |e^{i+1}| &\leq 4\overline{u}\int_0^t \theta(1,t-\tau)d\tau \\ &\leq 4\overline{u}\int_0^\delta \theta(1,\delta-\tau)d\tau = \ell. \end{aligned} \quad \text{(A.93)}$$

Thus, (A.92) still holds when $t \in [0,\delta]$.

Now, for any $t \in [0,T]$, taking λ-norm on both sides of (A.92) yields

$$|e^{i+1}|_\lambda \leq |1+2\rho\theta(1,\delta)|\,|e^i|_\lambda + (1+\rho_1)\,\ell + 2|\rho|\kappa_2\frac{1-\exp(-\lambda T)}{\lambda}|e^i|_\lambda.$$

Considering the fact that $2|\rho|\kappa_2(1-\exp(-\lambda T))/\lambda$ can be arbitrarily small by choosing a sufficiently large λ, it suffices to design ρ as in (7.13) such that

$$\begin{aligned} |e^{i+1}|_\lambda &\leq |1+2\rho\theta(1,\delta)|\,|e^i|_\lambda + (1+\rho_1)\,\ell \\ &\leq \gamma|e^i|_\lambda + (1+\rho_1)\,\ell, \end{aligned} \quad \text{(A.94)}$$

where $0 \leq \gamma < 1$. Applying (A.94) repeatedly leads to

$$\begin{aligned} |e^{i+1}|_\lambda &\leq \gamma(\gamma|e^{i-1}|_\lambda + (1+\rho_1)\,\ell) + (1+\rho_1)\,\ell \\ &\vdots \\ &\leq \gamma^{i+1}|e^0|_\lambda + (1+\rho_1)\,\gamma^i\ell + \cdots + (1+\rho_1)\,\ell \\ &= \gamma^{i+1}|e^0|_\lambda + \frac{1-\gamma^{i+1}}{1-\gamma}\cdot(1+\rho_1)\,\ell. \end{aligned} \quad \text{(A.95)}$$

Due to the boundedness of $|e^0|_\lambda$ and the fact $0 \leq \gamma < 1$,

$$\begin{aligned} \lim_{i\to\infty}|e^{i+1}|_\lambda &\leq \lim_{i\to\infty}\gamma^{i+1}|e^0|_\lambda + \lim_{i\to\infty}\frac{1-\gamma^{i+1}}{1-\gamma}\cdot(1+\rho_1)\ell \\ &= \frac{(1+\rho_1)\ell}{1-\gamma}. \end{aligned}$$

The proof is complete. ■

A.10 Proof of Lemma 7.2

Denote by u^{i+1} and u^i the control inputs in two consecutive iterations for system (7.1), whose corresponding states are v^{i+1} and v^i, respectively. Then, from (7.21), the respective integral equations for v^{i+1} and v^i can be differenced to yield

$$\begin{aligned} v^{i+1}-v^i &= -2\int_0^{t-\delta}\theta(x,t-\tau)(u^{i+1}(\tau)-u^i(\tau))d\tau \\ &\quad +\int_0^{t-\delta}\int_0^1\{\theta(x-\xi,t-\tau)+\theta(x+\xi,t-\tau)\} \\ &\quad \times(F^{i+1}-F^i)d\xi d\tau+\Xi^{i+1}-\Xi^i. \end{aligned} \tag{A.96}$$

By substituting the ILC law (7.10), it follows that

$$\begin{aligned} v^{i+1}-v^i &= -2\rho\int_0^{t-\delta}\theta(x,t-\tau)\dot{e}^i(\tau+\delta)d\tau \\ &\quad +\int_0^{t-\delta}\int_0^1\{\theta(x-\xi,t-\tau)+\theta(x+\xi,t-\tau)\} \\ &\quad \times(F^{i+1}-F^i)d\xi d\tau+\Xi^{i+1}-\Xi^i \\ &= -2\rho\,\theta(x,t-\tau)e^i(\tau+\delta)|_{\tau=0}^{t-\delta} \\ &\quad +2\rho\int_0^{t-\delta}e^i(\tau+\delta)\theta_\tau(x,t-\tau)d\tau \\ &\quad +\int_0^{t-\delta}\int_0^1\{\theta(x-\xi,t-\tau)+\theta(x+\xi,t-\tau)\} \\ &\quad \times(F^{i+1}-F^i)d\xi d\tau+\Xi^{i+1}-\Xi^i \\ &= -2\rho\,\theta(x,\delta)e^i(t)+2\rho\,\theta(x,t)e^i(\delta) \\ &\quad +2\rho\int_0^{t-\delta}e^i(\tau+\delta)\theta_\tau(x,t-\tau)d\tau \\ &\quad +\int_0^{t-\delta}\int_0^1\{\theta(x-\xi,t-\tau)+\theta(x+\xi,t-\tau)\} \\ &\quad \times(F^{i+1}-F^i)d\xi d\tau+\Xi^{i+1}-\Xi^i. \end{aligned} \tag{A.97}$$

Differentiating (A.97) with respect to x gives

$$\begin{aligned} v_x^{i+1} - v_x^i &= -2\rho\,\theta_x(x,\delta)e^i(t) + 2\rho\,\theta_x(x,t)e^i(\delta) \\ &\quad + 2\rho\int_0^{t-\delta} e^i(\tau+\delta)\theta_{\tau x}(x,t-\tau)d\tau \\ &\quad + \int_0^{t-\delta}\int_0^1 \{\theta_x(x-\xi,t-\tau) + \theta_x(x+\xi,t-\tau)\} \\ &\quad \times (F^{i+1} - F^i)d\xi\,d\tau + \Xi_x^{i+1} - \Xi_x^i. \end{aligned} \tag{A.98}$$

In the sequel, combining (A.97) and (A.98) and applying the Lipschitz continuous condition (7.26) and Assumption 7.1 lead to

$$\begin{aligned} &\sup_{0\le x\le 1}\left(|v^{i+1} - v^i| + |v_x^{i+1} - v_x^i|\right) \\ \le\ & 2\rho \sup_{0\le x\le 1}\left(|\theta(x,\delta)| + |\theta_x(x,\delta)|\right)\left|e^i\right| \\ &+ 2\rho \sup_{0\le x\le 1}\int_0^{t-\delta}\left(|\theta_\tau(x,t-\tau)| + |\theta_{\tau x}(x,t-\tau)|\right)|e^i(\tau+\delta)|d\tau \\ &+ C_F\int_0^{t-\delta}\sup_{0\le x\le 1}\int_0^1 \{|\theta(x-\xi,t-\tau) + \theta(x+\xi,t-\tau)| \\ &\quad + |\theta_x(x-\xi,t-\tau) + \theta_x(x+\xi,t-\tau)|\} \\ &\quad \times \left(|v_{i+1} - v_i| + |v_{i+1,\xi} - v_{i,\xi}|\right)d\xi\,d\tau \\ &+ \ell_1 + \ell_2 + 2\rho \sup_{0\le x\le 1}\left(|\theta(x,t)| + |\theta_x(x,t)|\right)\ell_1, \end{aligned} \tag{A.99}$$

where the relationship $\left|e^i(\delta)\right| \le \ell_1$ is used. Now, denote

$$\begin{aligned} a(t-\tau) &= C_F \sup_{0\le x\le 1}\int_0^1 (|\theta(x-\xi,t-\tau) + \theta(x+\xi,t-\tau)| \\ &\quad + |\theta_x(x-\xi,t-\tau) + \theta_x(x+\xi,t-\tau)|)\,d\xi, \\ b(t) &= \sup_{0\le x\le 1}(|v_{i+1}(x,t) - v_i(x,t)| \\ &\quad + |v_{i+1,x}(x,t) - v_{i,x}(x,t)|), \\ c_1(t) &= 2\rho \sup_{0\le x\le 1}(|\theta(x,t)| + |\theta_x(x,t)|), \\ c_2(t-\tau) &= 2\rho \sup_{0\le x\le 1}(|\theta_\tau(x,t-\tau)| + |\theta_{\tau x}(x,t-\tau)|). \end{aligned}$$

By Lemma 7.1, $c_1(t)$, $c_2(t-\tau)$, and $a(t-\tau)$, $\tau \in [0, t-\delta], t \in [\delta, T]$ are finite. Then, (A.99) can be rewritten as

$$\begin{aligned} b(t) &\leq c_1(\delta)|e^i| + \int_0^{t-\delta} c_2(t-\tau)|e^i(\tau+\delta)|d\tau \\ &\quad + \ell_1 + \ell_2 + 2c_1(t)\ell_1 + \int_0^{t-\delta} a(t-\tau)b(\tau)d\tau. \end{aligned} \tag{A.100}$$

Applying the Gronwall's inequality given in Lemma 1, there has

$$\begin{aligned} b &\leq \exp\left\{\int_0^{t-\delta} a(t-\tau)d\tau\right\} \\ &\quad \times \left(c_1(\delta)|e^i| + \int_0^{t-\delta} c_2(t-\tau)|e^i(\tau+\delta)|d\tau + \ell_1 + \ell_2 + 2c_1(t)\ell_1\right) \\ &\leq \kappa_5|e^i| + \kappa_6 \int_0^{t-\delta} |e^i(\tau+\delta)|d\tau + \kappa_7, \end{aligned} \tag{A.101}$$

where $\kappa_j, j = 5, \cdots, 7$ are defined as follows,

$$\begin{aligned} \kappa_5 &= c_1(\delta) \sup_{\delta \leq t \leq T} \exp\left\{\int_0^{t-\delta} a(t-\tau)d\tau\right\}, \\ \kappa_6 &= \sup_{\delta \leq t \leq T} \left(\exp\left\{\int_0^{t-\delta} a(t-\tau)d\tau\right\} \sup_{0 \leq \tau \leq t-\delta} c_2(t-\tau)\right), \\ \kappa_7 &= \sup_{\delta \leq t \leq T} \left((\ell_1 + \ell_2 + 2c_1(t)\ell_1)\exp\left\{\int_0^{t-\delta} a(t-\tau)d\tau\right\}\right). \end{aligned}$$

Due to the finiteness of c_1, $c_2(t-\tau)$, and $a(t-\tau)$ as $\tau \in [0, t-\delta]$, $\kappa_j, j = 5, \cdots, 7$ are finite and the proof is complete. ■

A.11 Proof of Theorem 7.2

By (7.22) and (7.24), it is easy to see that $|e^i| \leq \ell_1,\ i \in \mathscr{N}$ for $t \in [0, \delta]$. Next, it suffices to consider the scenario $t \in (\delta, T]$. Similarly as in (A.97) of Appendix B,

substituting the control law (7.10) into (7.25) renders to

$$\begin{aligned} e^{i+1} &= (1+2\rho\theta(1,\delta))e^i - 2\rho\theta(1,t)e^i(\delta) \\ &\quad -2\rho\int_0^{t-\delta} e^i(\tau+\delta)\frac{d\theta(1,t-\tau)}{d\tau}d\tau \\ &\quad +\int_0^{t-\delta}\int_0^1 \{\theta(1-\xi,t-\tau)+\theta(1+\xi,t-\tau)\} \\ &\quad \times (F^i - F^{i+1})d\xi d\tau - \Xi^{i+1}(1,t) + \Xi^i(1,t). \end{aligned} \tag{A.102}$$

By taking absolute value on both sides of (A.102) and considering the Lipschitz condition of F and Assumption 7.1, it follows

$$\begin{aligned} |e^{i+1}| &\leq |1+2\rho\theta(1,\delta)||e^i| \\ &\quad +2\rho\int_0^{t-\delta} |e^i(\tau+\delta)|\left|\frac{d\theta(1,t-\tau)}{d\tau}\right|d\tau \\ &\quad +\int_0^{t-\delta}\int_0^1 |\theta(1-\xi,t-\tau)+\theta(1+\xi,t-\tau)| \\ &\quad \times C_F(|v^{i+1}-v^i| + |v_\xi^{i+1}-v_\xi^i|)d\xi d\tau + (1+\rho_1)\ell_1, \end{aligned} \tag{A.103}$$

where $\rho_1 = 2|\rho|\sup_{t\in[0,T]}|\theta(1,t)|$. Then, by Lemmas 7.1 and 7.2, (A.103) further gives

$$\begin{aligned} |e^{i+1}| &\leq |1+2\rho\theta(1,\delta)||e^i| + 2\rho\kappa_2\int_\delta^t |e^i|d\tau + 2C_F\kappa_1\kappa_5\int_0^{t-\delta}|e^i|d\tau \\ &\quad +2C_F\kappa_1\kappa_6\int_0^{t-\delta}\int_0^{s-\delta}|e^i(\tau+\delta)|d\tau ds \\ &\quad +2C_F\kappa_1\kappa_7(t-\delta) + (1+\rho_1)\ell_1 \\ &< |1+2\rho\theta(1,\delta)||e^i| + 2(\rho\kappa_2 + C_F\kappa_1\kappa_5)\int_0^t |e^i|d\tau \\ &\quad +2C_F\kappa_1\kappa_6\int_0^t\int_0^s |e^i|d\tau ds + 2C_F\kappa_1\kappa_7 t + (1+\rho_1)\ell_1 \\ &\leq |1+2\rho\theta(1,\delta)||e^i| + \frac{2(\rho\kappa_2 + C_F\kappa_1\kappa_5)(\exp(\lambda t)-1)}{\lambda}|e^i|_\lambda \\ &\quad +\frac{2C_F\kappa_1\kappa_6(\exp(\lambda t)-\lambda t-1)}{\lambda^2}|e^i|_\lambda + 2C_F\kappa_1\kappa_7 t + (1+\rho_1)\ell_1 \end{aligned} \tag{A.104}$$

Since $|e^{i+1}| \leq \ell_1$ as $t \in [0, \delta]$ has been derived, the inequality (A.104) actually holds for any $t \in [0, T]$.

Taking λ-norm on both sides of (A.104) and noticing that

$$|t|_\lambda = \sup_{\tau \in [0,T]} e^{-\lambda\tau}\tau = e^{-\lambda\tau}\tau|_{\tau=\frac{1}{\lambda}} = \frac{1}{e\lambda},$$

it follows

$$\begin{aligned} |e^{i+1}|_\lambda &\leq |1+2\rho\theta(1,\delta)||e^i|_\lambda \\ &\quad + \frac{2(\rho\kappa_2 + C_F\kappa_1\kappa_5)(1-\exp(-\lambda T))}{\lambda}|e^i|_\lambda \\ &\quad + \frac{2C_F\kappa_1\kappa_6(1-\exp(-\lambda T))}{\lambda^2}|e^i|_\lambda + \frac{2C_F\kappa_1\kappa_7}{e\lambda} + (1+\rho_1)\ell_1. \end{aligned} \tag{A.105}$$

As λ is sufficiently large, it suffices to design ρ such that

$$\begin{aligned} |e^{i+1}|_\lambda &\leq |1+2\rho\theta(1,\delta)||e^i|_\lambda + (1+\rho_1)\ell_1 \\ &\leq \gamma|e^i|_\lambda + (1+\rho_1)\ell_1, \end{aligned} \tag{A.106}$$

where $0 \leq \gamma < 1$. The remaining part of proof is analogous to that of Theorem 1. ■

A.12 Proof of Lemma 8.1

First of all, from (8.8)-(8.10) the derivative of F with respect to the speed v is

$$\frac{\partial F}{\partial v}(\theta_m, f, v) = -v\rho A(l)(\frac{\partial h}{\partial x})^2. \tag{A.107}$$

According to the positiveness of v, ρ, $A(l)$, $(\frac{\partial h}{\partial x})^2$, it is obvious that $\frac{\partial F}{\partial v}(\theta_m, f, v) \leq 0$.

Furthermore, from the expression of F, its derivative with respect to the amplitude

θ_m can be obtained as follows

$$\begin{aligned}\frac{\partial F}{\partial \theta_m}(\theta_m, f, v) &= \frac{\partial H_1}{\partial \theta_m}(\theta_m, f) - \frac{\partial H_2}{\partial \theta_m}(\theta_m, f, v) \\ &= \frac{4\rho A(l)\pi^2 f^2 l^2}{9T}\int_0^T \theta_m \sec^4(\theta_m \sin(2\pi ft))\cos^2(2\pi ft) \\ &\quad \times[1+2\theta_m \tan(\theta_m \sin(2\pi ft))\sin(2\pi ft)]dt \\ &\quad -\frac{\rho A(l)v^2}{T}\int_0^T \tan(\theta_m \sin(2\pi ft)) \\ &\quad \times \sec^2(\theta_m \sin(2\pi ft))\sin(2\pi ft)dt. \end{aligned} \tag{A.108}$$

As shown in Fig. A.1, it is numerically found that $\frac{\partial F}{\partial \theta_m} > 0$. From the point view of practice, the speed of the robotic fish is bounded, namely, there exists a constant $\bar{v} > 0$ such that $0 \le v(t) \le \bar{v}$. Moreover, according to the boundedness of $0 \le \theta_m \le \theta_m^* < \pi/2$, (A.108) implies that there exists a constant $\vartheta > 0$ such that $0 < \frac{\partial F}{\partial \theta_m} \le \vartheta$. ■

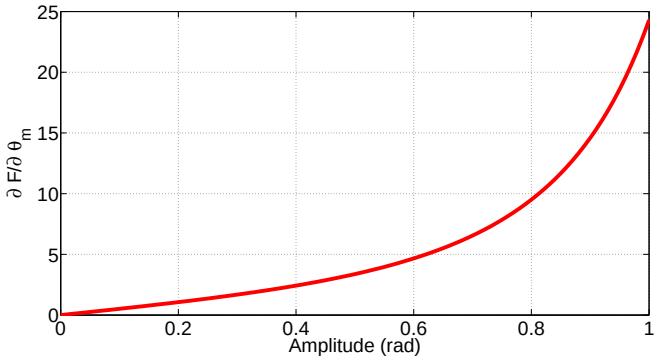

Figure A.1: The gradient $\partial F/\partial \theta_m$ vs. Amplitude.

Appendix B

Author's Publications

The author has contributed to the following publications:

Books:

[1] S. Yang, J.-X. Xu, X. Li. *Iterative Learning Control for Multi-agent Systems Coordination*, Wiley, 2016. (in press)

Journal Papers:

[1] X. Li, Q. Ren, J.-X. Xu, "Precise Speed Control of A Robotic Fish Based on Iterative Learning Control Approach," *IEEE Transactions on Industrial Electronics*, vol. 63, no. 4, pp. 2221-2228, 2016.

[2] X. Li, D. Huang, B. Chu, J.-X. Xu, "Robust Iterative Learning Control for Systems with Norm-bounded Uncertainties," *International Journal of Robust and Nonlinear Control*, vol. 26, no. 4, pp. 697-718, 2016.

[3] X. Li, J.-X. Xu, "A Mathematical Prognosis Model for Pancreatic Cancer Treatment Based on Clinical Data," *Journal of Theoretical Biology*, vol. 406, pp. 42-51, 2016.

[4] S. Yang, J.-X. Xu, X. Li, "Iterative Learning Control with Input Sharing for Multi-agent Consensus Tracking," *Systems & Control Letters*, vol. 94, pp. 97-106, 2016.

[5] X. Li, J.-X. Xu, "A Mathematical Model of Immune Response to Tumor Invasion Incorporated with Danger Model," *Journal of Biological Systems*, vol. 23, no. 3, pp. 505–526, 2015.

[6] X. Li, J.-X. Xu, Deqing Huang, "Iterative Learning Control for Nonlinear Dynamic Systems with Randomly Varying Trial Lengths," *International Journal of Adaptive Control and Signal Processing*, vol. 29, no. 11, pp. 1341-1353, 2015.

[7] X. Li, J.-X. Xu, "Lifted System Framework for Learning Control with Different Trial Lengths," *International Journal of Automation and Computing*, vol. 12, no. 3, pp. 273–280, 2015.

[8] Q. Ren, J.-X. Xu, X. Li, "A Data-Driven Motion Control Approach for A Robotic Fish," *Journal of Bionic Engineering*, vol. 12, no. 3, pp. 382–394, 2015.

[9] X. Li, J.-X. Xu, D. Huang, "An Iterative Learning Control Approach for Linear Time-invariant Systems with Randomly Varying Trial Lengths," *IEEE Trans. Automat. Contr.*, vol. 59, no. 7, pp. 1954–1960, 2014.

[10] D. Huang, X. Li, J.-X. Xu, C. Xu, W. He, "Iterative Learning Control for Linear Distributed Parameter Systems–Frequency Domain Design and Analysis," *Systems & Control Letters*, vol. 72, pp. 22–29, 2014.

[11] D. Huang, J.-X. Xu, X. Li, C. Xu, M. Yu, "D-type Anticipatory Iterative Learning Control for A Class of Inhomogeneous Heat Equations," *Automatica*, vol. 49, no. 8, pp. 2397–2408, 2013.

[12] X. Li, J.-X. Xu, S. Yang, D. Huang, "Comments on 'Decentralized Iterative Learning Control for a Class of Large Scale Interconnected Dynamical systems' by Hansheng Wu [J. Math. Anal. Appl. 327 (2007) 233-245]," *J. Math. Anal. Appl.*, vol. 403, no. 2, pp. 717–721, 2013.

Conference Papers:

[1] D. Huang, X. Li, W. He, S. Ding, "Boundary Control of Nonlinear Wave Equations: An Iterative Learning Control Scheme," in *35th Chinese Control Conference*, Chengdu, China, 27-29 July, 2016.

[2] X. Li, J.-X. Xu, "On Adaptive Iterative Learning From Tracking Tasks with Different Magnitude and Time Scales," in *28th Chinese Control and Decision Conference*, Yinchuan, China, 28-30 May, 2016.

[3] X. Li, J.-X. Xu, Q. Ren, "Motion Control of A Robotic Fish via Learning Control Approach with Self-adaption," in *41st Annual Conference of the IEEE Industrial Electronics Society*, Yokohama, Japan, 9-12 Nov, 2015.

[4] X. Li, J.-X. Xu, "A Mathematical Prognosis Model for Pancreatic Cancer Treatment Based on Clinical Data," in *14th Association of Pacific Rim Univeristies Doctoral Students Conference*, (Hangzhou, China), 23-27 Nov, 2015.

[5] X. Li, Q. Ren, J.-X. Xu, "Speed Trajectory Tracking of A Robotic Fish Based on Iterative Learning Control Approach," in *10th Asian Control Conference*, (Kota Kinabalu, Sabah, Malaysia), pp. 1–6, 31 May-3 June 2015.

[6] X. Li, Q. Ren, J.-X. Xu, "A Mathematical Model of Tumor-Immune Interactions Incorporated with Danger Model," in *10th Asian Control Conference*, (Kota Kinabalu, Sabah, Malaysia), pp. 1–6, 31 May-3 June 2015.

[7] Q. Ren, J.-X. Xu, X. Li, "A Motion Control Approach for A Robotic Fish with Iterative Feedback Tuning," in *IEEE International Conference on Industrial Technology*, (Seville, Spain), pp. 40–45, 17-19 March 2015.

[8] Q. Ren, J.-X. Xu, X. Li, Z. Guo, "Motion Controller Design for A Biomimetic Robotic Fish," in *The 40th Annual Conference of the IEEE Industrial Electronics Society*, (Dallas, Texas, USA), pp. 2816–2821, 29 October-1 November 2014.

[9] X. Li, J.-X. Xu, D. Huang, "An Iterative Learning Control Approach for Linear Time-invariant Systems with Randomly Varying Trial Lengths," in *International Conference on Control, Automation and Systems*, (Gwangju, Korea), pp. 564–569, 20-23 October 2013.

[10] D. Huang, X. Li, J.-X. Xu, C. Xu, "Iterative Learning Control for Linear Distributed Parameter Systems–Frequency Domain Design and Analysis," in *International Conference on Control, Automation and Systems*, (Gwangju, Korea), pp. 574–579, 20-23 October 2013.

[11] D. Huang, X. Li, "D-Type Anticipatory Iterative Learning Control for A Class of Inhomogeneous Heat Equations," in *3rd IFAC International Conference on Intelligent Control and Automation Science*, (Chengdu, China), pp. 68–73, 2-4 September 2013.